Radiochemistry in Nuclear Power Reactors (1996)

Pages
291

Size
8.5 x 10

ISBN
NI000156

Chien C. Lin, Committee on Nuclear and Radiochemistry, National Research Council

NUCLEAR
SCIENCE
SERIES

NAS-NS-3119

Radiochemical Techniques

Radiochemistry in Nuclear Power Reactors

by

Chien C. Lin

Vallecitos Nuclear Center
GE Nuclear Energy
Pleasanton, California

Prepared for the
Committee on Nuclear and Radiochemistry
Board on Chemical Sciences and Technology
Commission on Physical Sciences, Mathematics, and Applications
National Research Council

National Academy Press
Washington, D.C. 1996

NOTICE: The project that is the subject of this report was approved by the Governing Board of the National Research Council, whose members are drawn from the councils of the National Academy of Sciences, the National Academy of Engineering, and the Institute of Medicine. This monograph was prepared by an individual author for the Committee on Nuclear and Radiochemistry.

This report has been reviewed by a group other than the authors according to procedures approved by a Report Review Committee consisting of members of the National Academy of Sciences, the National Academy of Engineering, and the Institute of Medicine.

The National Academy of Sciences is a private, nonprofit, self-perpetuating society of distinguished scholars engaged in scientific and engineering research, dedicated to the furtherance of science and technology and to their use for the general welfare. Upon the authority of the charter granted to it by the Congress in 1863, the Academy has a mandate that requires it to advise the federal government on scientific and technical matters. Dr. Bruce Alberts is president of the National Academy of Sciences.

The National Academy of Engineering was established in 1964, under the charter of the National Academy of Sciences, as a parallel organization of outstanding engineers. It is autonomous in its administration and in the selection of its members, sharing with the National Academy of Sciences the responsibility for advising the federal government. The National Academy of Engineering also sponsors engineering programs aimed at meeting national needs, encourages education and research, and recognizes the superior achievements of engineers. Dr. William A. Wulf is interim president of the National Academy of Engineering.

The Institute of Medicine was established in 1970 by the National Academy of Sciences to secure the services of eminent members of appropriate professions in the examination of policy matters pertaining to the health of the public. The Institute acts under the responsibility given to the National Academy of Sciences by its congressional charter to be an adviser to the federal government and, upon its own initiative, to identify issues of medical care, research, and education. Dr. Kenneth I. Shine is president of the Institute of Medicine.

The National Research Council was organized by the National Academy of Sciences in 1916 to associate the broad community of science and technology with the Academy's purposes of furthering knowledge and advising the federal government. Functioning in accordance with general policies determined by the Academy, the Council has become the principal operating agency of both the National Academy of Sciences and the National Academy of Engineering in providing services to the government, the public, and the scientific and engineering communities. The Council is administered jointly by both Academies and the Institute of Medicine. Dr. Bruce Alberts and Dr. William A. Wulf are chairman and interim vice-chairman, respectively, of the National Research Council.

Support for this project was provided by the U.S. Department of Energy under Award Nos. DE-FG05-89ER14032 and DE-FG02-95ER14556.A000 and by the General Electric Company.

Available from

Board on Chemical Sciences and Technology
National Research Council
2101 Constitution Avenue, NW
Washington, DC 20418

Printed in the United States of America

FORWARD

The Committee on Nuclear and Radiochemistry existed as a standing committee under the Board on Chemical Sciences and Technology of the Commission on Physical Sciences, Mathematics, and Applications of the National Research Council from 1947 until 1993. The committee was charged with maintaining awareness of the chemical aspects of basic and applied nuclear science, stimulating scientific and technical progress, and identifying national problems and needs in nuclear and radiochemistry. Its members were drawn from academic, industrial, and government laboratories and represented the areas of nuclear chemistry, radiochemistry, and nuclear medicine. The committee concerned itself with those areas of nuclear science that involve the chemist, such as the collection and distribution of radiochemical procedures, specialized techniques and instrumentation, the place of nuclear and radiochemistry in college and university programs, the training of nuclear and radiochemists, radiochemistry in environmental science, and radionuclides in nuclear medicine.

A major interest of the committee was the publication of the Nuclear Science Series monographs on Radiochemistry, Radiochemical Techniques, and Nuclear Medicine. The committee endeavored to present monographs of maximum use to the working scientist. Each monograph presented pertinent information required for radiochemical work with an individual element or with a specialized technique or with the use of radionuclides in nuclear medicine. Experts on the various subjects were recruited to write the monographs, and the U.S. Department of Energy sponsored the printing of the series. This monograph, the last of the series, is an up-to-date review of the radiochemical considerations of importance in nuclear power reactors.

When the Committee on Nuclear and Radiochemistry was subsumed by the Board on Chemical Sciences and Technology in 1993, responsibility for the Nuclear Science Series of Monographs was transferred to the Division of Nuclear Chemistry and Technology of the American Chemical Society. Plans are for continuation of the Nuclear Science Series of monographs as review articles in the Journal of Radioanalytical and Nuclear Chemistry.

Steven W. Yates
University of Kentucky
Monograph Coordinator

DISCLAIMER OF RESPONSIBILITY

This document was prepared by the General Electric Company for the National Academy of Sciences–National Research Council. Neither the General Electric Company nor the National Academy of Sciences nor any of the contributors to this document:

A. Makes any warranty or representation, express or implied, with respect to the accuracy, completeness, or usefulness of the information contained in this document, or that the use of any information disclosed in this document may not infringe privately owned rights; or

B. Assumes any responsibility for liability or damage of any kind which may result from the use of any information disclosed in this document.

PREFACE

Radiochemical surveillance of a nuclear power plant is an important part of reactor operations. The plant operator is required to continuously monitor fuel performance, correctly account for release of radioactivity through gas and liquid effluents from the plant, and minimize the exposure of personnel to radiation. To satisfactorily accomplish these tasks, proper training must be given to the plant's chemists and technicians. A comprehensive textbook and/or manual is needed for their training, as well as for their use as a reference to develop good radiochemical procedures for routine analyses. Unlike a well-developed procedure in a research laboratory, a good procedure for routine analytical work in a nuclear power plant should be simple and easy to follow, yet accuracy should not be compromised. Therefore, the first main objective of this monograph is to provide the plant's chemists not only with the fundamentals, but also with some major practical procedures collected from many years of reactor experience. However, it must be pointed out that the information contained in this monograph is provided for reference purposes only and is not meant to establish a standard procedure. The second main objective of this monograph is to provide enough fundamental materials for academic professionals to bridge the gap between industry and academia in the area of radiochemistry in nuclear power plants. It also serves as an introduction to professionals in other related fields, such as health physics and nuclear engineering.

This monograph deals with two major types of light water reactors: the boiling water reactor (BWR) and the pressurized water reactor (PWR). The main body describes radiochemical technologies in six major areas: (1) radioactivity production and measurement, (2) fuel performance surveillance and fission product chemistry, (3) the chemistry and transport behavior of activation products, (4) radiation chemistry in the coolant, (5) assay of radioactive waste, and (6) special radiochemical studies and tests in the reactor system. Some selected procedures for sampling, radiochemical separation, and activity measurements are also included in the appendices. The subject matter presented in this monograph is the result of the author's gleanings from many sources, including lecture notes he used in 1980 at the Institute of Nuclear Science, National Tsing Hua University in Taiwan, and several reports published by the Electric Power Research Institute in Palo Alto, California. Some valuable materials provided by H.R. Helmholz of NWT Corporation and R.C. Huang of Taiwan Power Company are also included.

The author completed his education under the tutelage of nuclear chemistry pioneer Professor Arthur C. Wahl (retired) of Washington University and Professor Milton Kahn (retired) of the University of New Mexico, who were the first research team to report the anomalous chemical behavior of tracer-level iodine in aqueous solutions. After 40 years, the behavior of radioiodine in reactor systems continues to be one of the most elusive, but important, subjects in radiochemistry.

The author was fortunate to have worked under the late R.S. Gilbert, who was a master in fission product source term evaluation. More recently, he has benefited from association with, and guidance from, J.M. Skarpelos, R.N. Osborne, J.H. Holloway, H.R. Helmholz, G.F. Palino, C.P. Ruiz, and R.L. Cowan. He is grateful to GE Nuclear Energy for permission to publish this monograph. He would also like to express his appreciation to H.R. Helmholz, C.P. Ruiz, and G.C. Martin for reviewing the manuscript, and to Diane Parkinson for preparing the manuscript.

Finally, I must acknowledge a special debt to my wife, Jing, for her patience and encouragement during the writing of this monograph.

November 1994 Chien C. Lin

TABLE OF CONTENTS

TABLE OF CONTENTS (Continued)

TABLE OF CONTENTS (Continued)

TABLE OF CONTENTS (Continued)

LIST OF FIGURES

LIST OF FIGURES (Continued)

LIST OF FIGURES (Continued)

LIST OF FIGURES (Continued)

LIST OF TABLES

LIST OF TABLES (Continued)

LIST OF TABLES (Continued)

1. BRIEF DESCRIPTION OF NUCLEAR POWER REACTOR SYSTEMS AND PRIMARY COOLANT CHEMISTRY

1.1 BOILING WATER REACTOR (BWR)

The direct cycle boiling water reactor nuclear system (Figure 1-1) is a steam generating system consisting of a nuclear core and an internal structure assembled within a pressure vessel, auxiliary systems to accommodate the operational and safeguard requirements of the nuclear reactor, and necessary controls and instrumentation. High-purity water is circulated through the reactor core, serving as moderator and coolant. Saturated steam is produced in the reactor core, separated from recirculation water, dried in the top of the vessel, and directed to the steam turbine generator. The turbine employs a conventional regenerative cycle with condenser deaeration and condensate demineralization.

The reactor core, the source of nuclear heat, consists of fuel assemblies and control rods contained within the reactor vessel and cooled by the recirculating water system. A typical 1220 MWe BWR/6 core consists of 748 fuel assemblies and 177 control rods, forming a core array about 5 meters in diameter and 4.3 meters high. The power level is maintained or adjusted by positioning control rods up and down within the core. The BWR core power level is further adjusted by changing the recirculation flow rate without changing the control rods positions.

The boiling water reactor requires substantially lower primary coolant flow through the core than pressurized water reactors. The core flow of a BWR is the sum of the feedwater flow and the recirculation flow.

The function of the reactor water recirculation system is to circulate the required coolant through the reactor core. The system consists of two or more loops external to the reactor vessel, each loop containing a pump with a directly coupled water-cooled (air-water) motor, a flow control valve, and two shutoff valves.

High-performance jet pumps located within the reactor vessel are used in the BWR recirculation system. The jet pumps, which have no moving parts, provide a continuous internal circulation path for the total core coolant flow.

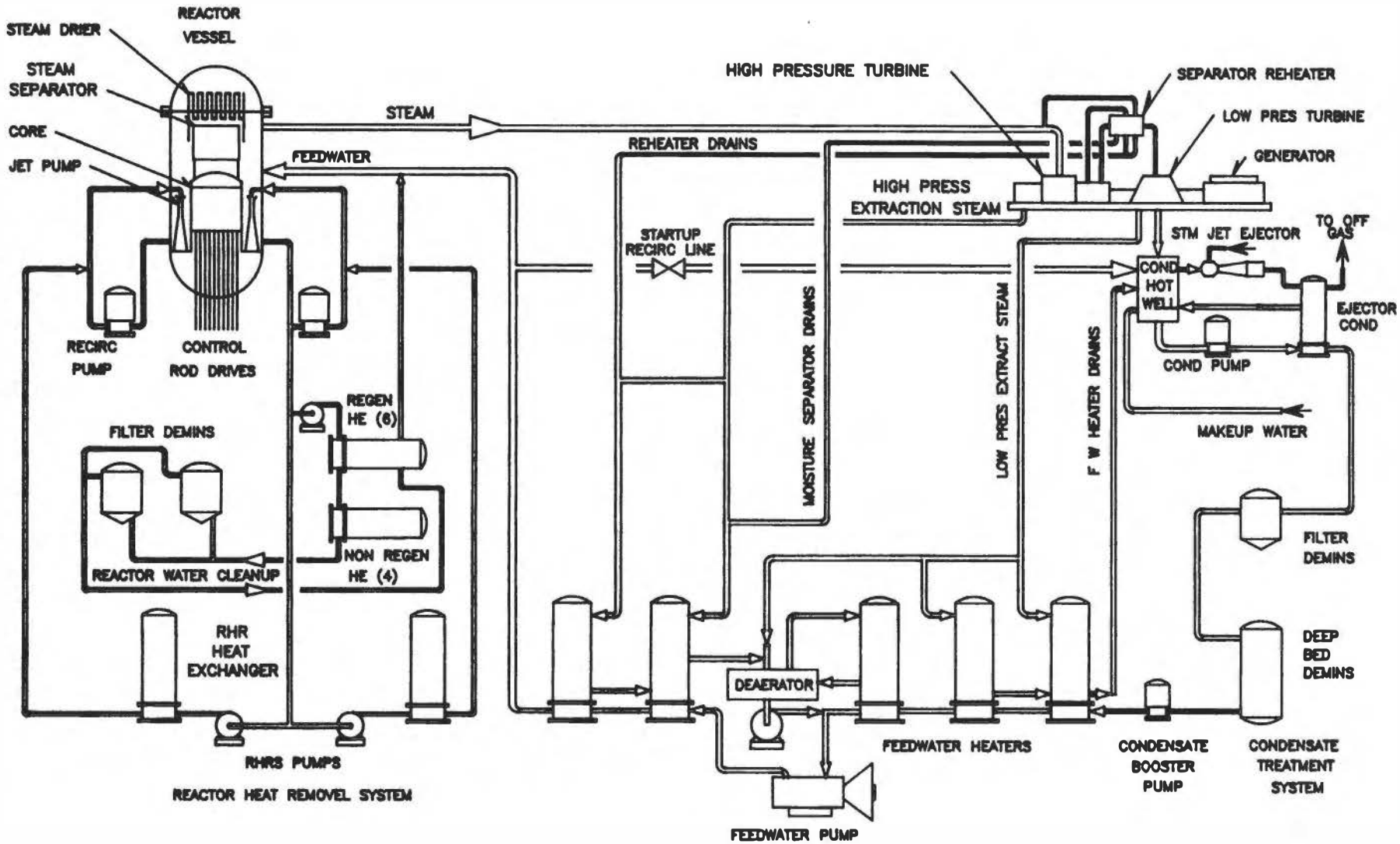

Figure 1-1. Direct Cycle Boiling Water Reactor System With Forward-Pumped Heater Drains

The BWR operates at a constant pressure of 1050 psi (or 68 kg/cm^2) and maintains a constant steam pressure, similar to most fossil boilers. The coolant temperature is maintained at approximately 280°C. A small portion of the recirculation water is removed from the reactor through the reactor recirculation pump suction line, passed through the heat exchangers and a reactor water cleanup (RWCU) system, and returned through the feedwater line. The purpose of the RWCU system is to maintain high reactor water quality by removing soluble and insoluble impurities, including corrosion products and radioactive species. In addition, the system provides a means for water removal from the primary system during periods of increasing water volume.

A summary of BWR water quality specifications is presented in Table 1-1. The main objectives for water quality control in a BWR system are to:

(1) Minimize the potential for stress corrosion cracking of structural materials.
(2) Minimize corrosion and corrosion product release from the primary system surfaces.
(3) Minimize fuel cladding failures due to zircaloy corrosion.
(4) Minimize corrosion product deposition and activation on the fuel cladding surfaces.
(5) Minimize the radiation field buildup on the system component surfaces due to deposition of activated corrosion products.

More detailed discussion on the BWR water chemistry quality control and guidelines can be found elsewhere[1].

As a result of water radiolysis-gas stripping in the core and recirculation, the reactor recirculation water contains dissolved oxygen and hydrogen peroxide in the concentration range from ~100 to ~300 ppb and somewhat less than stoichiometric concentration of dissolved hydrogen. Under this highly oxidizing environment, the radioactive impurities are normally found in the higher oxidation states in the coolant. Recently, hydrogen water chemistry (HWC) was developed to mitigate the intergranular stress corrosion on structure materials. In this technology, hydrogen gas is injected into the coolant through the feedwater system to suppress the water radiolysis in the core region and to control the dissolved oxygen concentration in the coolant at a very low level. More discussion on HWC is presented in Chapter 6.

Table 1-1
BWR WATER QUALITY SPECIFICATIONS

	Typical Warranty Limits		Operational Practices
	Normal Operating Limits	Maximum Operating Limits	Suggested * Administrative Limits
• Reactor Water			
• Power Operation			
– Conductivity (μS/cm)	1.0	10.0	0.2
– Chloride (ppb)	200	500	20
– pH	5.6-8.6	4.6-9.6	6.1-8.1
– Silica (ppb)	200	–	100
– Total Copper (ppb)	20	–	10
• Startup & Hot Standby			
– Conductivity (μS/cm)	1.0	2.0	0.2
– Chloride (ppb)	100	100	20
– Total Copper (ppb)	20	–	10
• Shutdown			
– Conductivity (μs/cm)	2.0	5.0	2.0
– Chloride (ppb)	100	500	50
– pH	5.3-8.6	4.6-9.6	5.3-8.6
– Silica (ppb)	200	–	100
– Total Copper	20	–	10
• Feedwater			
• Power Operation			
– Metallic Impurities(ppb)	15	60	–
– Iron (ppb)			
• Insoluble	10	40	2.0
• Soluble	1.0	2.0	0.5
– Total Copper (ppb)	0.5	2.0	0.1
– Oxygen (ppb)	35±15	110±90	25±5
– Conductivity (μs/cm)	0.005	0.1	0.06
• Startup and Hot Standby			
– Conductivity (μs/cm)	0.1	0.15	0.08
– Total Copper (ppb)	1.0	–	0.2
• Condensate Treatment System Effluent			
• Oxygen (ppb)	35±15	110±90	25±5
• Conductivity (μS/cm)	0.065	0.1	0.06
• Iron (ppb)			
– Insoluble	10.	–	2.0
– Soluble	1.0	–	0.5
• Total Copper (ppb)	0.5	–	0.1

* J.M. Skarpelas, GE Nuclear Energy, Private Communication (1990)

1.2 PRESSURIZED WATER REACTOR (PWR)

The primary side of a PWR system consists of a series of interrelated systems which directly or indirectly interface with the reactor itself. Each of the associated systems has its own specific functions which contribute to the fundamental safe operation and control of the reactor.

The major component of the primary side is the reactor vessel, which houses the reactor core. The reactor is operated at 2200 psi (or 142.5 kg/cm^2) with the coolant temperature at 350°C. Unlike the BWR system, there is no boiling in the core region.

Associated with the reactor vessel is a piping system through which the reactor coolant is pumped. The energy is transferred by the coolant from the reactor core to the steam generators where secondary steam is subsequently produced and routed to the unit turbine generator and main steam system.

The primary coolant system also includes the reactor, an electrically heated pressurizer, a pressurizer quench tank and inter-connecting piping, and the chemical and volume control system (Figure 1-2).

The pressurizer maintains primary coolant system operating pressure and compensates for changes in primary coolant volume during load changes. The quench tank is designed to receive and condense the normal discharges from the pressurizer relief valves and prevent the discharge from being released to containment.

The chemical and volume control system is designed to allow the operators to control the volume of primary coolant as well as its chemical composition through a dual interface with the primary coolant system. The major use of this system is to control the primary coolant boron concentration as a function of power level and core life. It is also used to control the reactor coolant pH through the addition or removal of lithium hydroxide. Some fission and activation products can be removed by the system's purification demineralizers. The system is designed to allow the addition or removal of boron in the form of boric acid, lithium hydroxide and hydrogen during normal operation. Hydrogen gas is dissolved in the reactor coolant to scavenge any trace amounts of dissolved oxygen which may be present in the coolant.

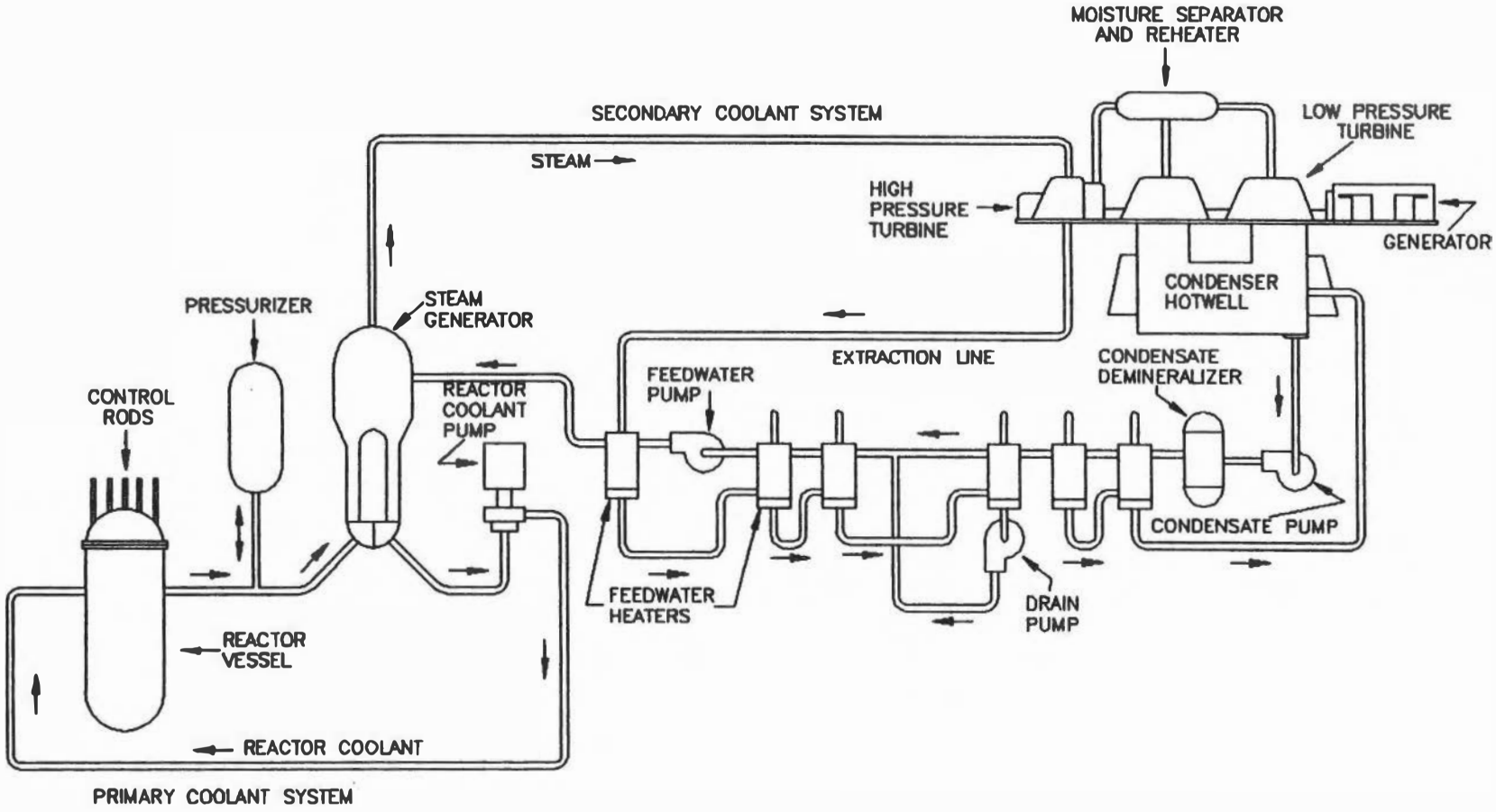

Figure 1-2. Schematic of a Pressurized Reactor System

The function of the primary coolant is to remove heat from the core, moderate the core, and transfer the heat to the steam generators. In order to perform these functions efficiently, chemistry controls are required. The purpose of these controls is to:

(1) Minimize the number of control rod movements by use of chemical shim (i.e., boron) for controlling core reactivity throughout the life of the core.
(2) Minimize corrosion of primary system surfaces including the steam generator tubing.
(3) Minimize Zircaloy corrosion and fuel cladding failures.
(4) Minimize corrosion product deposition and activation on the fuel cladding surfaces.
(5) Minimize corrosion product buildup on the steam generator which could reduce heat transfer.
(6) Minimize total activated corrosion product inventory and transport and plant radiation field buildup.

The vendor reactor coolant chemistry specifications may vary slightly from each other as shown in Table 1-2. Current Westinghouse specifications for the reactor coolant system are given in Table 1-3. Under the highly reducing chemistry environment, most of the radioactive impurities are expected to be present in the reduced or insoluble forms in the PWR coolant.

More detailed discussion on the principals of PWR coolant chemistry control and guidelines can be found in References 3 and 5.

1.3 REFERENCES

(1) BWR Owners Group, "BWR Water Chemistry Guidelines", EPRI NP-3589-SR-LD, Special Report (April 1985).
(2) A. Strasser et al, "Corrosion-Product Buildup on LWR Fuel Rods", EPRI NP-3789 (April 1985).
(3) PWR Primary Water Chemistry Guidelines Committee, "PWR Primary Water Chemistry Guidelines: Revision 2", EPRI NP-7070 Final Report (November 1990).
(4) S. Glasstone and A. Sesonske, "Nuclear Reactor Engineering," D. Van Nostrand Company, Inc., Princeton, New Jersey (1963).
(5) P. Cohen, "Water Coolant Technology of Power Reactors", Gordon and Breach Science Publishers, New York (1969).

Table 1-2

VENDOR REACTOR COOLANT CHEMISTRY SPECIFICATIONS FOR POWER OPERATION (Reproduced with Permission, EPRI NP-3789, Ref. 2)

Vendor	^{7}LiOH (as ppm Li)	Boron* (ppm)	Hydrogen (cc/kg, STP)
Westinghouse (W)	0.7-2.2 (formerly 0.2-2.2)	0-800 (0-1100 first cycle)	25-50 (normal operating range 30-40)
Combustion Engineering (CE)	1.0-2.0** (formerly 0.2-1.0)	<4400	25-50 (formerly 10-50)
Babcock and Wilcox (B&W)	0.2-2.0	0-2270	15-40

* Concentration varies from high levels early in cycle to low levels at end of cycle.

** Near end of life, when the deborating ion exchanger is placed in service (≈30 ppm B), the lithium range is 0.2-0.5 ppm.

Table 1-3

CURRENT WESTINGHOUSE SPECIFICATIONS FOR THE REACTOR COOLANT SYSTEM (Reproduced with Permission, EPRI NP-3789, Ref. 2)

Chemistry Parameter	Permissible Range
Electrical Conductivity	1-40 μmho/cm
pH	4.2-10.5
Dissolved Oxygen	≤5 ppb
Chloride	≤0.15 ppm
Fluoride	≤0.15 ppm
Suspended Solids	≤1.0 ppm
Hydrogen	25-50 cc/kg
Boron	0-4000 ppm
Lithium	0.7 to 2.2 ppm (recommendation depending on boron concentration)
Silica	≤0.2 ppm
Calcium	≤0.05 ppm
Magnesium	≤0.05 ppm
Aluminum	≤0.05 ppm

2. RADIOACTIVITY PRODUCTIONS IN NUCLEAR REACTORS

2.1 RADIOACTIVE SPECIES IN LIGHT WATER REACTORS

There are approximately one hundred major radioactive nuclides which can be found in a reactor system (see Appendix A, Table A-1). Each nuclide decays with emission from the nucleus of characteristic energetic elementary particles or energetic photons. In some cases, the change is accomplished by the capture by the nucleus of an extra-nuclear electron.

The various decay processes and the particles and radiations emitted are:

Decay Process	Radiation Emitted	Mass (amu)	Electrical Charge	Typical Energy (MeV)
Alpha Emission	Alpha particle (α)	4	+2	4-9
Beta Emission	Beta particle (β^-)	0.0005	-1	0-3
Positron Emission	Positron (β^+)	0.0005	+1	0-3
	Two gamma-rays (γ)	0	0	0.51
Electron Capture	Characteristic x-ray	0	0	0-0.1
Internal Transition	Gamma-ray (γ)	0	0	0.1-3
Internal Conversion	Converted electron(e^-)	0.0005	-1	0.1-1
	Characteristic x-ray	0	0	0.0-1
Neutron Emission	Neutron (n)	1	0	0-14
Spontaneous Fission (e.g., Cf-252)	Fission products and other radiations	-	-	≈200

The decay of a radioactive species is a random process dependent only on the number of radioactive atoms present at a given time (i.e., the decay rate is a first-order reaction):

$$-\frac{dN}{dt} = \lambda N \tag{2-1}$$

Upon integration, the result can be written as

$$N = N_0 e^{-\lambda t}, \tag{2-2}$$

where N = number of atoms present at time t;

N_0 = number of atoms present at t = 0;

λ = decay constant.

The constant λ is the characteristic decay constant for the radioactive species. The characteristic rate of radioactive decay may conveniently be stated in terms of the half-life ($t_{1/2}$), which is the time required for an initial number of atoms to be reduced to half that number by decay.

A sample of any radioactive substance which is decaying at the rate of 3.7×10^{10} disintegration per second is traditionally said to contain one curie (Ci) of radioactivity. A millicurie (mCi) is 10^{-3} curies and a microcurie (μCi) is 10^{-6} curies. The microcurie is probably the most frequently used activity unit in the nuclear industry. The SI unit for the activity is Becquerel (Bq). One Bq is equal to one disintegration per second of activity, thus one Ci equals 3.7×10^{10} Bq.

The concentrations of radioactive species in different types of samples may be expressed in different ways. For example:

Sample Form	Recommended Expression	Recommended Unit
Liquid	Concentration	μCi/L or Bq/mL
Reactor water or condensed steam	Concentration	μCi/kg or Bq/gm
Gas	Concentration	μCi/cc or Bq/cc
Solid	Solid concentration	μCi/gm or Bq/gm of specified solid substance
Surface	Surface concentration	μCi/cm^2 or Bq/cm^2
Any form of target substance	Specific activity	μCi/gm or Bq/gm of target element

It should be noted that the activity concentration in reactor water or condensed steam is commonly reported in μCi/kg or Bq/gm. Using the mass instead of volume avoids the confusion of water density differences at different temperatures.

The radioactive species may be produced in a reactor by different nuclear reactions from various target materials in the system.

2.2 NUCLEAR FISSION

The fission process is usually accompanied by the emission of neutrons and much more rarely by the emission of α particles and possibly other light fragments. Tritium is also emitted in some fission processes. Fission has been produced in some nuclides (notably U-235, U-238, and Th-232) by neutrons, protons, deuterons, helium ions, and γ and x-rays of moderate energies. In a reactor by far the most important of these reactions is neutron-produced fission. The species U-232, U-233, U-235 , Pu-239, Am-241, and Am-242 undergo fission either with thermal or fast neutrons, whereas fission of U-238 requires fast neutrons.

2.2.1 Mass Distribution and Fission Product Chains

The fission process may occur in many different modes, and a very large number of fission products, ranging from Z = 30 (zinc) to Z = 65 (terbium) and from A = 72 to A = 161 in the thermal neutron fission of U-235, are known. Fission into two equal fragments is by no means the most probable mode in thermal-neutron fission. Asymmetric modes are much more favored, the maximum fission product yields occurring at A = 95 and A = 138. The asymmetry appears to become less pronounced with increasing bombarding energy. When the total fission yield at each mass number is plotted against mass number, the curve shown in Figure 2-1 results. The curve is essentially symmetrical about the minimum at A = 233.5/2 and has two rather broad maxima around mass numbers 95 and 138. The yields in each of the two peaks sum to approximately 100%.

Sufficient information is available on the fission yields in the thermal- neutron fission of Pu-239 to draw a mass-yield curve for this case. The general shape is similar to the U-235 curve, but there are certain significant differences (see Figure 2-1). The yield at the minimum is not as low as for U-235; it is about 0.04 percent of the fission yield at A = 119. The heavy peak appears not to be appreciably displaced, compared to U-235 fission, but the light peak has its maximum at about A = 99.

An enormous amount of radiochemical work was required to arrive at the present state of knowledge about fission products. It was necessary to develop chemical separation procedures, to analyze radioactive decay and growth patterns, to determine beta- and gamma-ray energies, to establish mass assignments of many previously unknown nuclides and to measure the fission yields. The fission yield of a nuclide is the fraction or the percentage of the total number of fissions which lead directly or indirectly to that nuclide.

As would be expected from the different neutron-proton ratios for U-235 and the stable elements in the fission product region, the primary products of fission are generally on the neutron-excess side of stability. Each such product decays by successive β^- processes to a stable isobar. Chains with as many as six β^- decays have been established, and undoubtedly some fission products still further removed from stability (higher on the parabolic slope of the stability valley) have escaped detection because of their very short half-lives. No neutron-deficient nuclides have been found among the products of thermal-neutron fission.

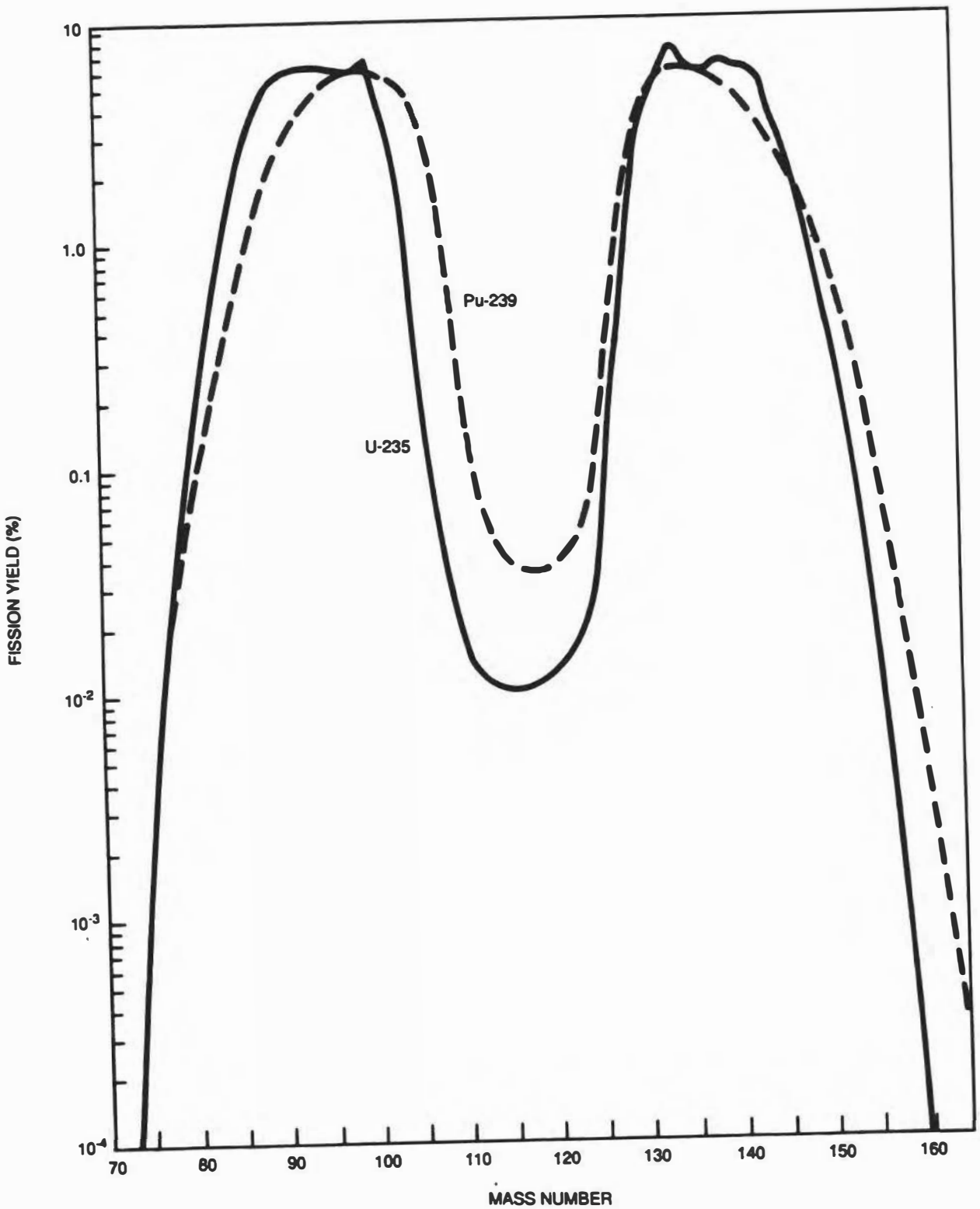

Figure 2-1. Yields of Fission Product Chains as a Function of Mass Number for the Thermal-Neutron Fission of U-235 and Pu-239

2.2.2 Charge Distribution

Direct information on the distribution of yields along any given chain is confined to the relatively few good measurements of independent fission yields of individual chain members and of the shielded nuclides. An hypothesis which appears to account fairly well for most of the data is the postulate of "equal charge displacement." To state this, we make use of the quantity Z_A, the value of Z corresponding to the highest binding energy for a given A. Furthermore, we define Z_p as the most probable charge for a primary fission fragment of mass number A. The postulate of equal charge displacement is that the two complementary fragments in a given fission event always have equal $Z_A - Z_p$ values and, furthermore, that the probability distribution around Z_p is the same for all values of A. Remembering that on the average 2.5 neutrons are emitted per U-235 fission, we can write $Z_A - Z_p = Z_{233.5-A} - (92 - Z_p)$, or $Z_p = 46 + 1/2(Z_A - Z_{233.5-A})$. From this formula and Z_A, Z_p can be calculated for any A. The measured independent yields indicate a probability distribution such that 50% of the total chain yield occurs for $Z = Z_p$, about 25% each for $Z = Z_p \pm 1$, about 2% for $Z = Z_p \pm 2$, and much less for other Z values. The isobaric yield distribution around Z_p appears to be Gaussian, and the postulate of a universal distribution in Z at all values of A is borne out by experiment, but not understood theoretically. As an example, the charge dispersion among products with A=93 from thermal-neutron fission of U-235 is shown in Table 2-1 and Figure 2-2. As can be seen in Figure 2-2, the fractional independent yield or relative probability P(Z) of formation of a product with atomic number Z is well-represented by a Gaussian curve,[3]

$$P(Z) = f_{o.e.}\,(C\pi)^{-1/2} \exp\left[-(Z-Zp)^2/C\right],$$

in which P(Z) is the fractional independent yield of the fission product with atomic number Z, $f_{o.e.}$ is the odd-even effect factor, and C is nearly constant for all fission product mass chains.

The fractional cumulative yield of a fission product with charge Z is given by:[4]

$$\sum P(Z) = \frac{f_{o.e.}}{(C\pi)^{1/2}} \int_{-\infty}^{Z+1/2} \exp\frac{-(Z-Z_p)^2}{C}\, dZ$$

Table 2-1

BETA DECAY CHAIN FOR MASS NUMBER 93
(Yields are for thermal-neutron fission of U-235)

Nuclide	Fractional Independent Yield	Cumulative Yield %
Br-93 (0.81s)	4.9×10^{-4}	0.003
Kr-93 (1.3s)	0.075	0.49
Rb-93 (5.8s)	0.48	3.54
Sr-93 (7.5m)	0.39	6.21
Y-93 (10.2h)	0.19	6.37
Zr-93 (9.5×10^{5}y)	2×10^{-4}	6.37
Nb-93 (Stable)	27×10^{-9}	6.37

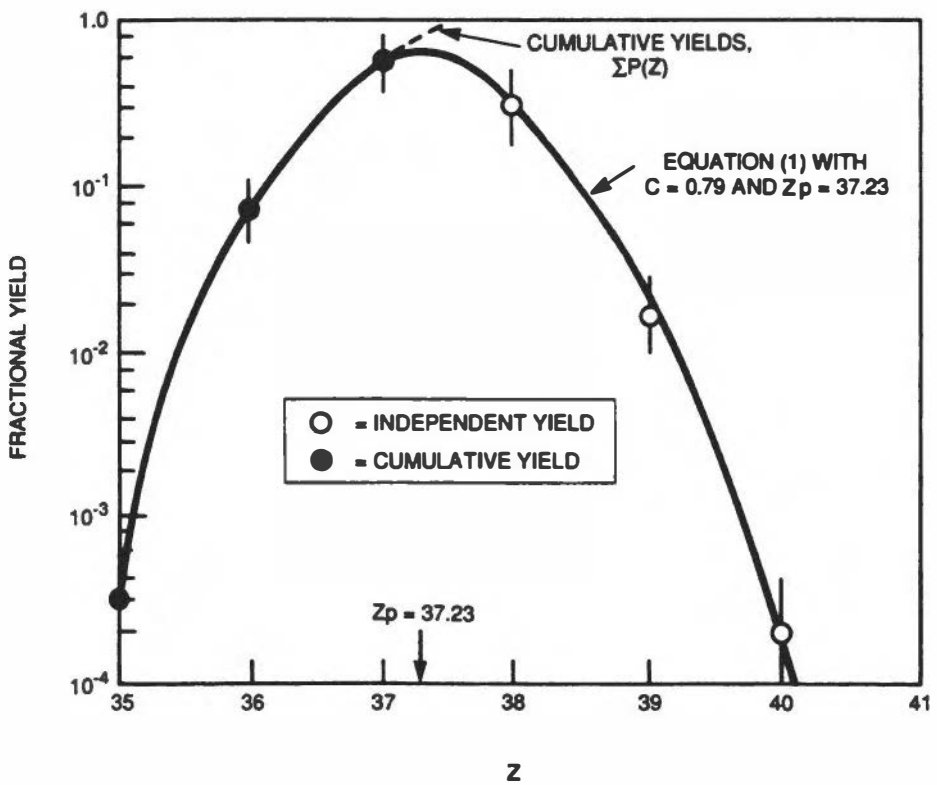

Figure 2-2. Charge Dispersion for Products with A = 93 from Thermal-Neutron Fission of U-235

The value of C is related to the Gaussian curve width parameter (σ) which is nearly constant (σ = 0.56) for all masses.*[5] Z_p for each mass chain has been empirically determined based on many values of Z_p found experimentally.

Based on the charge distribution probability, Rider[6] has calculated by both the independent and cumulative fission yields for all fission products from various fission reactions. A summary of major fission product yields in thermal-neutron fission of U-235 and Pu-239 is given in Table 2-2.

2.3 TRANSURANIC NUCLIDES

The transuranic elements are those produced by successive neutron capture of uranium and its products in a reactor. The chain of production and the radiation characteristic of each isotope are shown in Figure 2-3. In this production chain, the major products are:

Neptunium	-237, -239;
Plutonium	-238, -239, -240, -241, -242;
Americium	-241, 243;
Curium	-242; -244.

Except for Np-239 and Pu-241, all the isotopes above are alpha emitters. Np-239 is a beta emitter and decays to Pu-239 with 2.36-day half-life. Pu-241 is also a beta emitter and decays to Am-241 with a 14.4-year half-life. A small fraction (0.0023%) of Pu-241 also decays to U-237 by emitting alpha particles.

Experimental measurements, as well as theoretical calculations of each transuranic isotope buildup in the fuel element as a function of fuel burnup, have been reported by several investigators[8,9,10] for various fuel materials. Variations of transuranic isotope content with fuel burnup relative to total uranium are shown in Figure 2-4 for 2.5% enriched UO_2 fuel. The transuranic activity buildup varies quite rapidly with the fuel burnup; however, the predominant alpha activity at the end of irradiation is Cm-242 (90 to 95%) because of its shorter half-life. As the fuel exposure increases, the fissionable nuclides (Pu-239 and Pu-241) are created in the fuel, and a large fraction of fission may be attributed to plutonium isotopes near the end of fuel life (Figure 2-5).

---

* $C \approx (\sigma^2 + 1/12)$

Table 2-2

CUMULATIVE YIELDS OF MAJOR FISSION PRODUCTS IN THERMAL NEUTRON FISSION OF U-235 AND Pu-239

Nuclide	Half-life		Decay constant λ, 1/s	Fission yields(Y),% U-235	Pu-239	(U+Pu) 2	Y*λ U-235	(U+Pu)/2
Br-84	31.80	m	3.63E-04	0.967	0.444	0.706	3.51E-06	2.56E-06
Kr-85m	4.48	h	4.30E-05	1.300	0.565	0.933	5.59E-07	4.01E-07
Kr-85	10.72	y	2.05E-09	0.285	0.128	0.207	5.86E-12	4.24E-12
Kr-87	1.37	h	1.41E-04	2.520	0.990	1.755	3.54E-06	2.47E-06
Kr-88	2.84	h	6.78E-05	3.550	1.320	2.435	2.41E-06	1.65E-06
Kr-89	3.15	m	3.67E-03	4.600	1.440	3.020	1.69E-04	1.11E-04
Kr-90	32.30	s	2.15E-02	4.860	1.400	3.130	1.04E-03	6.72E-04
Rb-88	17.70	m	6.53E-04	3.570	1.360	2.465	2.33E-05	1.61E-05
Rb-89	15.40	m	7.50E-04	4.770	1.680	3.225	3.58E-05	2.42E-05
Rb-90	2.60	m	4.44E-03	4.500	1.390	2.945	2.00E-04	1.31E-04
Rb-90m	4.30	m	2.69E-03	1.240	0.680	0.960	3.33E-05	2.58E-05
Rb-91	58.00	s	1.19E-02	5.670	2.160	3.915	6.77E-04	4.67E-04
Sr-89	50.50	d	1.59E-07	4.780	1.690	3.235	7.59E-09	5.14E-09
Sr-90	29.10	y	7.55E-10	5.910	2.110	4.010	4.46E-11	3.03E-11
Sr-91	9.51	h	1.93E-04	5.930	2.490	4.210	1.14E-05	8.11E-06
Sr-92	2.71	h	7.10E-05	5.910	3.040	4.475	4.20E-06	3.18E-06
Sr-93	7.40	m	1.56E-03	6.370	3.920	5.145	9.94E-05	8.03E-05
Y-90	2.67	d	3.00E-06	5.920	2.110	4.015	1.78E-07	1.21E-07
Y-91	58.50	d	1.37E-07	5.930	2.490	4.210	8.13E-09	5.77E-09
Y-92	3.54	h	5.44E-05	5.980	3.060	4.520	3.25E-06	2.46E-06
Y-93	10.20	h	1.89E-05	6.370	3.920	5.145	1.20E-06	9.71E-07
Zr-95	64.00	d	1.25E-07	6.490	4.890	5.690	8.14E-09	7.13E-09
Zr-97	16.80	h	1.15E-05	5.930	5.320	5.625	6.80E-07	6.45E-07
Nb-95	34.97	d	2.29E-07	6.490	4.890	5.690	1.49E-08	1.31E-08
Nb-97	1.23	h	1.57E-04	5.950	5.370	5.660	9.31E-06	8.86E-06
Mo-99	2.79	d	2.88E-06	6.120	6.160	6.140	1.76E-07	1.77E-07
Mo-101	14.60	m	7.91E-04	5.180	5.940	5.560	4.10E-05	4.40E-05
Tc-98m	6.02	h	3.20E-05	5.380	5.420	5.400	1.72E-06	1.73E-06
Tc-101	14.20	m	8.14E-04	5.180	5.950	5.565	4.21E-05	4.53E-05
Tc-104	18.00	m	6.42E-04	1.920	5.960	3.940	1.23E-05	2.53E-05
Ru-103	39.27	d	2.04E-07	3.040	6.950	4.995	6.21E-09	1.02E-08
Ru-105	4.44	h	4.34E-05	0.972	5.360	3.166	4.22E-07	1.37E-06
Ru-106	1.02	y	2.15E-08	0.403	4.280	2.342	8.68E-11	5.05E-10
Rh-105	35.40	h	5.44E-06	0.972	5.360	3.166	5.29E-08	1.72E-07
Sb-125	2.76	y	7.96E-09	0.029	0.115	0.072	2.31E-12	5.73E-12
Te-129m	33.60	d	2.39E-07	0.127	0.270	0.199	3.03E-10	4.74E-10
Te-132	3.26	d	2.46E-06	4.280	5.230	4.755	1.05E-07	1.17E-07
I-131	8.04	d	9.98E-07	2.880	3.850	3.365	2.87E-08	3.36E-08
I-132	2.28	h	8.44E-05	4.320	5.390	4.855	3.65E-06	4.10E-06
I-133	20.80	h	9.26E-06	6.690	6.930	6.810	6.19E-07	6.30E-07
I-134	52.60	m	2.20E-04	7.710	7.270	7.490	1.69E-05	1.65E-05
I-135	6.57	h	2.93E-05	6.300	6.450	6.375	1.85E-06	1.87E-06
I-136	1.39	m	8.31E-03	2.970	1.740	2.355	2.47E-04	1.96E-04

Table 2-2 (Continued)

Nuclide	Half-life		Decay constant λ, 1/s	Fission yields(Y),% U-235	Pu-239	(U+Pu) 2	Y*λ U-235	(U+Pu)/2
Xe-133	5.24	d	1.53E-06	6.700	6.980	6.840	1.03E-07	1.05E-07
Xe-133m	2.23	d	3.60E-06	0.189	0.232	0.211	6.80E-09	7.57E-09
Xe-135m	15.30	m	7.55E-04	1.000	1.680	1.340	7.55E-06	1.01E-05
Xe-135	9.10	h	2.12E-05	6.540	7.600	7.070	1.38E-06	1.50E-06
Xe-137	3.82	m	3.02E-03	6.060	6.040	6.050	1.83E-04	1.83E-04
Xe-138	14.20	m	8.14E-04	6.420	5.120	5.770	5.22E-05	4.69E-05
Xe-139	39.70	s	1.75E-02	5.040	3.050	4.045	8.80E-04	7.06E-04
Xe-140	13.70	s	5.06E-02	3.620	1.600	2.610	1.83E-03	1.32E-03
Cs-137	30.17	y	7.29E-10	6.220	6.690	6.455	4.53E-11	4.70E-11
Cs-138	32.20	m	3.59E-04	6.640	5.910	6.275	2.38E-05	2.25E-05
Cs-139	9.30	m	1.24E-03	6.280	5.350	5.815	7.80E-05	7.22E-05
Ba-139	83.70	m	1.38E-04	6.350	5.600	5.975	8.76E-06	8.25E-06
Ba-140	12.75	d	6.29E-07	6.270	5.540	5.905	3.95E-08	3.72E-08
Ba-141	18.30	m	6.31E-04	5.790	5.230	5.510	3.66E-05	3.48E-05
Ba-142	10.70	m	1.08E-03	5.730	4.600	5.165	6.19E-05	5.58E-05
La-140	40.27	h	4.78E-06	6.280	5.550	5.915	3.00E-07	2.83E-07
La-141	3.90	h	4.94E-05	5.810	5.310	5.560	2.87E-06	2.74E-06
La-142	92.50	m	1.25E-04	5.830	4.910	5.370	7.28E-06	6.71E-06
Ce-141	32.50	d	2.47E-07	5.800	5.260	5.530	1.43E-08	1.37E-08
Ce-143	33.00	h	5.83E-06	5.940	4.430	5.185	3.47E-07	3.03E-07
Ce-144	284.60	d	2.82E-08	5.470	3.740	4.605	1.54E-09	1.30E-09
Nd-147	10.99	d	7.30E-07	2.250	2.040	2.145	1.64E-08	1.57E-08
Np-239	2.35	d	3.41E-06	60.000	60.000	60.000	2.05E-06	2.05E-06

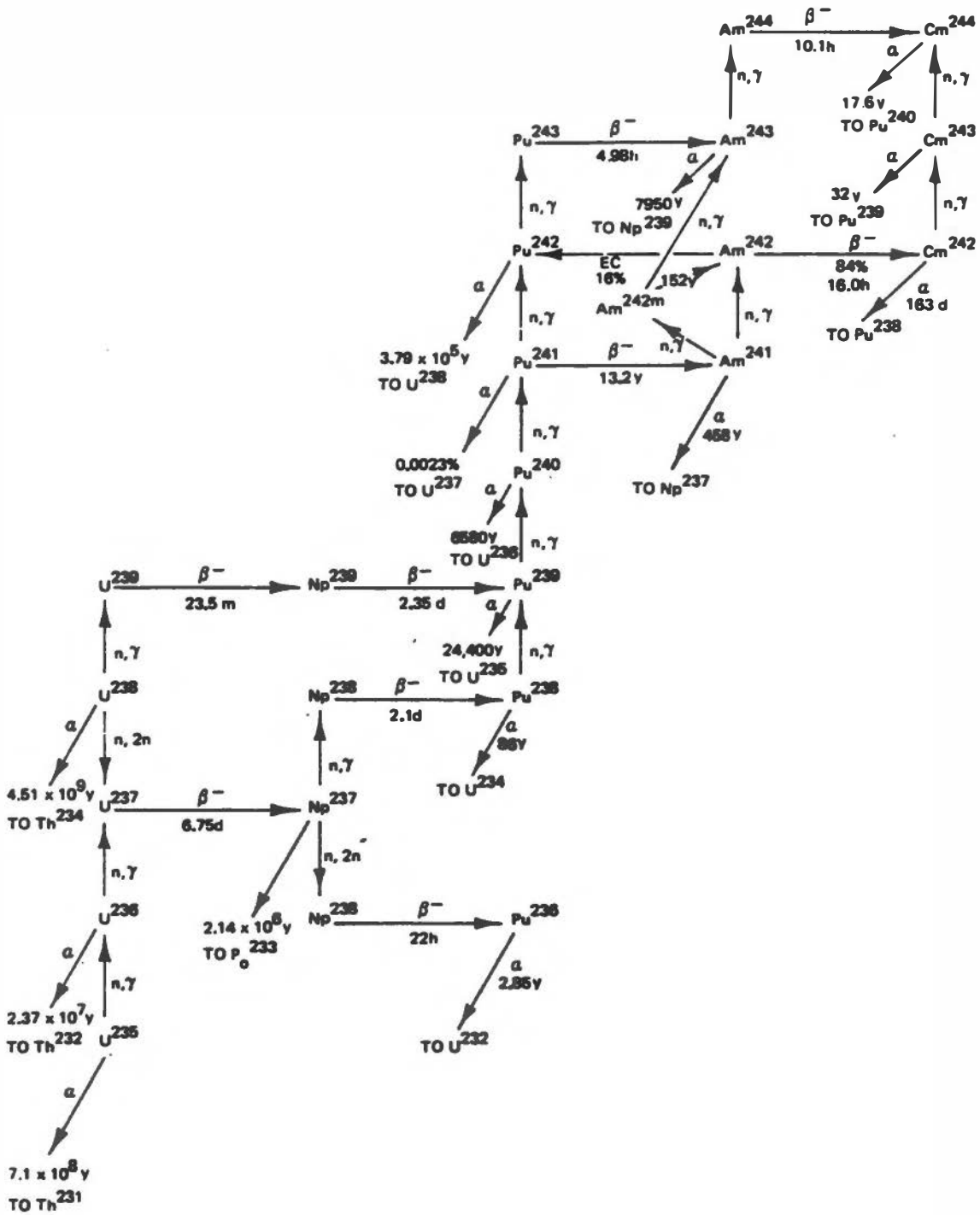

Figure 2-3. Actinide Chains in Uranium-Plutonium Fuel (Reproduced with Permission, from Ann. Rev. Nucl. Sci., Ref. 7)

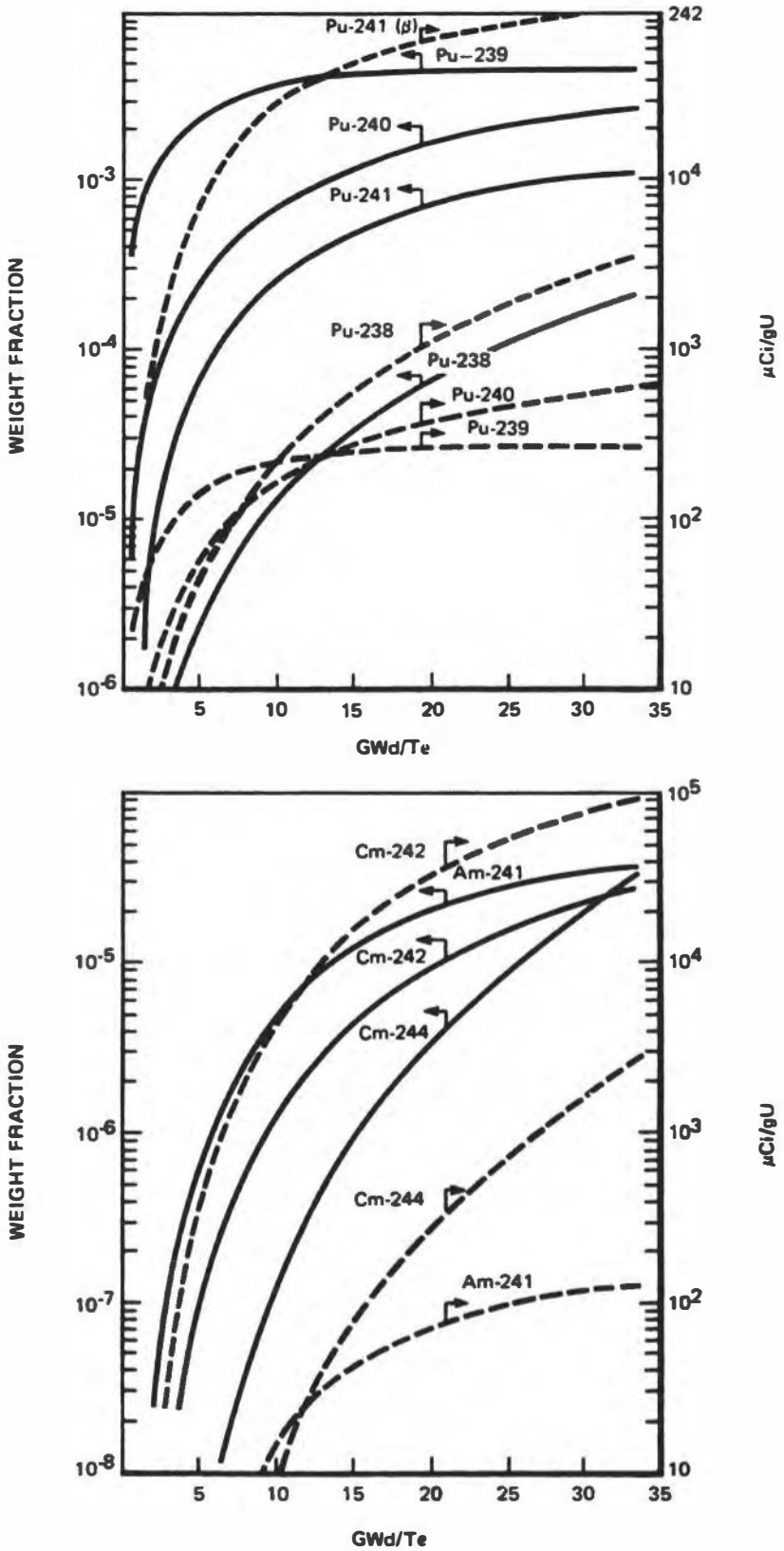

Figure 2-4. Variation of Transuranic Isotope Content with Fuel Exposure in UO_2 Fuel

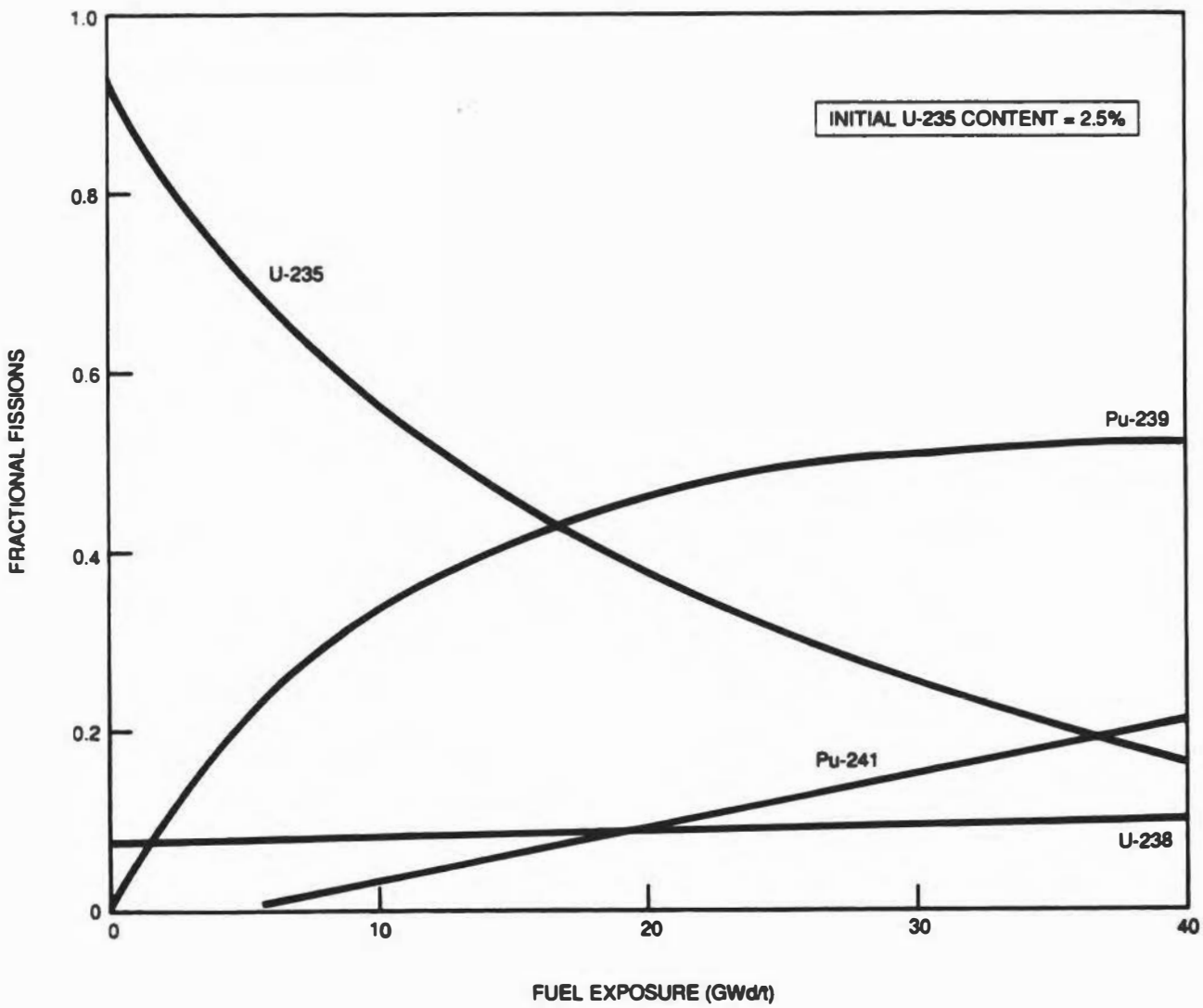

Figure 2-5. Variation of Fractional Fissions from Fissionable Nuclides in UO_2 Fuel (2.5% U-235) with Fuel Exposure

2.4 ACTIVATION OF WATER AND IMPURITIES IN REACTOR COOLANT

Water and impurities in water are activated only when the water flows through the core region; the residence time in the flux zone is only a few seconds for each path. The relevant nuclear data for major activation products in the BWR coolant are given in Table 2-3. Among these nuclides, N-16 ($t_{1/2}$ = 7.1 s) is probably the most important nuclide because of its high-energy gamma ray (6.1 MeV) where the radiological effect is concerned. The chemistry and transport behavior of N-16 and other semi-volatile species in the BWR primary system will be discussed later (Subsection 5.4).

The production rates of radioactive species in water depend on the concentrations of their parent targets in water. The equilibrium concentration of a radioactive nuclide can be estimated as follows:

$$\frac{dN}{dt} = N^{o}P\phi\sigma - (\lambda + \beta_c)N \qquad (2\text{-}3)$$

where

N^o = number of parent target atoms

N = number of activation product atoms

n = parent target input rate, atom/s

λ = decay constant, s^{-1}

β_c = reactor water cleanup time constant, s^{-1}.

$$= \frac{\text{reactor water cleanup system flow rate (kg / s)}}{\text{reactor water mass (kg)}}$$

P = reactor power and core geometric factor

ϕ = effective neutron flux for target activation

σ = effective activation cross section

Table 2-3

MAJOR WATER AND IMPURITY ACTIVATION PRODUCTS IN REACTOR COOLANT

Nuclide	Half-Life	Reaction	Natural Isotopic Abundance (%)	Average Activation Cross Section[a]
^{3}H	12.3 y	$^{2}H(n,\alpha)^{3}H$	0.015	0.53 mb(T)
		$^{6}Li(n,\alpha)^{3}H$	7.5	942 b (F)
		$^{10}B(n,2\alpha)^{3}H$	-	5.6 mb (F)
		$^{10}B(n,\alpha)^{7}Li$	-	3838 b (F)
		$^{235}U(n,f)^{3}H$	-	0.01% fy
^{14}C	5730 y	$^{13}C(n,\gamma)^{14}C$	1.11	0.9 mb (T)[b]
		$^{14}N(n,p)^{14}C$	99.63	1.8 b (F)[b]
		$^{17}O(n,\alpha)^{14}C$	0.038	240 mb (F)[b]
^{15}C	2.45 s	$^{18}O(n,\alpha)^{15}C$	0.204	1.5 mb (F)
^{13}N	9.97 m	$^{16}O(p,\alpha)^{13}N$	99.76	50 mb (P)[c]
^{16}N	7.13 s	$^{16}O(n,p)^{16}N$	99.76	19 mb (F)
^{19}O	26.9 s	$^{18}O(n,\gamma)^{19}O$	0.204	160 mb (T)
^{18}F	1.83 h	$^{18}O(p,n)^{18}F$	0.204	300 mb (P)
^{24}Na	14.96 h	$^{23}Na(n,\gamma)^{24}N$	100	528 mb (T)
^{32}P	14.28 d	$^{31}P(n,\gamma)^{32}P$	100	190 mb (T)
		$^{32}S(n,p)^{32}P$	95	69 mb (F)
^{38}Cl	37.2 m	$^{37}Cl(n,\gamma)^{38}Cl$	24.23	430 mb (T)

(a) Data for 20°C; T, F, and P in the parentheses indicate thermal and fast neutron and proton reactions, respectively; the activation cross-section data are adopted from References 1 and 2.

(b) P. J. Magno, et al, Proc. 13th AEC Air Cleaning Conf., P1047 (1972).

(c) M. S. Singh and L. Ruby, Nucl. Tech., 17, 104 (1973).

At equilibrium condition during normal operation,

$$\frac{dN}{dt} = 0, \text{ and}$$

$$\frac{N_{eq}}{N^{o}_{eq}} = \frac{P\phi\sigma}{\lambda + \beta_c}, \quad \text{or} \quad N_{eq} = N^{o}_{eq}\left(\frac{P\phi\sigma}{\lambda + \beta_c}\right) \tag{2-4}$$

Thus, by measuring N_{eq} and N^{o}_{eq}, P can be calculated.

For the parent nuclide,

$$\frac{dN^{o}}{dt} = n - \beta_c N^{o} \tag{2-5}$$

At equilibrium,

$$\frac{dN^{o}}{dt} = 0, \quad N^{o}_{eq} = \frac{n}{\beta_c} \tag{2-6}$$

Thus, the total active impurity at equilibrium condition can be estimated by:

$$N_{eq} = \frac{nP\phi\sigma}{\beta_c(\lambda + \beta_c)} \tag{2-7}$$

The core average neutron flux in a light water reactor may be approximately related to the power density of the core. For a BWR with the core power density at 50 W/cm^3, the average fluxes for thermal, epithermal and fast neutrons in the core region are estimated at 1.35×10^{14}, 6×10^{13} and 3.9×10^{13} $n/cm^2/s$, respectively.

2.5 ACTIVATION OF CORROSION PRODUCTS

The metallic impurities are released into the coolant from the struc-tural materials in the feedwater and primary systems as a result of corrosion/erosion. When they are deposited on the fuel surfaces, they become activated by the neutron flux in the core. Some activation products are also produced in the structural materials in the core. The pertinent nuclear data for the major activated corrosion products are given in Table 2-4. The activity (A) produced in the structural material in the core region at time to can be calculated by

$$A = \lambda N = \phi N^{o} \sigma \left(1 - e^{-\lambda t}\right) \tag{2-8}$$

All symbols have the meanings given previously.

The calculated specific activities as a function of irradiation time at a constant neutron flux for the major activation products generally found in lightwater reactors are shown in Figure 2-6.

The calculation of activity production in the fuel deposit is rather complex; it involves variations in corrosion product deposition rate, neutron flux, release of activities, etc. The details of model calculations are discussed and compared with the experimental data in Section 4.

Table 2-4

MAJOR ACTIVATED CORROSION PRODUCTS IN LIGHT WATER REACTORS

Nuclide	Half-Life	Formation Reaction	Nature Isotopic Abundance (%)	Activation Cross Section (Barns)[a]		
				Thermal	Epithermal	Fast
^{51}Cr	27.7 d	$^{50}Cr(n,\gamma)^{51}Cr$	4.35	16.0	0.68	
^{54}Mn	312.2 d	$^{54}Fe(n,p)^{54}Mn$	5.8			0.11
^{56}Mn	2.58 h	$^{55}Mn(n,\gamma)^{56}Mn$	100	13.3	1.13	
^{55}Fe	2.73 y	$^{54}Fe(n,\gamma)^{55}Fe$	5.8	2.5	0.1	
^{59}Fe	44.51 d	$^{58}Fe(n,\gamma)^{59}Fe$	0.3	1.14	0.1	
^{58}Co	70.88 d	$^{58}Ni(n,p)^{58}Co$[b]	68.3			0.146
^{60}Co	5.27 y	$^{59}Co(n,\gamma)^{60}Co$	100	37.5	6.05	
^{63}Ni	100 y	$^{62}Ni(n,\gamma)^{63}Ni$	3.6	14.6	0.77	
^{65}Ni	2.52 h	$^{64}Ni(n,\gamma)^{65}Ni$	0.9	1.50	0.07	
^{64}Cu	12.7 h	$^{63}Cu(n,\gamma)^{64}Cu$	69.2	4.4	0.40	
^{65}Zn	243.8 d	$^{64}Zn(n,\gamma)^{65}Zn$	48.6	0.82	0.13	
^{76}As	26.3 h	$^{75}As(n,\gamma)^{76}As$	100	4.4	5.08	
^{95}Zr	64.02 d	$^{94}Zr(n,\gamma)^{95}Zr$	17.4	0.075	0.031	
^{110m}Ag	249.8 d	$^{109}Ag(n,\gamma)^{110m}Ag$	48.17	4.7		
^{113}Sn	115.1 d	$^{112}Sn(n,\gamma)^{113}Sn$	1.01	0.71	2.2	
^{124}Sb	60.2 d	$^{123}Sb(n,\gamma)^{124}Sb$	42.7	4.0	9.7	
^{181}Hf	42.4 d	$^{180}Hf(n,\gamma)^{181}Hf$	35.2	12.6	2.26	
^{182}Ta	114.43 d	$^{181}Ta(n,\gamma)^{182}Ta$	100	22.0	56.4	
^{187}W	23.9 h	$^{186}W(n,\gamma)^{187}W$	28.6	37.2	33.9	

[a]Data for 20°C.
[b]Burnup cross section, σ_b, for Co-58 is 1.9×10^{-21} cm^2.

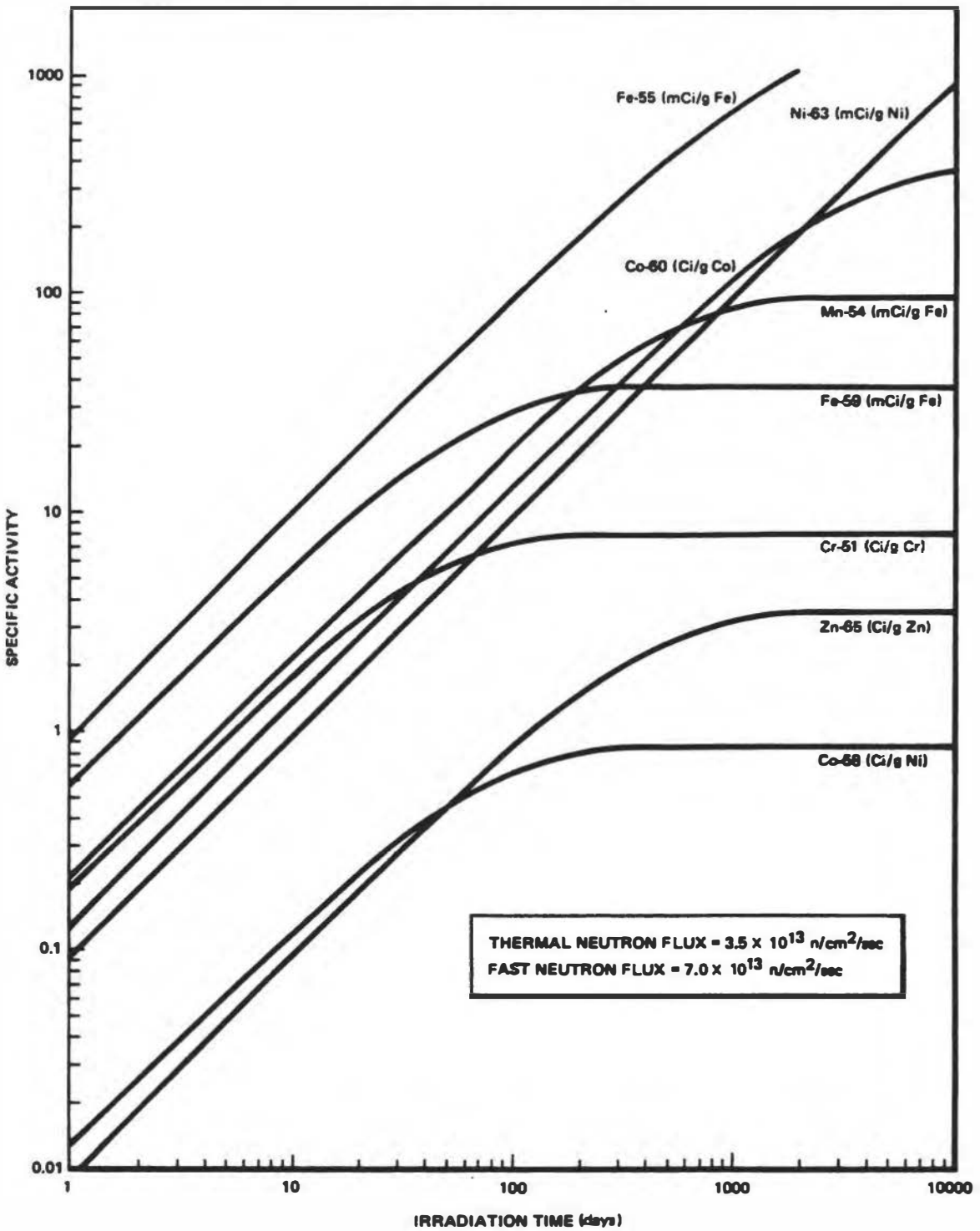

Figure 2-6. Specific Activity of Major Corrosion Products as a Function of Irradiation Time with Neutron Flux

2.6 REFERENCES

(1) C.M. Lederer et al., "Table of Isotopes," 7th ed., John Wiley & Sons, Inc., New York (1978).

(2) "Handbook on Nuclear Activation Cross Sections," Technical Report Series No. 156, IAEA, Vienna (1974).

(3) A.C. Wahl, "Mass and Charge Distribution in Low-Energy Fission," Proc. 1st International Atomic Energy Symposium on Physics and Chemistry of Fission, Vienna, Austria (IAEA, 1965).

(4) B. Ehrenberg and S. Amiel, Phys., Rev. C, 6, p. 618 (1972).

(5) A.C. Wahl et al., Proc. 2nd International Atomic Energy Symposium on Physics and Chemistry of Fission, Vienna, Austria, p. 813 (IAEA, 1969).

(6) B.F. Rider, "Compilation of Fission Product Yields," Vallecitos Nuclear Center, 1981 (NEDO-12154-3C), ENDF-322 (October 1981).

(7) T.H. Pigford, "Environmental Aspects of Nuclear Energy Production," Am. Rev. Nucl. Sci., Vol. 24, 1974, p. 515.

(8) H.S. Bailey, et al., Nucl. Tech., 17, 1973, p. 217.

(9) H. Umezawa, et al., J. Nucl. Sci. Tech., 10, 1973, p. 489.

(10) W.B. Wilson, et al., Nucl. Safety, 29, 2, 177 (1988).

2.7 BIBLIOGRAPHY

G. Friedlander, J.W. Kennedy, E.S. Macias and J.M. Miller, "Nuclear and Radiochemistry," 3rd ed., John Wiley & Sons, Inc., New York (1981).

D. C. Layman and G. Thorton, "Remote Handling of Mobile Nuclear Systems," U.S. AEC, January 1966 (TID-21719).

3. FISSION PRODUCTS

3.1 FISSION PRODUCT RELEASE CALCULATION - A THEORETICAL MODEL

The main purpose of measuring the fission product release from the reactor is to monitor the fuel integrity, as well as the activity release as part of radiological surveillance in the power plant. The fission products from the defective fuel are released into the primary coolant, and some volatile species are subsequently released through the offgas system. The magnitude and composition of the released fission products depend on the size of the defect and the number of defective fuel rods in the core. Some fission products are also released as a result of fission recoil from tramp uranium or natural uranium contaminate in the Zircaloy fuel cladding.

In practice, empirical methods are used to characterize the fission product release behavior. However, it is worthwhile describing a theoretical model for comparison with the empirical models which will be discussed in the subsequent sections.

3.1.1 Release of Fission Products into Fuel Gap

It has been generally accepted that diffusion is the primary release mechanism for volatile fission products from oxide fuel pellets. Based on the equivalent sphere model originally proposed by Booth,[1] solutions for the appropriate diffusion equations for a sphere in which production and decay of the fission product are taken into account have been obtained by Beck.[2]

For reactor operating times that are long with respect to the half-life of a radioactive fission product, the fraction of non-decayed atoms outside the sphere (G) approaches the equilibrium value:

$$G = 3\left[\left(1/\sqrt{\mu}\right)\coth\left(\sqrt{\mu}\right) - 1/\mu\right] \qquad (3\text{-}1)$$

where $G = \frac{\lambda N}{B}$ = the fraction of non-decayed atoms in the fuel gap at equilibrium

B = fission product production rate inside the sphere, atom/s

N = the accumulation of undecayed atoms in the fuel gap

λ = decay constant, s^{-1}

$\mu = \lambda a^2/D = \lambda/D'$

a = equivalent-sphere radius, cm

D = diffusion coefficient, cm^2/cm

$D' = D_o/a^2 \exp(-Q/RT) \times [100(MWd/t)/28000]$

D_o = limiting diffusion coefficient, cm^2/s

Q = activation energy for diffusion, cal/g-mole

R = gas constant, (cal/deg) • (g-mole)

T = absolute temperature, °K

MWd/t = fuel burnup

For a small G (≈5%)* , i.e., μ>100,

$$G = 3\left(\frac{D'}{\lambda}\right)^{1/2} \tag{3-2}$$

or

$$\frac{\lambda_i N_i}{B_i} = 3\left(\frac{D'}{\lambda_i}\right)^{1/2} \tag{3-2A}$$

where the subscript i indicates nuclide i. At equilibrium, the release rate of nuclide i into the fuel gap is:

$$R_i^o = \lambda_i N_i = 3B_i\left(\frac{D'}{\lambda_i}\right)^{1/2} \tag{3-3}$$

*For iodine and noble gas isotopes, an average of <5% was adopted in the Rasmussen report, WASH-1400 (NUREG-75/014). A smaller value has been reported in the most recent experimental measurement.[3,4]

For convenience,

$$R_i^o = F(p)Y_i\lambda_i^{-1/2} \qquad (3\text{-}4)$$

where $F(p)Y_i = 3B_iD^{-1/2}$, atom/s

$F(p)$ = fission rate as a function of power and diffusion coefficient, fission/s.

Y_i = fission yield of nuclide i. Normally, thermal neutron fission of U-235 is used in calculation; however, in the case with high burnup fuel, contribution from Pu-239 should be considered.

3.1.2 Release of Fission Product from Defective Fuel into Reactor Coolant

The one compartment model of volatile fission product released into the reactor coolant from defective fuel cladding is schematically described in Figure 3-1, and the release rate is derived as follows:

$$\frac{dN_i}{dt} = R_i^o - \lambda_iN_i - \nu_iN_i - \phi\sigma_iN_i \qquad (3\text{-}5)$$

where N_i = inventory in fuel gap, atom

R_i = $F(p)Y_i\lambda i$ (Eq. 3-4)

ν_i = escape time constant, s^{-1}

$\phi\sigma_i$ = burnup rate, s^{-1}

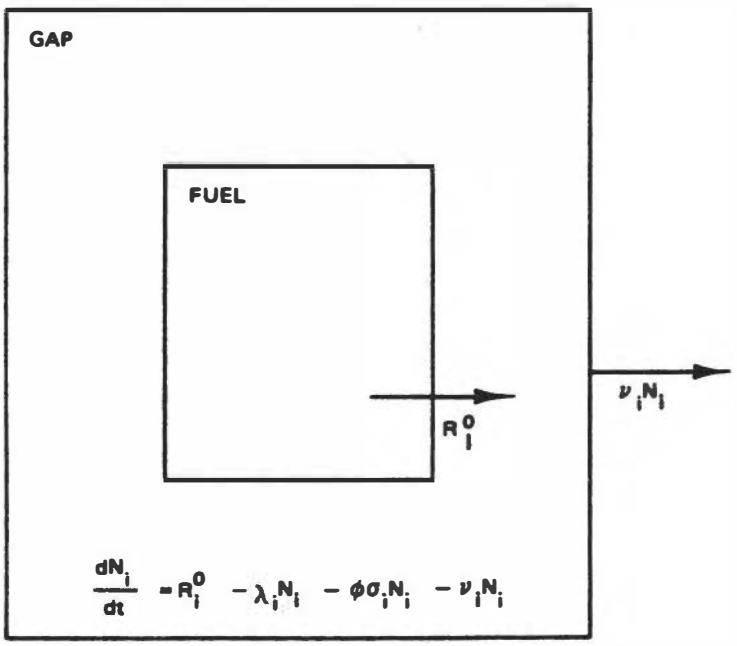

Figure 3-1. Schematic of One Compartment Model

Upon integration

$$N_i = \frac{F(p)Y_i\lambda^{-1/2}}{\lambda_i + \nu_i + \phi\sigma_i}\left[1 - e^{-(\lambda_i + Y_i + \phi\sigma_i)t}\right]$$

when $t \rightarrow \infty$,

$$N_i = F(p)Y_i \frac{\lambda_i^{-1/2}}{\lambda_i + \nu_i + \phi\sigma_i} \tag{3-6}$$

The release rate in atom/s can be calculated by:

$$N_i\nu_i = F(p)Y_i \frac{\nu_i\lambda_i^{-1/2}}{\lambda_i + \nu_i + \phi\sigma_i} \tag{3-7}$$

and the activity release rate in Bq/s is

$$A_i = N_i \nu_i \lambda_i = F(p) Y_i \frac{\nu_i \lambda_i^{-1/2}}{\lambda_i + \nu_i + \phi\sigma_i} \qquad (3\text{-}8)$$

The burnup rate, $\phi\sigma$, is generally very small except for Xe-135; the value of $\phi\sigma$ for Xe-135 is 8.9×10^{-5} s^{-1}, which is larger than the decay constant of Xe-135, 2.1×10^{-5} s^{-1}. The value of the escape time constant, ν, depends on the size of defect and communication in the fuel gap*; neither are very well defined. Thus, if

$$\nu \gg \lambda, \quad A_i = F(p) Y_i \lambda_i^{1/2} \qquad (3\text{-}9)$$

or, if $$\nu \ll \lambda, \quad A_i = F(p) Y_i \nu_i \lambda_i^{-1/2} \qquad (3\text{-}10)$$

It must be noted that if there is more than one defective fuel rod, and the defect sizes are different, then this model prediction of fission product release may not be applicable.

3.1.3 Release of Fission Products from Fuel Contaminant

Even though the reactor core may contain no defective fuel, natural uranium contamination of core construction materials and Zircaloy cladding, as well as enriched uranium contamination of the external cladding surfaces, could be the source of fission products in the coolant during power operations. The recoil range of a fission product is approximately 10 microns; therefore, only the fissions that occur within ≈10 microns of the outer surface of the Zircaloy cladding can introduce fission products into the coolant. It is safe to assume that half of the recoils from the fissioning nuclei will escape to the coolant and the other half will be embedded in the host material. Thus, the activity release into the coolant may be predicted by:

$$A_i' = \frac{1}{2} F(p)' Y_i \lambda_i \qquad (3\text{-}11)$$

---

* Typical values of ν for volatile fission products are in the range of 10^{-9} to 10^{-7} s^{-1}.

where A_i' = activity release rate from fuel contaminant, Bq/s.

$F(p)'$ = fission rate, as a function of power, of fissionable material ("tramp" fuel) in contaminants, fission/s.

3.2 CHARACTERIZATION OF FISSION PRODUCT RELEASE PATTERNS IN BWR

3.2.1 Empirical Methods

In the GE source term document,[5] the release rate A_i is defined by the empirical relation

$$A_i = KY_i\lambda_i^{1-b} \tag{3-12}$$

or

$$R_i = \frac{A_i}{Y_i\lambda_i} = K\lambda_i^{-b} \tag{3-13}$$

where A_i = release rate in Bq/sec (or μCi/s)

R_i = release rate in fission/s

K = a dimensional constant establishing the level of release.

b = a dimensionless constant establishing the relative amount of each nuclide in a mixture of similar chemical group (i.e., noble gas or iodine isotopes).

Y_i = fission yield of species i

λ_i = decay constant of species i, in s^{-1}.

By plotting log (R_i) versus log (λ_i) for noble gases or iodine isotopes, a theoretical straight line can be obtained with a characteristic slope of b. An example of such a plot is shown in Figure 3-2.

It should be noted that: (1) the noble gas release rate is always equal to or greater than the iodine release rate for the isotopes of comparable half-life, (2) the "b" value for noble gas activities is always equal to or greater than the "b" value for iodine activities, and (3) when $b \approx 0$, the noble gas and iodine activities fall into a same horizontal line.

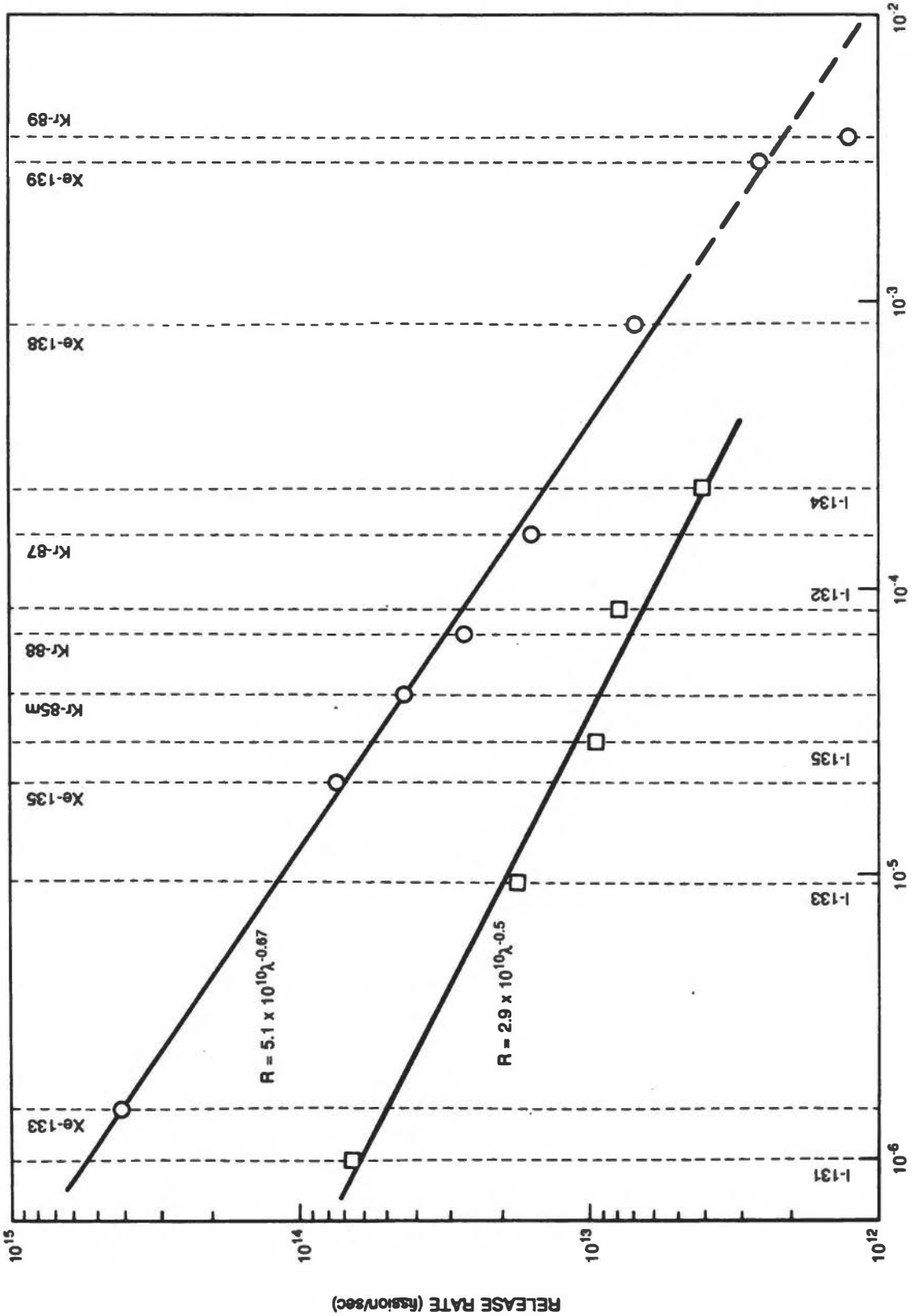

Figure 3-2. Typical Example of Log (Release Rate) vs. Log (Decay Constant) for Noble Gases and Iodine Isotopes

It is convenient to characterize the release pattern or the composition of fission product mixture in three types as follows:

Release Pattern	Value of b	Release rate, R_i	Characteristics of fuel defect and activity release
Recoil	0	K	No defect; activity release from tramp fuel; proportional to reactor power.
Equilibrium	1.0	$K\lambda_i^{-1}$	Pin hole defect; no consistent correlation of release rate with reactor power.
Diffusion	0.5	$K\lambda_i^{-0.5}$	Split cladding defect; activity release changes exponentially with power.

The source term equations, Equation 3-12 or 3-13 can be directly related to the model calculations given in Section 3-1. When b = 0, the "recoil" release is identified with Equation 3-11,

$$R_i \text{ (recoil)} = K_r, \text{ and}$$

$$K_r = 1/2\ F(p)', \tag{3-14}$$

where K_r is the recoil release rate.

When $b \neq 0$, the source term equation is related to Equation 3-8,

$$A_i = F(p) Y_i \lambda_i^{1/2} \left(\frac{\nu_i}{\lambda_i + \nu_i + \phi\sigma_i} \right) = K\, Y_i \lambda_i^{1-b} \tag{3-15}$$

and

$$R_i = \frac{A_i}{Y_i \lambda_i} F(p) \lambda_i^{-1/2} \left(\frac{\nu_i}{\lambda_i + \nu_i + \phi\sigma_i} \right) = K\lambda_i^{-b} \tag{3-16}$$

Since $\phi\sigma_i$ is generally very small and negligible, and

if $\nu >> \lambda$, $b = 0.5$ and $K_d = F(p)$

if $\nu << \lambda$, $b = 1.5$ and $K_e = F(p)\nu_i$,

where K_d and K_e are "diffusion" and "equilibrium" release rate constants, respectively. It should be noted that the equilibrium release pattern is characterized by b = 1, but the theoretical maximum value of b is 1.5. The value of b>1 has been frequently observed experimentally. It is also important to note that the release rate is proportional to the escape time constant, ν_i, in the equilibrium case.

3.2.2 Release of Noble Gas Activities

The total activity in the offgas is a direct measure of the total noble gas fission product mixture released from the reactor core, and the analysis of radionuclide distribution of the noble gas fission product mixture is used to determine the specific mechanisms of the activity release. The release rate A_i for each isotope is calculated from the measured concentration C_i in the offgas and the radiolytic gas flow rate, F_{gas},

$$A_i = C_i F_{gas}$$

The release rates of the six major noble gases (Xe-138, Kr-87, Kr-88, Kr-85m, Xe-135, and Xe-133) have been commonly used to characterize the type and magnitude of fuel failures. The activity release rates can be approximately expressed by Equation 3-12 or 3-13. Since the actual distribution observed may be composed of a mixture of releases characterized as "recoil" (b=0), "equilibrium" (b=1), and "diffusion" (b=0.5), Equation 3-13 can be written as

$$R_i = \frac{A_i}{Y_i \lambda_i} K \lambda_i^{-b} = K_r + K_e \lambda_i^{-1} + K_d \lambda_i^{-0.5} \qquad (3\text{-}17)$$

There may be no definite "equilibrium" or "diffusion" type release in the actual case, and for the practical purpose, the release mechanisms may be resolved into two components, "recoil" and a mixture of non-recoil release from failed fuel, so that

$$R_i = K_r + K_f \lambda_i^{-b'} \quad (3\text{-}18)$$

where K_r is the recoil level of release, K_f is a constant establishing the level of release from failed fuel, and b′ is a dimensionless constant establishing the relative amount of each nuclide in the mixture of noble gas activities released from failed fuel.

Fuel performance, as defined in a narrow sense by fuel rod reliability, is typically monitored in a BWR by the measurement of the "sum of six" major noble gas activities at the steam jet air ejector (SJAE). The recoil fraction of the total offgas activity should be subtracted from the total release rate to determine the release rate from failed fuel. The recoil level of fission product release may be estimated by a number of techniques using the noble gas activity data or the soluble fission product activities measured in reactor water. These techniques are briefly described and compared below:

	Technique	Comment
(1)	Extrapolation of 6 major noble gas data to the interception with $\lambda = 10^{-2}$ s^{-1} vertical line (see Figure 3-2).	Very rough estimate.
(2)	Mathematically resolving Eq. (3-17) into 3 components using 6 major noble gas data.	Popular practice with computer programming; not accurate.
(3)	Determination from shorter-lived noble gas activities, Kr-89 (3.16 m) Kr-90 (32 s), Xe-137 (3.8 m), Xe-139 (40 s).	Difficulty in sampling and decay correction.
(4)	Determination from soluble cationic fission products, Rb-89, Sr-91, Sr-92, Cs-138, Cs-139, Ba-139, Ba-140, Np-239 (see Section 3.2.4).	Easy to measure for some isotopes, reliable.
(5)	Determination from iodine activities, recoil level ≈ 1/2 of I-134 release rate (see Section 3.2.3).	Easy to measure, reliable.

By knowing the recoil level K_r, the $\sum_{i}^{6}(A_i)_{recoil}$ can be easily estimated from:

$$\sum_{i}^{6}(A_i)_{recoil} = K_r \sum_{i}^{6}(Y_i\lambda_i)_{recoil} \qquad (3\text{-}19)$$

If the fission yields from the thermal neutron fission of U-235 are used in calculation, more typical of new low exposure core,

$$\sum_{i}^{6}(A_i)_{recoil} = 1.6 \times 10^{-9} K_r \qquad (\text{in } \mu Ci/s)^*$$

If the fission yields are taken from 50% U-235 and 50% Pu-239, more typical of an equilibrium core,

$$\sum_{i}^{6}(A_i)_{recoil} = 1.4 \times 10^{-9} K_r \qquad (\text{in } \mu Ci/s)^*$$

The non-recoil fuel activity release rate can then be calculated by:

$$\sum_{i}^{6}(A_i)_{fuel} = \sum_{i}^{6}(A_i)_{total} - \sum_{i}^{6}(A_i)_{recoil} \qquad (3\text{-}20)$$

Alternatively, it is convenient to use the release rate R_i (in fission/s) to subtract the recoil fraction, since the value of R_i for recoil is identical for all fission products ($R_i = K_r$). The non-recoil fraction for each isotope is then converted to the activity release rate A_i (in $\mu Ci/s$), and the total non-recoil release rate can be calculated.

Based on experience, the offgas activity release rate (sum of six) per one leaking fuel rod measured at SJAE ranges from a few hundred to a few thousand $\mu Ci/s$ with the average at approximately 2000 $\mu Ci/s$[6].

---

* 1 $\mu Ci/s = 3.7 \times 10^4$ Bq/s.

3.2.3 Release of Iodine Activities

The release rate of iodine activity, A_i, can be calculated from the activity concentration in reactor water C_i by the following equations:

$$\frac{dC_i}{dt} = \frac{A_i + A_f}{W} - (\lambda_i + \beta_c + \beta_s)C_i \qquad (3\text{-}21)$$

where A_i = release rate to coolant from fuel, Bq/s or μCi/s.

A_f = return of the same activity species from the feedwater, Bq/s or μCi/s. (Except for the forward pumping plants, A_f is generally very small compared with A_i.)

W = reactor water mass, kg.

λ_i = decay constant of species i, s^{-1}.

β_c = reactor water cleanup (RWCU) system removal time constant, sec^{-1}, which is defined as $\beta_c = f/W$, assuming _ 100% efficient.

f = RWCU flow rate, kg/s

β_s = steam removal time constant, s^{-1}, which is defined as $\beta_s = \varepsilon F/W$

ε = iodine carryover, defined as the ratio of

$$\frac{\text{the concentration of species i in condensate}}{\text{the concentration of species i in reactor water}}$$

F = steam flow rate, kg/s

Upon integration,

$$C_i = \frac{A_i + A_f}{W(\lambda_i + \beta_c + \beta_s)}\left[1 - e^{-(\lambda_i + \beta_c + \beta_s)t}\right] \qquad (3\text{-}22)$$

when t -> ∞, and the equilibrium concentration is established by the release rate A_i if the activity returned from the feedwater is negligible, (i.e., $A_i >> A_f$):

$$C_i = \frac{A_i}{W(\lambda_i + \beta_c + \beta_s)} \tag{3-23}$$

$$A_i = C_i W(\lambda_i + \beta_c + \beta_s) \tag{3-24}$$

The characteristics of the iodine activity release then can be evaluated by using Equations 3-17 and 3-18 again.

Similar to the noble gas activities, the mixture of iodine activities can be characterized by the b value and also can be separated into "recoil", and fuel release ("equilibrium" and "diffusion") components. It has been experimentally determined that the "recoil" level of release may be established from the iodine activities more easily than from the noble gas activities. The empirical method is such that when the measured fission/s value for I-134 is greater or equal to that for I-132, the I-134 fission/s value is approximately equal to the true recoil level.* On the other hand, when I-134 < I-132,** the recoil level is approximately equal to one-half the I-134 fission/s value. This empirical method is more reliable when the reactor is operated at near 100% power.

3.2.4 Calculation of Nonvolatile Soluble Fission Product Release Rate

The isotopes of rubidium, cesium, strontium, barium, technetium, and molybdenum are included in this group. It is believed that these nuclides occur in the coolant primarily as the result of fission fragment recoil or as a result of the decay of short-lived noble gas precursors in water. The release rate (μCi/s) for the individual nuclides in this group can be calculated from the concentration of the activities in the reactor water by Equation 3-25:

$$A_i = C_i W(\lambda_i + \beta_c) \tag{3-25}$$

---

* The "true" recoil level is established from the cationic fission products in reactor water and the shorter-lived noble gas activities.

** The normal release rates (in fission/s) for iodine isotopes from non-recoil source are generally higher for the longer-lived isotopes. However, I-134>I-132 has been observed when the recoil contribution is relatively high.

The release rate can be related to the decay constant and the fission yield by the equation of a recoil mechanism

$$A_i = KY_i'\lambda_i \tag{3-26}$$

where Y′ is the fission yield modified to include the release produced by the decay of the noble gas precursor,

$$Y' = Y_{ind} + \frac{\lambda_g Y_g}{\lambda_g + \alpha} \tag{3-27}$$

where Y_{ind} = independent fission yield of i^{th} nuclide

Y_g = cumulative yield of the precursor gas

λ_g = decay constant of the precursor gas, and

α = the removal rate constant of the gas precursor from the reactor coolant, s^{-1}. The value of α is approximately 0.2 s^{-1} estimated from the ratio of steam flow (by volume) to the steam volume in the reactor pressure vessel.

The measurement of activities in this group can be used to establish a recoil level of activity release. The value of R_i for each isotope should be independent of λ_i and nearly constant. Among the activities in this group, Rb-89, Sr-91, Sr-92, Cs-138, Cs-139, Ba-139, Ba-140 and Np-239 (activation product of U-238) are easier to measure and generally give more consistent results.

3.2.5 Estimation of the Exposure for Defective Fuel Rods

In theory, the measurements of Cs-134 and Cs-137 activities in the reactor coolant may be used as an indicator of the exposure (burnup) of a failed fuel rod from which the fission products are released. Cs-137 (30 y) is produced directly from fission, and Cs-134 (2.1 y) is produced by neutron activation on Cs-133, a stable fission product. Since the Cs-134 activity increases (proportionally to the square of the fuel exposure) faster than Cs-137 in the fuel as the fuel exposure increases, the ratio of Cs-134 to Cs-137 increases as the fuel exposure increases, as shown in Figure 3-3. It should be pointed out that if Cs-134 and

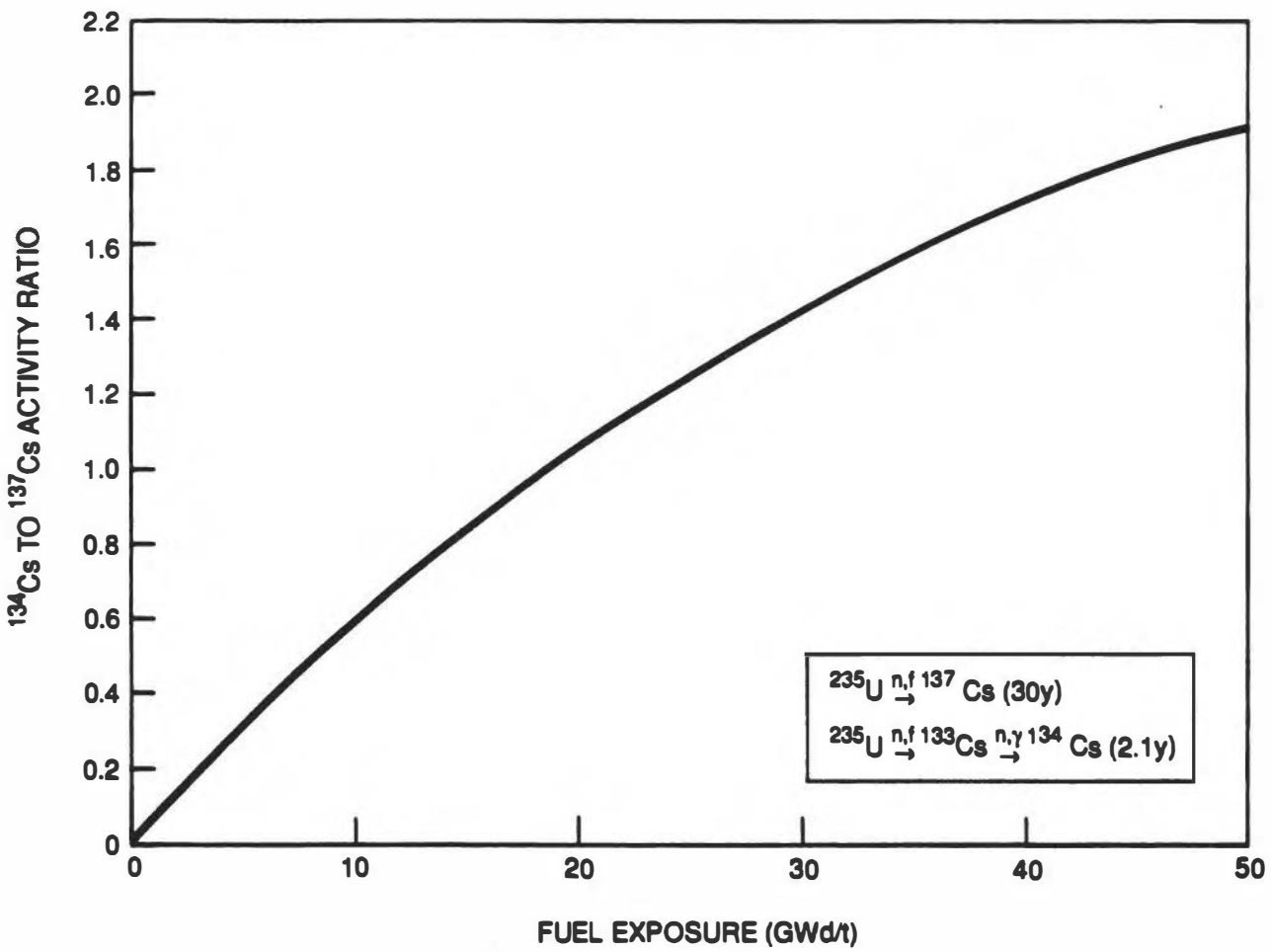

Figure 3-3. Calculated Cs-134 to Cs-137 Ratio in the fuel as a Function of Fuel Burnup

Cs-137 are released from different defective fuel rods with different exposures and different sizes of defects, it would be more difficult to accurately estimate the exposures of defective fuel.

3.2.6 BWR Radioactivity Source Terms* and Fission Product Activities in the Primary Coolant

Based on previous experience, the BWR activity release source term was established in 1971 for design purposes.(5) The activity release rate is represented by the empirical relationship given in Equation 3-28,

$$A_i(\mu Ci/s) = KY_i\lambda_i^{1-b} \tag{3-28}$$

where b=0.6 is adopted for the noble gas release. By setting the total noble gas activity release rate at 10^5 μCi/s measured at t=30 minutes (delay time), the release rate for each noble gas isotope can be calculated from

$$A_i(\text{gas}) = 2.6\times10^7\, Y_i\lambda_i^{0.4}\, e^{-\lambda_i t} \tag{3-29}$$

Similarly, the 1971 source term for iodine activities defines b = 0.5 and 700 μCi/s I-131 leakage rate. The release rate for all halogen isotopes can be calculated by

$$A_i(\text{iodine}) = 2.4\times10^7\, Y_i\lambda_i^{0.5}\, e^{-\lambda_i t} \tag{3-30}$$

The calculated release rates using U-235 fission yields for the major noble gas and halogen activities are given in Table 3-1.

The steady state concentrations of fission product activities in water and steam systems vary from reactor to reactor, sometimes by two to three orders of magnitude, depending on the size of the fuel defect, the number of defective fuel rods in the core, and the capacity of reactor water cleanup system. In the case of iodine activities, the concentration also depends on the level of steam carryover. Selected American Nuclear Society standard radionuclide concentrations in principal fluid streams of the light water reactors are given in Table 3-2.(7)

---

* The source term is loosely defined as the most likely maximum release of radioactivity in a reactor.

Table 3-1

STANDARD PLANT DESIGN BASIS NOBLE GAS AND HALOGEN LEAKAGE RATES

Radioisotope	Half-Life	Leakage Rate at t = 0 (μCi/s)	Leakage Rate at t = 30 m (μCi/s)
Kr-83m	1.86 h	3.4×10^3	2.9×10^3
Kr-85m	4.48 h	6.1×10^3	5.6×10^3
Kr-85	10.73 y	10 to 20*	10 to 20*
Kr-87	1.37 h	2.0×10^4	1.5×10^4
Kr-88	2.84 h	2.0×10^4	1.8×10^4
Kr-89	3.15 m	1.3×10^5	1.8×10^2
Kr-90	32.3 s	2.8×10^5	–
Kr-91	8.6 s	3.3×10^5	–
Xe-133m	2.19 d	2.9×10^2	2.8×10^2
Xe-133	5.24 d	8.2×10^3	8.2×10^3
Xe-135m	15.3 m	2.6×10^4	6.9×10^3
Xe-135	9.1 h	2.2×10^4	2.2×10^4
Xe-137	3.82 m	1.5×10^5	6.7×10^2
Xe-138	14.1 m	8.9×10^4	2.1×10^4
Xe-139	39.7 s	2.8×10^5	–
Xe-140	13.6 s	3.0×10^5	–
Br-83	2.40 h	1.1×10^3	
Br-84	31.8 m	4.3×10^3	
I-131	8.04 d	7.0×10^2	
I-132	2.28 h	$9/4 \times 10^3$	
I-133	20.8 h	2.8×10^3	
I-134	52.6 m	2.8×10^4	
I-135	6.57 h	7.9×10^3	
Total noble gases			$\sim 1.0 \times 10^5$

*Estimated from experimental observations.

Table 3-2

SELECTED ANS STANDARD RADIONUCLIDE CONCENTRATIONS IN REACTOR COOLANTS - FISSION PRODUCTS (μCi/kg) (Ref. 7)

	BWR[a]		PWR[b]	
Nuclide	Reactor Water	Steam	Reactor Water	Secondary Coolant
Kr-85m	–	1.0		
Kr-85	–	0.004		
Kr-87	–	3.3		
Kr-88	–	3.3		
Kr-89	–	21		
Xe-133m	–	0.049		
Xe-133	–	1.4		
Xe-135m	–	4.4		
Xe-135	–	3.8		
Xe-137	–	26.		
Xe-138	–	15		
I-131	2.2	0.033	45	0.0018
I-132	22	0.33	210	0.0031
I-133	15	0.23	140	0.0048
I-134	43	0.65	340	0.0024
I-135	22	0.33	260	0.0066
Rb-89	5	0.005	190	
Cs-134	0.03	–	7.1	
Cs-136	0.02	–	0.87	
Cs(Ba)-137	0.08	–	9.4	
Cs-138	10	0.01	–	
Sr-89	0.1	–	0.14	
Sr(Y)-90	0.0007	–	0.012	
Sr-91	4	–	0.96	
Sr-92	10	–	–	
Y-91	0.04	–	0.0052	
Zr(Nb)-95	0.0008	–	0.39	
Mo(Tc)-99	2	–	6.4	
Ru(Rh)-103	0.02	–	7.5	
Ru(Rh)-106	0.003	–	90	
Te-132	0.01	–	1.7	
Ba(La)-140	0.4	–	25	
Ce-141	0.03	–	0.15	
Ce-144	0.003	–	4	
Np-239	8	–	2.2	

[a]A reference BWR is a 3400 MWt BWR/5.
[b]A reference PWR is a 3400 MWt PWR with U-tube steam generators.

3.3 CHARACTERISTICS OF FISSION PRODUCT RELEASE PATTERNS IN PWR

3.3.1 Activity Release Rate

In PWRs, the fuel performance is usually characterized by analysis of iodine activities in the primary coolant. The level of I-131 activity is measured for the purpose of estimating the number of fuel failures, and the ratio of I-131/I-133 is measured to characterize the type of defect.

As shown in Section 3.1.2, the activity release from failed fuel may be characterized by Equation 3-8. Depending on the magnitude of the escape time constant, ν, Equation 3-8 can be simplified to Equations 3-9 and 3-10:

$$A_i = F(p)Y_i\lambda_i^{0.5} \qquad \text{for } \nu >> \lambda \tag{3-9}$$

$$A_i = F(p)Y_i\nu_i\lambda_i^{-0.5} \qquad \text{for } \nu >> \lambda \tag{3-10}$$

For practical purposes, the value of ν is assumed to be identical for all iodine isotopes. Thus, the ratio of I-131/I-133 release rate may be estimated by:

$$\frac{A_{131}}{A_{133}} = \left(\frac{Y_{131}}{Y_{133}}\right)\left(\frac{\lambda_{131}}{\lambda_{133}}\right)^{0.5} \qquad \text{for } \nu >> \lambda \tag{3-31}$$

or

$$\frac{A_{131}}{A_{133}} = \left(\frac{Y_{131}}{Y_{133}}\right)\left(\frac{\lambda_{131}}{\lambda_{133}}\right)^{-0.5} \qquad \text{for } \nu << \lambda \tag{3-32}$$

It is safe to assume that the activity release rate ratio would be between these two extreme limits for the iodine activities released from a failed fuel.

When the activities are released only from the tramp fuel, the activity release ratio can be estimated from Equation 3-11.

$$\frac{A_{131}}{A_{133}} = \left(\frac{Y_{131}}{Y_{133}}\right)\left(\frac{\lambda_{131}}{\lambda_{133}}\right) \tag{3-33}$$

3.3.2 Fission Product Activities in the Primary Coolant and Characterization of Fuel Failure Pattern

Similar to that described for the BWR (Section 3.2.4), the steady-state activity release rate can be calculated from the measured activity concentration in the coolant by:

$$A_i = C_i W(\lambda_i + \beta) \tag{3-34}$$

where A_i = activity release rate from fuel, μCi/s or Bq/s

C_i = activity concentration in the coolant, μCi/kg or Bq/s

W = reactor coolant mass, kg (excluding the pressurizer mass)

λ_i = decay constant, s^{-1}

β = letdown coefficient, s^{-1}, given by $F\varepsilon/W$ where F = letdown flow rate (kg/s) and ε = letdown demineralizer efficiency

The activity release rate ratio can be calculated from:

$$\frac{A_{131}}{A_{133}} = \frac{C_{131}(\lambda_{131} + \beta)}{C_{133}(\lambda_{133} + \beta)}, \tag{3-35}$$

and the concentration ratio can be calculated from:

$$\frac{C_{131}}{C_{133}} = \frac{A_{131}(\lambda_{133} + \beta)}{A_{133}(\lambda_{131} + \beta)} \tag{3-36}$$

By substituting the A_{131}/A_{133} ratio from Equation 3-33 for the recoil release from the tramp fuel, the concentration ratio can be calculated by:

$$\frac{C_{131}}{C_{133}} = \left(\frac{Y_{131}}{Y_{133}}\right)\left(\frac{\lambda_{131}}{\lambda_{133}}\right)\left(\frac{\lambda_{133} + \beta}{\lambda_{131} + \beta}\right) \tag{3-37}$$

By using a typical value of $\beta = 2 \times 10^{-5}\ s^{-1}$, the concentration ratio from the recoil source can be estimated:

$$\left(\frac{C_{131}}{C_{133}}\right)_{recoil} = 0.065$$

Similarly, the concentration ratio from the failed fuel can be estimated by:

$$\frac{C_{131}}{C_{133}} = \left(\frac{Y_{131}}{Y_{133}}\right)\left(\frac{\lambda_{131}}{\lambda_{133}}\right)^{0.5}\left(\frac{\lambda_{133}+\beta}{\lambda_{131}+\beta}\right) \qquad (3\text{-}38)$$

for a large release, and

$$\frac{C_{131}}{C_{133}} = \left(\frac{Y_{131}}{Y_{133}}\right)\left(\frac{\lambda_{131}}{\lambda_{133}}\right)^{-0.5}\left(\frac{\lambda_{133}+\beta}{\lambda_{131}+\beta}\right) \qquad (3\text{-}39)$$

for a small release. The ratio values are approximately 0.2 and 1.85, respectively. It can be easily seen as the release source changing from tramp fuel to failed fuel, due to the faster decay of the shorter-lived isotope (I-133) inside the fuel and fuel gap, the activity concentration ratio increases from ≈ 0.065 for the recoil source to ≈ 0.2 or greater, depending on the nature and size of fuel defect. By using the measured I-131/I-133 concentration ratio in the coolant, the nature of the fuel defect may be characterized as follows:

I-131/I-133 Concentration Ratio	Defect Nature	Comment
≤0.1	Possibly no defect	Release from tramp fuel or fuel contaminate
0.1-0.3	Open hole or large crack	Coolant in contact with fuel in cladding
0.3-0.5	Small hole	Release by diffusion
≥0.5	Pin hole or tight crack	Activity release in equilibrium with activity inside the fuel cladding

It should be mentioned that when the iodine activity concentrations in a reactor are compared with that in other reactors, there are usually "normalized" to a common value of letdown coefficient, $\beta = 2 \times 10^{-5}\ s^{-1}$.

From Equation 3-34, the iodine concentration measured in a reactor with letdown coefficient β may be normalized to a normalized concentration C_i^n for comparison:

$$C_i^n W(\lambda_i + 2\times 10^{-5}) = C_i W(\lambda_i + \beta)$$

or

$$C_i^n = C_i \frac{\lambda_i + \beta}{\lambda_i + 2\times 10^{-5}} \qquad (3\text{-}40)$$

Similarly, the concentration may also be normalized to a same reactor coolant mass, W^n:

$$C_i^n = C_i \frac{W(\lambda_i + \beta)}{W^n\left(\lambda_i + 2\times 10^{-5}\right)} \qquad (3\text{-}41)$$

In addition to characterizing the nature of fuel failure, the measured activity ratio of Cs-137/Cs-134 may be used to estimate the exposure of failed fuel as discussed previously for the BWR.

3.3.3 Estimation of the Number of Failed Fuel Rods

In spite of some suggested techniques to estimate the number of failed fuel rods, the most practical and accurate method is to compare the normalized I-131 concentration from failed fuel (total minus recoil) with the previously established empirical data. The I-131 activity concentrations per leaking fuel rod are:(6)

	Tight Defect (I-131/I-133 >> 0.7)	Open Defect (I-131/I-133 ≈ 0.2-0.5)
Typical	5 μCi/kg	80 μCi/kg
Range	1-10 μCi/kg	10-100 μCi/kg

Similar to that discussed in Section 3.2, for the BWR, the correction of the measured activity concentration for the contribution due to tramp fuel must be calculated. It has been suggested[6] that I-134, which has a 52.6 min. half-life, comes primarily from direct recoil sources. The measured I-134 activity may be used to correct the recoil contribution for I-131. According to Equation 3-37, the recoil fraction of I-131 may be calculated by:

$$\left(\frac{C_{131}}{C_{134}}\right)_{recoil} = \left(\frac{Y_{131}}{Y_{134}}\right)\left(\frac{\lambda_{131}}{\lambda_{134}}\right)\left(\frac{\lambda_{134}+\beta}{\lambda_{131}+\beta}\right) \qquad (3\text{-}42)$$

By using the typical value of $\beta = 2 \times 10^{-5}\ s^{-1}$,

$$\left(\frac{C_{131}}{C_{134}}\right)_{recoil} = 0.0194$$

Thus, the I-131 concentration from leaking fuel is:

$$(C_{131})_{recoil} = (C_{131})_{total} - 0.0194\ C_{134}$$

It must be cautioned that, by assuming the I-134 activity release is totally from recoil, a large error could be introduced in calculating I-131 for a small fuel leakage. It is suggested that the recoil level would be more accurately determined from other shorter-lived isotopes, similar to that in the BWR. In many cases, only a fraction (1/4 to 1/2) of I-134 comes from recoil sources.

3.3.4 Steady-State Concentrations of Fission Product Activities in the Primary Coolant

The steady-state concentrations of fission product activities in the primary coolant vary from reactor to reactor, depending on the size of the fuel defect, the number of defective fuel rods in the core, and the capacity of letdown cleanup system. The American Nuclear Society Standards Committee has published a set of typical (or "standard") radionuclide concentrations in principal fluid streams of the light water reactors.[7] The "standard" concentrations of fission products in the reference PWR are given in Table 3-2. For evaluating the long-term environmental impact, the recommended relationship for estimating the expected I-131 concentration in the reactor coolant system of PWR is:

$$\text{I-131}\ (\mu Ci/g) = 0.003\ (P/L)^{(8)}$$

where P = power rating (MWt) and L = letdown flow rate (GPM)

3.4 FISSION PRODUCT TRANSPORT IN THE COOLANT SYSTEM

3.4.1 Fission Products in the Steam/Condensate System in BWR

There are three mechanisms of steam transport ("carryover")* in the BWR primary systems: (1) mechanical entrainment, (2) vapor transport, and (3) grow-in with the decaying noble gas activities.

(1) Mechanical entrainment is very small compared to the other two mechanisms. The magnitude of mechanical entrainment can be determined by measuring the soluble activities (e.g., Na-24) in the steam condensate. The ratio of Na-24 in the condensate to that in the reactor water is normally on the order of 0.01%.

(2) Vapor transport is the partitioning of a volatile species between liquid and gas phases and is subject to equilibrium restraints. The magnitude of iodine carryover in BWRs has been found to vary from ≈ 0.1% to ≈ 2.5%, depending on the coolant chemistry and the metallic impurity content. A correlation has been established between the iodine carryover and the copper ion concentration in the feedwater, as shown in Figure 3-4. Copper is believed to be a key impurity in water which will alter the radiation chemistry in reactor water. It has been postulated that the volatile species of iodine in steam transport are HIO and/or H_2O-I.[9,10] The chemical forms of iodine in reactor water have been found to be iodide (I^-) and iodate (IO_3^-). More discussion on the radiochemistry of iodine will be presented in Section 8.3. A study on the effects of hydrogen water chemistry on the behavior of radioiodine has been performed and the results will be published elsewhere.[14]

A detailed iodine-131 transport distribution in the steam/condensate and feedwater cycle measured at Brunswick-2, which has a forward-pumping system design (the high-pressure turbine condensate and reheater drains are pumped back to the reactor via the feedwater train without going through the condensate demineralizer system), are shown in Figure 3-5.[10] Both measured and calculated data are indicated in individual flowing streams. It

---

* Carryover is traditionally defined as:

$$\% \text{ carryover} = 100 \times \frac{\text{concentration of species i in condensate } (\mu Ci / kg)}{\text{concentration of species i in reactor water } (\mu Ci / kg)}$$

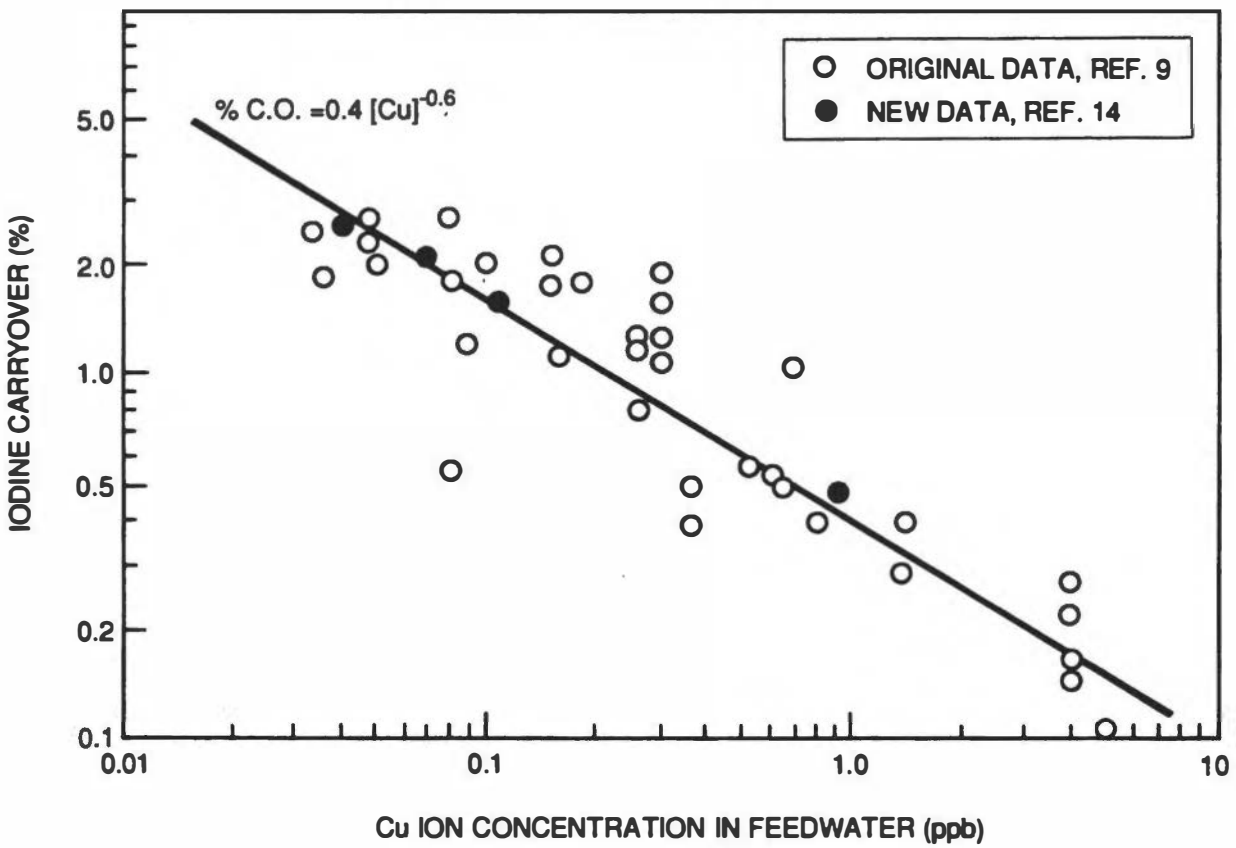

Figure 3-4. Iodine Carryover As A Function of Copper Ion Concentration in Feedwater

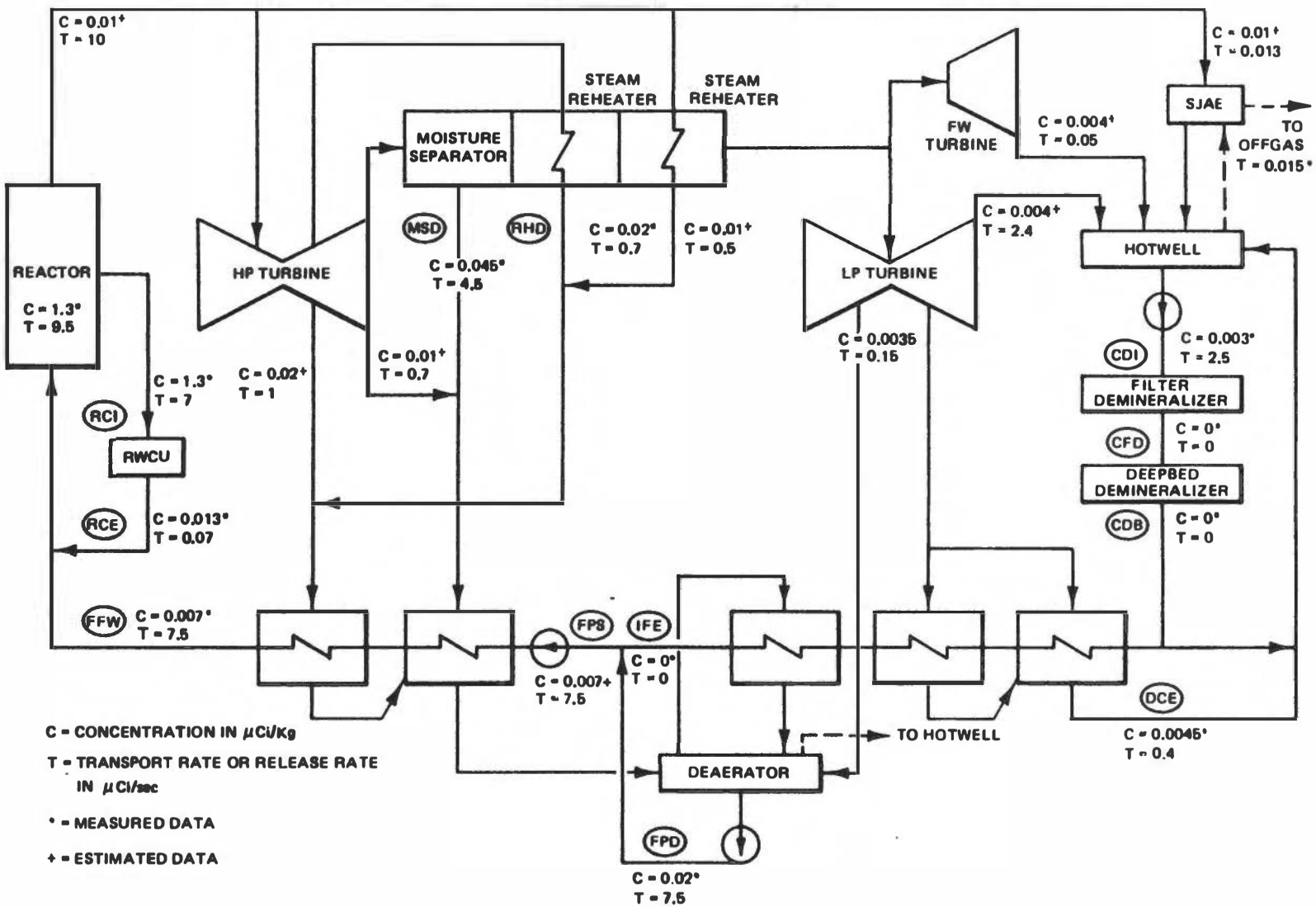

Figure 3-5. Iodine-131 Transport Distribution in the Steam, Condensate and Feedwater Systems of a BWR (Ref. 10)

is important to note that greater than 99% of steam phase I-131 is condensed with the steam, and only a small fraction of non-condensable I-131 activity is released in the offgas and eventually stopped in the offgas filter system.

(3) Noble gas daughters grow into the steam/condensate system during the transient time. It normally takes approximately two minutes for steam carrying noble gas activities to pass through the steam/turbine system (see Section 8.1). Some fundamental equations for the parent-daughter activity calculations have been shown in Section 2.4.

3.4.2 Fission Products in the Secondary Coolant System in PWR

It is obvious that the radioactivities in the secondary system are the result of steam generator leakage. The "standard" concentrations of fission products in the reference PWR secondary coolant are given in Table 3-2. The steam generator leakage rate can be estimated from the measurement activity concentration in the secondary coolant and a material balance equation.

$$\frac{dS_i}{dt} = \frac{LC_i}{V} - \frac{\beta S_i}{V} - \lambda_i S_i \qquad (3\text{-}43)$$

where S_i = secondary coolant activity of species i (μCi/kg)

C_i = primary coolant activity of species i (μCi/kg)

λ_i = decay constant of species i (s^{-1})

L = primary to secondary leakage rate (kg/s)

V = mass of secondary coolant system (kg)

β = losses from secondary system (kg/s)

Upon integration

$$S_i = \frac{LC_i}{(\beta + \lambda V)}\left[1 - \exp - \left(\frac{\beta}{V} + \lambda_i\right)t\right] \qquad (3\text{-}44)$$

For steady state equilibrium conditions,

$$S_i = \frac{LC_i}{(\beta + \lambda_i V)} \tag{3-45}$$

or

$$L = \frac{S_i}{C_i}(\beta + \lambda_i V) \tag{3-46}$$

The value of β includes total blowdown rate and total system losses by leakage. If a noble gas activity (e.g., Xe-133) is monitored, the same equations can be used. In this case, β represents the air ejector flow rate and S_i the gas-phase Xe-133 activity.

Care must be exercised to determine the leakage rate because the time required to reach equilibrium conditions may vary, depending on the relative values of λ and β/V in the exponential term in the equation. A leakage rate on the order of 4 kg/s or 75 lb/day is commonly adopted in source term studies.(7)

As discussed in the BWR, a small fraction of the fission products or other radioactive species leaking from the primary to secondary system is expected to be transported into the steam phase in the steam generator. With the exception of noble gas and tritium activities, most of fission products are transported by the mechanical entrainment mechanism. This is also true for iodine species because of the basic and reducing nature in the secondary coolant chemistry. The iodine carryover in the steam generator system is commonly found to be on the order of 0.1%.

3.5 FISSION PRODUCT RELEASE DURING POWER TRANSIENT

Fission product releases from defective fuel during power transients occur similarly in BWRs and PWRs. During normal operation, the defective fuel gap is filled with steam and/or water, equilibrating with the coolant pressure, and the fission product release rate depends on the size of defect. During power reduction or shutdown, the release mechanism is totally different, and the activity spike has been seen in most cases. One typical example of I-131 spiking in a BWR is shown in Figure 3-6. The following important features in fission product spiking have been observed:

(1) When a reactor is shut down in an orderly manner, at least two spiking peaks are generally seen: one at zero power and another immediately after total depressurization.

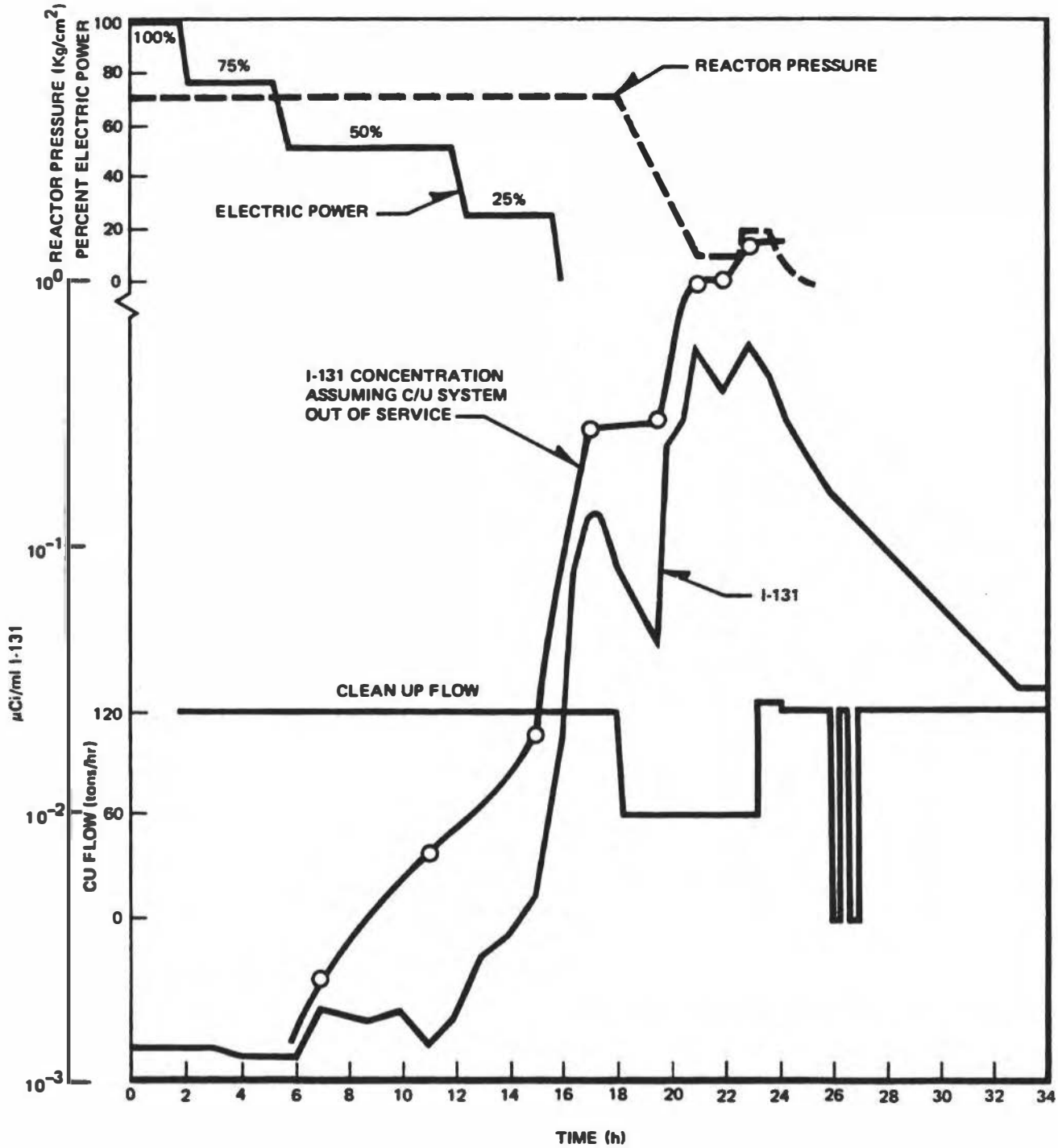

Figure 3-6. Behavior of Iodine-131 Spiking During Shutdown in a BWR (Ref. 11)

(2) Frequently there are some smaller spiking peaks between two major spiking peaks.
(3) Only a small spike occurs if the reactor is brought down to the hot standby state (without depressurization).
(4) After the peak is reached during spiking, very little activity is released from the fuel, and the concentration of activity in water decreases, depending on the reactor water cleanup flow (BWR) or the letdown flow (PWR).
(5) Iodine is not the only fission product spike; Cs, Sr, and other soluble fission products behave similarly.
(6) Iodine spike also occurs during startup, but the magnitude is much smaller than shutdown spiking.
(7) Obviously, if the fission product is released only by recoil from cladding surface contamination during power operation, no fission product spike is expected.

3.5.1 Release Mechanisms

Based on these observations, the mechanisms of fission product release during power transients are proposed as follows:

(1) During power reduction, a portion of the fuel cools down, and the liquid water is forced into the defect fuel gap. The decay heat is still high enough to evaporate the water into steam, and some fission products leak out with the steam. The process reaches a peak when the reactor is shut down at zero power.
(2) While the reactor is down, the pressure in the RPV is maintained at high pressure, the fission product release rate is slow, and the concentration of fission product in water decreases as the cleanup system removes the activities.
(3) When the pressure starts to drop, the higher pressure inside the fuel cladding begins to push the water- and steam-carrying fission products out of the cladding through the defect hole. The process reaches a peak when the pressure drops and the water temperature decreases to near ambient conditions.
(4) Because the fuel gap spaces and plenum in a fuel rod may not be in total communication, some smaller spiking peaks between two large peaks may be seen.

3.5.2 Magnitude of I-131 Spike

The magnitude of iodine spiking depends on the nature of the cladding defect. For a large split cladding defective fuel, the magnitude of spiking* is much smaller than that for a pin hole defective fuel. Basically, the inventory in the defective fuel available for release during shutdown will determine either the magnitude of spiking or the total release during shutdown. (The total release of I-131 can be easily estimated from the I-131 concentration in the coolant, the total mass of the coolant, and the coolant cleanup flow rate during reactor shutdown.) There is no direct relationship between the total release and the equilibrium release rate during normal operation (Figure 3-7). However, Brutschy et al.[11] were able to correlate either the spiking magnitude or the total release with the relative inventory of I-131 in the defective fuel in BWRs. The original data reported by Brutschy et al. and some additional new data are shown in Figure 3-8.

The relative inventory is related to the ratio of the "fission gas" release rate (in fission/s) to the I-131 release rate (in fission/s) during normal operation. The "fission gas" is assumed to be an imaginative noble gas nuclide with the I-131 decay constant. This ratio represents the ratio of "total release" to "partial release" of I-131 from a defective fuel during normal operation. Thus, a large ratio represents a smaller I-131 release during normal operation, or a larger inventory available for release during shutdown.

An example for predicting the magnitude of I-131 spike is illustrated by using the data shown in Figure 3-2. The "fission gas" (FG) release rate (~5.2×10^{14} fission/s) is taken from the noble gas line at the I-131 decay constant. The I-131 release rate is read directly from the data (3.4×10^{13} fission/s).

---

* The magnitude of spiking is defined as the ratio of (I-131 concentration in reactor coolant at peak during shutdown) to (the steady I-131 concentration in reactor coolant prior to shutdown.)

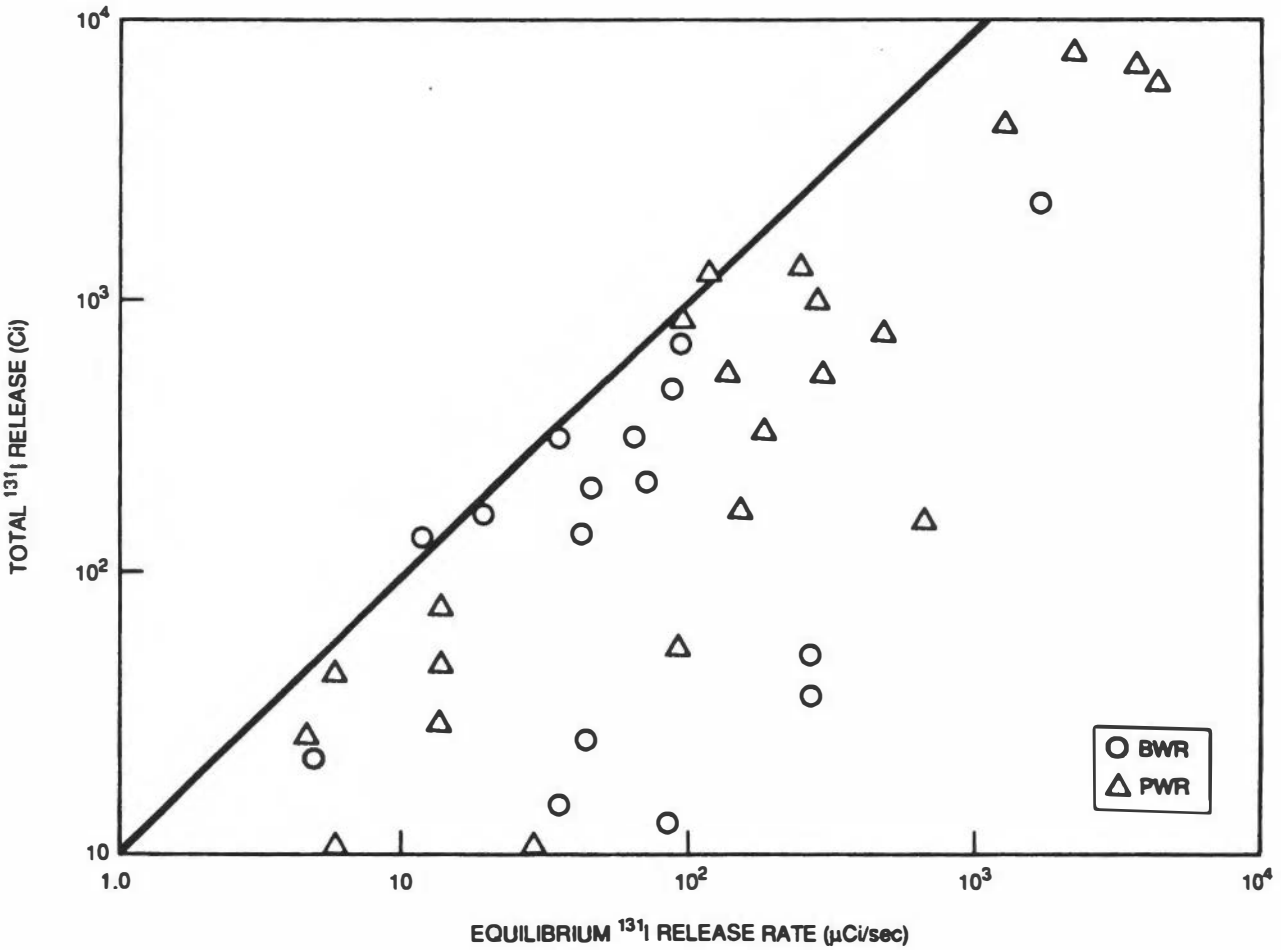

Figure 3-7. Total I-131 Release During a Spiking Sequence (Ref. 12)

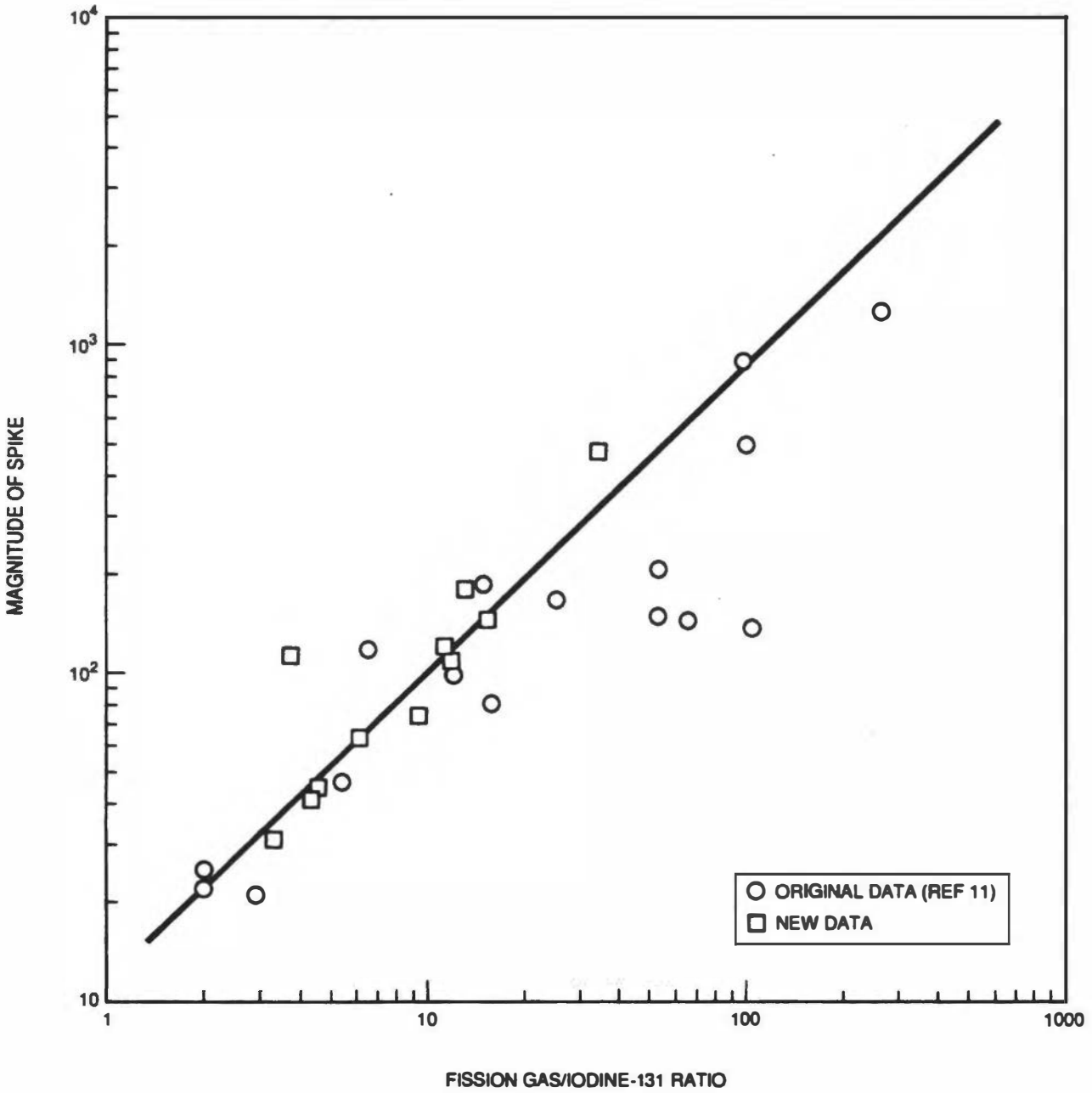

Figure 3-8. Magnitude of I-131 Spike as a Function of the Ratio of Fission Gas to I-131 Release Rate During Power Operation in BWRs (Ref. 11)

The ratio of FG/I-131 is estimated to be ~16. The spike magnitude is therefore predicted to be ~200 (Figure 3-8). It should be noted that the correlation shown in Figure 3-8 may be qualitatively predicted by the measurement of six major noble gas release rates during normal operation. If the defect size is small and therefore the value of "b" in the source term equation (Equation 3-13) is large, the magnitude of I-131 spiking would be large, and vice versa. If one assumes the equilibrium pattern of release during power operation, the I-131 activity inventory (μCi) in the fuel gap may be estimated from the "FG" release rate (in μCi/s):

$$\text{I}-131 \text{ inventory in fuel gap} = \frac{\text{FG release rate}}{\lambda_{(\text{I-131})}}$$

Based on spiking data, it is estimated that only a maximum of ~10% release from the fuel gap inventory has ever been observed in BWRs.

3.5.3 Iodine Release Rate in PWR

The release rate of I-131 from the fuel to the reactor coolant system in a PWR can be estimated by using the following equation[15]:

$$R = \frac{L_t\left[A - A_o \exp(-L_t t)\right]}{1 - \exp(-L_t t)}, \qquad (3\text{-}48)$$

where R = transient iodine release rate (Ci/h)

L_t = total iodine removal rate (h^{-1})

A = maximum transient RCS iodine inventory (Ci)

A_o = steady-state RCS iodine inventory (Ci)

t = time from iodine spike initiating event to maximum iodine concentration (h),

and $$L_t = L_d + L_p, \qquad (3\text{-}49)$$

where L_d = ^{131}I decay constant = $3.59 \times 10^{-3}\ h^{-1}$

L_p = purification removal constant

$$= \frac{F(1-1/DF)}{M}$$

F = purification system flow rate (kg/h)

M = RCS mass inventory (kg)

DF = purification system decontamination factor.

An example of calculation can be found in the literature[16].

3.5.4 Soluble Fission Products Releases

As mentioned earlier, Cs, Sr and other soluble fission products also spike during reactor shutdown. An example of Cs isotopes spiking in a PWR is shown in Figure 3-9.

3.6 REFERENCES

(1) A.H. Booth, A Method of Calculating Fission Gas Diffusion from UO_2 and Its Application to the X-2-F Loop Test, September 1957 (AECL CRDC-721).

(2) S.D. Beck, The Diffusion of Radioactive Fission Products from Porous Fuel Elements, April 1960 (BMI-1433).

(3) American Nuclear Society, "Method for Calculating the Fractional Release of Volatile Fission Products from Oxide Fuel," ANSI/ANS-5.4-1982.

(4) R.A. Lorenz, J.L. Collins, and A.P. Malinauskas, Nucl. Tech. Vol 46, 404 (1979).

(5) J.M. Skarpelos and R.S. Gilbert, "Technical Derivation of BWR 1971 Design Basis Radioactive Material Source Terms," March 1971 (NEDO-10871).

(6) EPRI, "Failed Fuel Action Plan Guidelines," NP5521-SR (Nov. 1987).

(Continued)

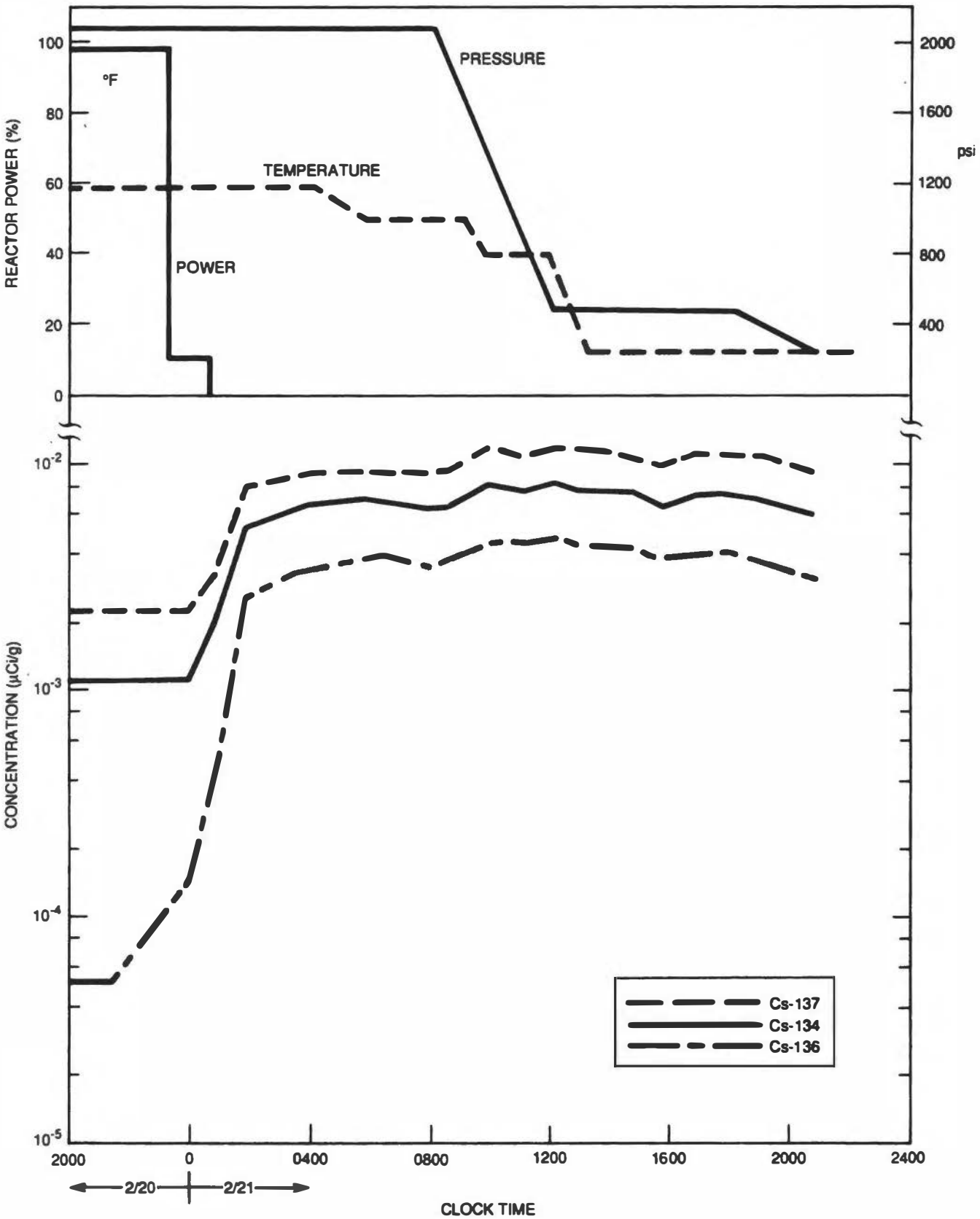

Figure 3-9. Behavior of Cs Isotopes Spiking During Shutdown in a PWR (Ref. 13)

(7) American Nuclear Society, American National Standard Radioactive Source Term for Normal Operation of Light Water Reactors, ANSI/ANS-18.1-1984.

(8) Westinghouse Electric Corporation "Source Term Data for Westinghouse Pressurized Water Reactors," WCAP 8253, (May 1974).

(9) C.C. Lin, J. Inorg. Nucl. Chem. 42, 1093 (1980).

(10) C.C. Lin, "Chemical Behavior and Distribution of Volatile Radionuclides in a BWR System with Forward-Pumped Heater Drains" Water Chemistry of Nuclear Reactor System 3, 103, BNES, London (1983).

(11) F.J. Brutschy et al., Behavior of Iodine in Reactor Water During Plant Shutdown and Startup, August 1972 (NEDO-10585).

(12) W.G. Pasedaq, "Iodine Spiking in BWR and PWR Coolant Systems," Proc. Topical Meeting on Thermal Reactor Safety, Sun Valley, Idaho, July 31, 177, Conf. 770708.

(13) J.E. Cline and E.D. Barefoot, "Study of Reactor Shutdown Radioactivity Spiking at Three Mile Island Nuclear Power Station During Feb. 20-21, 1976," Science Applications, Inc. (1976).

(14) C.C. Lin, "Chemical Behavior of Radioiodine in BWR Systems (II). Effects of Hydrogen Water Chemistry," Nucl. Tech., 97, 71 (1992).

(15) R.J. Lutz, Jr., "Iodine Behavior Under Transient Conditions in the Pressurized Water Reactor," WCAP-8637, Westinghouse Electric Corporation (1975).

(16) J.P. Adams and C.L. Atwood "Iodine Spike Release Rate During a Steam Generator Tube Rupture" Nucl. Tech. 94, 36 (1991).

4. ACTIVATED CORROSION PRODUCTS

4.1 INTRODUCTION

Activated corrosion products are produced by neutron activation of either the corrosion product deposit on the fuel surface or the in-core structure materials. The activation cross sections and specific activities for some major corrosion products are given in Table 2-5 and Figure 2-12, respectively. The activated corrosion products are released from fuel surface deposits by erosion and spalling caused by hydraulic shear forces in some cases and by dissolution in other cases. Some activated products are released from in-core materials by dissolution and wear. The activation products in the coolant can be soluble or insoluble, and they are transported by water to all parts of the primary system. This presents problems with regard to accessibility and safe maintenance of various components because of radiation fields. Among those activated corrosion products, the γ-emitting activities (Co-60, Co-58, Zn-65, Mn-65 and Fe-59) are more important in creating the radiation field problems. The longer-lived species (Fe-55, Ni-63 and Co-60) are of more concern with the problems in the radioactive waste handling and disposal. Radioactive waste production and handling will not be the major subject in this monograph, but some important aspects of radioassays of radioactive waste will be discussed separately in Section 7.

Since the coolant chemistries in BWRs and PWRs are totally different, the behavior of corrosion product transport and radiation field buildup in the two reactor systems should be expected to be different, and they will be discussed separately in the following sections.

4.2 ACTIVATED CORROSION PRODUCTS IN BWRs

4.2.1 Activation of Corrosion Products on Fuel Surfaces

A great number of fuel deposit samples have been analyzed and the results can be found in the literature[1,2,3]. Some typical data of corrosion product and activity distribution along the length of the fuel rod are shown in Figures 4-1 and 4-2. The corrosion product deposits are generally found to be heaviest at ~50-100 cm from the bottom of the fuel rod, where the boiling starts. The specific activities are generally proportional to the exposure along the fuel length.

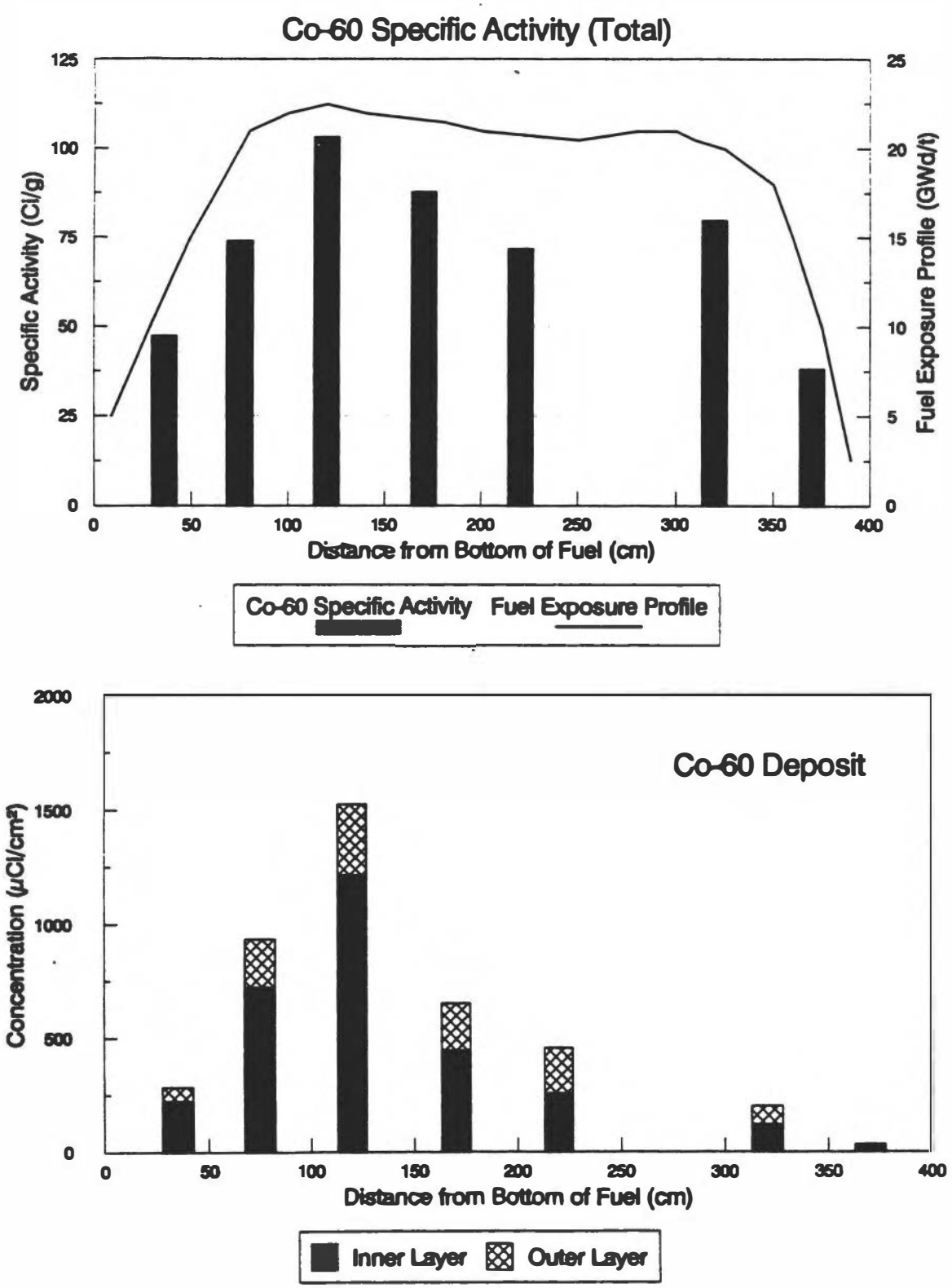

Figure 4-2. Axial Distribution of Co-60 and Co-60 Specific Activity on Fuel Surface (Reproduced with Permission, J. Nucl. Sci. Tech., Ref. 4)

The deposit samples are taken from the fuel cladding surface under water in the fuel pool using a special sampling device similar to that described by Uchida et al.[4] (Figure 4-3). An area of ~2 cm^2 is first "brushed" to remove the loosely-adherent deposit (outer layer). The same area is then "scraped" with a scraping stone to remove the tenacious deposit (inner layer). While the brushing or scraping process is in progress, the deposit removed from the fuel cladding surface is sucked in with water in the sampling device, transported through the sampling tube out of the fuel pool, and collected on a membrane filter.

As shown in Figure 4-1, the activated corrosion products in the outer layer are only a small fraction of the total activities in the deposit. The specific activities in the inner layer are also generally higher, as expected, because of longer residence time on the cladding surface.

The levels of fuel deposit and its chemical composition depend on the corrosion product input from the condensate and feedwater systems, and the levels of feedwater input vary significantly, depending on the materials used in the condensate system and the type of condensate treatment system. With the deepbed demineralizer system, the ionic species in the condensate are more effectively removed than the insoluble particulate species. On the other hand, the removal efficiencies for the ionic and insoluble species are just reversed in the filter-demineralizer system. Thus, the fuel deposit in the deepbed system contains a higher percentage of iron than that in the filter- demineralizer system. This fundamental difference may cause some differences in the activity concentration and chemical behavior of activated corrosion products in the coolant (Section 4.2.2).

The corrosion product (mainly represented by iron, customarily called "crud") deposition on a heating surface can be described by a simple equation:

$$\frac{dW}{dT} = DC - kW \qquad (4\text{-}1)$$

$$= \left(P\frac{Q}{L}\right)C - kW$$

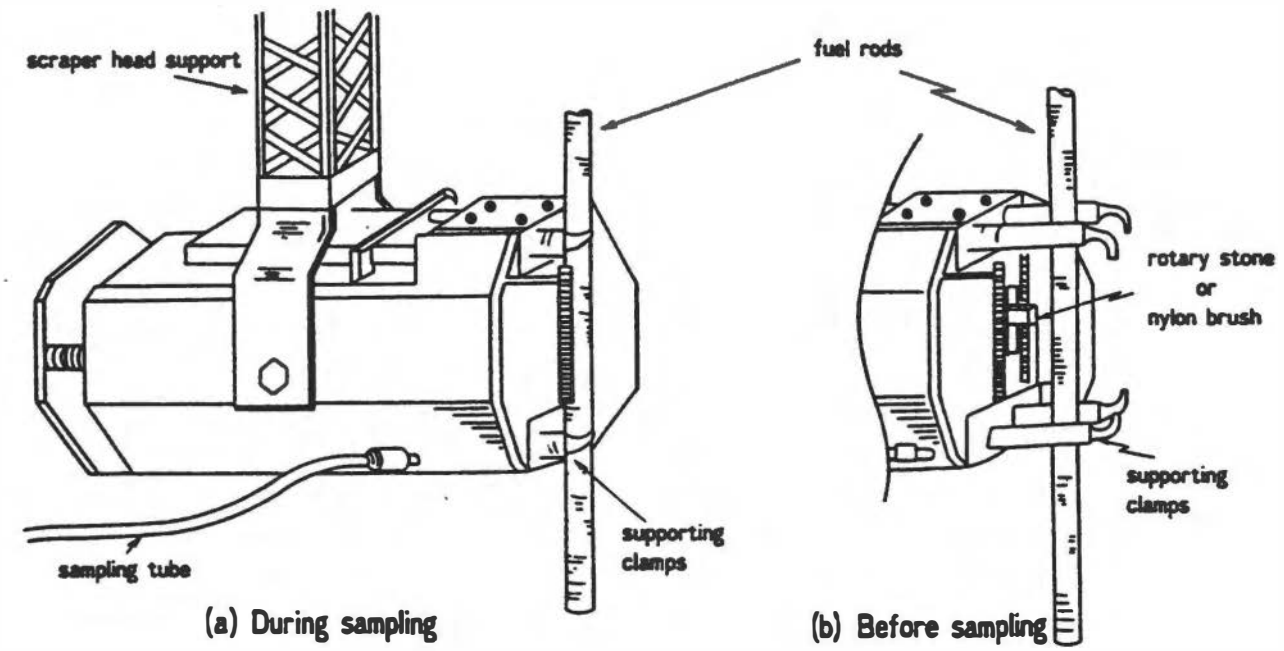

Figure 4-3. Fuel Cladding Deposit Sampling Device (Reproduced with Permission, J. Nucl. Sci. Tech., Ref. 4)

where: D = deposition rate constant, $kg/cm^2/day$

W = weight of crud deposit at time t, g/cm^2

C = crud concentration in reactor water, g/kg

Q = heat flux on fuel surface, $kcal/cm^2/day$

L = latent heat of water vaporization, $kcal/kg$

p = probability of deposition, dimensionless

k = release constant, day^{-1}

At steady state, Equation 4-1 can be integrated as:

$$W = \frac{D}{k} \cdot C \cdot \left(1 - e^{-kt}\right) \tag{4-2}$$

$$= \frac{p}{k} \cdot C \cdot \frac{Q}{L} \left(1 - e^{-kt}\right)$$

Initially when W is small,

$$W = P \cdot C \cdot \frac{Q}{L} \cdot t \ ,$$

and the initial linear deposition rate

$$\frac{W}{t} = P \cdot C \cdot \frac{Q}{L} \tag{4-3}$$

If k is large, and/or t is long, W may reach an equilibrium value,

$$W = \frac{p}{k} \cdot C \cdot \frac{Q}{L} \tag{4-4}$$

In the boiling region with steam, the deposition rate constant has to be modified by a factor of (1 - V), where V is the steam void fraction in the region. The release constant k may vary as a function of water flow velocity and the thickness and chemical composition of the crud deposit.

A mathematical model has also been developed to describe the activation of corrosion products in the fuel deposits. The assumptions for model development, the derivation of the model and a comparison of experimental data with the results of model calculations are given below:

Assumptions:

(1) The parent atoms in the deposit increase linearly with time, and no release of the parent nuclide from the deposit is assumed. (This is generally true for a BWR with low crud input)
(2) The active atoms carried in by feedwater are insignificant.
(3) The active atoms are uniformly distributed in the fuel deposit.
(4) The release of active atoms is a first-order reaction regardless of the true mechanism.

From these assumptions, the rate of formation of active atoms in the deposit on a fuel unit surface is described by Equation 4-5:

$$\frac{dN}{dt} = PN^{o}\phi\sigma - \lambda N - kN - P\phi\sigma_{b}N \qquad (4\text{-}5)$$

where: N = number of active atoms in the deposition unit surface area (atoms)

N^{o} = number of parent atoms deposited on unit surface area at time t (atoms), $N^{o} = nt$

n = constant rate of deposition of parent atoms from water to unit surface area on the fuel (atoms/s)

P = reactor power and geometric factor

k = a pseudo net release rate constant of active atoms from deposit into water (s^{-1})

t = time of irradiation (s)

λ = decay constant (s^{-1})

ϕ = effective neutron flux ($n/cm^2/s$), assumed constant

σ = activation cross section (cm^2)

σ_b = burnup cross section (cm^2)

Replacing N^o with nt, Equation 4-5 becomes:

$$\frac{dN}{dt} = Pn\phi\sigma t - \lambda N - kN - P\phi\sigma_b N \qquad (4\text{-}6)$$

Equation 4-6 can be rearranged to become:

$$dN = Pn\phi\sigma t\ dt - C\ Ndt \qquad (4\text{-}7)$$

where

$$C = \lambda + k + P\phi\sigma_b$$

Multiplying both sides of Equation 4-7 by e^{Ct} and rearranging the equation, one obtains

$$d\left(n e^{Ct}\right) = Pn\phi t e^{Ct}\, dt \qquad (4\text{-}8)$$

Integrating Equation 4-8 gives

$$Ne^{Ct} = n\phi\sigma \frac{e^{Ct}}{C^2}(Ct - 1) + K \qquad (4\text{-}9)$$

where K is an integration constant.

At t=0, N=0, therefore $K = \frac{Pn\phi\sigma}{C^2}$

Putting K back in Equation 4-9.

$$Ne^{Ct} = \frac{Pn\phi\sigma}{C^2}\left[(Ct-1)e^{Ct}+1\right],$$

or

$$N = \frac{Pn\phi\sigma}{C^2}\left(Ct-1+e^{-Ct}\right)$$

Since activity $A = N\lambda$ and $N^\circ = nt$, therefore,

$$A = \frac{PN^\circ\phi\sigma\lambda}{tC^2}\left(Ct-1+e^{-Ct}\right), \qquad (4\text{-}10)$$

and the specific activity can be calculated by Equation 4-9:

$$\frac{A}{N^\circ} = \frac{P\phi\sigma\lambda}{tC^2}\left(Ct-1+e^{-Ct}\right) \qquad (4\text{-}11)$$

Based on some earlier reactor data[2], the values of k and C are empirically determined for the activities in BWR fuel deposits (Table 4-1). Also given in Table 4-1 are estimated equilibrium specific activities for some common activated corrosion products. A comparison of the calculated specific activities with the experimental data* obtained in several reactors is shown in Figure 4-4. It is apparent that the specific activities of the shorter-lived isotopes become saturated (or reach equilibrium) much sooner than the longer-lived isotopes. As shown in Table 4-1, Co-60 has the highest specific activity, and it is also the dominate activity in the deposit in most cases.

* Each data point represents the average of all samples taken from a fuel bundle.

4.2.2 Concentrations and Chemical Behavior of Activated Corrosion Products in Reactor Water

The concentrations of activated corrosion products in reactor water vary from reactor to reactor, depending largely on the materials used in the entire reactor and condensate systems. Some activated corrosion products (mainly Co-60 and Co-58) may be released from the in-core structure materials, but most of the other activities are released from the fuel deposit. Some selected American National Standard activation products concentrations in reactor coolants are given in Table 4-2. More recent data have shown much lower activity concentrations, as shown in Table 4-3, in which the activated corrosion products are determined as "soluble" and "insoluble" species separately.

Table 4-1

EMPIRICAL RELEASE CONSTANTS AND EQUILIBRIUM SPECIFIC ACTIVITIES FOR ACTIVATION PRODUCTS IN BWR FUEL DEPOSITS

Nuclide	$k(day^{-1})$	$\lambda(day^{-1})$	$P\phi\sigma_b(day^{-1})$	$C\ (day^{-1})$*	Equilibrium Specific Activity **
Co-60	1.26×10^{-3}	3.6×10^{-4}	0	1.62×10^{-3}	80 Ci/g
Co-58	5.9×10^{-3}	9.8×10^{-3}	4.8×10^{-3}	2.05×10^{-2}	0.65 Ci/gNi
Fe-55	8.56×10^{-4}	7.03×10^{-4}	0	1.56×10^{-3}	0.6 Ci/g
Fe-59	7.09×10^{-3}	1.55×10^{-2}	0	2.26×10^{-2}	25. mCi/g
Mn-54	2.28×10^{-3}	2.2×10^{-3}	0	4.48×10^{-3}	35. mCi/gFe
Zn-65	2.42×10^{-3}	2.8×10^{-3}	0	5.22×10^{-3}	1.8 Ci/g
Ni-63	1.03×10^{-3}	19×10^{-5}	0	1.05×10^{-3}	90 mCi/g

* $C = k + \lambda + P\phi\sigma_b$

** Based on average thermal neutron flux = 3.5×10^{13} $n/cm^2/s$ and fast neutron flux = 7×10^{13} $n/cm^2/s$

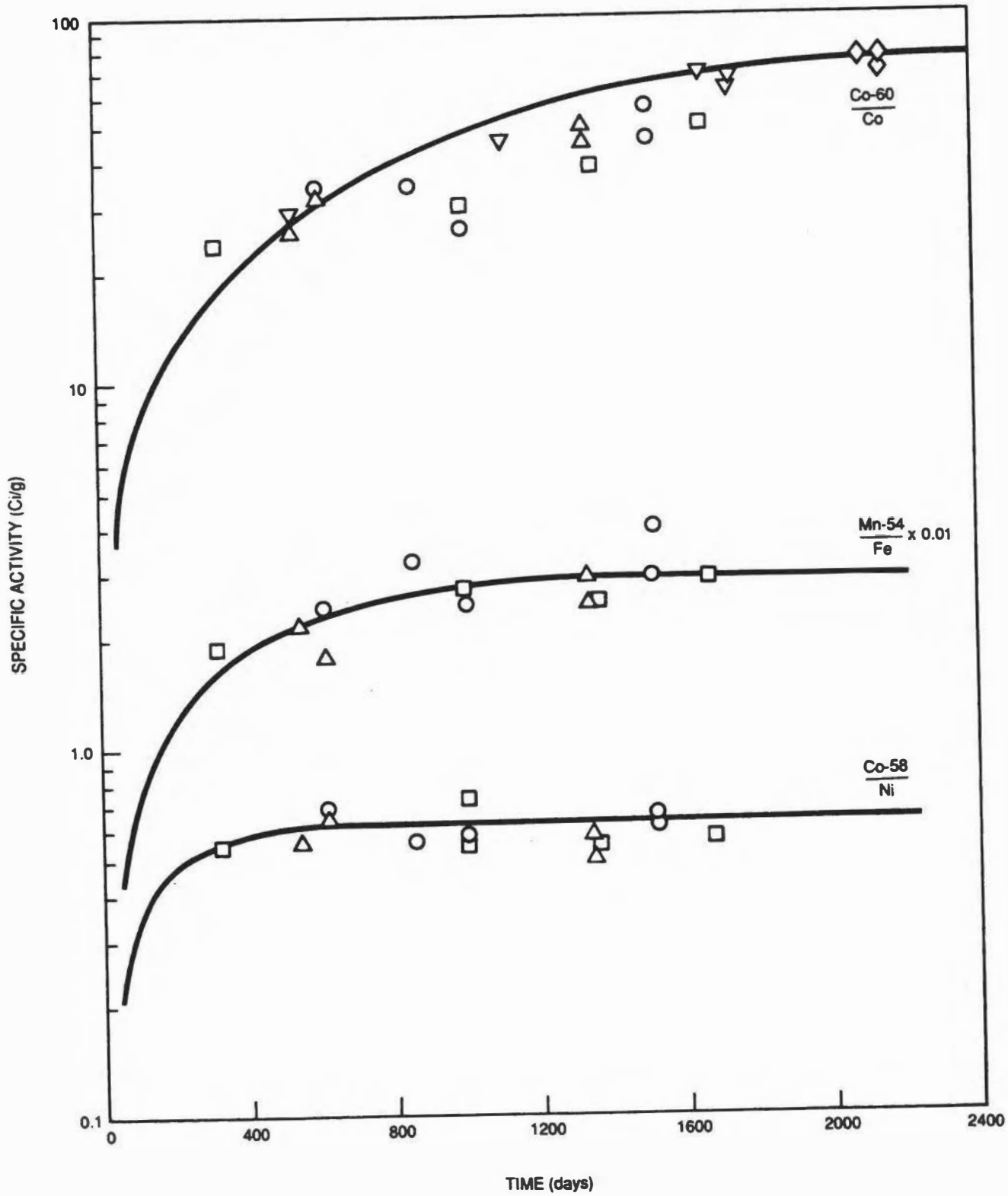

Figure 4-4. Bundle Average Specific Activities of Activated Corrosion Products in Fuel Deposits

Table 4-2

SELECTED ANS STANDARD RADIONUCLIDE CONCENTRATIONS IN REACTOR COOLANTS - ACTIVATION PRODUCTS (μCi/kg) (Ref. 5)

Nuclide	BWR[a]	PWR[b]
H-3	10	1,000
N-16	60,000	60,000
F-18	1.0	-
Na-24	10	47
P-32	0.2	-
Cr-51	6.0	3.1
Mn-54	0.07	1.6
Mn-56	50	-
Fe-55	1.0	1.2
Fe-59	0.03	0.3
Co-58	0.2	4.6
Co-60	0.4	0.53
Ni-63	0.001	-
Cu-64	30	-
Zn-65	0.2	0.51
Ag-110m	0.001	1.3
W-187	0.3	2.5

[a] A reference BWR is a 3400 MWt BWR/5.
[b] A reference PWR is a 3400 MWt PWR with U-tube steam generators.

Table 4-3

TYPICAL CONCENTRATIONS OF MAJOR ACTIVATED CORROSION PRODUCTS IN REACTOR WATER (x 0.01 μCi/kg) (Ref. 3)

Operation Time (days)	Co-60		Co-58		Mn-54		Fe-59		Cr-51	
	Crud*	Filt-rate*	Crud	Filt-rate	Crud	Filt-rate	Crud	Filt-rate	Crud	Filt-rate
83	0.47	2.7	1.1	7.5	1.5	8.1	1.0	-	4.0	89
210	2.0	4.5	3.6	7.9	7.2	8.0	7.5	0.65	4.3	110
325	0.21	2.3	0.17	3.9	0.39	3.4	0.12	0.34	0.13	230
475	1.1	5.7	0.55	14	3.4	6.3	1.7	-	1.0	180
604	1.2	13	1.2	14	0.74	8.2	-	-	1.3	200
730	1.3	8.2	5.7	23	0.68	4.5	0.35	-	1.6	230
830	0.52	7.6	2.4	24	0.24	4.2	0.17	-	1.1	250
896	0.11	5.7	0.51	23	0.07	4.1	0.03	-	0.61	120
1020	0.45	6.6	1.8	26	0.23	3.7	0.10	-	0.94	170
1175	0.22	6.3	0.53	30	0.14	3.8	-	-	0.21	170
1292	0.33	6.5	0.55	29	0.14	5.3	0.08	-	0.27	980
1417	0.11	7.7	0.45	35	0.05	3.7	0.03	-	0.96	130

* Crud = insoluble activities filtered by a 0.45 μm membrane filter.
Filtrate = soluble activities filtered through a 0.45 μm membrane filter.

Generally, the activities in reactor water can be separately sampled in three fractions: "insoluble", cationic and anionic (See Appendix B for details of sampling technique). Under normal operating conditions, among common activated corrosion products, only Fe-55, and Fe-59 are found truly insoluble.* They are all the nuclear reaction products of iron. Cr-51 is normally found in soluble anionic forms, most likely as $HCrO_4^-$ or CrO_4^{-2}. Cu-64 and Zn-65 are found mostly in soluble cationic forms and as a trace insoluble. Co-58, Co-60, Mn-54 and Mn-56 can be found in either soluble cationic or insoluble forms, depending on the iron crud concentration in reactor water. The Co-58 and Co-60 activities may not exhibit the same chemical characteristics, particularly with regard to "solubility", since Co-58 is the product of an (n,p) reaction on Ni-58 and Co-60 is the result of an (n,γ) reaction on Co-59.

* The solubility of iron oxide (α-Fe_2O_3) is extremely low in reactor water, <1 ppb at 280°C.

In most cases, the concentrations of the activities which are found as "insolubles" are much lower than their true solubility limits.** Many transition metal ions are easily adsorbed onto the insoluble iron oxides (α -Fe_2O_3), and most of them are transformed into more stable mixed oxides in the ferrite forms ($NiFe_2O_4$ or $CoFe_2O_4$). It has been experimentally observed that the ratio of Co-60 in "insoluble" to "soluble" forms depends on the iron oxide concentration in reactor water (see Figure 4-5).

4.2.3 Corrosion Product Spiking in Reactor Coolant During Power Transients

Corrosion product spiking in the reactor coolant during the reactor shutdown has been observed in practically all operating boiling water reactors (BWRs or PWRs). However, the spiking magnitude and the total released activities may vary from reactor to reactor, depending on the activity inventory and the characteristics of the deposit on the fuel cladding surfaces. The corrosion product deposit on the fuel cladding surfaces is known to have two distinguishable layers: the inner tenacious layer and the loosely attached outer layer. The characteristics of the deposit depend largely on the thickness of the deposit and the metallic elemental composition in the deposit (or metallic impurity level in reactor water). There are at least three major causes for the release of the corrosion product deposit from the fuel cladding surfaces during power transients:

(1) Mechanical and/or hydraulic disturbance.
(2) Coolant chemistry change caused by temperature and radiation field changes.
(3) Decreasing temperature which increases the solubilities of some corrosion product oxides in the deposit.

It is obvious that immediately after a reactor shutdown or scram, the crud burst occurs due to mechanical and/or hydraulic disturbance in the core. A portion of the outer layer is believed to be easily shaken off by the mechanical disturbance. Smaller crud spikes can also continue for some time after the reactor shutdown. Such small spikes may be attributed to continued water boiling at lower pressure and/or water chemistry upset at lower temperatures. Since the crud deposition on the cladding surfaces may be partially due to a weak interaction between the charged particles and the stationary surface, when

** For example, the solubility of CoO in BWR coolant is 10-20 ppb. Typical CoO concentration in reactor water is on the order of 0.1 ppb.

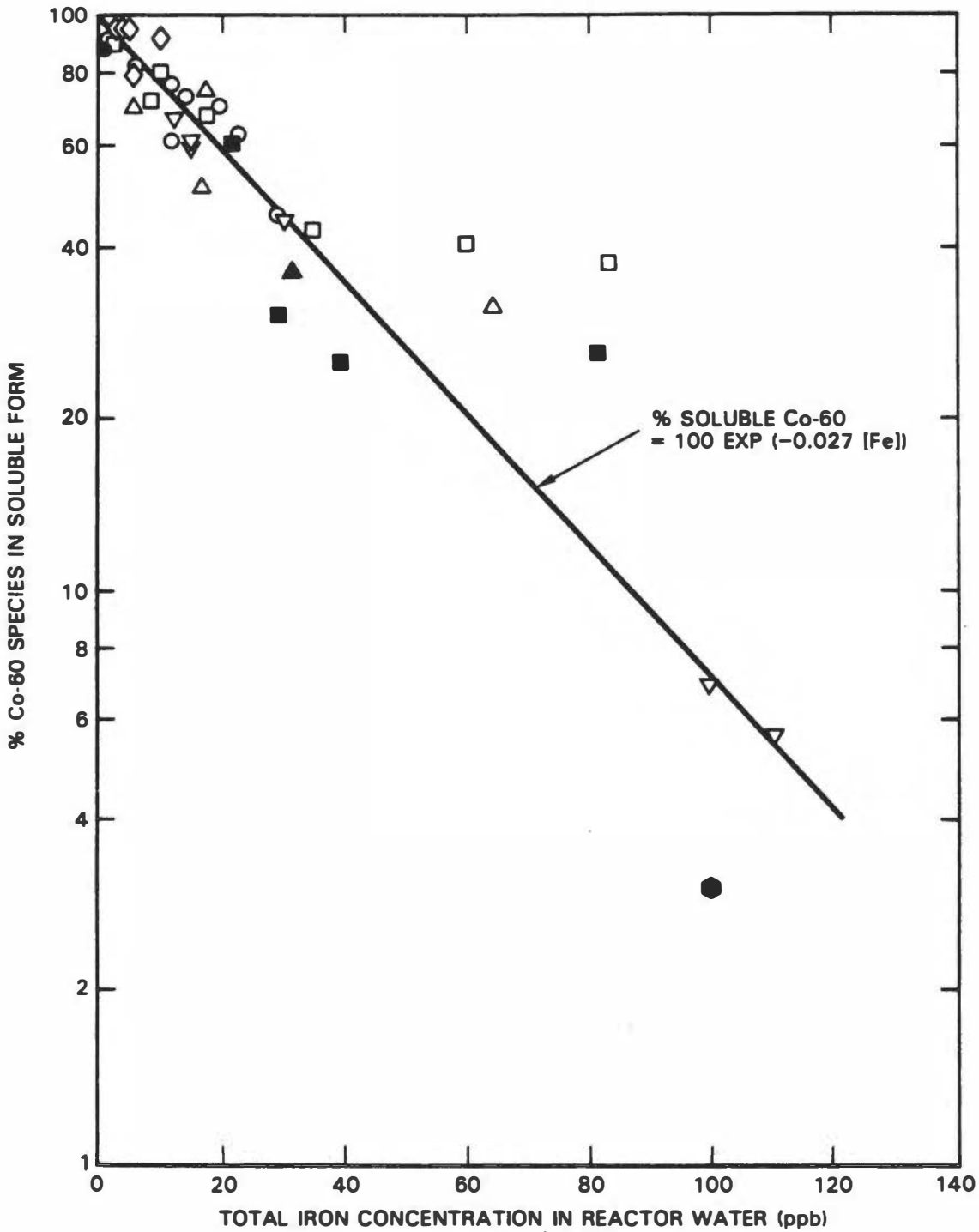

Figure 4-5. Percent Soluble Co-60 as a Function of Iron Concentration in Reactor Water

a slight change in water chemistry occurs, the weak attraction force may be broken and particles released from the surface.

The corrosion product spiking is not limited to the release of insoluble crud. The spiking of soluble species can sometimes account for the majority of the released activities. The decrease in the reactor water temperature is probably responsible for the release of soluble species, which is normally observed long after the first crud spike and the temperature is about 200°C. Based on the known solubilities of many corrosion product oxides (or mixed oxides) in water, it is predictable that most of the activities in the fuel deposit should become more soluble at lower temperatures. However, there are two factors (thermodynamics and kinetics) that control the dissolution rate of the corrosion product oxide during the cooling down process. At lower temperatures, the solubility is high but the dissolution rate may be quite slow. On the other hand, at elevated temperatures the dissolution process may be fast enough but the equilibrium is in favor of the insoluble form. A typical example of activated corrosion product spiking release during reactor shutdown is shown in Figure 4-6.

4.2.4 Corrosion Product Transport and Radiation Field Buildup in the Primary System

The major radiation source in the BWR for personnel exposure during shutdown maintenance has been identified to be the activated corrosion products, mainly Co-60, deposited on the primary system walls. The average shutdown radiation levels on the recirculation lines in some mature BWRs are shown in Figure 4-7. The radioisotopic composition of the contamination on the inside of the primary system piping has been determined using a shielded and collimated IGe detection system. A summary of the surface activity concentration data obtained in several reactors is presented in Table 4-4. The approximate conversion factors for the surface activity concentration to dose rate are given in Table 4-5. Obviously, the data are widely scattered, and the activity transport process is a complex chemical reaction which can be affected by many water chemistry parameters.

A semi-empirical phenomenological model has been developed[6] to describe and calculate the corrosion product transport in the BWR primary system. The basic transport phenomena are presented in a block diagram shown in Figure 4-8. Some major transport processes in the model are summarized below:

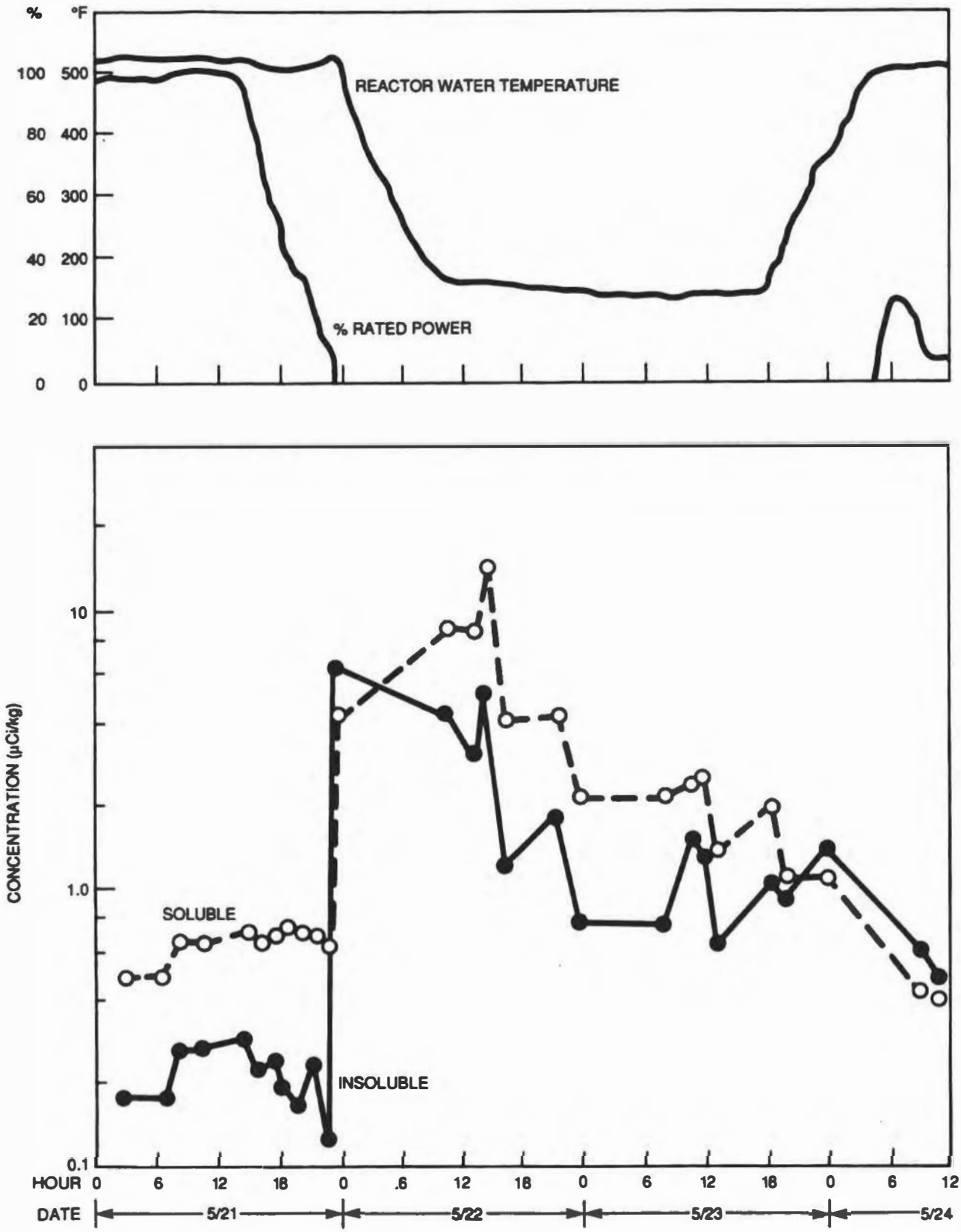

Figure 4-6. Variation of Co-60 Concentration in Reactor Water During Shutdown

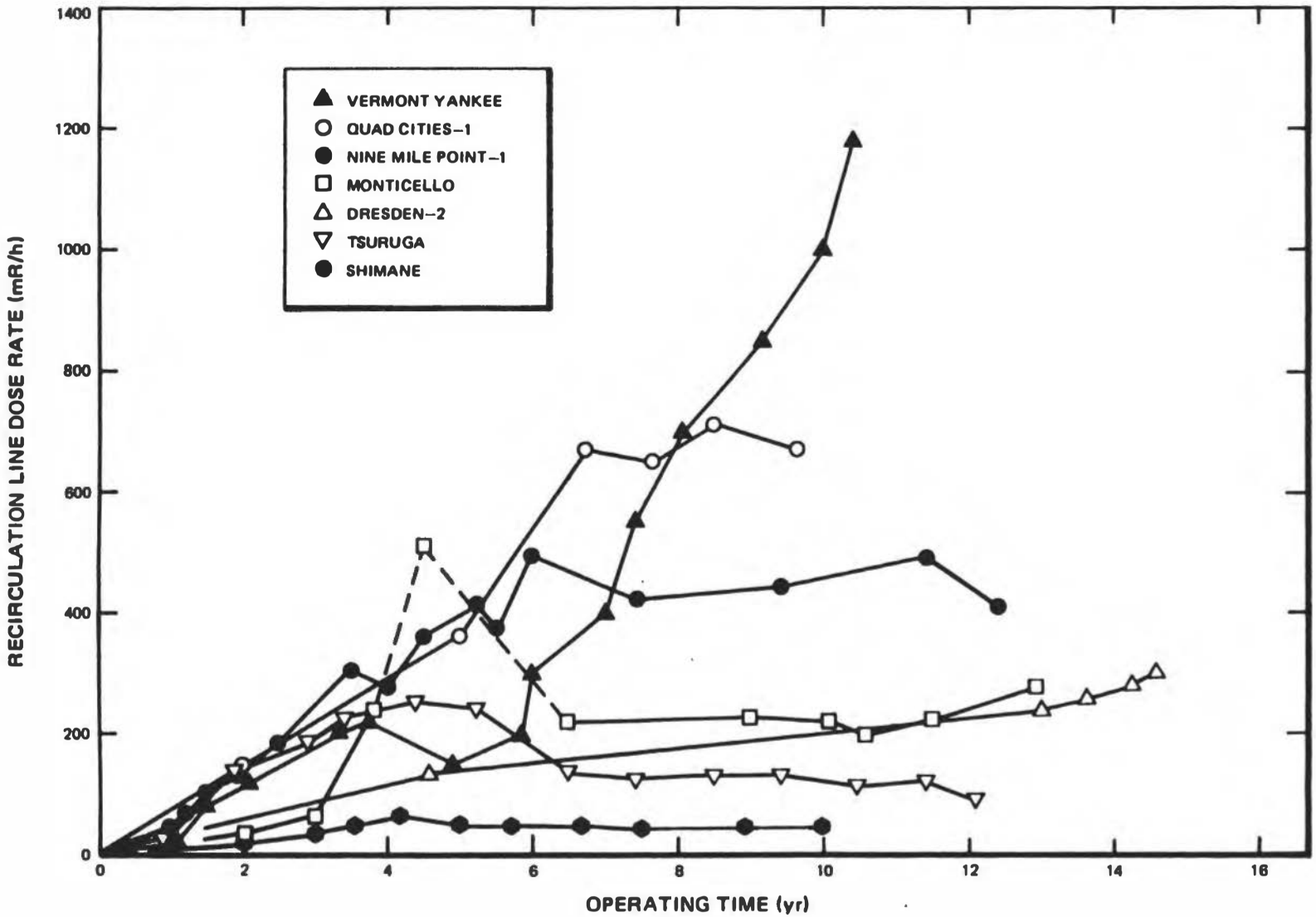

Figure 4-7. Radiation Fields on BWR Recirculation Lines (Ref. 7)

Table 4-4

AVERAGE RADIOISOTOPE CONCENTRATIONS ON BWR RECIRCULATION LINES
(Reproduced with Permission, EPRI NP-3114, Ref.3)

		Concentration ($\mu Ci/cm^2$)					
BWR	EFPY	Co-60	Co-58	Mn-54	Zn-65	Zr-95	Ru-103
Brunswick-2	0.32	0.3	0.9	0.2	0.2	0.05	N.O.[1]
	0.96	2.2	1.7	0.9	0.8	N.O.	N.O.
	2.19	5.1	2.1	1.1	0.9	N.O.	N.O.
Quad Cities-1	2.79	25.5	1.7	1.4	N.O.	N.D.[2]	0.3
	4.06	34.7	1.6	2.1	N.O.	3.3	4.5
	4.71	38.5	1.5	1.5	N.O.	0.9	3.9
	5.27	39.9	1.0	2.1	N.O.	N.O.	1.6
	6.05	38.3	1.6	1.6	N.O.	0.3	1.8
Quad Cities-2	2.85	27.9	0.9	1.0	N.O.	N.O.	0.3
	4.13	34.8	1.5	1.5	N.O.	2.1	2.8
	4.63	43.1	1.5	1.6	N.O.	3.4	4.9
	5.10	36.9	1.1	1.5	N.O.	N.O.	1.8
	5.80	39.3	1.3	2.3	N.O.	N.O.	1.2
Hatch-2	0.61	0.5	1.8	0.1	1.8	0.06	N.O.
Millstone-1	1.20	3.4	1.8	1.5	0.1	0.2	0.2
	1.28	3.3	0.7	1.0	0.1	0.04	0.1
	2.04	7.1	1.7	3.1	0.6	0.4	1.2
	2.72	5.8	1.1	1.6	0.1	0.9	2.2
	3.44	8.9	1.5	2.3	N.O.	0.8	3.2
Monticello	1.31	0.5	0.4	0.1	1.0	0.2	0.2
	1.88	1.2	1.3	0.3	1.2	1.0	1.2
	2.35	4.0	1.0	1.0	3.5	12.4	12.5
	2.83	7.9	1.3	1.1	4.5	7.8	9.8
	4.41	8.5	0.6	0.5	1.3	0.7	2.0
Nine Mile Point-1	1.80	12.6	1.5	1.5	0.3	0.6	0.7
	2.49	13.6	1.4	1.3	N.O.	0.8	0.9
	3.47	14.5	1.3	1.5	0.7	1.5	2.7
	4.44	19.5	1.5	1.2	N.O.	1.7	2.7
	5.82	21.0	1.5	1.4	N.O.	N.D.	N.D.
Tsuruga	3.45	5.7	0.6	3.4	N.O.	0.8	1.5
	6.09	5.3	0.7	1.4	N.O.	0.02	0.7
Shimane	3.55	1.8	0.6	0.2	N.O.	N.O.	N.O.

[1] N.O. - Not observed
[2] N.D. - Not determined

Table 4-5

CALCULATED DOSE RATE CONVERSION FACTORS FOR 20-28 IN O.D. PIPE*
(mR/h per μCi/cm^2)

Wall thickness (inch)	Co-58 (0.81 MeV)	Mn-54 (0.834 MeV)	Zn-65 (1.12 MeV)	Co-60 (1.25 MeV)
0.90	7.39	7.71	6.10	27.30
0.95	7.05	7.36	5.85	26.15
1.00	6.70	7.00	5.60	25.00
1.05	6.36	6.65	5.35	23.85
1.10	6.01	6.29	5.10	22.70
1.15	5.67	5.94	4.85	21.55
1.20	5.32	5.58	4.60	20.40
1.25	4.98	5.23	4.35	19.25
1.30	4.63	4.87	4.10	18.10
1.35	4.29	4.52	3.85	16.95
1.40	3.94	4.16	3.60	15.80
1.45	3.60	3.81	3.35	14.65
1.50	3.25	3.45	3.10	13.50

* Data obtained from Reference 6, Nucl. Tech. 54, 253 (1981)
Co-60 : Y = 48.0 - 23. X
C0-58 : Y = 13.6 - 6.9 X
Zn-65 : Y = 10.6 - 5.0 X
Mn-54 : Y = 14.1 - 7.1 X
Y = conversion factor, mR/h per μCi/cm^2 at 15 cm from pipe surface
X = wall thickness, inch

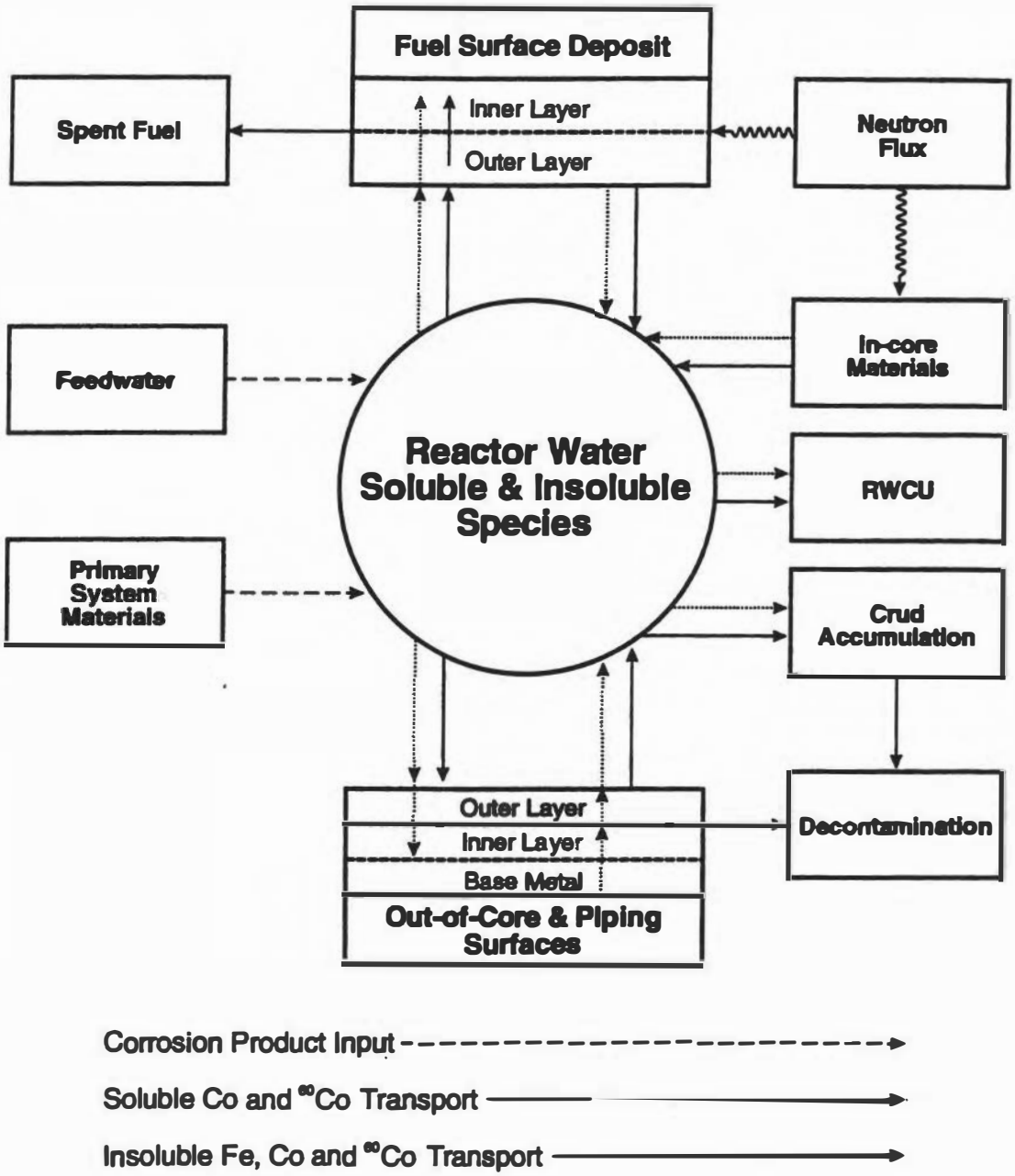

Figure 4-8. Block Diagram for Co/Co-60 Transport Model

- Metallic impurities in ionic, colloidal, and insoluble oxide forms (called crud) are released to the condensate and feedwater from hardware and piping surfaces and subsequently appear in the reactor coolant. In some plants forward-pumped heater drains contribute corrosion products and in all plants there is leakage through the condensate treatment system.

- Metal ions are also released to the coolant from the corroding surfaces in the primary system. Colloids and particles of oxide or hydroxide are formed in the coolant when the saturation limit is exceeded.

- Some interactions between soluble ionic species and crud particles occur and result in adsorption (scavenging) of ionic species on the crud particles suspended in the water.

- Both crud and soluble species deposit on the fuel surface with different mechanisms. The nature of the crud plays an important role in the rate of soluble species deposition. Some of the loosely attached deposit in the outer layer may be transformed into a tenacious layer on the fuel surface.

- The deposits on the fuel surface and the in-core structure materials are activated by neutrons. The radioactive species are released from in-core materials by dissolution and wear, and the species are released from fuel surface deposits by erosion and spalling caused by hydraulic shear forces. Dissolution and ion exchange processes also are other possible release mechanisms.

- The radioactive species redistribute themselves into "soluble" and "insoluble" species, depending on the solubility of the oxide and the concentration of iron crud which acts as a scavenger. Soluble and insoluble radioactive species deposit on the out-of-core surfaces by different mechanisms. Material corrosion plays an important role in soluble species deposition, and slow ion-exchange reactions may also be involved (see below).

- Double layer formation on out-of-core surfaces is caused by base metal corrosion and water-borne crud deposition. Transformation of the oxidation state on the material surface takes place and a small fraction of the corrosion products, both radioactive and nonradio-active, is released mostly from the outer oxidized layer into the coolant.

4.2.5 Summary of Major Laboratory Test Results for Co-60 Deposition on Stainless Steel Surfaces

An extensive research program[7] has been completed to understand the fundamental mechanisms of the Co-60 deposition on stainless steel surfaces. The effects of key water chemistry parameters on the Co-60 deposition have been identified, and some major results are qualitatively summarized below:

- The Co-60 activity buildup on as-received stainless steel samples under normal water chemistry conditions can be described by a simple logarithmic rate law. Prefilming the stainless steel surfaces under proper conditions has been shown to reduce the initial activity buildup (Figure 4-9).

- High water conductivity in water (~0.5 μS/cm at 25°C) has shown obvious enhancement in Co-60 buildup on all samples tested. The enhancement effect is more significant in slightly basic solution (pH ≈ 8 at 25°C) (Figure 4-10).

- Maintaining a low concentration (5-15 ppb) of non-radioactive metallic ions in solution has been found to significantly suppress the Co-60 activity buildup on stainless steel samples. Zinc and nickel are obviously more effective than copper in reducing the activity buildup (Figure 4-11). The effect of metallic ions in water can be explained by assuming an ionic competition for the limited adsorption/reaction sites on the corroding surface. The number of Co-60 ions which can reach the reaction sites are apparently diluted by other competing non-radioactive ions.

- Under hydrogen water chemistry (HWC) conditions, where the dissolved O_2 was approximately 15 ppb compared to approximately 200 ppb under NWC conditions, the activity buildup rate was apparently larger than that predicated by a logarithmic corrosion rate law. It is of particular interest to note that when the samples, prefilmed or as-received, had previously been exposed to NWC and then changed to HWC, the activity level started to increase at a higher deposition rate (see Figure 4-12). Although it is not certain how the HWC affects the existing oxide film, it is apparent the oxide film has become more receptive to Co-60 deposition under HWC conditions. One possible explanation is that the oxide layer may have experienced a "chemistry shock" when the O_2 level in

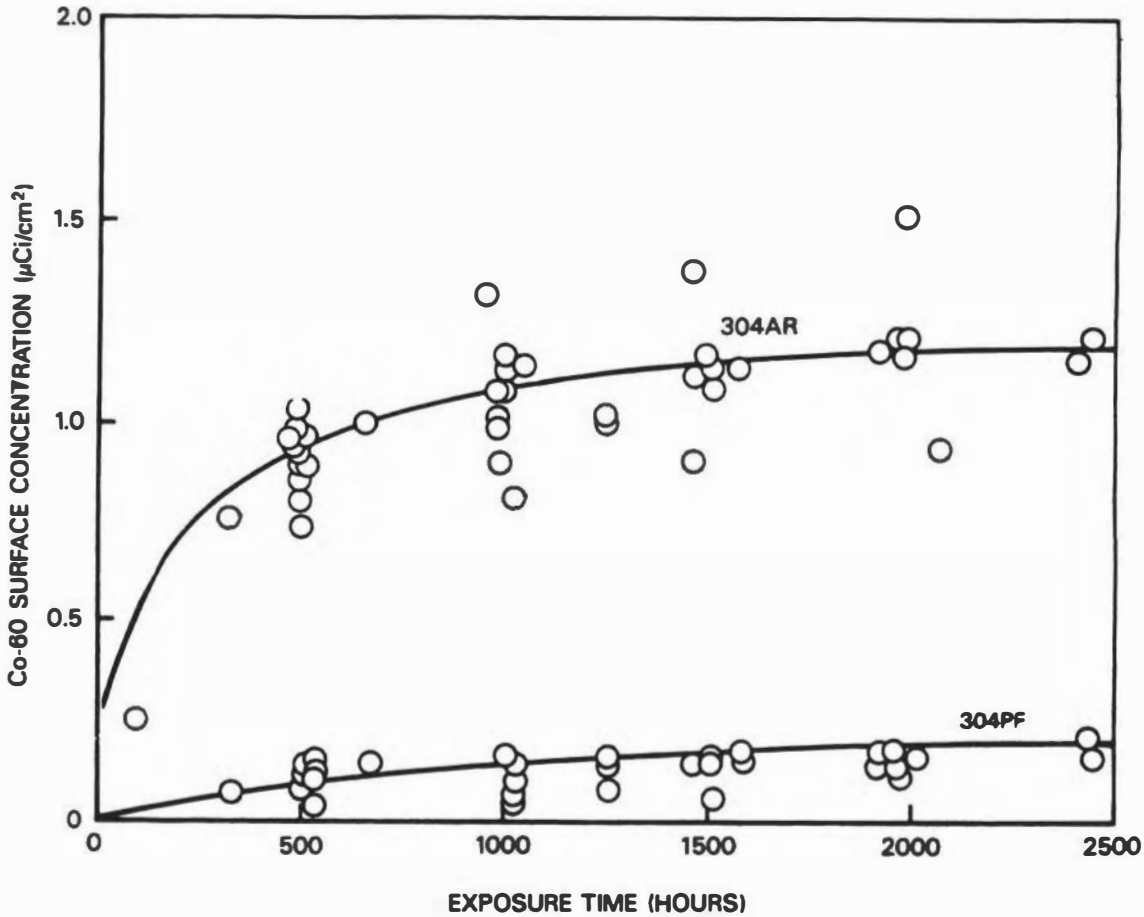

Figure 4-9. Co-60 Deposition on As-Received (304AR) and Prefilmed (304 PF) 304 SS Samples Under Normal Water Chemistry Conditions. The curves represent the best fit of the data to a logarithmic rate law:

$$A = RC \ln (kt+1), \text{ and}$$

$$A = RC [\ln(kt+1) - \ln(kt_o+1)]$$

where:

- A = Co-60 activity on surface, μCi/cm
- R = deposition rate constant, kg/cm
- k = corrosion kinetic constant, hr^{-1}
- C = Co-60 concentration in water, μCi/kg
- t = exposure time, hr
- t_o = the time in hours of prefilming period under the same water chemistry conditions

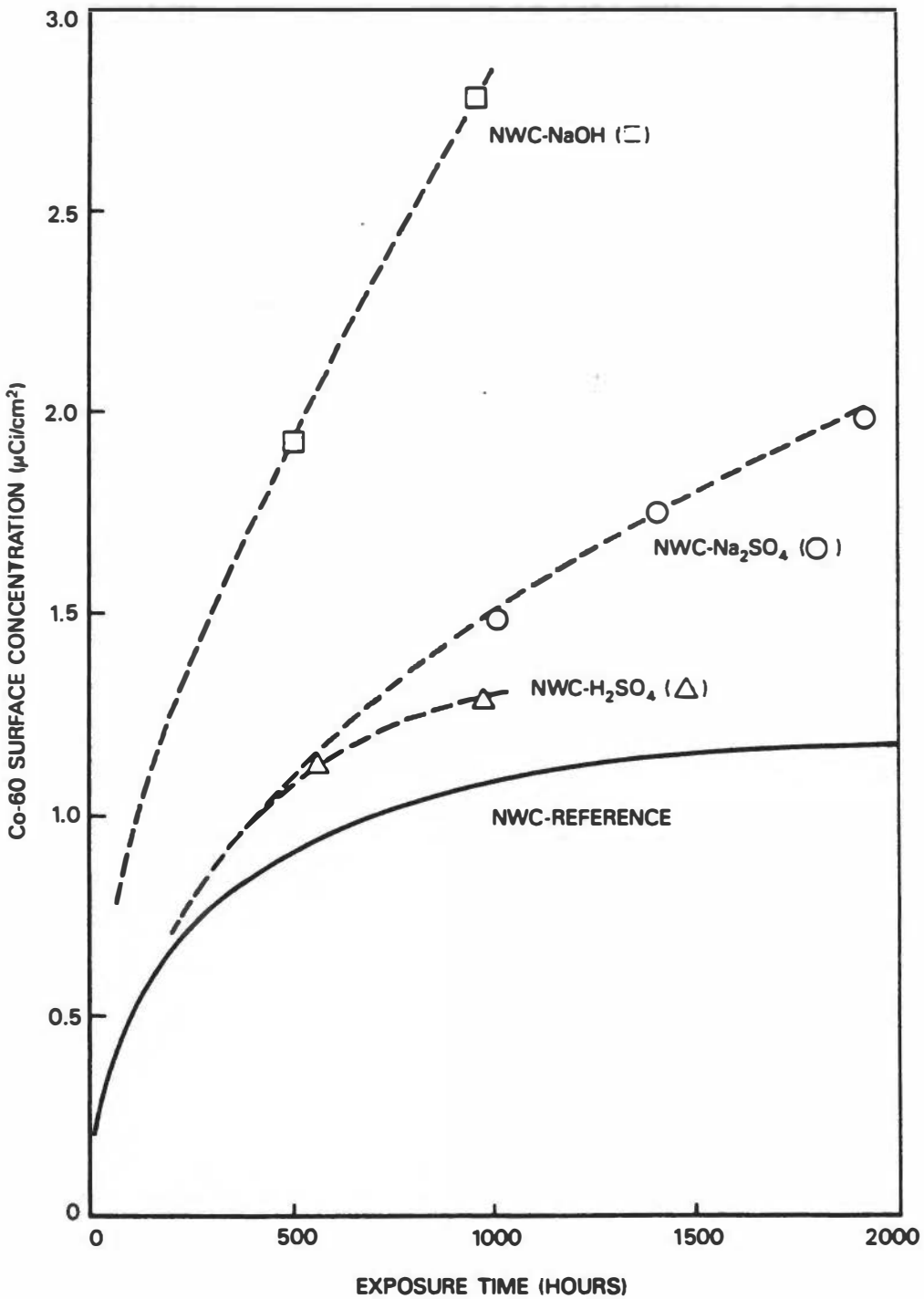

Figure 4-10. Effects of Chemical Additives on Co-60 Deposition on As-received 304 SS Samples Under Normal Water Chemistry Conditions

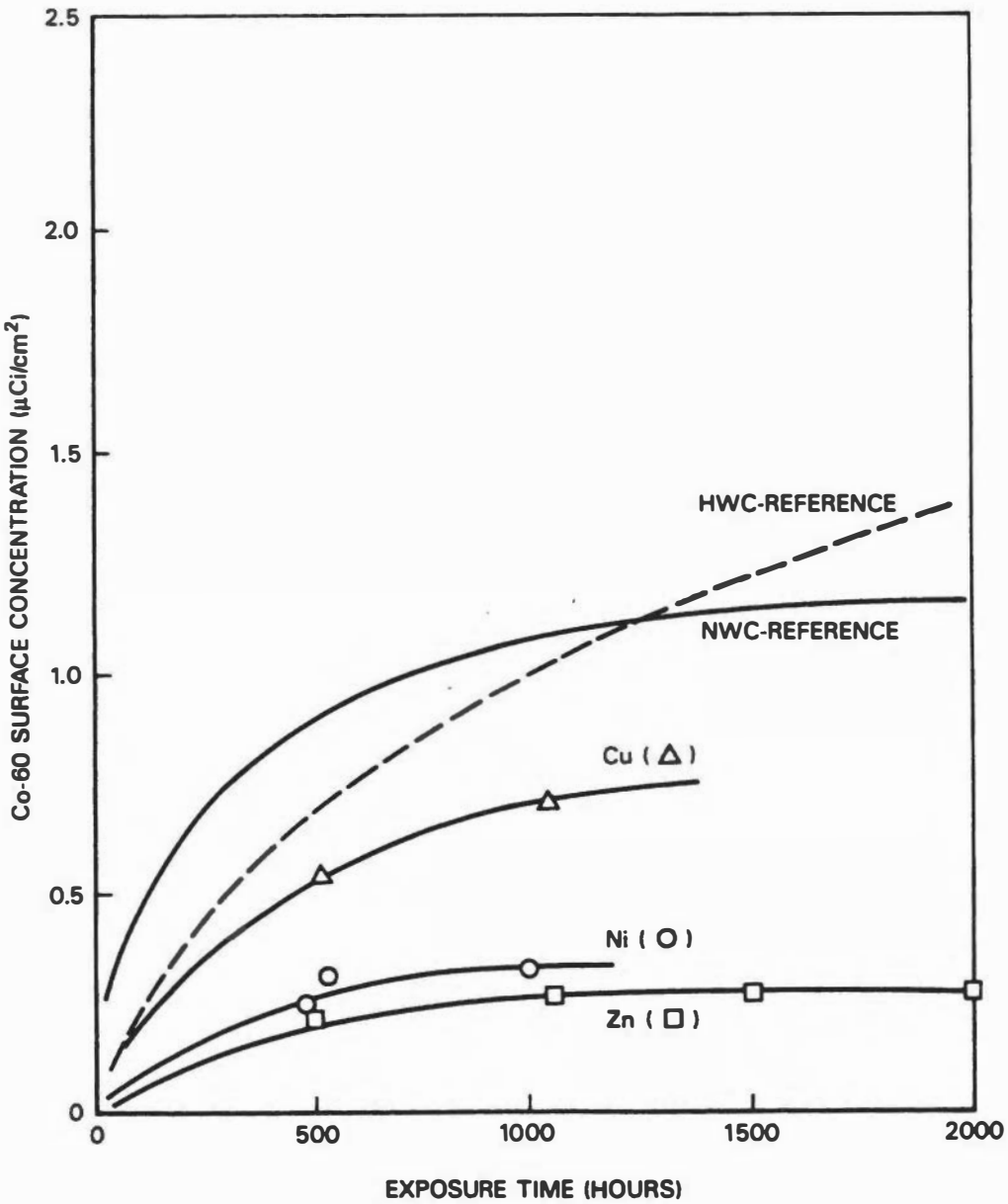

Figure 4-11 Comparison of Co-60 Deposition on As-Received 304SS Samples Under Normal Water Chemistry Conditions with Metallic Ions at 15 ppb

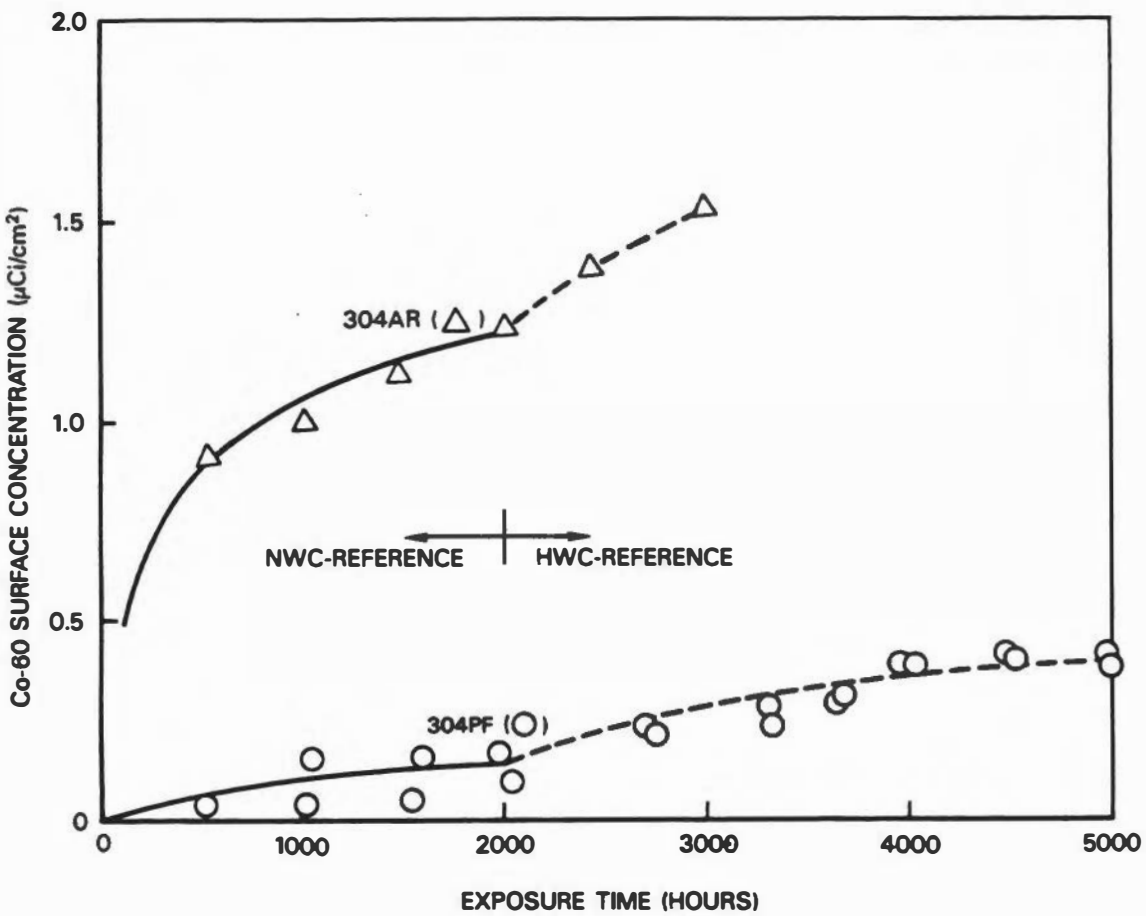

Figure 4-12. Variation of Co-60 Deposition on 304SS Samples Changing from Normal to Hydrogen Water Chemistry

water has changed from ~200 ppb to ~20 ppb. The oxide morphology is expected to undergo some transformation to equilibrate with the new O_2/H_2 environment in water. Consequently, some oxide particle surfaces may become more receptive to Co-60 during this transient period until a new equilibrium is established. More recently, Lin, et al.[20] have suggested that the formation of Cr-enriched oxides under HWC conditions could enhance the deposition of Co-60 on stainless steel surfaces.

- The mechanisms of Co-60 deposition on stainless steel surfaces have been hypothesized, based on the known stainless steel corrosion process and the observed test results. The proposed mechanisms, which are summarized in Table 4-6, are able to explain most of the test results obtained in the present program. It is clear that the presence of metallic ions in water is the dominant controlling factor Co-60 deposition. However, the water chemistry also plays a key role when the oxide film thickness and characteristic are considered in the Co-60 deposition process.

More test results obtained under hydrogen water chemistry (HWC) conditions, detailed discussion on the reaction mechanisms, prefilming techniques, and the oxide film characterization have been reported elsewhere.[7]

Table 4-6

SUMMARY OF COBALT DEPOSITION MECHANISMS

Reaction	Location	Relative Rate and Key Controlling Factor
• Direct chemical reacton	Basal film/oxide interface	Very fast. Limited by corrosion rate; affected by metallic ions in water
• Absorption/ recrystallization	Oxide layer	Slow. Increasing with water pH; increasing with Cr-enriched oxides under HWC condition; affected by metallic ions in water
• Ion-Exchange reaction	Oxide layer	Slow. Increasing with excessive metallic ions in oxide layer; affected by water chemistry changes.

4.2.6 Radiation Fields and Personnel Exposure Reduction at BWRs

The main objective of radiation control and reduction in a nuclear power plant is to minimize the collective personnel exposures in accordance with the spirit of ALARA. It is clear that the best run reactors with low radiation exposures are those having highest purity in reactor water containing extremely low levels of metallic impurities.(18)

Reduction of radiation fields is a major step toward the reduction of occupational radiation exposure, but other approaches, such as improvement of maintenance equipment and procedures, and reduction of maintenance requirements, could also significantly reduce the total exposure. Increasing shielding on the hot-spot, control of contamination dispersion, and decontamination would be effective in reducing radiation fields.

The radiation fields commonly measured in a BWR at the straight section of recirculation pipes are considered to be most representative for the purposes of radiation buildup trending and comparing with the similar fields in other plants. It is believed that radiation field buildup in many other locations in the primary system may not occur by similar mechanisms nor at the same rate.

Furthermore, occupational exposures are generally accumulated at high radiation field locations where maintenance work is frequently needed. The recirculation line is not normally one of such locations. Therefore, occupational exposures are not always expected to be proportional to the contact dose rates measured on the recirculation pipes. A long-term solution to the problem is to reduce the activity production in the core and minimizing the activity concentrations in the reactor water. Some fundamental approaches to controlling radiation field buildup in BWRs are discussed elsewhere.(18,19)

4.3 ACTIVATED CORROSION PRODUCTS IN PWRs

4.3.1 Deposition of Corrosion Products on Fuel Surfaces

Unlike BWRs, corrosion product deposition on fuel surfaces depends on the solubilities of crud which consists of mostly substituted nickel ferrite, $Ni_xFe_yO_4$, where $x+y=3$ and $x/y \approx 0.25$. After careful examination of numerous core crud samples, it was concluded(2) that the corrosion product transport in the PWR primary system is a continuous process of crud transport from one surface to another via the primary

coolant. The crud can be quite mobile, and the major factors affecting crud transport (deposition/dissolution) are believed to be the coolant pH and the hydrogen concentration. Some qualitative observations which have been reported elsewhere[8,9,10] are summarized below:

- The axial thickness distribution of crud seems to be inversely proportional to the local power. A typical axial power and temperature distribution in a PWR core is shown in Figure 4-13.

- The activity profile along the fuel assemblies shows little correlation with neutron flux (Figure 4-14), since one would expect the highest activity at or below the middle of the assemblies. A typical set of radiochemical data is given in Table 4-7.

- Radioactivity in a given core crud sample is noted to have very little correlation with the chemical composition of that sample. Despite a very wide variation in parent element ratios, the activated product ratios are noted to be nearly uniform. These data suggest that (1) there is a very high crud turnover rate in which there was no strong bond among the particles in the crud core deposits, and (2) activated isotopes were released into the coolant and circulating in the system and depositing on material surfaces, nearly independent of the target materials.

Although it is known that the major circulating and core-deposit crud are not magnetite (they are substituted nickel ferrites), it is worthwhile to use the well-known chemical properties of magnetite to qualitatively explain the transport behavior of corrosion product on the fuel surfaces. The dependence of solubility of magnetite on pH and temperature has been published by Sweaton and Baes [11] and are partially reproduced in Figure 4-15. "Depending on the pH and the temperature, the temperature coefficient of the solubility of iron can be either negative or positive. Thus, iron may be dissolved from the fuel deposit or precipitate onto the fuel surface depending on the temperature difference (ΔT) between the fuel clad and bulk water. The driving force is related to ΔT, which, in turn, is a function of power level and axial and radial location in the core."[8] It is probably more appropriate to describe the transport of corrosion products as functions of the coolant system pH at average temperature (T_{av}).

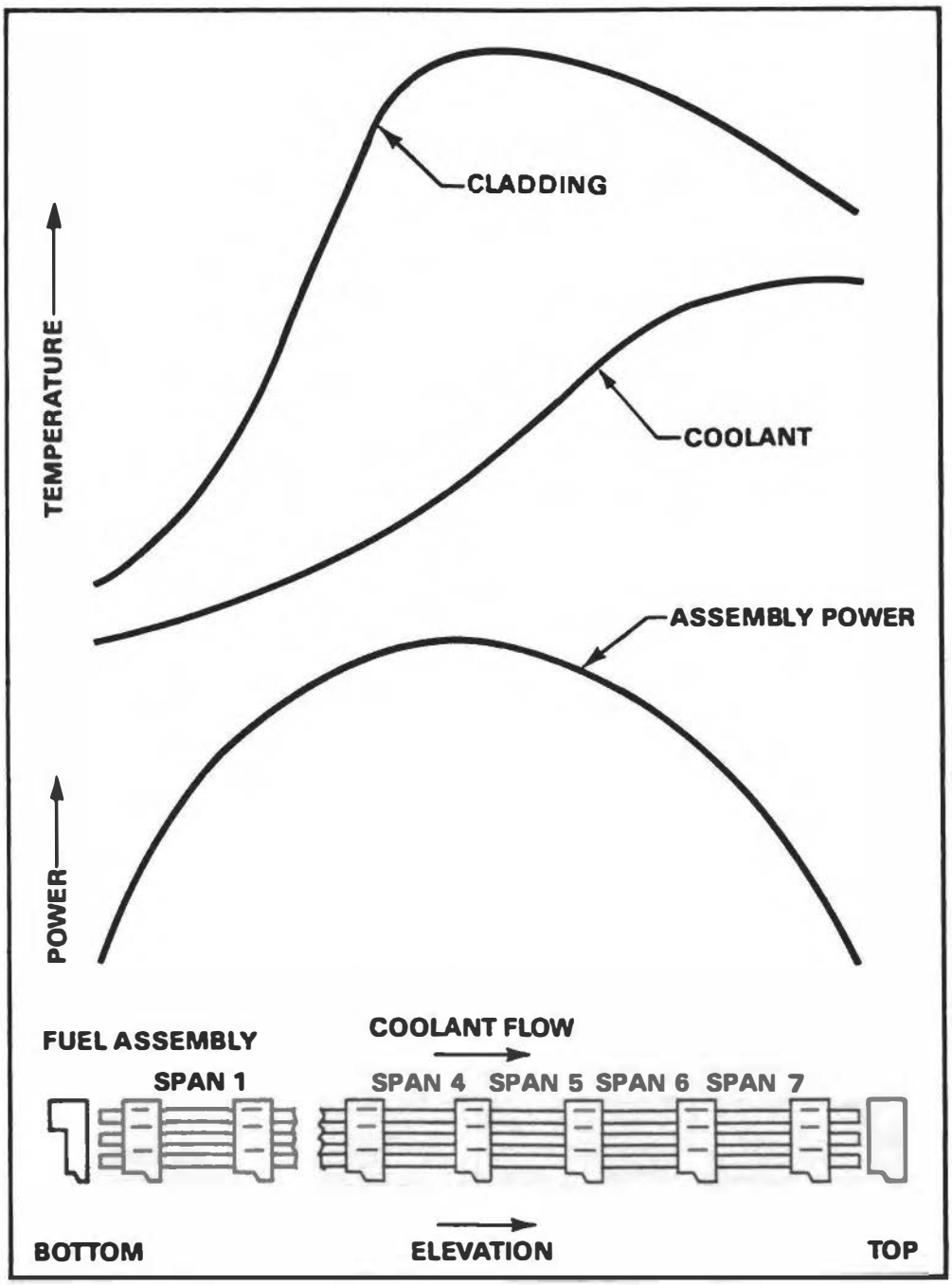

Figure 4-13. Typical Axial Power and Temperature Distribution in a PWR Core (Reproduced with Permission, EPRI NP-4247, Ref. 9)

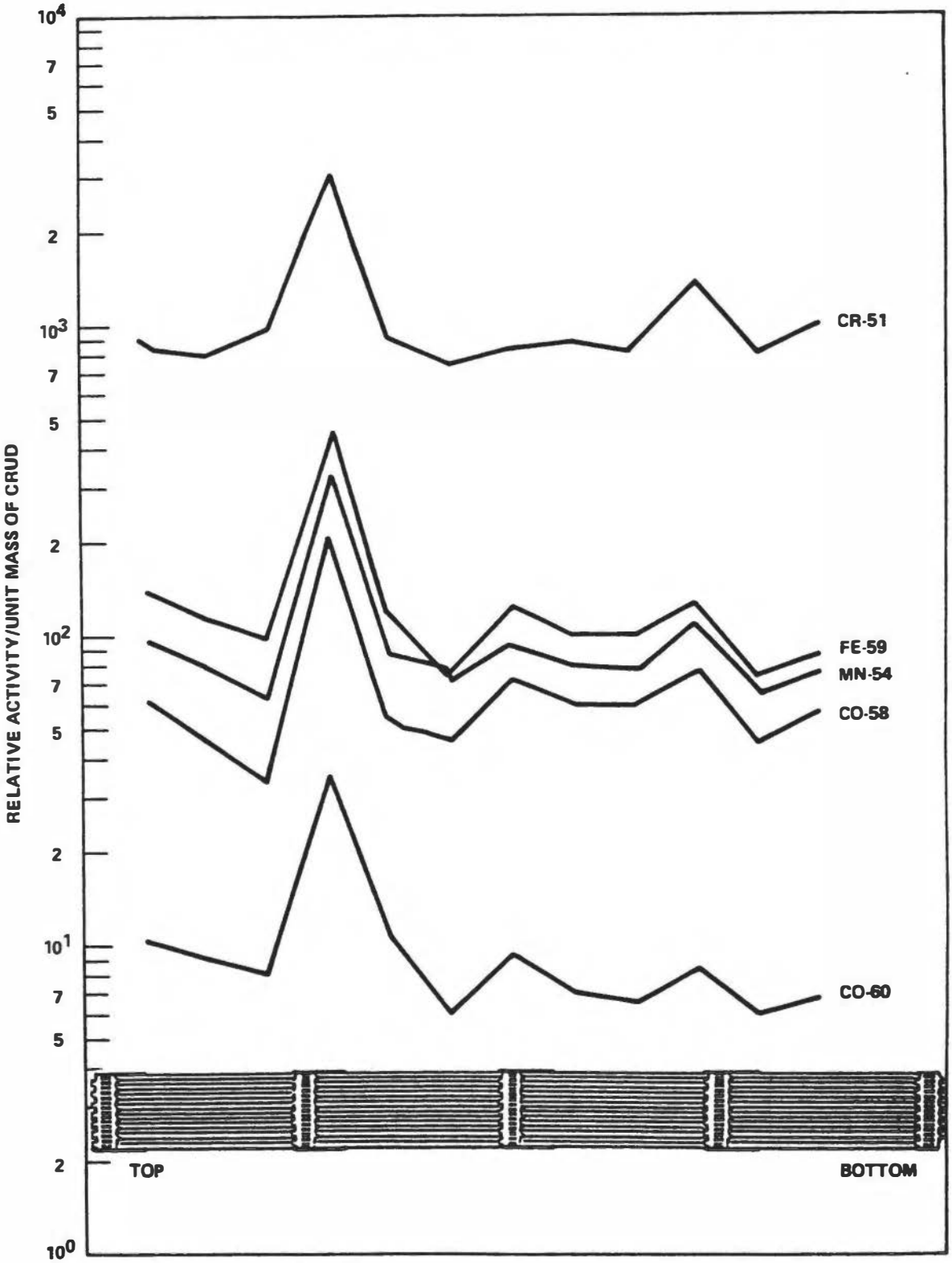

Figure 4-14. Relative Specific Crud Activity of Fuel Deposits (Reproduced with Permission, EPRI NP-4246, Ref. 10)

Table 4-7

AVERAGE RADIOCHEMICAL COMPOSITION OF DEPOSITS ON THE FUEL SURFACE IN A PWR AFTER ONE CYCLE
(Reproduced with Permission, EPRI NP-3463, Ref.8)

Core Region	Span	Specific Activities in μCi/mg crud ± σ					Co-58
		Cr-51	Fe-59	Mn-54	Co-58	Co-60	Co-60
	7	68±18	15±4	18±3	215±40	15±4	15±1
A	6	ND[a]	ND	30±8	916±858	27±9	37±35
	5	52±26	13±5	17±5	211±51	14±8	16±2
	7	50±6	12±1	18±3	226±24	12±2	19±3
B	6	65±11	16±5	24±6	261±46	15±2	17±3
	5	71±9	13±2	20±2	301±19	14±1	21±2
	7	35±8	10±3	16±5	198±61	8±1	24±4
C	6	—	—	—	—	—	—
	5	25±1	6±1	10±1	136±15	6±1	25±6
Average	7	52±14	13±3	18±3	236±35	12±3	19±4
Average	6	65±10	16±7	27±5	613±668	21±9	28±26
Average	5	57±22	11±5	17±4	239±79	12±4	21±5
Core Avg.		66±37	13±7	20±4	337±387	15±7	22±14

[a]ND - Not determined.
Error indicators are standard deviations

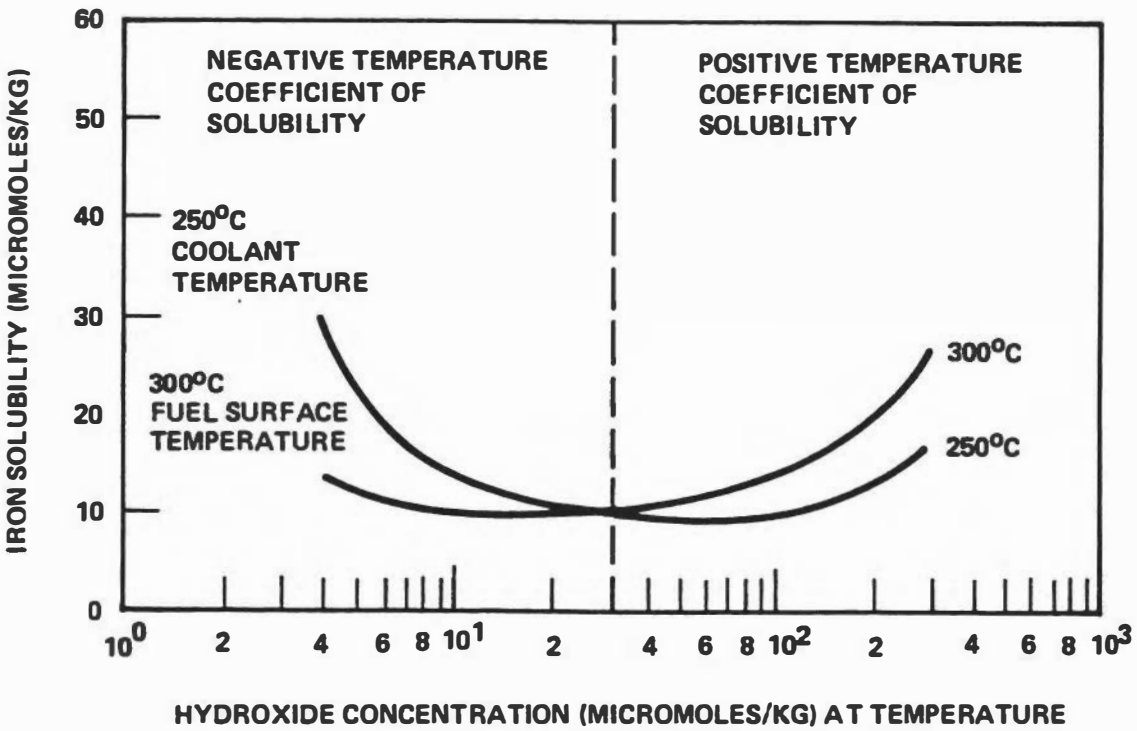

Figure 4-15. Iron Solubility for Magnetite as a Function of Hydroxide Concentration at 250°C and 300°C, at Hydrogen Partial Pressure of 1 atm (Reproduced with Permission, EPRI NP-3463, Ref. 8)

4.3.2 Radiochemical Composition in PWR Coolants

The radiochemical composition of a typical PWR reactor coolant given by American National Standard Radioactive Source Term[5] is compared with the BWR data in Table 4-2. The average activity concentrations of selected nuclides measured in two reactors are compared in Table 4-8.

If one can extrapolate the measurement at ambient to operating temperatures in the coolant, the data given in Table 4-8 suggest that Cr-51 tends to occur in reactor coolant predominately in solids, while others have been found in both soluble and insoluble forms. However, Mn-54 seems to be more soluble and Co-58, Co-60 and Fe-59 are more insoluble.

At shutdown, the spiking activities are dominated by the solubles (Table 4-8). Typical spiking data for Co-58 and Co-60 are shown in Figure 4-16. The cobalt activities increased dramatically when boration was essentially completed and the coolant temperature was reduced below 300°F. Another spike occurred after hydrogen peroxide had been added.

One must be cautious when the reactor coolant corrosion product data are evaluated. Problems in withdrawing representative samples from a PWR primary coolant through long sample lines are well recognized.[10,12,13]

Unlike the high-purity water in the BWR coolant, the PWR coolant chemistry is rather complex, and it presents a special environment for some radiochemical species which may easily change their solubilities and undergo certain interactions with the oxide film on the sample line when the coolant is cooled down and water pH is changed. Experience at Ringhals[13] suggests that, in general, the measured concentrations of some activated corrosion products do not bear any useful relationship to the concentrations of corrosion products in the coolant at operating temperatures. The measured concentrations of some corrosion products (e.g., soluble Co-60 and Mn-54) are strongly dependent on sampling flow rate and the boron concentration. (See sampling procedures in Appendix B.)

Table 4-8

AVERAGE ACTIVITIES OF SELECTED NUCLIDES IN REACTOR COOLANTS FROM THE BEAVER VALLEY AND TROJAN PLANTS (Activities in nCi/kg) (Reproduced with Permission, EPRI NP-3463, Ref. 8)

	Beaver Valley				Trojan			
	Operating		Shutdown		Operating		Shutdown	
Nuclide	Solids	Solutes	Solids	Solutes	Solids	Solutes	Solids	Solutes
Cr-51	159±209	3.2±1.2[a]	62	ND[c]	232±362	41[b]	466	1364
Mn-54	8.9±15.8	69±41	6.3	2994	17±18	21±40	55	113
Fe-59	12±17	6.8±5.3	281	ND	17±21	10±10	37	52
Co-58	162±240	183±403	1135	1.7×10^5	437±657	210±249	680	4253
Co-60	45±82	30±35	96	5823	22±27	9±11	86	384
Co-58/Co-60	3.9±3.0	11±20	12	29	15±6	34±17	8	11

Error indications are standard deviations. Entries without error indications are single measurements.

[a] Average of four measurements; nine additional measurements were ND.

[b] One real value, the remaining measurements were ND.

[c] ND = Not detected.

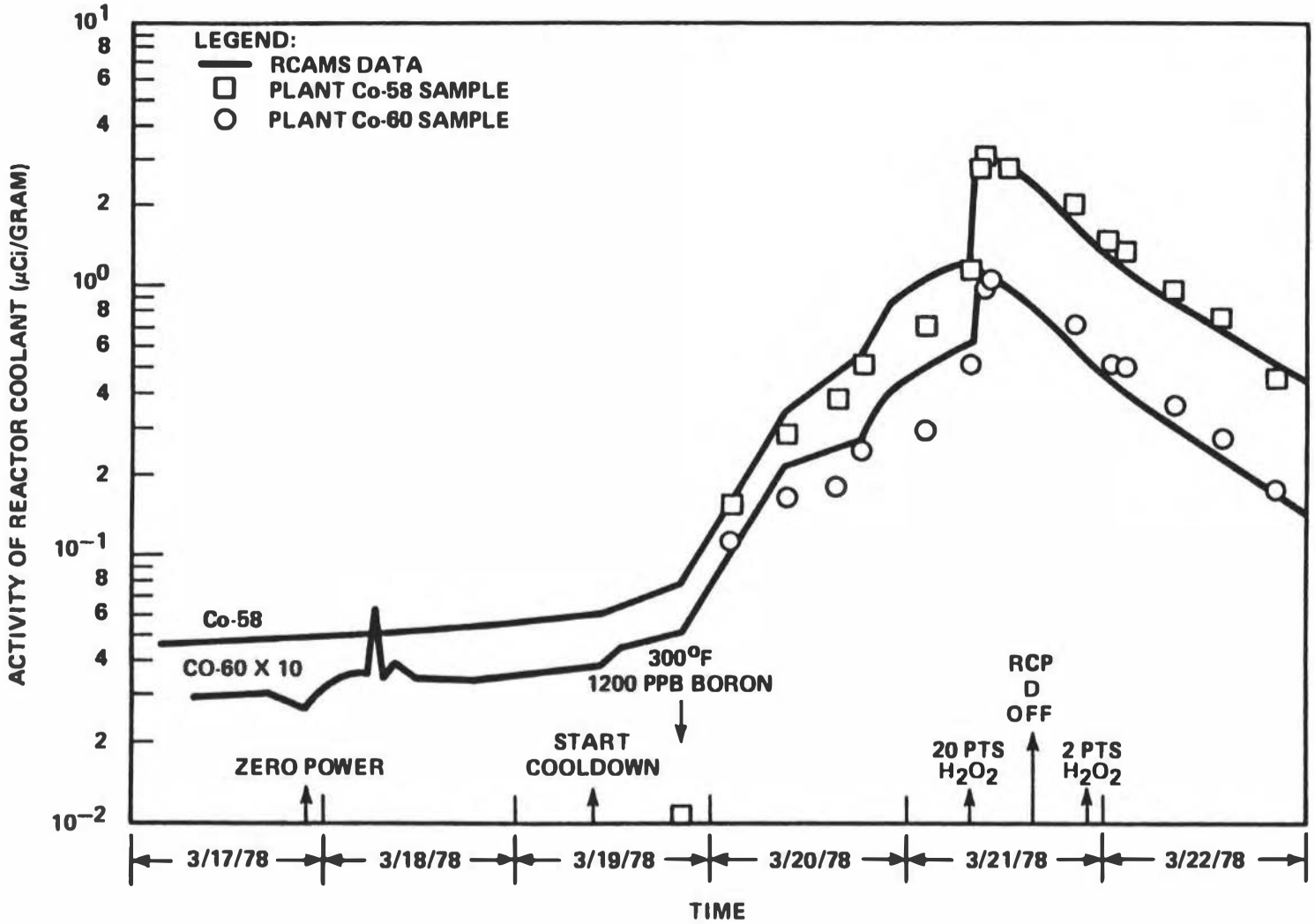

Figure 4-16. Concentrations of Co-58 and Co-60 Activities in a PWR Primary Coolant During Shutdown Operation (RCAMS = Reactor Coolant Activity Monitoring System (Reproduced with Permission, EPRI NP-3463, Ref. 8)

4.3.3 Corrosion Product Deposition On Out-Of-Core Surfaces

The corrosion product activity transport processes and radiation buildup on the main coolant piping and steam generator have been the main subject of a recent investigation.[8,9] Coolant chemistry in PWRs plays an important role in the radiation field buildup. The primary long-term source of radiation fields in either BWR or in PWR plants is Co-60, but in PWR Co-58 can also be a significant source, especially early in life. Cobalt-58 has a half-life of 71 days and hence reaches an equilibrium level in a few months.

A review of the data obtained from the various out-of-core locations shows that the specific activity of the crud deposits varies, depending upon location and the base material. A comparison of the surface activity concentration on the piping, steam generator tubing, and fuel surfaces of a Westinghouse PWR plant is shown in Figure 4-17. The difference in activity deposition could be caused by the corrosion mechanism of Inconel tubing versus that of stainless steel piping, the effects of the smooth surface of the tubing versus that of the rougher piping surface, or the amount of activity and flow rates of the coolant passing through a tube compared with that in a section of piping. In terms of Co-60 activity, inventories on the various surfaces are approximately 1000 Ci on the core, 500 Ci on the steam generator tubing and 100 Ci on the piping after several years of operation.[10]

In the primary coolant system, the corrosion product activities (mainly Co-60 and Co-58) can be transported throughout the system in either soluble forms or insoluble crud. Because of the complexity of the coolant chemistry, it is almost impossible to quantitatively identify which form of the activity is more important. A mathematical model (CORA) has been developed to describe the transport of corrosion products in the PWR system[10]. The computer code nodal diagram is shown in Figure 4-18. Figure 4-19 shows the widely spread dose rate data measured on the steam generator channel head and the range of CORA results.

Recent studies on the role of coolant chemistry on PWR radiation field buildup[9,14,15] have concluded that control of pH is an important factor in reducing the radiation buildup. Lower radiation fields are generally observed at plants which were operated with constant, or higher, pH, and the fuel crud deposits were thinner. The effect of pH on the solubility and the mobility of the crud is obvious. The key in reducing the radiation field is to minimize the deposition of corrosion products on the fuel surfaces, where they are

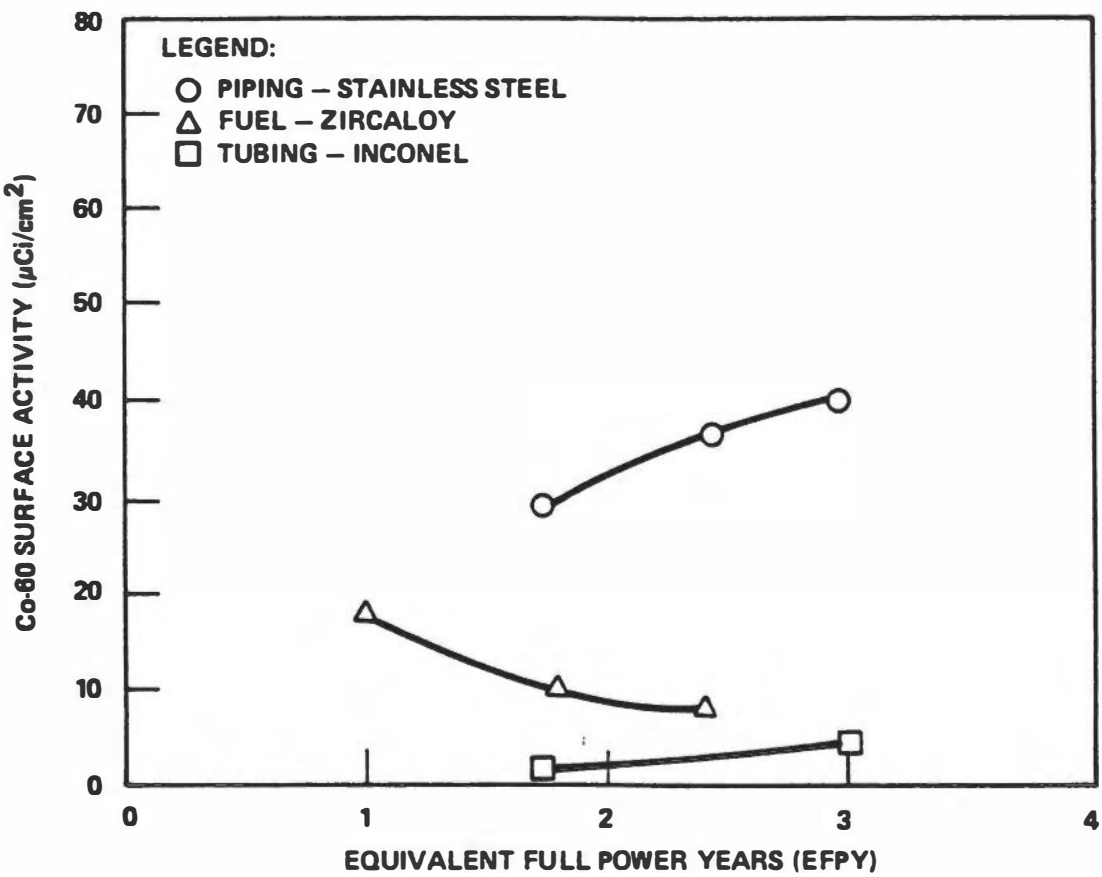

Figure 4-17. Comparison of Unit Surface Activities at Three Different Locations and Materials of Construction (Reproduced with Permission, EPRI NP-4246, Ref. 10)

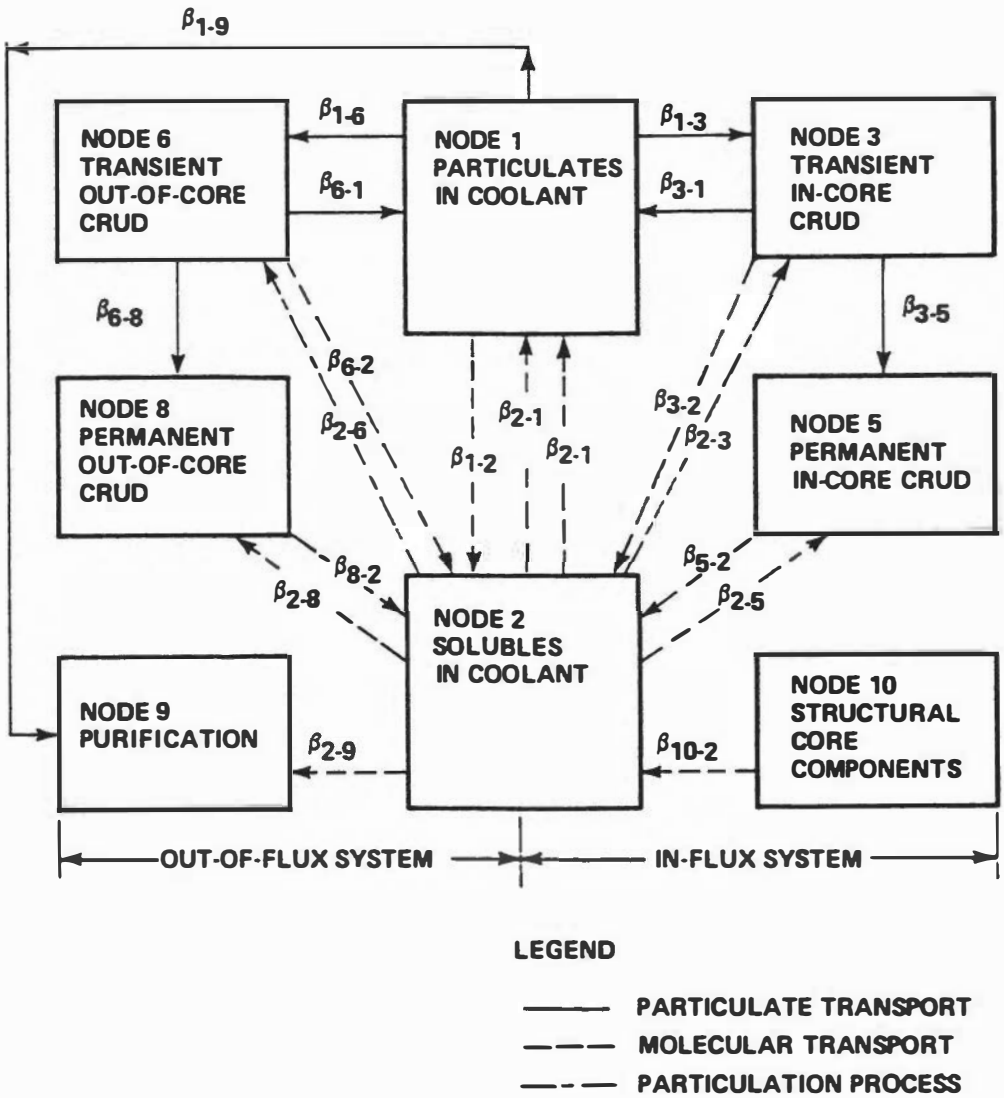

Figure 4-18. CORA Model Nodel Diagram
(Reproduced with Permission, EPRI NP-4246, Ref. 10)

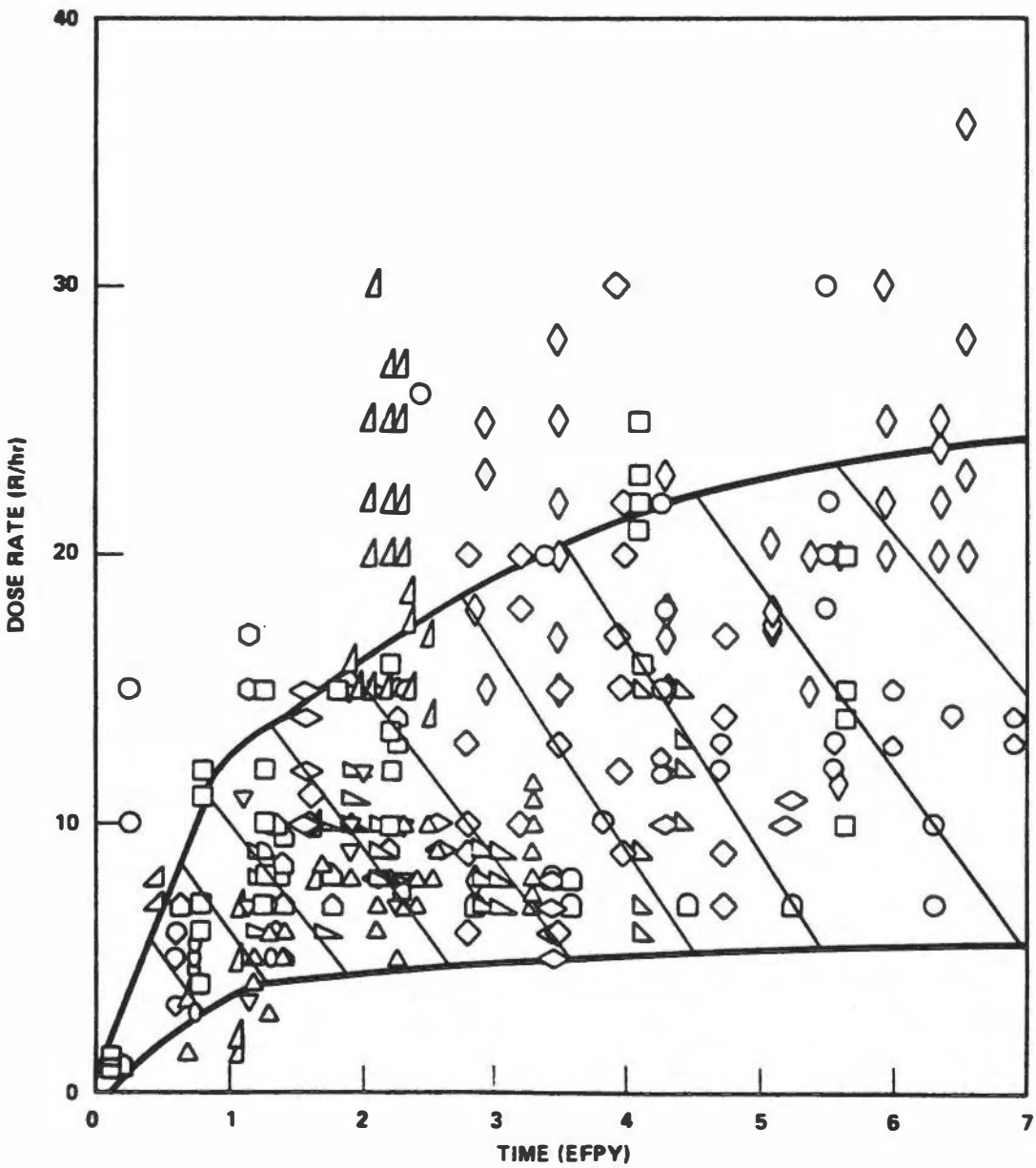

Figure 4-19. Measured Steam Generator Channel Head Dose Rates and Range of CORA Results (Reproduced with Permission, EPRI NP-4246, Ref. 10)

being activated by the neutron flux and subsequently being released and transported to other parts of the primary system. Laboratory measurements[16] of the solubility of several nickel ferrite stoichiometries as a function of pH, temperature and dissolved hydrogen indicate that solubilities tend to increase at higher temperatures when the solution pH is higher. Most recently, initial results from the high pH tests at Ringhals-4 in Sweden[17] have shown that the radiation fields are significantly lower than the typical plants at the comparable operation time. Ringhals-4 has operated at a pH of 7.3 (maximum LiOH concentration of 3.3 ppm) for much of its ~2 years of operations. It must be cautioned that operating at higher LiOH concentrations (Li $\geq$ 3.5 ppm) in the coolant may result in higher fuel surface oxidation.

4.4 REFERENCES

(1) L.D. Anstine, et. al., "BWR Corrosion-Product Transport Survey", EPRI NP-3687 (September 1984).

(2) A. Strasser, et. al., "Corrosion-Product Buildup on LWR Fuel Rods", EPRI NP-3789 (April 1985).

(3) L.D. Anstine, "BWR Radiation Assessment and Control Program: Assessment and Control of BWR Radiation Fields", Volume 2, EPRI NP-3114 (May 1983).

(4) S. Uchida, et. al., J. Nucl. Sci. Tech., 24, 385-392 (May 1987).

(5) American Nuclear Society, "American National Standard Radioactive Source Term for Normal Operation of Light Water Reactor" ANSI/ANS-18.1-1984.

(6) C.C. Lin, et. al, "Corrosion Product Transport and Radiation Field Buildup Modeling in the BWR Primary System", 2nd Int. Conf. Water Chemistry of Nuclear Reactor System, BNES, October 1980, Paper 46; Nuc. Tech. 54, 253 (1981).

(7) C.C. Lin and F.R. Smith, "BWR Cobalt Deposition Studies, Final Report", EPRI NP-5808 (May 1988).

(8) C.A. Bergmann and J. Roesmer, "Coolant Chemistry Effects on Radioactivity at Two Pressurized Water Reactor Plants", EPRI NP-3463 (March 1984).

(9) C.A. Bergmann, et. al., "The Role of Coolant Chemistry in PWR Radiation-Field Buildup", EPRI NP-4247 (October 1985).

(10) S. Kang and J. Sejvar, "The CORA-II Model of PWR Corrosion-Product Transport", EPRI NP-4246 (September 1985).

(11) F.H. Sweeton and C.F. Bass, J. Chem. Thermodynamics, 2, 479 (1970).

(12) N.R. Large, et. al., "Studies of Problems of Corrosion Problem Sampling from PWR Primary Coolant", Water Chemistry of Nuclear Reactor System 5, Vol. 1, P. 63, BNES, London (1984).

(13) M.V. Polley and P.O. Andersson, "Study of the Integrity of Radioisotope Sampling from the Primary Coolant of Ringhals 3 PWR", ibid, P. 71, (1989).

(14) M. Yamada and Z. Ojima, "Correlation Between Deposition Fuel, pH Control and Radiation Field Trend", 1988 JAIF Int. Conf. Water Chemistry in Nuclear Power Plants, Vol. 1, P. 162 (April 1988), Japan Atomic Industrial Forum, Tokyo.

(15) H. Takiguchi, et. al., "Radiation Buildup Control by High pH Chemistry in the Tsuruga-2 Primary Coolant System", ibid. P. 168.

(16) R.H. Kunig and Y. Sandler, "Solubility of Simulated PWR Plant Corrosion Products", EPRI NP-2448 (1985).

(17) K. Egner, "Getting the Dose Down at Sweden's PWR Plants", Nucl. Engng. Int. 31 49 (1986).

(18) C.C. Lin, "Foreign Approaches to Controlling Radiation Field Buildup in BWRs", EPRI NP-6942-D (August 1990).

(19) C.C.Lin, "Optimum Water Chemistry in Radiation Field Buildup Control", Third International Workshop on Implementation of ALARA at Nuclear Power Plants, Paper 1-2, May 8-11, 1994, Hauppauge, New York.

(20) C.C. Lin, F.R. Smith and R.L. Cowan, "Effects of Hydrogen Water Chemistry on Radiation Field Buildup in BWRs", International Conference on Chemistry in Water Reactors: Experience and New Developments, Vol. 1, 271 (April 24-27) 1994, Nice, France.

5. WATER AND IMPURITY ACTIVATION PRODUCTS

5.1 INTRODUCTION

There are numerous water activation products and activated water impurities in the coolant (Table 2-4). Among those nuclides, only a few nuclides are radiologically significant in reactor operation. The following activities have been studied in detail: H-3, N-13, N-16, F-18, Na-24 and Cl-38. The chemistry of nitrogen activities and their transport behavior in the steam/condensate systems in a BWR has become an interesting and important subject of investigation under hydrogen water chemistry conditions(1).

5.2 TRITIUM IN PWRs

The study of tritium in PWRs is important because tritium's long half-life (12.3 years) permits long-term buildup within the plant systems. Since reactor coolant is recycled, tritium is retained within the plant as tritiated water and release may occur as liquid, water vapor or gaseous tritium. The primary sources of tritium in the reactor coolant system in a PWR are: (1) diffusion of tritium from the fuel through the zircaloy cladding; (2) neutron activation of boron in the burnable poison rods and subsequent tritium diffusion through the stainless steel cladding; and (3) neutron activation of boron, duterium and ^{6}Li in the reactor coolant. The fission yield of tritium for U-238 is ~0.01%.

Two major neutron reactions with boron resulting in tritium production are:

(1) $^{10}B\ (n,2\alpha)^{3}T$
(2) $^{10}B\ (n,\alpha)\ ^{7}Li\ (n,n\alpha)^{3}T$

It has been estimated (2) that approximately 10% of the tritium produced in stainless-clad burnable poison rods is released into the coolant, which contributes ~2/3 of the observed tritium buildup.

The production of tritium from the $^{6}Li\ (n,\alpha)^{3}T$ reaction in the coolant is controlled by limiting the ^{6}Li impurity in the $^{7}LiOH$ used in the reactor coolant and in the lithium from demineralizers with 99.9% ^{7}Li. However, it has been experienced that an increase in ambient reactor coolant system tritium levels may be used as an indicator of inadequate ^{7}Li enrichment. The tritium produced by the neutron activation of deuterium in water (~0.015%) is less than 5 Ci/year, a few percent of total production

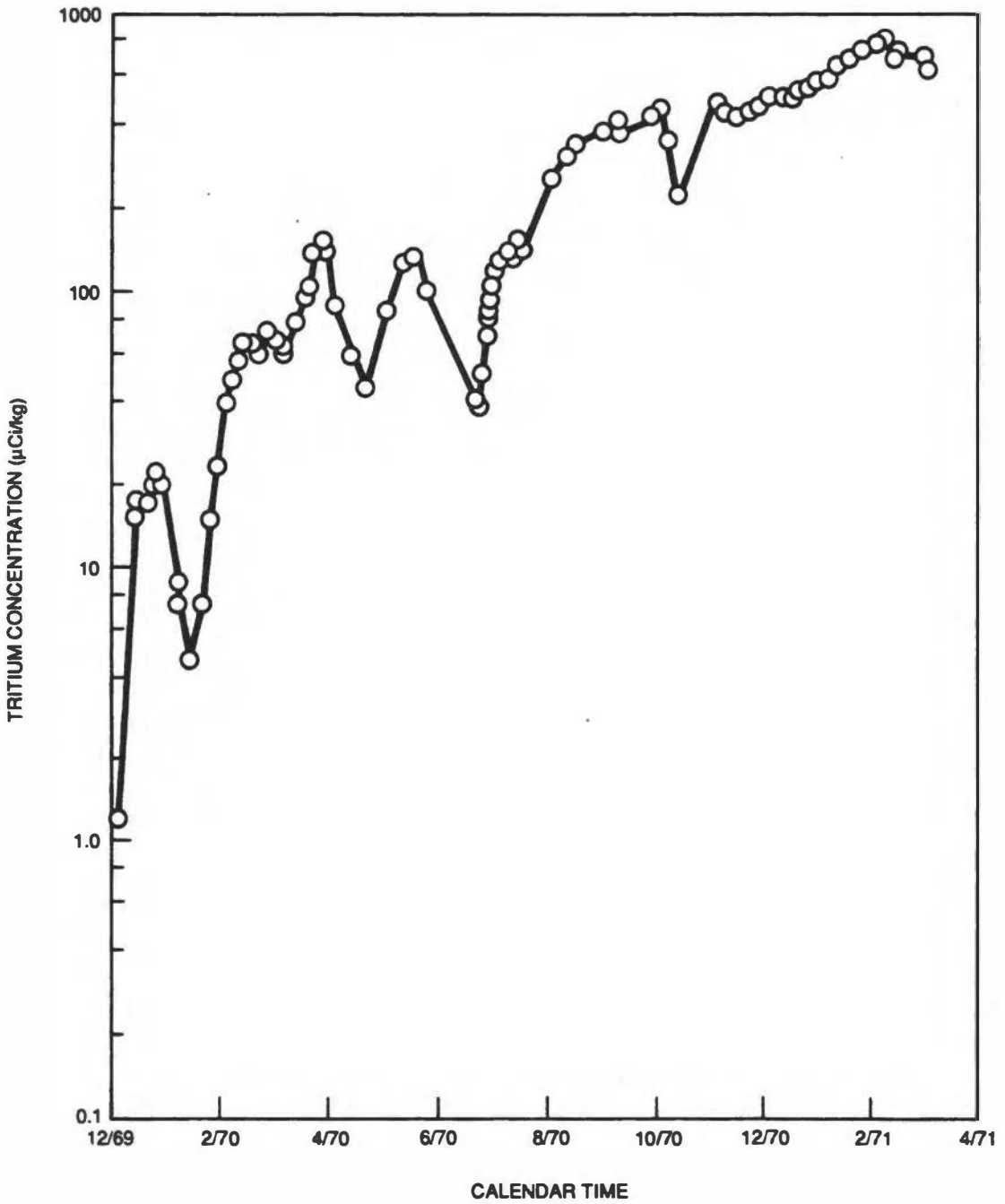

Figure 5-1. Tritium Level in A PWR Primary Coolant (Ref. 2)

5.3 Na-24 AND Cl-38 IN BWRs

Na-24 and Cl-38 activities are two major activated products from water impurities. The main source of NaCl is believed to be the inleakage of the secondary coolant in the condensate-feedwater system. However, a significant "leaching-out" of sodium from the deep bed demineralizer system may also be an important contributor during normal operation.

It is rather difficult to calculate directly the activity production from the core average neutron flux and the average coolant residence time in the core region (Section 2.7). Instead, based on a number of measurements in operating BWRs, it has been estimated that the equilibrium production rates of Na-24 and Cl-38 in the coolant during normal operation are, respectively:

$$R_{Na\text{-}24} = 1.9 \times 10^{-3}\ \mu Ci/s/MW_t/ppb\ Na$$

$$R_{Cl\text{-}38} = 5.9 \times 110^{-3}\ \mu Ci/s/MW_t/ppb\ Cl$$

The equilibrium activity concentration per unit target material in the coolant can be calculated from:

$$C_{eq} = \frac{R}{W(\lambda + \beta_c)}$$

where C_{eq} = equilibrium activity concentration per unit target material, μCi/Kg/ppb

R = activity production rate, μCi/kg/ppb

W = reactor coolant mass, kg

λ = decay constant, s^{-1}

β_c = reactor cleanup time constant, sec^{-1}

$$= \frac{(\text{cleanup flow rate, kg/sec})}{(\text{reactor coolant mass, kg})}$$

If the equilibrium activity concentration is measured, the equilibrium target material concentration (C^o_{eq}) as well as the constant target source input rate (n) can be easily estimated. An example of calculation is shown in Table 5-2. A detailed model calculation

of activity buildup in the coolant during a no-cleanup test will be presented in Section 8.2.

Table 5-2

EQUILIBRIUM CONCENTRATIONS AND SOURCE INPUT RATES OF Na^+ (Na-24) AND Cl^- (Cl-38) DURING NORMAL OPERATION IN A BWR*

	Na^+	Na-24	Cl^-	Cl-38
Production rate, R, μCi/s/MW_t/ppb	—	1.9×10^{-3}	—	5.9×10^{-3}
Equilibrium conc., μCi/kg/ppb				
$C_{eq} = \frac{R}{V(\lambda + \beta_c)}$	—	0.14	—	0.125
Equilibrium conc., μCi/kg (Observed)	—	2.6	—	2.9
Equilibrium conc.,				
C^o_{eq}, ppb	18.6		23.2	
Constant source input rate, ppb/hr				
$n = C^o_{eq}\beta_c$	8.04		10	

* Reactor power = 1820 MW_t
Reactor water mass, W = 2×10^5kg
Feedwater flow rate, F = 920 kg/s
Cleanup flow rate, f = 24 kg/s
Cleanup time constant, $\beta_c = 1.2 \times 10^{-4} s^{-1}$

5.4 N-13 AND N-16 IN BWRS

The N-16 activity is the primary source of radiation fields in the coolant and steam systems during power operation. In a BWR, the total nitrogen activity carried by the steam is only a few percent of the total nitrogen activity produced in the core under normal BWR water chemistry (NWC) conditions[3]. However, during recent tests in BWRs with hydrogen addition in the coolant, the radiation fields in the steam-turbine

systems increased by a factor of ~5[1,4], mainly due to the increase of the N-16 activity in the steam phase (Figure 5-2).

The gamma-ray spectrum of N-16 and other nuclides (O-19 and C-15) observed at an operating BWR is shown in Figure 5-3. The higher levels of radiation fields in the steam-turbine systems are the major concern in reactor operation under hydrogen water chemistry (HWC) conditions.

The N-13 ($t_{1/2}$ = 10 min) and N-16 ($t_{1/2}$ = 7.1 s) are two radioactive nuclides produced from oxygen by the ^{16}O $(p,\alpha)^{13}N$ and ^{16}O $(n,p)^{16}N$ reactions, respectively, in the reactor coolant. The recoil energies for the nitrogen nuclides from nuclear transformations are estimated at ~0.4 MeV, which is several orders of magnitude larger than required to break a chemical bond (~3 eV). Thus, these two activated nuclides are expected to behave similarly in chemical reactions after they become thermalized. Because of its short half-life, the chemical forms of N-16 have never been measured. However, the chemistry and steam transport behavior of N-13 have been extensively studied [3,5].

As a result of radiation effects, the nitrogen activities can exist in many chemical forms in water and steam (Section 6.7). In some early reactor measurements under normal operating conditions, most of the N-13 and N-16 activities were found in the anion forms in the reactor coolant, presumably NO_2^- and NO_3^-, while most of the activities in the steam condensate were found in the cationic form, most likely NH_4^+. In recent radiochemical studies in four reactors during hydrogen chemistry tests[5], the cationic form of nitrogen activity has been identified as NH_4^+ by ion chromatographic separation, and the anion fraction was found to contain two major species, NO_3^- and NO_2^-, in both reactor coolant and steam condensate. The test results are summarized in Table 5-3, and the typical results are shown in Figures 5-4 and 5-5, in which the N-13 concentrations in both cation and anion fractions in the reactor recirculation water and the steam condensate are shown as a function of dissolved H_2 in reactor recirculation water. The dissolved O_2 is also shown in each figure for comparison.

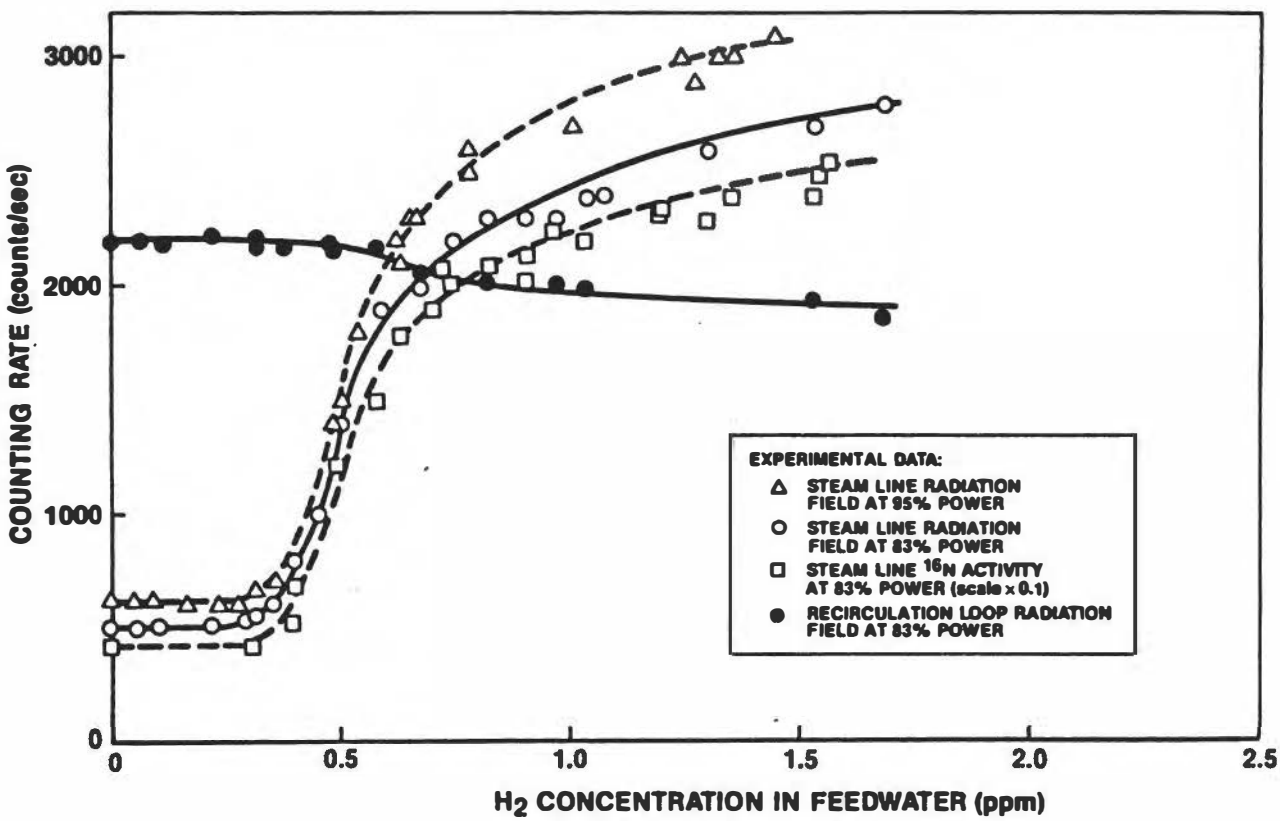

Figure 5-2. Variation of Radiation Fields and N-16 Concentrations in Steam as a Function of H_2 Concentration in Feedwater (Ref. 3)

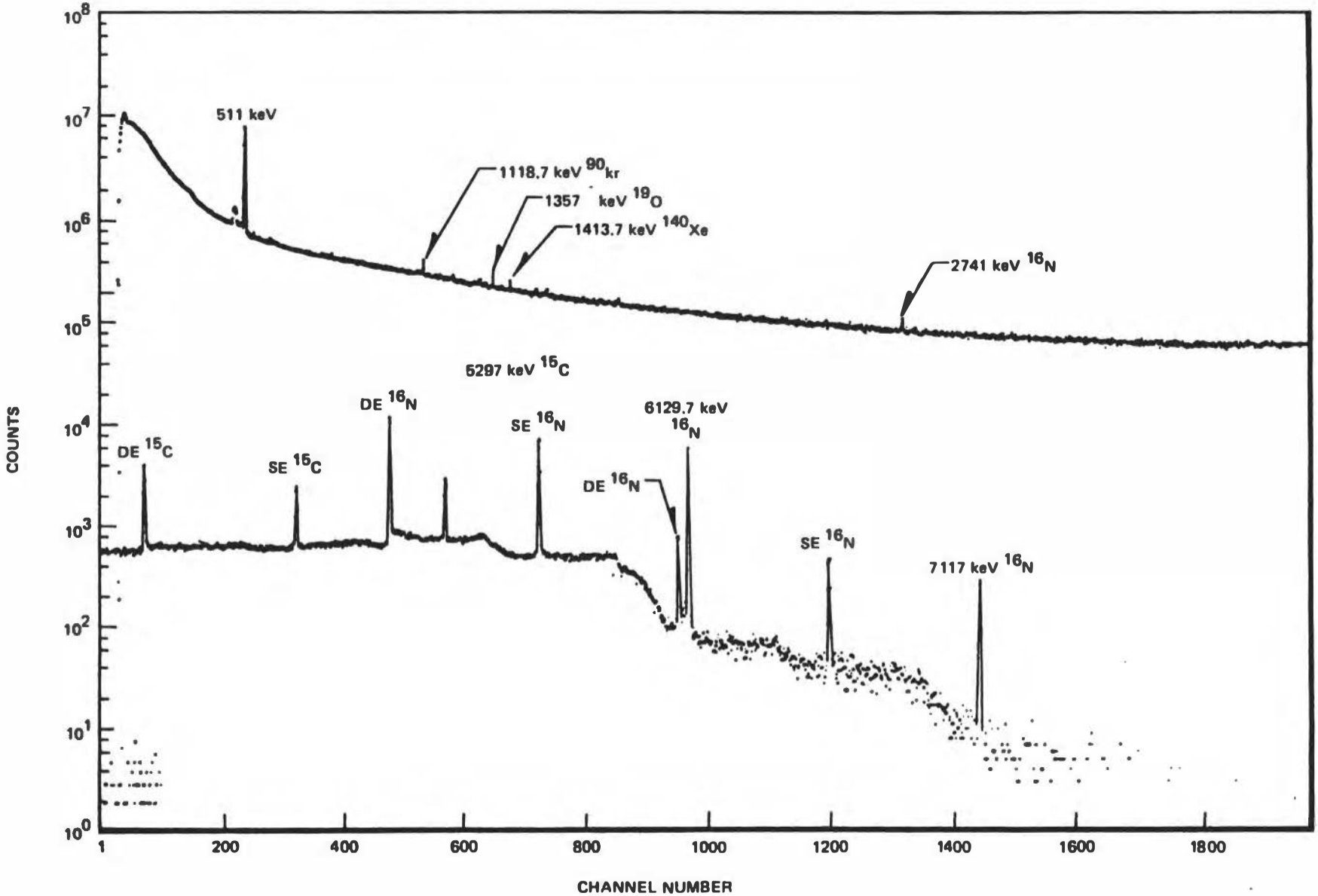

Figure 5-3. Gamma-Ray Spectrum Observed at a High Pressure Turbine with a Shielded Collimator

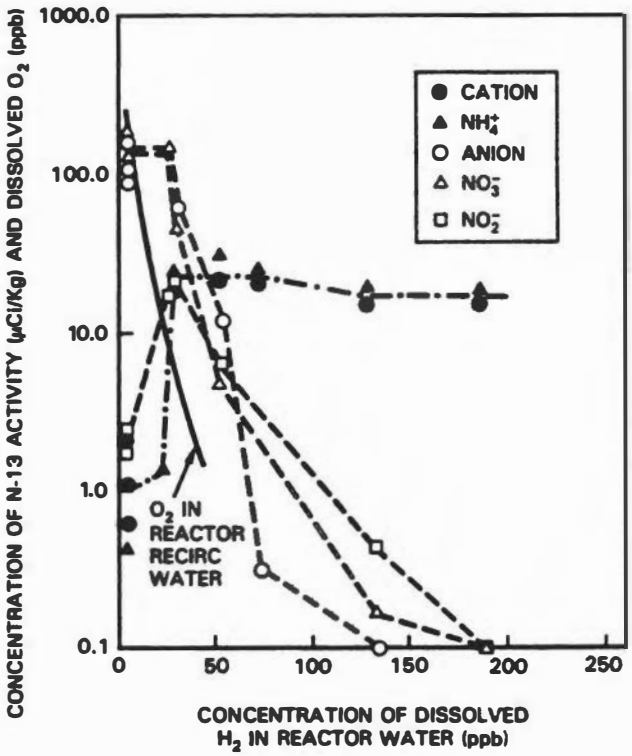

Figure 5-4. Variation of N-13 Species in Reactor Water with H_2 Concentration. (Ref. 1,5)

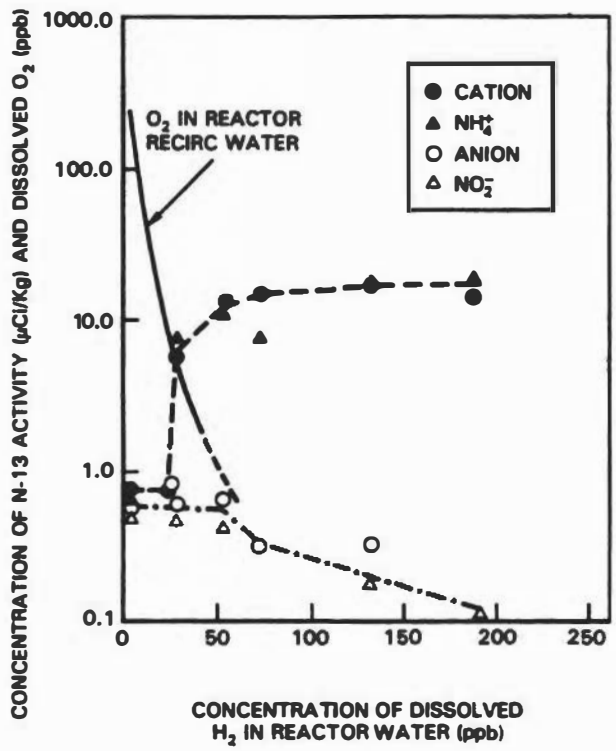

Figure 5-5. Variation of N-13 Species in Steam Condensate with H_2 Concentration in Reactor Water. (Ref. 1,5)

Table 5-3

SUMMARY OF N-13 CHEMICAL FORMS MEASURED DURING HWC TESTS (Ref. 5)
(in % of chemical fraction)

	NWC		HWC*	
Reactor	**Cation**	**Anion**	**Cation**	**Anion**
In Reactor Water:				
Pilgrim	0.6	99.4	80.0	20.6
FitzPatrick	1.2	98.8	97.7	2.3
Hatch-1	1.8	98.2	59.2	40.8
NMP-1	1.2	98.8	81.0	19.0
NMP-1 (Incore)	4.6	95.4	56.4	43.6
In Steam Condensate:				
Pilgrim	55.6	44.4	99.5	0.5
FitzPatrick	52.5	47.5	98.7	1.3
Hatch-1	58.7	41.3	100.0	0.0
NMP-1	65.7	34.3	100.0	0.0

* HWC conditions are: 130-140 ppb H_2 and 1-2 ppb O_2 in reactor recirculation water.

System chemistry has been found to have a profound influence on the chemical forms and the distribution of nitrogen activities in the BWR primary coolant system. Apparently, the NO_3^- or anion fraction dominate the N-13 activity in reactor water under NWC condition. As the dissolved H_2 increases and dissolved O_2 decreases, the NO_3^- fraction decreases quickly and the cation fraction, or NH_4^+ increases significantly. Similarly, the anion fraction (NO_2^-) of N-13 in steam decreases and the cation fraction (NH_4^+) increases sharply and becomes dominant as the dissolved H_2 in water increases.

The average total N-13 production rate is experimentally determined to be ~25 μCi/s/MWt, which is in excellent agreement with the theoretically calculated value of 23 μCi/s/MWt[6]. The production rate of ^{16}N is rather difficult to determine; however, based on the measured ^{16}N concentration in steam lines, the core exit N-16 concentrations have been estimated to be 54 ± 15 μCi/g under normal water chemistry conditions and 240 ± 65 μCi/g under hydrogen water chemistry conditions (Table 5-4).

The activity presented in non-condensable chemical forms and released through the off-gas system was only a few percent of the total production, and the release rate decreased by a factor of ~2 under HWC conditions, in spite of the increase in steam activity. Apparently, the chemical form of N-13 in the offgas was dominated by the NO and/or NO_2 under NWC conditions.

Table 5-4.

N-16 STEAM CONCENTRATION AT VARIOUS LOCATIONS IN THREE CLASSES OF BWRs (μCi/g Steam) (Ref. 1)

	BWR/2	BWR/3		BWR/4	
Location	NMP-1	Pilgrim	Dresden-2	Hatch-1	PB-3
Measurement Point					
NWC	34	25	24	46	21
HWC	159	129	104	201	78
Vessel					
Nozzle					
NWC	38	28	27	51	23
HWC	180	139	117	221	87
Core Exit					
NWC	64	46	49	73	37
NWC Ave: 54 ± 13					
HWC	300	230	212	319	137
HWC Ave: 240 ± 65					

5.5 F-18 IN BWR

F-18 ($t_{1/2}$=110 min) is formed in the reactor coolant by the $^{18}O(p,n)^{18}F$ reaction. Its production rate has been theoretically estimated to be 0.67 μCi/s/MWt[6], which is in good agreement with the experimentally measured values (~0.6 μCi/s/MW_t). The F-18 activity has been observed only in the fluoride (F^-) form in either the reactor coolant or the BWR steam condensate, which is the most stable and only form of fluorine in water. The typical concentrations of F-18 in the BWR coolant and the steam condensate are 1.0 and 2.0 μCi/kg, respectively, independent of water pH and conductivity in reactor water.

Frequently, the F-18 activity has been found to be the major source of radiation fields in the BWR hotwell. More than 90% of the F-18 activity produced in the coolant is transported through the steam system and condenses in the condensate system.[3] The mechanism responsible for the formation of the volatile form of fluorine in steam is not clear. A complex of $H_2O.F$ or its equivalent has been proposed to explain the appearance of F-18 in the steam phase.[3] In a water environment, the newly formed F-18 may tend to be associated with H_2O molecule as a complex $H_2O.F$ when its recoil energy from the nuclear reaction is totally reduced by numerous collisions. $H_2O.F$ may

be transported with the steam, and the F atom is reduced to F^- as the steam condenses in the water phase at lower temperatures.

Since the F^- concentration in reactor water is believed to be very low ($\leq$ 1ppb), the volatility of F-18 as HF in steam transport may be very low.

5.6 REFERENCES

(1) C.P. Ruiz, C.C. Lin and T.L. Wong "Control of N-16 in BWR Main Steam Lines Under Hydrogen Water Chemistry Conditions", EPRI NP-6424-SD (July 1989).

(2) Westinghouse Electric Corporation, "Source Term Data for Westinghouse Pressurized Water Reactors", WCAP-8253 (May 1974).

(3) C.C. Lin, "Chemical Behavior and Distribution of Volatile Radionuclides in a BWR System Water Forward-Pumped Heater Drains", Water Chemistry of Nuclear Reactor Systems 3, Vol. 1, 103 (1983), BNES (London).

(4) R.J. Law, et al, "Suppression of Radiolytic Oxygen Porduced in a BWR by Feedwater Hydrogen Addition; ibid, Vol. 2, 23 (1983).

(5) C.C. Lin, J. Radioanal. Nucl. Chem., 130, 129 (1989).

(6) M.S. Single and L. Ruby, Nucl. Tech., 17, 104 (1973).

6. RADIATION CHEMISTRY IN REACTOR COOLANT

6.1 INTRODUCTION

The radiation energy generated in the reactor core and absorbed in the coolant is mainly attributed to fast neutrons and gamma rays. Absorption of energy in the coolant results in water radiolysis, which occurs in both BWR and PWR. However, because of hydrogen gas over-pressure in the PWR system, there is no net water decomposition nor oxygen gas production in the PWR system (Section 6.4). The addition of hydrogen in the BWR coolant has become an important technique to reduce the dissolved oxygen level in the coolant and minimize the susceptibility of intergranular stress corrosion cracking (IGSCC) of stainless steel in the BWR primary system.

Because of its reducing nature in the PWR coolant, practically all radioactive and non-radioactive impurities in the coolant are in the reduced chemical forms. On the other hand, the BWR coolant under normal operating conditions is under oxidizing condition and the chemistry of the BWR coolant system is rather complicated due to many oxidizing species (both radicals and stable species). An attempt will be made to describe this complicated system in a limited scope.

6.2 WATER RADIOLYSIS IN BWR COOLANT

Boiling water reactors use high purity water as the neutron moderator and primary coolant in the production of steam. In an operating BWR, most of the radiolysis occurs in the high flux core region. Under normal operating conditions, the core contains an average steam void of ~30% and the core radial average void fraction increases from 0 at core inlet to ~70% at the top of the core.

A brief overview of radiation chemistry in the BWR coolant has been reported by Lin.[1] The radiation energy generated in the reactor core and absorbed in the coolant is mainly attributed to fast neutrons and gamma rays; the contributions from thermal neutron and beta particles are relatively small. The core average total neutron dose rate is estimated at 1.5×10^9 R/hr and the total gamma dose rate is estimated at 3.1×10^8 R/hr for a 50 W/cm^3 power density standard plant. The total radiation dose rate in the core region

is nearly proportional to the core power density. As a result of water radiolysis, liquid-vapor phase equilibrium and recirculation, the reactor recirculation water contains oxygen and hydrogen peroxide in the concentration range from 100 to 300 ppb, and about 10 ppb (less than stoichiometric ratio of 8 to 1) of dissolved hydrogen.

It is known that the dose rates decrease as the distance from the core increases, and the fast neutron fluxes decrease faster than the gamma fluxes. At out-of-core regions, the total dose rate could be ≈0.1-1% of the core dose rate. The production of radiolytic species is not important in the peripheral regions, but the levels of radiation are still high enough to initiate the "recombination" of dissolved O_2 and excess H_2 in the coolant (see Section 6.4).

The overall simplified general expression for the radiation-induced water decomposition can be written as:

$$H_2O \rightarrow e^-_{aq}, H, H_2, OH, H_2O_2, HO_2, H^+ \qquad (6\text{-}1)$$

which is not chemically balanced.

Although the detailed mechanism of water radiolysis is complex, a simple scheme has been well established to explain the observed effects.[2,3] The primary process is to produce H and OH radicals,

$$H_2O \rightarrow H + OH. \qquad (6\text{-}2)$$

Many of these radicals react with each other in regions of high local concentration to form molecular products, H_2 and H_2O_2, or reform water according to the reactions:

$$H + H \rightarrow H_2 \qquad (6\text{-}3)$$

$$H + OH \rightarrow H_2O \qquad (6\text{-}4)$$

$$OH + OH \rightarrow H_2O_2 \qquad (6\text{-}5)$$

The molecular products H_2 and H_2O_2 may be destroyed and water is reformed by the following chain reaction:

$$OH + H_2 \rightarrow H + H_2O \quad (6\text{-}6)$$

$$H + H_2O_2 \rightarrow OH + H_2O \quad (6\text{-}7)$$

Production of molecular O_2 is brought about by the following reactions:

$$H_2O_2 + OH \rightarrow HO_2 + H_2O \quad (6\text{-}8)$$

$$HO_2 + OH \rightarrow H_2O + O_2 \quad (6\text{-}9)$$

$$HO_2 + HO_2 \rightarrow H_2O_2 + O_2 \quad (6\text{-}10)$$

$$H_2O_2 + HO_2 \rightarrow H_2O + OH + O_2 \quad (6\text{-}11)$$

The O_2 is destroyed mainly by the reaction:

$$O_2 + H \rightarrow HO_2 \quad (6\text{-}12)$$

Within seconds of irradiation, steady-state concentrations of molecular and radical species can be reached in a static system which contains pure water. The examples of radiolysis model calculations[21] for the production of H_2, O_2, and H_2O_2 in air-free and air-saturated water at ambient temperature are shown in Figure 6-1. In air-free water, all three radiolytic products reach steady state concentrations at ~200 Gy of total dose (Figures 6-1, A and B). In the presence of excess oxygen in water, both H_2 and H_2O_2 increase and they may continue to increase until the oxygen is consumed to an equilibrium level (Figure 6-1, C).

The chemical yield of the decomposition product is denoted by the symbol G. The G value is defined as

$$G = \frac{\text{Number of species produced or destroyed}}{100 \text{ eV absorbed}}$$

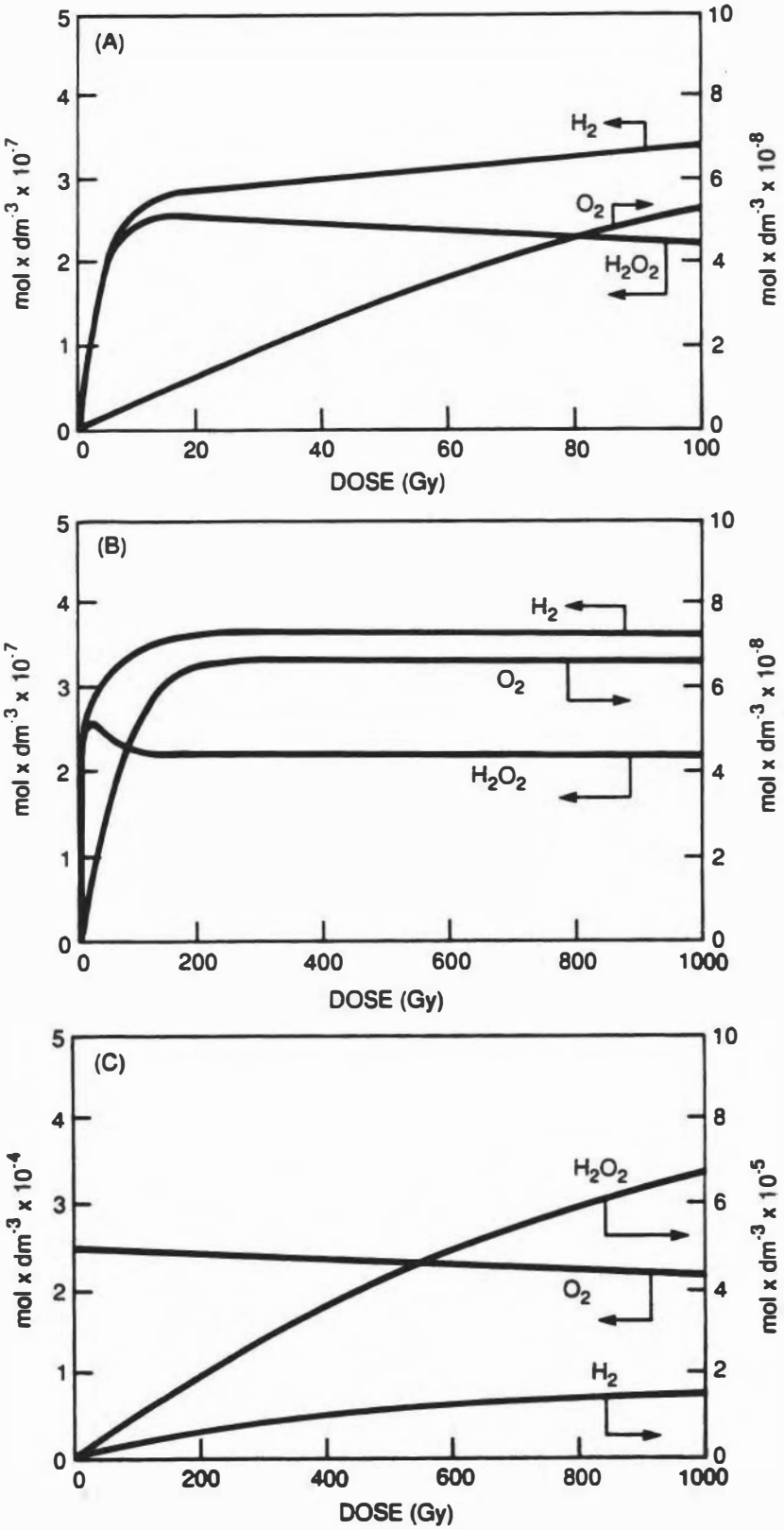

Figure 6-1. Radiolytic Products in Water Radiolysis with 1 Gy/s Dose Rate (Reproduced with Permission, Radiochim. Acta, Ref. 21)
A. In air-free pure water, doses up to 100 Gy
B. In air-free pure water, doses up to 1000 Gy
C. In air-saturated water

The symbols G_H, G_{H_2}, $G_{H_2O_2}$, etc., refer to primary radical and molecular yields, while G(H), $G(H_2)$, $G(H_2O_2)$, etc., refer to the observed yield under experimental conditions. When a species is decomposed by radiation, the negative yield is indicated by a minus sign, i.e., G_{-H_2O}.

The chemical yield (G value) for a species in the radiolysis of water may vary as a function of several factors in an irradiation system. Variations of radical and molecular yields with water pH, temperature, LET*, and does rate have been well documented.[4] The variation of chemical yields with temperature is significant at reactor operating conditions, and the LET is probably the most important factor when one calculates the chemical yields from gamma rays (low LET) and fast neutron (high LET) in a reactor. The yields of some major species at ambient and higher temperatures are compared in Table 6-1.[5]

Table 6-1

G-VALUES OF PRIMARY RADIOLYTIC SPECIES IN WATER (Ref. 5)

Temperaure	Radiation	$e_{(aq)}^-$	H^+	H	H_2	OH	HO_2	H_2O_2
25°C	Gamma	2.70	2.70	0.61	0.43	2.86	0.03	0.61
	Neutron	0.93	0.93	0.50	0.88	1.09	0.04	0.99
280°C	Gamma	3.76	3.76	0.7	0.8	5.5	–	0.28
(Tentative)**	Neutron	1.4	1.4	0.75	1.32	1.64	0.06	1.49

* The rate at which energy is lost (locally absorbed) per unit of length traveled by an ionizing particle, -dE/dx, is called the linear energy transfer (LET).

**Best estimated values from current literatures.

6.3 RADIOLYTIC GAS PRODUCTION IN BWRS

In an operating BWR, most of the radiolysis occurs in the high flux core region where boiling takes place. The net average production rate of radiolytic gases (containing approximately stoichiometric mixtures of H_2 and O_2) in BWRs has been determined to be 0.041 SCFM/MWt (19.35 cc/s/MWt) (Figure 6-2). The majority of the data shown in Figure 6-2 were determined by measuring the radiolytic gas (H_2 + O_2) content in a gas sample vial and the offgas flow rate. As shown in Figure 6-2, considerable variation in the measured radiolytic gas production rate can be seen. The variation may be partly attributed to analytical error and the difficulty in accurately calibrating the gas flow rate in the off-gas line. However, the data measured in steam samples appear to be more consistent with the average production rate. It should be noted that the actual production rate in the BWR core may slightly vary due to differences in design and/or operating characteristics (e.g., core power density, steam void fraction, operating pressure, coolant flow rate, and impurity levels in the coolant).

For the average offgas production rate of 0.041 SCFM/MWt in BWRs, the "apparent" H_2 and O_2 yields are $G(H_2)_{BWR}$ = 0.0056 and $G(O_2)_{BWR}$ = 0.0028, respectively. These apparent yields are produced by a mixture of neutron and gamma radiation in the core region. It is entirely possible that most of the radiolytic gases are produced in the boiling region and quickly partition between the steam phase and the liquid phase. The steady-state concentrations of dissolved gases in non-boiling water are expected to be relatively low. In the presence of excess H_2 in water, the production of O_2 may be effectively suppressed in non-boiling water.

6.4 SUPPRESSION OF WATER RADIOLYSIS BY H_2 ADDITION

In the presence of excess H_2 in water, the water decomposition and production of O_2 can be suppressed through a chain reaction which rapidly reduces the concentration of OH and H_2O_2, in the reactions.

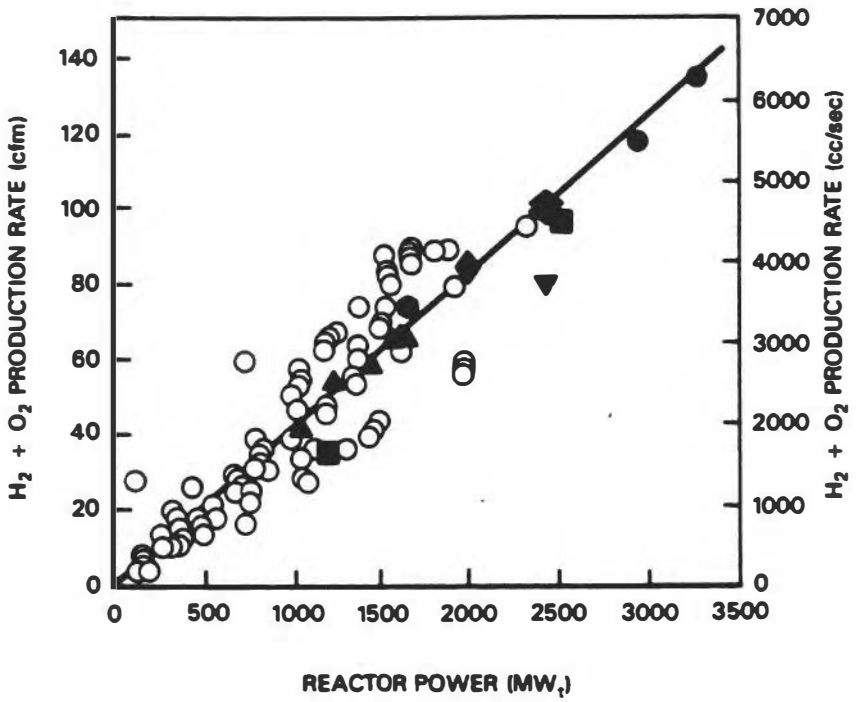

SYMBOL	REACTOR	RATED POWER MW_t	POWER DENSITY KW/L	STEAM FLOW Kg/sec	SAMPLE TYPE
○ -	•	•	•	•	OFFGAS
▲	DRESDEN-2	2527	36.6	1230	OFFGAS
■	DRESDEN-2	2527	36.6	1230	STEAM
●	PEACH BOTTOM-3	3293	50.0	1686	STEAM
◆	PILGRIM	1988	38.8	1006	STEAM
◆	FITZPATRICK	2436	51.2	1319	STEAM
▼	HATCH-1	2435	51.2	1319	STEAM
●	DUANE ARNOLD	1593	51.0	862	STEAM

*INCLUDING 10 UNNAMED REACTORS OF VARIOUS SIZES DURING STARTUP BEFORE 1971.

Figure 6-2. Radiolytic Gas Production Rates In BWRs (Ref. 6)

$$H_2 + OH \rightarrow H_2O + H \quad (6\text{-}13)$$

$$H + H_2O_2 \rightarrow H_2O + OH. \quad (6\text{-}14)$$

These two species are normally the precursors of O_2 in the reactions

$$OH + H_2O_2 \rightarrow HO_2 + H_2O \quad (6\text{-}15)$$

$$HO_2 + OH \rightarrow O_2 + H_2O. \quad (6\text{-}16)$$

When H_2 is in excess, the O_2 concentration is reduced by the fast reaction

$$H + O_2 \rightarrow HO_2 \quad (6\text{-}17)$$

and the decrease in H_2O_2 concentration occurs finally because the overall rate of reactions which destroy H_2O_2 is faster than that of reactions which produce H_2O_2 including its radiolytic formation. For the recombination of H_2 and O_2, a balanced set of reactions can be written as:

$$H_2O \rightarrow H + OH$$

$$2H_2 + 2OH \rightarrow 2H_2O + 2H$$

$$O_2 + H \rightarrow HO_2$$

$$H + HO_2 \rightarrow H_2O_2$$

$$H_2O_2 + H \rightarrow H_2O + OH$$

$$2H_2 + O_2 \rightarrow 2\,H_2O$$

An example of a radiolysis model calculation for the suppression of dissolved O_2 by surplus H_2 in water at ambient temperature is shown in Figure 6-3. A set of reactions and rate constants used in water radiolysis simulation is given in Table 6.2.

Table 6-2

REACTION AND RATE CONSTANTS USED IN WATER RADIOLYSIS SIMULATION (Ref. 8)

Chemical Reactions	Rate Constant at 25°C ($l\ mole^{-1}\ s^{-1}$)	Activation Energy K cal $mole^{-1}$
$e_{aq}^- + H_2O \rightarrow H + OH^-$	1.6×10^1	3.0
$e_{aq}^- + H^+ \rightarrow H$	2.4×10^{10}	3.0
$e_{aq}^- + OH \rightarrow OH \rightarrow OH^-$	2.0×10^{10}	3.0
$e_{aq}^- + H_2O_2 \rightarrow OH + OH^-$	1.3×10^{10}	3.0
$H + H \rightarrow H_2$	1.0×10^{10}	3.0
$e_{aq}^- + HO_2 \rightarrow HO2^-$	2.0×10^{10}	3.0
$e_{aq}^- + O_2 \rightarrow O_2^-$	1.9×10^{10}	3.0
$2e_{aq}^- \rightarrow 2OH^- + H_2$	5.0×10^9	3.0
$2OH \rightarrow H_2O_2$	4.5×10^9	3.0
$OH + HO_2 \rightarrow H_2O + O_2$	1.2×10^{10}	3.0
$OH + O_2^- \rightarrow OH^- + O_2$	1.2×10^{10}	3.0
$OH^- + H \rightarrow e_{aq}^- + H_2O$	2.0×10^7	4.5
$e_{aq}^- + H + H_2O \rightarrow OH^- + H_2$	2.5×10^{10}	3.0
$e_{aq}^- + HO_2^- + H_2O \rightarrow OH + 2OH^-$	3.5×10^9	3.0
$H^+ + OH^- \rightarrow H_2O$	1.44×10^{11}	3.0
$H_2O \rightarrow H^+ + OH^-$	2.6×10^{-5}	3.0
$H + OH \rightarrow H_2O$	2.0×10^{10}	3.0
$OH + H_2 \rightarrow H + H_2O$	4.0×10^7	4.6
$OH + H_2O_2 \rightarrow H_2O + HO_2$	2.25×10^7	3.45
$H + H_2O_2 \rightarrow OH + H_2O$	9.0×10^7	4.5
$H + O_2 \rightarrow HO_2$	1.9×10^{10}	3.0
$HO_2 \rightarrow O_2^- + H^+$	8.0×10^5	3.0
$O_2^- + H^+ \rightarrow HO_2$	5.0×10^{10}	3.0
$2HO_2 \rightarrow H_2O_2 + O_2$	2.7×10^6	4.5
$2O_2^- + 2H_2O \rightarrow H_2O_2 + O_2 + 2OH^-$	1.7×10^7	4.5
$H + HO_2 \rightarrow H_2O_2$	2.0×10^{10}	3.0
$H + O_2^- \rightarrow HO_2^-$	2.0×10^{10}	3.0
$e_{aq}^- + O_2^- \rightarrow HO_2^- + OH^-$	1.3×10^8	4.5
$OH^- + H_2O_2 \rightarrow HO_2^- + H_2O$	1.8×10^8	4.5
$2H_2O_2 \rightarrow 2H_2O + O_2$	$0.3/H_2O_2$	-

6.5 THE ROLE OF IMPURITIES

Some ionic impurities, especially halide and metallic ions, are known as "radical scavengers" which have profound effects on water radiolysis as well as radiation induced chemical reactions. The examples of reactions involving Br^- and Cu^{++} ions are illustrated by:

$$OH + Br^- \rightarrow Br + OH^-$$
$$H + Br \rightarrow Br^- + H^+$$

and

$$H + Cu^{++} \rightarrow Cu^+ + H^+$$
$$OH + Cu^+ \rightarrow Cu^{++} + OH^-$$

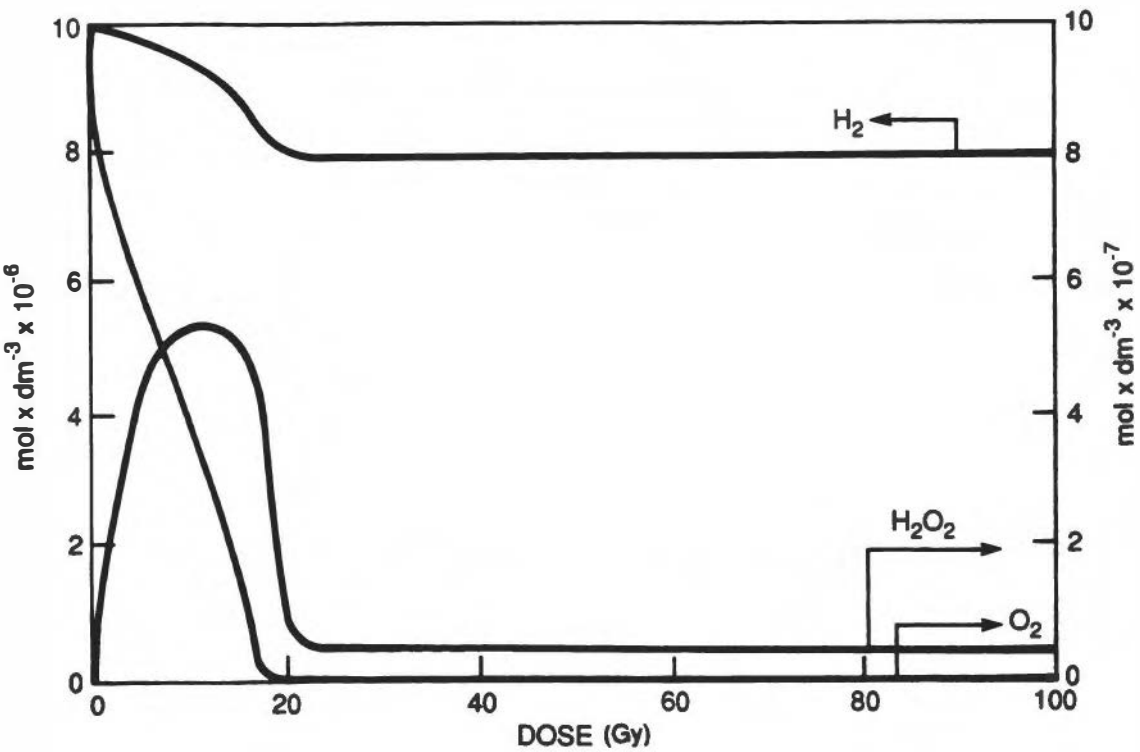

Figure 6-3. Depletion of O_2 in Water by Irradiation in the Presence of Surplus H_2. Dose Rate at 1 Gy/s (Reproduced with Permission, Radiochim. Acta, Ref. 21)

The scavengers compete with H_2 and H_2O_2 in reactions (6-6) and (6-7) for OH and H radicals. The reaction rate constants for some reactions involving Cu^+/Cu^{++} and halide ions can be found in the literature.[7] As shown in Table 6-3, the reaction rates for the Cu^+/Cu^{++} ions are comparable to most of the free radical reactions involved in radiolysis (Table 6-2). Thus, if the impurity levels are high enough (e.g., ≥10 ppb), the scavenging effect would significantly interrupt the radiolytic chain reactions.

Table 6-3

EXAMPLES OF IMPURITY REACTION RATE CONSTANTS[7]

Reaction					k(L/mol/s)
CL^-	+	OH	→	$Cl + OH^-$	10^6
Br^-	+	OH	→	$Br + OH^-$	10^9
I^-	+	OH	→	$I + OH^-$	1.5×10^{10}
Cu^{+2}	+	H	→	$Cu^+ + H^+$	9.8×10^8
Cu^{+2}	+	e^-_{aq}	→	$Cu^+ + (H_2O)$	4.0×10^{10}
Cu^+	+	H_2O_2	→	$Cu^{+2} + OH + OH^-$	2.3×10^9

6.6 HYDROGEN WATER CHEMISTRY IN BWR COOLANT

The first full-scale hydrogen water chemistry (HWC) test in the U.S. was performed at Dresden-2 in 1982.[9] Subsequently, similar tests have been carried out in several reactors. A typical example of the H_2 and O_2 concentrations in steam as a function of H_2 concentration in reactor water is shown in Figure 6-4. It can be shown (Section 6-4) that the excess H_2 provides the initial H radicals for a chain reaction and there is no net consumption of H_2 in the process. That is, for each H_2 molecule that is added to the coolant and consumed to remove 1/2 O_2, one H_2 molecule is liberated by water radiolysis. The steam phase is dominated by the H_2 added in the feedwater. The initial decrease of the H_2 content in the steam may be due to some direct recombination of H_2 and O_2 in the core region when the O_2 concentration is sufficiently high.

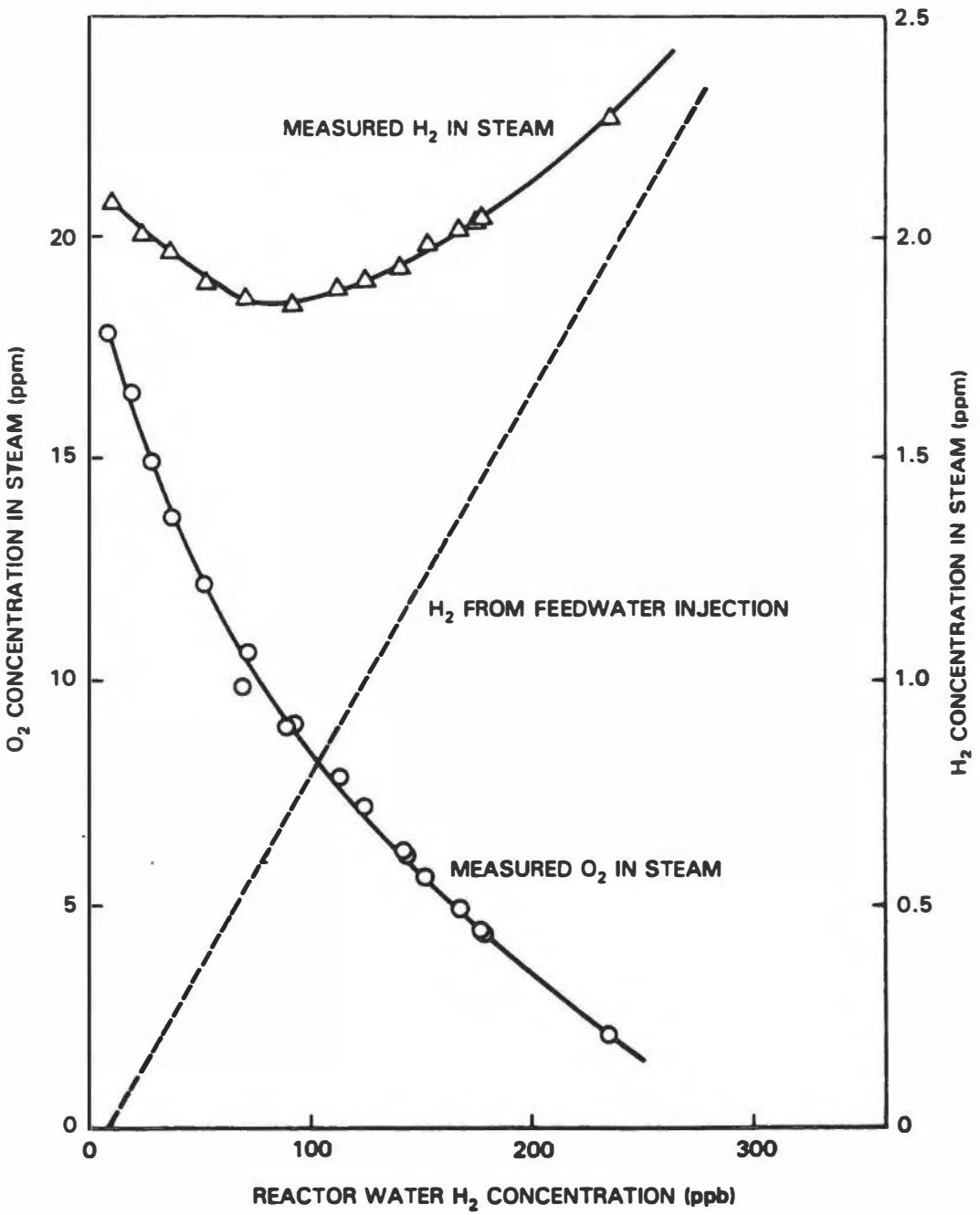

Figure 6-4. Hydrogen and Oxygen Concentrations in Steam as a Function of Hydrogen Concentration in Reactor Water

The dissolved O_2 concentration in the recirculation system also responds very quickly to hydrogen addition to the reactor water. When sufficient H_2 is added, the O_2 concentration decreases with increasing H_2 concentration according to the following equation:

$$[O_2] = K_{eq}/[H_2]^2$$

Experimental data obtained at three reactors are shown in Figure 6-5. It has been hypothesized that a radiation induced water decomposition-recombination equilibrium.

$$2\,H_2O \rightleftarrows 2\,H_2 + O_2$$

$$K_{eq} = [H_2]^2\,[O_2]$$

is established in the downcomer region when sufficient H_2 is added to the reactor water. The equilibrium constant K_{eq} is a strong function of the radiation field in the downcomer region. [22]

Measurements have not detected H_2O_2 in any of the plant measurements of the recirculation system chemistry. Ullberg and Rooth[10] have suggested that H_2O_2 may be present in the large diameter pipe, but decomposes heterogenously on high temperature, small diameter sample piping surfaces, to be measured as oxygen. Recently, a laboratory study[11] has shown that indeed H_2O_2 decomposes quickly in a stainless steel tubing at higher temperatures. However, the same study also shows there is no evidence of reactions between H_2 and O_2 or H_2O_2 in high-purity water. Thus, it is certain that in high purity water the dissolved H_2 measured in a BWR coolant sample line is representative of the concentration in the coolant from which the sample is taken.

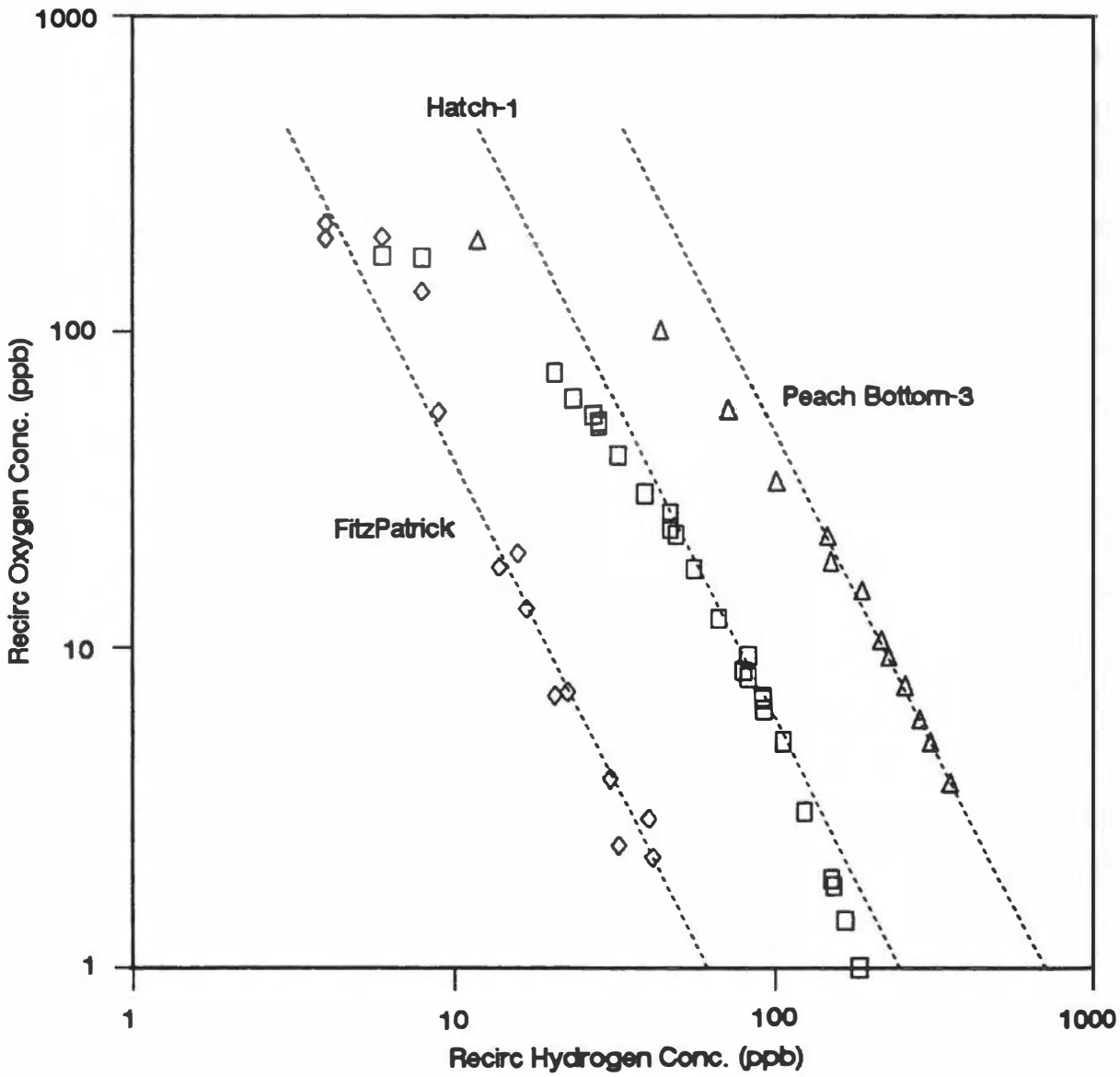

Figure 6-5. Recirculation Water Oxygen Concentration as a Function of Recirculation Water Hydrogen Concentration. (Ref. 22)

Similarly, the measured dissolved O_2 should be the combined concentrations of H_2O_2 and O_2 in the coolant. Nevertheless, with impurities in water, the same study indicates that copper ions at ~30 ppb would catalyze the reaction between H_2 and H_2O_2 to some extent at higher temperatures.

6.7 CHEMICAL EFFECTS OF RADIATION IN BWR COOLANT

Radiolytic oxidation of impurities including corrosion products ($CrO_4^=$) fission products (IO_3^-, $TcO_4^=$, NpO_2^+), and water activation products (NO_3^-) in the primary coolant under normal water chemistry conditions are well known,[12] but the actual reaction mechanisms may not be easily understood.

The radiation effects on nitrogen species have been extensively investigated.[13-16] When dealing with N-13 and N-16, which are activated from the oxygen atoms in water (Section 5.4), the reactions of "hot atoms" also have to be considered. In an earlier study, Schlieffer and Adlogg[17] reported that the chemical forms and distribution of N-16 produced in pure water were:

Chemical Form:	N_2	NO	NO_2^-	NO_3^-	NH_4^+	NH_2OH
Distribution (%)*:	1	9	25	10	30	16

This result suggests that when a newly produced N-16 atom is broken away from an H_2O molecule, the thermalized nitrogen atom (N*) may react equally with various radicals, ions and molecules in the immediate surrounding area. Under a high radiation field, such as in the reactor core, the nitrogen atoms are expected to react with radiolytic species from water radiolysis. The initial reactions may include:

$$N^* + OH \rightarrow NO + H$$

$$N^* + H \rightarrow NH$$

$$N^* + H_2O \rightarrow NH + OH$$

* The data do not total 100% as reported in Ref. (17).

$$N^* + O_2 \rightarrow NO + O$$
$$N^* + H_2O_2 \rightarrow H_2O + NO$$
$$N^* + HO_2 \rightarrow HNO_2,$$

and the following subsequent reactions may occur until stable compounds are formed:[13]

$$NO + OH \rightarrow HNO_2$$
$$HNO + OH \rightarrow NO_2 + H_2O$$
$$2NO + O_2 \rightarrow 2NO_2$$
$$NH + H_2 \rightarrow NH_3$$
$$NO_2 + H_2O \rightarrow HNO_3 + HNO_2$$
$$NO_2 + OH \rightarrow H^+ + NO_3^-$$

It may be expected that under oxidizing conditions, more NO_3^- and NO_2^- will be formed. Even if ammonia is present in reactor water at low concentrations, ammonia will be converted to nitric acid in the reactor core under conditions of unsuppressed radiolysis of water,[14,15,16] according to the following equations:

$$NH_3 + OH \rightarrow NH_2 + H_2O$$
$$NH_2 + O_2 \rightarrow H_2NO_2$$
$$H_2NO_2 + HO_2 \rightarrow HNO_3 + H_2O_2 \text{ or}$$
$$H_2NO_2 + O_2 \rightarrow NO_2^- + NO_3^-$$

On the other hand, when H_2 is added to suppress water radiolysis, more NH_3 is expected to form as most of the oxidizing species are eliminated. Although N_2 is thermodynamically stable, its formation from two nitrogen atoms at very low concentrations in reactor coolant is very unlikely. The results of measurements in reactor coolant and steam in several reactors have been described in Section 5.4.

The radiation chemistry of iodine is as complex as nitrogen chemistry. Iodine can exist in several stable and unstable chemical forms in aqueous solutions, particularly at very low concentrations similar to those normally observed in reactor coolant. The effect of gamma-ray radiation on the I-131 activity in aqueous solutions was investigated in a laboratory study at ambient temperature.[18] The I-131 activity in the iodide (I^-) form was found easily oxidized to iodate (IO_3^-) as a result of high intensity (>10^5 R/h) gamma-ray irradiation. The chemical yield of IO_3^- was found to vary with water pH, dose rate and concentration. Thermodynamically the primary oxidizing species, OH and HO_2 (oxidation potentials are 2.8 and 1.35 V, respectively)[19] are capable of oxidizing all iodine species to IO_3^-, and, in the core region, the concentration of OH is expected to be higher than iodine species in the coolant. Thus, the mechanisms may consist of successive oxidation of iodine by OH, with I, IO, HIO, IO_2, and HIO_2 as possible intermediate species. The reactions may be represented by:

$$I^- \xrightarrow{OH} I(I_2) \xrightarrow{OH} HIO \xrightarrow[OH]{OH} IO_3^-$$

A number of studies on the chemical behavior of radioiodine in the BWR system have been reported.[20] The results of those studies are summarized in Section 8.3.

6.8 REFERENCES

(1) C.C. Lin "An Overview of Radiation Chemistry in Reactor Coolants", Proc. 2nd. Int. Symp. Environmental Degradation of Materials in Nuclear Power Systems - Water Reactors." Monterey, California, p. 160, (September 1988).

(2) C.J. Hochanadel, J. Phys. Chem., 56., 587 (1952).

(3) A.O. Allen, et al., J. Phys. Chem., 56., 575 (1952).

(4) See for example, I.G. Draganic and Z.D. Draganic "The Radiation Chemistry of Water" Academic Press, New York (1971).

(5) W.G. Burns and P.B. Moore, "Radiation Enhancement of Zircaloy Corrosion in Boilng Water System. A Study of Simulated Radiation Chemical Kinetics", Water Chemistry of Nuclear Reactor System 1, BNES, paper 33, 229 (1977); private communication (1991).

(6) C.C. Lin, Nucl. Sci. Eng., 99, 340 (1988).

(7) National Bureau of Standards, NSRDS-NBS-43 (1973) and 43 Supplement (1975), ibid-46 (1973), ibid-51 (1975), ibid-59 (1977).

(8) C.P. Ruiz and C.C. Lin, "Modeling Hydrogen Water Chemistry for BWR Applications", EPRI NP-6386 (June 1989).

(9) R.J. Law, et al., "Suppression of Radiolytic Oxygen Produced in a BWR by Feedwater Hydrogen Addition," Water Chemistry of Nuclear Reactor System 3, BNBS Vol. 2, 23 (1983).

(10) M. Ullberg and T. Rooth, "Hydrogen Peroxide in BWRs," Water Chemistry of Nuclear Reactor System 4, BNES, Vol. 2, 67 (1986).

(11) C.C. Lin and F.R. Smith, "Decomposition of Hydrogen Peroxide at Elevated Temperatures," EPRI NP-6733 (March 1990); Int. J. Chem. Kinet. Vol. 23, 971 (1991).

(12) C.C. Lin and H.R. Helmholz, "Radiochemical studies of the BWR at Monticello Nuclear Generation Plant," NEDE-12586 (June 1975) (GE Internal Report).

(13) M.T. Dmitriev, Zh. Prik. Khim., 36, 1123 (1963).

(14) J.E. LeSurf, G.M. Allison, Nucl. Tech., 29., 160 (1976).

(15) L. Hammar, et al., Water Chemistry Research at the Halden Boiling Water Reactor, Proc. Int. Conf. Peaceful Uses of Nuclear Energy, 3rd: Geneva, 1964, Vol. 9, 408 (1965).

(16) F.W. Fessenden, et al., J. Phys. Chem., 82, 1875 (1978).

(17) P.J.J. Schlieffer and J.P. Adlogg, Radiochem, Acta, 3 145 (1964).

(18) C.C. Lin, J. Inorg. Nucl. Chem., 42, 1101 (1980).

(19) E.J. Henley and E.R. Johnson, "The Chemistry and Physics of High Energy Reactions", University Press, Washington, D.C. (1969).

(20) C.C. Lin, J. Inorg. Nucl. Chem., 42, 1093 (1980).

(21) E. Bjergbakke, Z. D. Draganic, K. Sehested, and I. G. Draganic, Radiochimica Acta, 48, 65 (1989).

(22) C.C. Lin "Prediction of Electrochemical Potentials in BWR Primary System". Vol. 1: Evaluation of Water Chemistry and ECP Measurements under HWC", EPRI TR-102766, Vol. 1 (August 1993).

7. ASSAY OF RADIOACTIVE WASTE

7.1 INTRODUCTION

The determination of levels of radioactivity for the disposal of low-level radwaste has historically been done more on a semi-quantitative basis than a quantitative one. The use of gamma spectrometry and/or direct radiation measurements on bulk containers of waste has been the general approach. General difficulty in quantitative sampling and analysis is a well-known fact, and the radiation exposure costs associated with such sampling and analysis is also a factor in determining the methodology of radioactivity assay of radwaste. Nevertheless, the methods which have been used in the management of these low-level wastes have produced satisfactory results and have not led to circumstances inimical to the public health and safety.

In December 1983, the U.S. Nuclear Regulatory Commission (NRC) put into effect new standards and criteria (known as Regulation 10CFR61) governing the land disposal of radioactive wastes. The new rules defined three classes of low-level waste (designated classes A, B and C) based on the half-lives and quantities of radioactivity of specified radionuclides and assumed pathway models. The radionuclide concentration limits from 10CFR61 are reproduced in Table 7-1.[1] Some major characteristics of the nuclides needed to be analyzed are listed in Table 7-2 Many of these nuclides do not emit measurable gamma rays in their decay and can be measured only through difficult and time-consuming radiochemical and nuclear counting processes, requiring techniques and equipment beyond the capability of most nuclear power plant on-site laboratories. Even in some reputable laboratories, significant differences in the results of some comparative analyses have been reported[2].

The NRC has accepted an indirect methodology for the difficult-to-measure nuclides (i.e., nuclides which do not emit easily measured gamma rays) listed in 10CFR61. One of these involves establishing ratios or scaling factors between the difficult-to-measure nuclides and those which are both easy to measure and possess similar chemical and physical properties.

Table 7-1

10 CFR 61 WASTE CLASSIFICATION ACTIVITY LIMITS (Ref. 1)
(From 10 CFR Part 61.55)

Nuclide	Concentration, μCi/cm³		
	Class A	Class B[a]	Class C
Long Lived			
C-14	0.8	NA	8
C-14 in activated metal	8.0	NA	80
Ni-59 in activated metal	22.0	NA	220
Nb-94 in activated metal	0.02	NA	0.2
Tc-99	0.3	NA	3
I-129	0.008	NA	0.08
Alpha emitting transuranics with half-lives greater than 5 years	10[b]	NA	100[b]
Pu-241	350[b]	NA	3,500[b]
Cm-242	2,000[b]	NA	20,000[b]
Short Lived			
Total of all nuclides with half-lives less than 5 years	700	(c)	(c)
H-3	40	(c)	(c)
Co-60	700	(c)	(c)
Ni-63	3.5	70	700
Ni-63 in activated metal	35	700	7,000
Sr-90	0.04	150	7,000
Cs-137	1	44	4,600

a. There is no Class B category for waste exceeding the Class A limit for long lived nuclides. Such wastes are automatically Class C or are unacceptable for shallow burial. For waste containing a mixture of nuclides, the sum of the fractions of limits must be less than one with each section (long or short lived) considered separately. The appropriate limits must all be taken from the same column in the table.

b. Units are nanocuries per gram.

c. There are no specific limits for these nuclides in these classes. Practical considerations such as heating effect, external package radiation on shipping, or maximum specific activity determine the maximum concentration for these nuclides.

Table 7-2

NUCLEAR DATA FOR DIFFICULT-TO-MEASURE RADIONUCLIDES

Isotope	Half Life (years)	Radiation Emitted	Principal Means of Production	Nuclides Origin
H-3	12.3	Beta	Fission; Li-7 (n,nα); B-10 (n,2α); H-2 (n,γ)	Fuel & Coolant
C-14	5730	Beta	N-14 (n, p), 0-17 (n,α)	Fuel & Coolant
Fe-55	2.76	x-ray	Fe-54 (n,γ)	In-core surfaces
Ni-63	99.5	Beta	Ni-62 (n,γ)	In-core surfaces
Ni-59	7.5×10^4	x-ray	Ni-58 (n,γ)	In-core surfaces
Sr-90	28.1	Beta	Fission	Fuel
Tc-99	2.12×10^5	Beta	Fission; Mo-98 (n,γ) Mo-99 (beta)	Fuel
I-129	1.57×10^7	Beta, Gamma	Fission	Fuel
TRU*	Variable	Mostly alpha	Multiple n-capture	Fuel

* TRU = Transuranic isotopes, excluding beta emitter Pu-241 and shorter-lived Cm-242

Some typical BWR and PWR nuclide concentrations in various waste streams are shown in Tables 7-3 and 7-4, respectively. Some reports dealing with the methodologies for the radionuclide assay and correlations in radwaste have been published[2-8]. A brief review and discussion of those methodologies are presented in the following sections.

7.2 SAMPLING AND SAMPLE PREPARATION

The primary objective of sampling is to obtain a small quantity of the waste material which is representative of the whole quantity of the waste. The nuclide concentrations measured in the sample are then extrapolated to the whole waste quantity. In practice, true homogeneity of the waste is rarely achieved in a system to be sampled. It can only be approached by the application of mixing and sampling techniques. Thus, the accuracy of radionuclide determination depends largely on the sampling technique, more than the techniques of radiochemical analysis. An excellent discussion of radwaste sampling methodology and sample size requirements can be found elsewhere[6].

The mixing and sampling techniques applied to a given system depend on the property of waste material being measured. Radwaste streams can best be characterized as complex mixtures containing various components, each with different properties and concentrations. Due to these variabilities, they should be considered as heterogeneous substances from a sampling standpoint, which may vary both in time and space depending on system conditions. In order to obtain a representative sample, one should:

(1) control process conditions to approximate a homogeneous solution,
(2) utilize sampling equipment/techniques which do not bias samples, and
(3) adopt sampling techniques which approximate random sampling.

Controlling process conditions to approximate a homogenous solution cannot always be accomplished in a radwaste system. However, since the most practical application of automatic sampling equipment would be in pipe systems on holding tanks, the following guidelines should be observed[6].

Table 7-3

TYPICAL BWR NUCLIDE CONCENTRATION BY WASTE STREAM ($\mu Ci/cm^3$)
(Reproduced with Permission, EPRI NP-5983, Ref. 2)

Nuclide	RWCU Resins	Condensate Resins	Radwaste Resins	Evaporator Bottoms	DAW[c]
Co-60	25.0	2.6	11.2	3.4	4.0E-3
Cs-137	14.1	1.1	6.1	1.9	1.6E-3
Ni-63	3.6E-1	2.3E-1	1.1E-1	1.2E-1	1.0E-4
Fe-55	10.6	2.5	1.3	2.2	4.6E-3
C-14	3.7E-3	7.7E-3	4.6E-3	4.6E-4	2.6E-6
I-129	3.6E-5	3.7E-5	3.0E-5[a]	3.0E-5[a]	1.6E-7
Tc-99	5.6E-4	2.3E-4	2.4E-4[a]	7.6E-5[a]	1.8E-7
Sr-90	4.5E-2	4.9E-2	1.8E-6	5.6E-2	3.2E-5
Pu-241[b]	8.5	3.0	7.8E-1	6.7	8.8E-6
Cm-242[b]	1.2E-1	4.1E-2	1.1E-2	9.3E-2	2.4E-7
TRU[b]	1.5E-1	5.2E-2	1.4E-2	1.2E-1	2.4E-7

a. Values derived from Cs-137 concentrations multiplied by industry-wide scaling factors.

b. Concentration units for these nuclides are nCi/g.

c. DAW = dry active waste; concentrations are based on contact dose rates of 10mR/h.

Table 7-4

TYPICAL PWR NUCLIDE CONCENTRATIONS BY WASTE STREAM ($\mu Ci/cm^3$)
(Reproduced with Permission, EPRI NP-5983, Ref. 2)

Nuclide	Primary Resins	Primary Filters	Non-Primary Resins	Non-Primary Filters	Evaporator Bottoms	DAW[c]
Co-60	50	247	3.1	32.0	5.3E-2	2.6E-3
Cs-137	51.0	–	8.41	–	3.5E-2	2.0E-3
Ni-63	16.1	76.2	1.8	18.0	1.1E-1	1.14E-3
Fe-55	5.5	250	3.6	26.5	5.2E-2	7.25E-3
C-14	6.2E-2	1.4	3.1E-2	5.5E-1	1.0E-3	3.25E-5
I-129	1.7E-4	–	6.1E-5	–	4.0E-7[a]	1.3E-7
Tc-99	6.6E-4	–	1.8E-4	–	4.0E-6[a]	9.0E-8
Sr-90	1.9E-1	1.4E-1	1.4E-2	1.8E-2	7.7E-5	5.4E-6
Pu-241[b]	1400	3822	94	289	9.4E-1	6.2E-5
Cm-242[b]	19.4	53	1.3	4.0	1.3E-2	9.4E-7
TRU[b]	25	68	1.7	5.1	1.7E-2	1.6E-6

a. These values were derived by applying industry scaling factors to the cesium-137 concentrations.

b. The unit of concentration for these nuclides is nCi/g.

c. DAW = dry active waste; concentrations are based on contact dose rates of 10 mR/h.

(1) Prior to transfer and/or sampling, holding tanks should be thoroughly mixed with mixing systems which promote homogeneity.
(2) The time interval between mixing and sampling should be a minimum to prevent settling of particles.
(3) The location of sampling points should be selected where stream stratification is not expected.
(4) Pump speed for transferring the waste stream should provide sufficient velocity to prevent settling and stratification of particles in the line or pipe being sampled.

It is important that the sampling equipment produces the required size and quantity of individual grabs required for compositing a representative sample which can be handled for laboratory analytical evaluations. The sampling process should be performed on the transfer line to the waste container during the period of transfer. The initiating factor for each grab may be time, flow, radiation level, or other variable depending on the objective of sampling.

Sampling variations have been identified[2] as one of the major uncertainties in the 10CFR61 compliance program. One way to reduce sampling error is to increase both the number and size of samples, but the sampling error is frequently compromised by personnel radiation exposure and operation costs associated with sampling.

The composite sample is further properly mixed in a laboratory and prepared for radiochemical analysis. Figure 7-1 shows a flow diagram of the necessary sample preparation required to properly analyze the waste sample[5].

7.3 RADIOCHEMICAL ANALYSIS

As pointed out earlier, due to difficulties of some analyses, most of the waste radioassay has been performed by outside contractor laboratories. However, the on-site laboratory can generally perform relatively easy-to-measure nuclides, including major gamma-emitting nuclides, which can be measured directly by gamma spectrometry, and some of

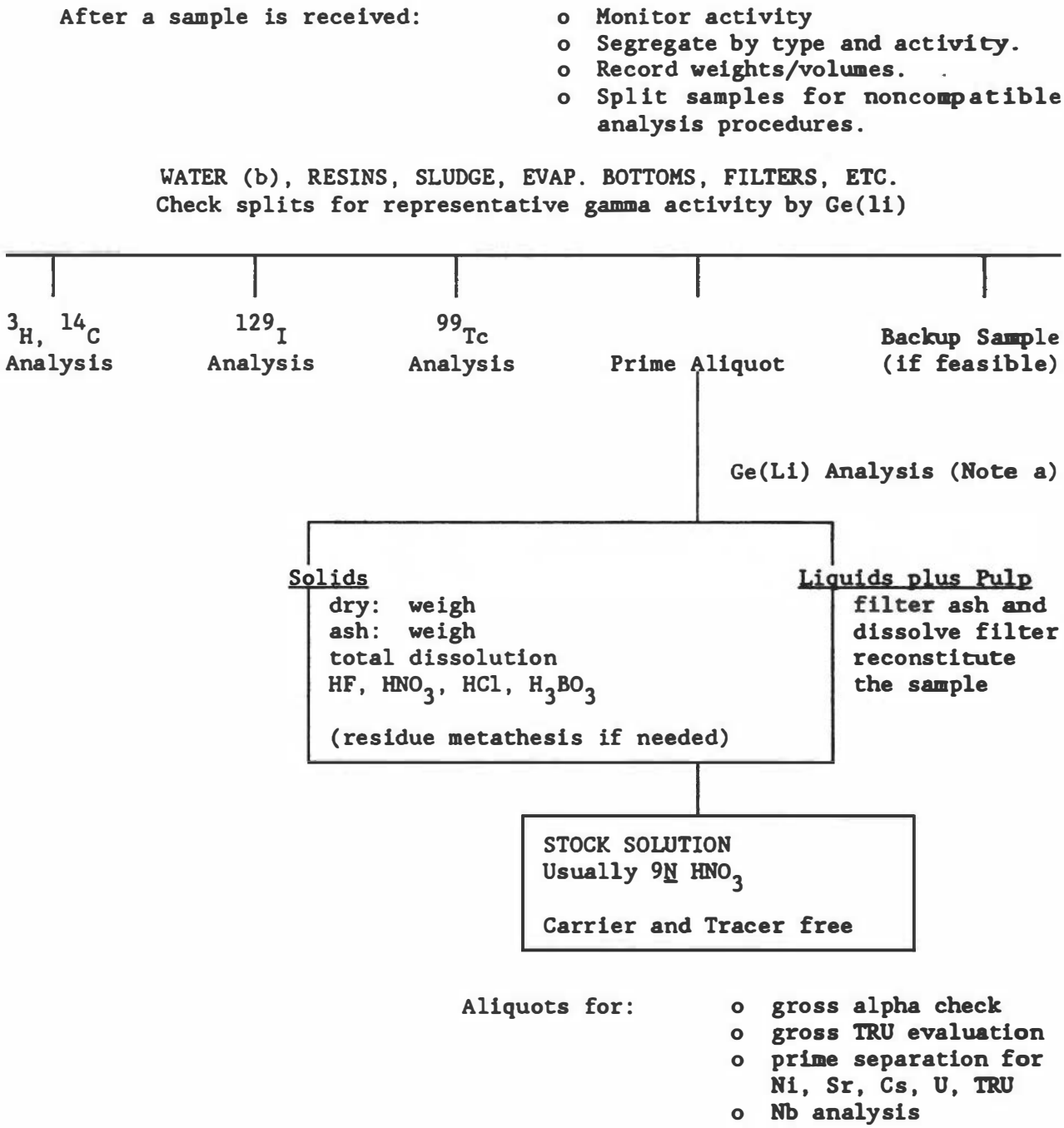

Figure 7-1. Flow Diagram of Sample Preparation (Reproduced with Permission, EPRI NP-4037, Ref. 5)

Note (a) Ge(Li) analysis is performed on the appropriate counting form for the sample type, such as Marinelli beaker or other container for water, counting dish for evaporated water, petri dish for dried or ashed solids, etc.

(b) Water with reducing preservative for ^{3}H, ^{14}C, ^{129}I and ^{99}Tc. Water with pulp for "prime".

the beta-emitting nuclides H-3, Sr-90/Y-90, Fe-55 and Ni-63 which have been frequently measured in liquid waste stream samples. The radiochemical procedures for these nuclides are given in Appendix E. In many cases, the major gamma-emitting nuclides can be measured directly in transfer lines or in waste drums. Discussion of direct assay techniques will be presented in the next section.

Description of the analytical procedures used by outside contractor laboratories should be available in their literature. A schematic of the typical analysis program used by Science Applications International Corporation (SAIC) is shown in Figure 7-2. A brief summary of measurement methods developed by EAL Corporation has been described by Wassman and Leventhal[5].

There are two primary problems associated with the radiochemical analyses of the difficult-to-measure nuclides. These are analytical sensitivity and radiochemical purity. The former is mainly a function of sample size, length of counting times, and measurement equipment. These are variables which are well-defined and easily controlled. In the case of the long-lived, beta-emitting nuclides, the requirement of radiochemical purity is extremely severe and the degree of purity is difficult to measure or control, particularly as many of the potential impurities are also pure beta emitters. Thus it is not unusual to require chemical separation factors on the order of 10^6 to 10^7. Detailed evaluation of published radiochemical procedures for those difficult-to-measure nuclides is beyond the scope of this monograph. However, some of the major concerns in the analyses of those nuclides have been reported by Vance et al.[2].

7.4 DIRECT ASSAY TECHNIQUES

Direct assay of waste radioactivity by gamma-ray spectrometry is a well-established technique. Generally, a high resolution germanium detector is installed in a heavily shielded collimator, which is positioned properly toward the target waste container or waste transfer line. The direct assay technique generally gives fast and accurate assays of bulk waste with no personnel radiation exposure from sampling.

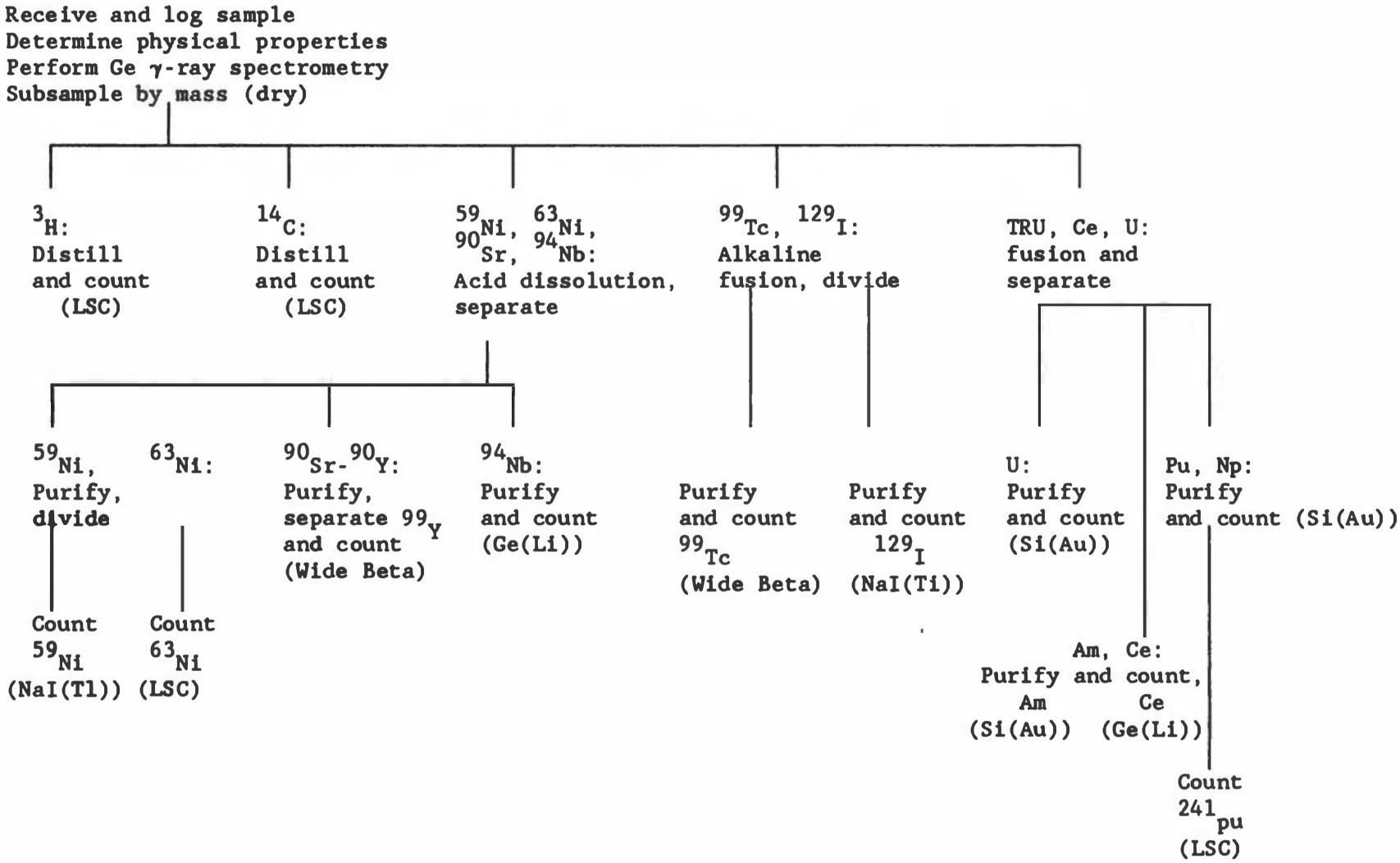

Figure 7-2. Schematic of the Sample Chemical Analysis Program (Ref. 3)

LSC: Liquid Scintillation Counter
NaI(Tl): Thin window thallium activated sodium iodide scintillation counter
Si(Au): Barrier type, silicon alpha energy counter

Direct assay is of particular importance for heterogeneous wastes, since representative sampling of those wastes is nearly impossible. Similar to all other radioactivity counting systems, the direct gamma-ray assay system requires a quantitative calibration. Calibration of the system makes it possible to convert the measured gamma-ray intensities into concentrations of gamma-emitting nuclides contained in the radwaste. The conversion factors should include the correction factors for various collimators, detector configurations and counting geometries, in addition to counting efficiencies as a function of gamma-ray energy.

Unlike the laboratory counting system, it is rather difficult* to use a known "standard" for counting efficiency and geometry calibration in the counting system for the radwaste. Different calibration techniques have been reported by several investigators.[6-9] One of those calibration procedure has been developed by SAIC[6,7] and used with the direct assay gamma scanner. The procedure incorporates a semi-empirical model for detector efficiency that treats the detector as a point on the axis whose location is a function of gamma-ray energy and whose response to volume elements located off the axis is a function of both energy and the off-axis distance. The calibration procedure for each collimator and detector configuration is to determine the model parameters by mapping the response to a calibrated gamma-ray source (standard) located anywhere in front of the detector-collimator system. The model calculates detection efficiencies for a source-detector geometry through numerical integration of the detector response function over the volume of the source. Calculations include gamma-ray self-attenuation in the source material as well as the attenuation by the source container and any external absorber.

There are at least three general rules of practice in application of the gamma-ray direct-assay technique to the assay of radwaste: (1) the background radiation fields in the area should be low, so that a clear gamma-ray spectrum can be obtained from the radwaste for analysis (the background spectrum is always needed for the net activity calculation); (2) establish the proper detection efficiency for the chosen geometry; and (3) choose

*It is difficult, but not impossible, to prepare a simulated waste material, spiked with known quantity of radioactivity, contained in a waste container for direct calibration.

the geometry of scan optimal to the waste container. Choosing the optimal scan geometry is often a practical as well as an accuracy consideration. Since the waste is frequently inhomogeneously mixed in the container, it is desirable to scan the entire portion of the container containing the waste. An ideal geometry is with the axis of the detector collimator aligned with the center of the waste, and there is a sufficient space between the detector and the waste container so that the entire container can be scanned.[10]

A technique of direct assay of transuranics by passive neutron measurement has been developed by PNL (Battelle Pacific Northwest Laboratories)[6]. Neutrons can be produced in the radwaste containing transuranic isotopes, either by spontaneous fission or by the (α, n) reaction. Although the technique has been demonstrated to be a viable technique for assaying measurable levels of transuranics, the efficiency of the counting system is unlikely to achieve the required LLD of 0.1 nCi/g.

7.5 RADIONUCLIDE CORRELATIONS AND SCALING FACTORS

As mentioned earlier, in order to report the content of radionuclide in the radwaste, the "difficult-to-measure" nuclides may be inferred by taking a ratio of their activity to the activity of nuclides that can be readily measured. These ratios are referred to as scaling or correlation factors and are expected to be developed on a plant and waste stream specific basis.

Ideally, the nuclides used for scaling factors should meet the following criteria:

(1) There should be a constant ratio in the rate of formation and release of both nuclides.
(2) Both nuclides should possess similar chemical and physical transport properties.
(3) The nuclide on which the correlation is based should be readily measurable by gamma-ray spectrometry.

Studies have been undertaken [3-5,11] to determine or review the scaling factors for all the difficult-to-measure nuclides. A careful examination of the correlation pairs used by many operating reactors reveals that most of the correlations are based on either Co-60 or Cs-137. There is a considerable disparity between the actual and ideal correlation pairs. As a result, the correlation ratios are considerably dispersive; differences of orders of magnitude have been reported.

Variation in the correlation ratios is expected to arise from at least three major areas, which could be significantly different from plant to plant, and could change from time to time. The first area is a change in defective fuel conditions which would give rise to different release rates between nuclides. Detailed discussion on the variation of fission product release rate as a function of fuel failure condition has been presented previously in Section 3. The second area is a change in the primary system materials, from which most of the activated corrosion products originate. In recent years considerable effort has been made in many plants to remove the sources of cobalt (Co-60) as the major step taken to reduce personnel exposures. The Co-60 concentration in the BWR primary coolant has been seen decreasing from ≈ 0.5 μCi/kg in earlier years to < 0.1 μCi/kg in some reactors. Reduction of iron crud input from feedwater is also an example of changing the source of activated corrosion products. The third area is a change in the source of inputs to the radwaste system. The compositions of nuclides in different waste streams are expected to be different. These areas and the difficulties of developing the reliable scaling factors for those difficult-to-measure nuclides are discussed below:

Tritium (H-3) is produced in the coolant by neutron capture in the $^{2}H(n, \gamma)^{3}H$ reaction. It is also produced by high energy neutron reactions with lithium isotopes, $^{6}Li(n, \alpha)^{3}H$, and $^{7}Li(n, n\alpha)^{3}H$, and with boron isotopes $^{10}B(n, 2\alpha)^{3}H$, $^{10}B(n, \alpha)^{7}Li$ $(n, n\alpha)^{3}H$. The boron and lithium reactions are predominant sources of tritium in PWR. Tritium is also produced by ternary fission of U-235, but only a small fraction ($\approx 1\%$) of the total H-3 produced in the fuel is believed to diffuse through the cladding into the coolant.

H-3 does not relate to any other nuclide in the waste but can be estimated from the coolant content of the radwaste. The concentration of tritium in the coolant is used to calculate the tritium content. The coolant content of the specific stream of the radwaste is, in fact, predetermined by measuring the H-3 concentration in a series of representative samples.

Carbon-14 is produced by neutron capture from the $^{17}O(n,\alpha)^{14}C$ and $^{14}N(n,p)^{14}C$ reactions. Carbon-14 is released from PWRs in the gaseous radwaste system as organic species, predominantly methane. In BWRs, it is released in the condenser offgas system as CO_2. A small fraction of C-14 as $CO_3^=$ or HCO_3^- is retained in the reactor water cleanup system. No suitable correlation nuclide can be found in the radwaste.

Iron-55 and Ni-63 are produced by neutron activation of Fe-54 and Ni-62, $^{54}Fe(n,\gamma)^{55}Fe$ and $^{62}Ni(n,\gamma)^{63}Ni$, respectively. These two nuclides and Co-60 result from the activation of reactor material corrosion and/or wear products. All three species have similar chemical properties, although cobalt and nickel are probably more soluble than iron in the reactor coolant. The major activation process involves the deposition of corrosion products on the fuel surfaces followed by their activation and subsequent release and transport to the radwaste system. There are also some important sources of Co-60 and Ni-63 in the core construction materials. Because there are some differences in the material sources, and the primary coolant chemistry conditions are entirely different between BWRs and PWRs, the ratios of Fe-55/Co-60 and Ni-63/Co-60 are expected to be different between BWRs and PWRs.

Nickel-59 is produced by the $^{58}Ni(n,\gamma)^{59}Ni$ reaction. Since the ratio of Ni-58 and Ni-62 in natural nickel is invariant, and the product of Ni-59 is quite similar to that of Ni-63, the ratio of the production rate of Ni-59 to Ni-63 should be a constant. This Ni-59/Ni-63 activity ratio has been calculated to be approximately 0.01 irrespective of the flux or core location. Since the Ni-63/Co-60 correlation factor can be measured and established for a specific waste stream, the Ni-59/Co-60 can also be estimated.

Strontium-90 is produced by fission. It decays by beta emission to Y-90 which is also a beta emitter. The Y-90 ($t_{1/2}$ = 64 hour) is practically in equilibrium with Sr-90, but unlike Sr-90, Y-90 is normally in insoluble forms. Since Sr-90 and Cs-137 are generally found in soluble cationic forms, the activity ratio may be easier to establish as long as the fuel conditions do not change significantly.

Technitium-99 is mainly produced by fission. The valence states of technitium may vary from -1 to +7. In the BWR coolant, shorter-lived technitium activities (Tc-99m, -101, -104) are normally found in the anionic forms, most likely TcO_4^-, but they would behave

totally differently in the PWR coolant. It is very difficult to find a good correlation partner. Although Cs-137 has been suggested, there are not only differences in chemical properties, but the release mechanisms from fuel are also significantly different. Tc-99 is also produced by activation of Mo-98.

Iodine-129 is produced by fission as a decay product of Te-129. Iodine activities are always found in either the BWR or PWR coolant as anion species. In BWRs, iodine activities are also volatile and a large fraction of iodine activities released from the failed fuel can be transported with steam into the condensate (Section 3,4). Similar to Tc-99, a gamma-emitting correlation partner for I-129 may not exist.

Transuranic isotopes are those produced by successive neutron activation of uranium and its products in a reactor. The chain of production and the radiation characteristic of each isotope are shown in Figure 2-9 in Section 2.6. As discussed earlier, the activity buildup varies quite rapidly with the fuel burnup (Figure 2-10); however, the predominant alpha activity is Cm-242 (90 to 95%) because of its shorter half-life.

In the reactor coolant, most of the transuranic (TRU) alpha activities are found to be in insoluble forms, and can be correlated with insoluble fission products, Zr-95 and Ru-103 (Section 8.5) and Ce-144[6]. The determination of the TRU content of low-level waste has long been a problem confronting utilities, and the determination of gamma-emitting nuclides Zr-95, Ru-103 or Ce-144 is also very difficult by direct spectrometry because of their low intensities and short half-lives (relative to Cs-137, Co-60 and other major activities in the radwaste).

In summary, the correlation or scaling factors for those difficult-to-measure nuclides in the radwaste are very difficult to determine accurately and consistently. The plant and stream specific correlation factors can only be determined for a short operating duration because the correlation may vary from time to time depending on many factors discussed previously.

7.6 REFERENCES

(1) U.S. Nuclear Regulatory Commission, "Licensing Requirements for Land Disposal of Radioactive Waste," Code of Federal Regulations, Title 10, Part 61, Federal Register, 47, p. 57446, December 1982.

(2) J.N. Vance, et al., "Assessing the Impact of NRC Regulation 10CFR61 on the Nuclear Industry", EPRI NP-5983 (August 1988).

(3) J.E. Cline, et al., "Assay of Long-Lived Radionuclides in Low-Level Wastes from Power Reactors", U.S. Nuclear Regulatory Commission NUREG/CR-4101 (April 1985).

(4) J.A. Lieberman, et al., "Methodologies for Classification of Low-Level Radioactive Wastes from Nuclear Power Plants", AIF/NESP-027 (December 1983).

(5) W.T. Best, et al., "Radionuclide Correlations in Low-Level Radwaste", EPRI NP-4037 (June 1985)

(6) J.E. Cline, et al., "Advanced Radioactive Waste Assay Methods", EPRI NP-5497 (November 1987).

(7) J.E. Cline, et al., "Direct Assay of Drummed Evaporator Bottoms, Dry-Active Waste and Filter Cartridges at the GINNA Nuclear Station", ANS Int. Topical Meeting on Waste Management and Decontamination and Decommissioning (1987).

(8) M. Tsutsumi, T. Gato and H. Kato, "Assay System for Gamma Radionuclides in Miscellaneous Solid Waste Packed in Drums", 1988 JAIF International Conf. Water Chemistry in Nuclear Power Plants, Tokyo, Japan, Vol. 2, p. 813, (1988).

(9) W. Inder Schmitten, B. Sohnius and E. Wehner, Nucl. Tech., 92, 374 (1990).

(10) R.L. Brodzinski, et al., "Design and Operation of a Passive Neutron Monitor for Assaying the TRU Content of Solid Wastes", PNL-4966 (February 1984).

(11) W.T. Best and A.D. Miller, "Updating Scaling Factors in Low-Level Radwaste", EPRI NP-5077 (March 1987).

8. SPECIAL RADIOCHEMICAL STUDIES

8.1 ESTIMATION OF NOBLE GAS TRANSIT TIME IN THE BWR TURBINE SYSTEM

The decay of the short-lived noble gases and buildup of their daughter product activities in the steam and condensate are unique features of the BWR system. The noble gas activities, which are exhausted from the Steam Jet Air Ejector (SJAE), decay during the transit in the steam path, and they and their daughter activities follow many separate paths through the low pressure turbine and the heater drain system, while ≈1% of the high-pressure steam is used to drive the SJAEs. The daughter activities will either be washed out by the condensed steam or deposited on the turbine and heater surfaces. In order to estimate the parent decay and daughter buildup in the steam paths in the turbine, the transit time as well as the activity release rate must be known. It is estimated that a major portion (≈60%) of the gaseous activities passes the turbine in a few seconds, but the "apparent" transit time, defined for the gaseous parents by the equation $t_i = (1/\lambda_i)\ln(A^o_i/A_i)$*, may vary from several seconds to a few minutes, depending on the half-life of the individual gaseous isotopes.

The "apparent" transit time, T, can be calculated from the parent-daughter pair activities:

$$A_2 = \frac{\lambda_2}{\lambda_2 - \lambda_1} A_1 \left[1 - e^{(\lambda_1 - \lambda_2)T}\right]$$

where A_2 = daughter activity transport rate (μCi/s)

A_1 = parent activity release rate (μCi/s) measured at the same SJAE sample point

---

* e.g., in more familiar form, $A_i = A^o_i e^{-\lambda_i t_i}$. In case of multiple pathes, $A_i = \sum_j F_j A^o_i e^{-\lambda_i t_i}$

where F_j is the fraction of A^o_i passing through the steam path j.

A smooth curve of T vs. the half-life of the parent nuclide from the data obtained in an operating BWR is shown in Figure 8-1. Qualitatively, the curve would be expected to flatten out for short half-lives as a limiting point is reached where only a single flow delay is significant, and all other delays are so long relative to the half-life that they do not contribute to the release. The apparent transit time for other gaseous activities can be obtained from this curve. If the transit time from the outlet of the reactor pressure vessel (RPV) to the SJAE is known, the gaseous activity release rate at the RPV can be estimated.

Similarly, using the parent-daughter relationship, the delay time in the condensate (hotwell) can be estimated from the noble gas daughter and granddaughter activities. In the reactor coolant, the delay time in the sample line or any specific system can also be estimated from the parent-daughter pair activities. Some major parent-daughter pairs and their decay constants have been summarized in Table 2-1.

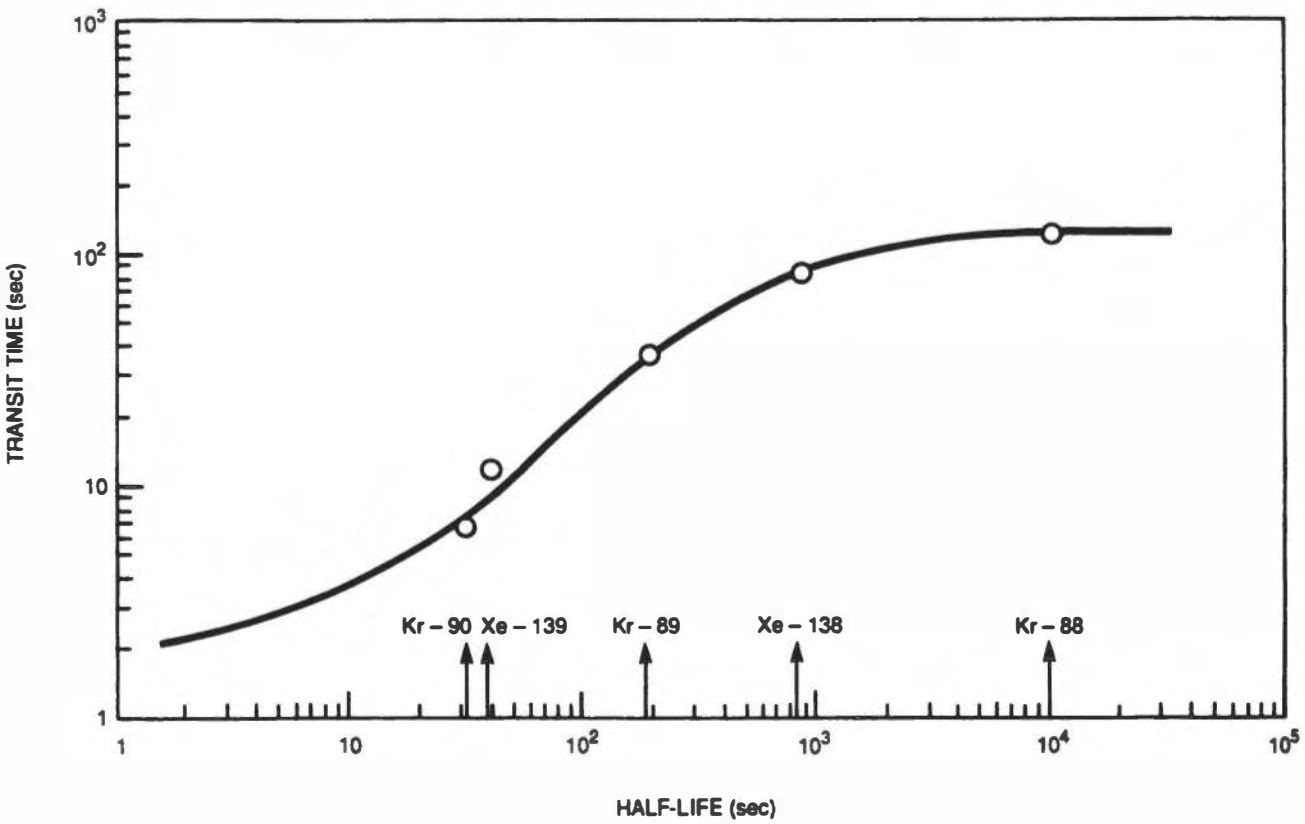

Figure 8-1. Apparent Transit Time for Gaseous Activities from RPV to SJAE

8.2 NO-CLEANUP TEST IN A BWR

A no-cleanup test is generally referred to as a test of measuring the water chemistry and the distribution of fission products in the primary coolant system when the RWCU system is removed from service. During a no-cleanup test, a number of practical operation parameters can be measured, such as the mass of reactor coolant, water cleanup half-time, iodine carryover, impurity input rate, etc. A typical example of no-cleanup test data is shown in Figure 8-2. In this test, the water conductivity was allowed to increase to 2.4 μS/cm before the cleanup system was returned to service. By measuring the decrease in water conductivity after return to service, the cleanup half-time can be estimated (Figure 8-3). Also, by knowing the water cleanup flow rate and efficiency, the apparent reactor coolant mass may be calculated (it should not be a surprise that the measured reactor coolant mass during operation may not be consistent with that estimated from the design drawing).

The radioactivity buildup in the coolant may be easily calculated. Some examples of calculations are compared with the measured data below.

8.2.1 Na-24 and Cl-38 Activity Buildup

The total active impurity at equilibrium condition during normal operation has been shown in Section 2.7, Equation 2-17:

$$N_{eq} = \frac{n\phi\sigma}{\beta_c(\lambda + \beta_c)} \qquad (8\text{-}1)$$

During the time of no-cleanup service, the production of active nuclides N_{nc} can be described by Equation 8-2:

$$\frac{dN_{nc}}{dt} = N^{o}_{nc}\ \phi\sigma - \lambda N \qquad (8\text{-}2)$$

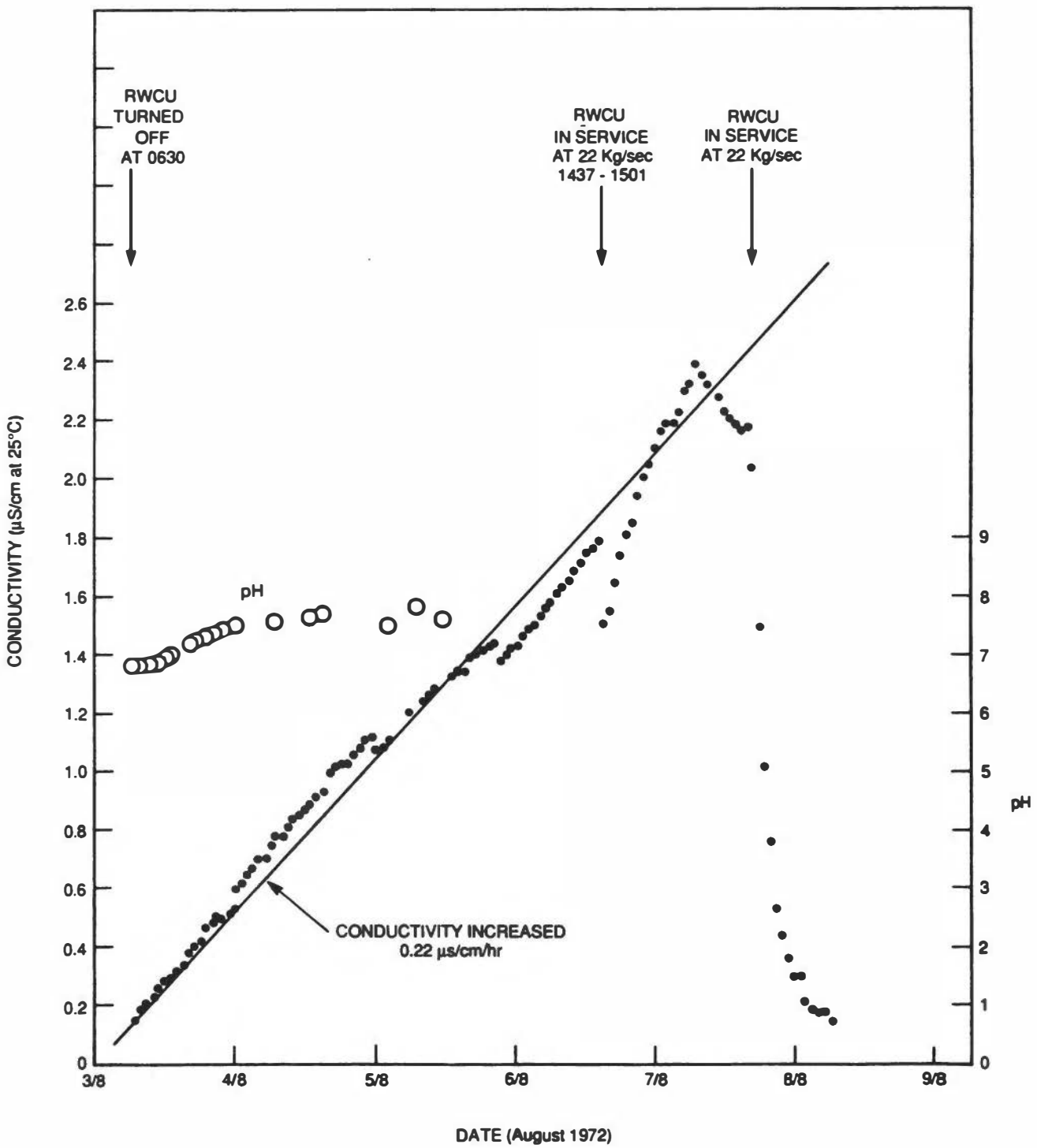

Figure 8-2. Variation of Conductivity and pH Value in Reactor Water During a No-Cleanup Test

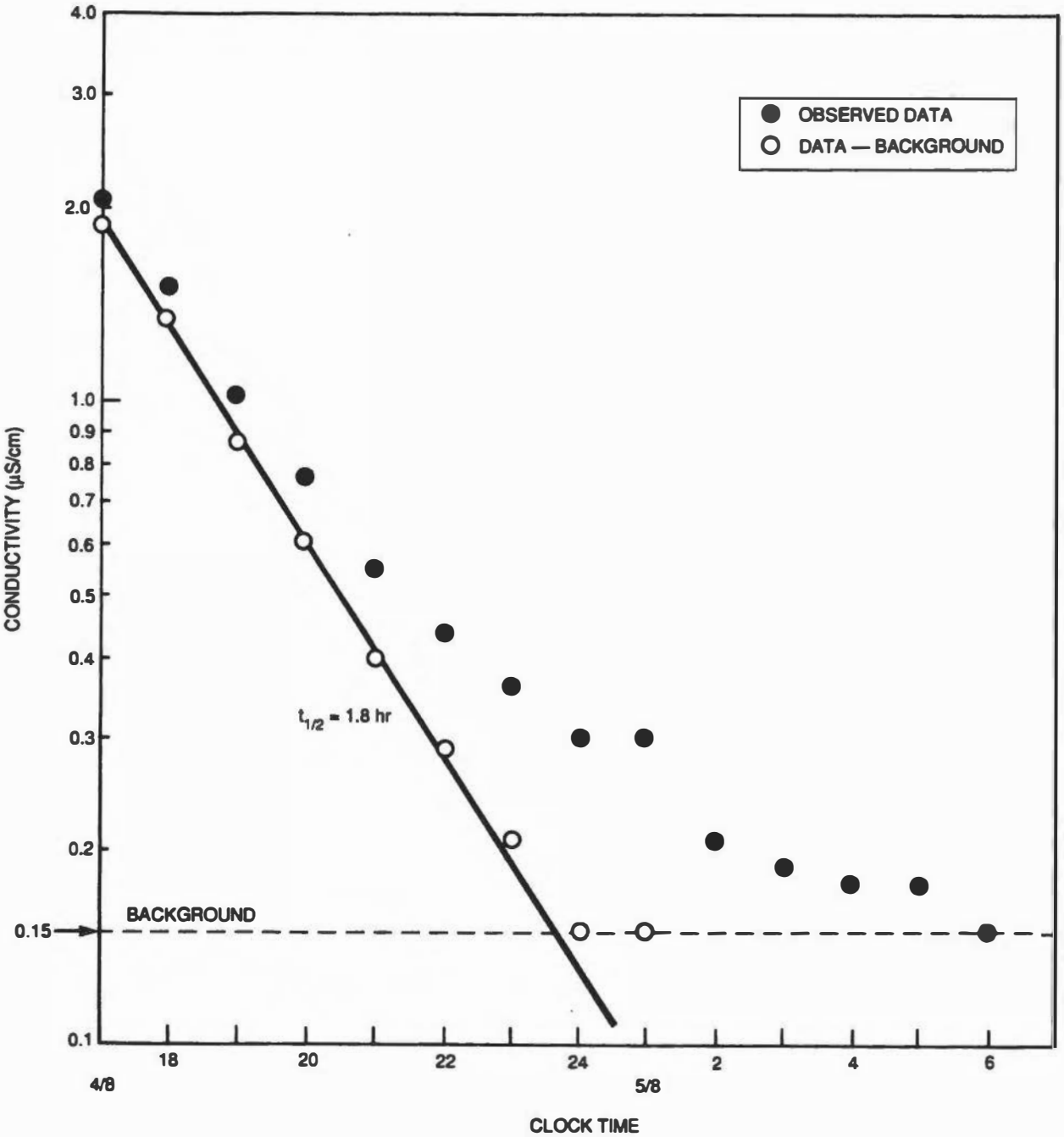

Figure 8-3. Variation of Reactor Water Conductivity with RWCU Returning to Service

By replacing $N^{o}_{nc} = nt$, Equation (8-2) can be integrated to become

$$N_{nc} = \frac{n\phi\sigma}{\lambda^2}(\lambda t - 1 + e^{-\lambda t}) \qquad (8\text{-}3)$$

Replacing $n\phi\sigma = N_{eq}\beta_c(\lambda + \beta_c)$ from Equation (8-1),

$$N_{nc} = \frac{N_{eq}\beta_c(\lambda+\beta_c)}{\lambda^2}(\lambda t - 1 + e^{-\lambda t}) \qquad (8\text{-}4)$$

The total activity in the reactor water at time t after the cleanup service is turned off, can be calculated by the summation of Equation 8-4 and the following two items:

$N'_{nc} = N_{eq}e^{-\lambda t}$ — active nuclide produced during normal operation

$N''_{nc} = N^{o}_{eq}\phi\sigma(1-e^{-\lambda t})$ — activation of parent nuclide input to reactor water during normal operation.

$$= N_{eq}(\lambda+\beta_c)(1_c - e^{-\lambda t})$$

$$N_{nc}(\text{total}) = N_{eq}\left[\frac{\beta_c(\lambda+\beta_c)}{\lambda^2}(\lambda t - 1 + e^{-\lambda t}) + (\lambda+\beta_c)(1-e^{-\lambda t}) + e^{-\lambda t}\right] \qquad (8\text{-}5)$$

Equation 8-5 predicts that the concentrations of Na-24 and Cl-38 activities should increase with time after the RWCU system is out of service for a period of a few half-lives. The observed increases of Na-24 and Cl-38 activity concentrations are shown in Figure 8-4. The data are also compared with the calculated concentrations from Equation 8-5.

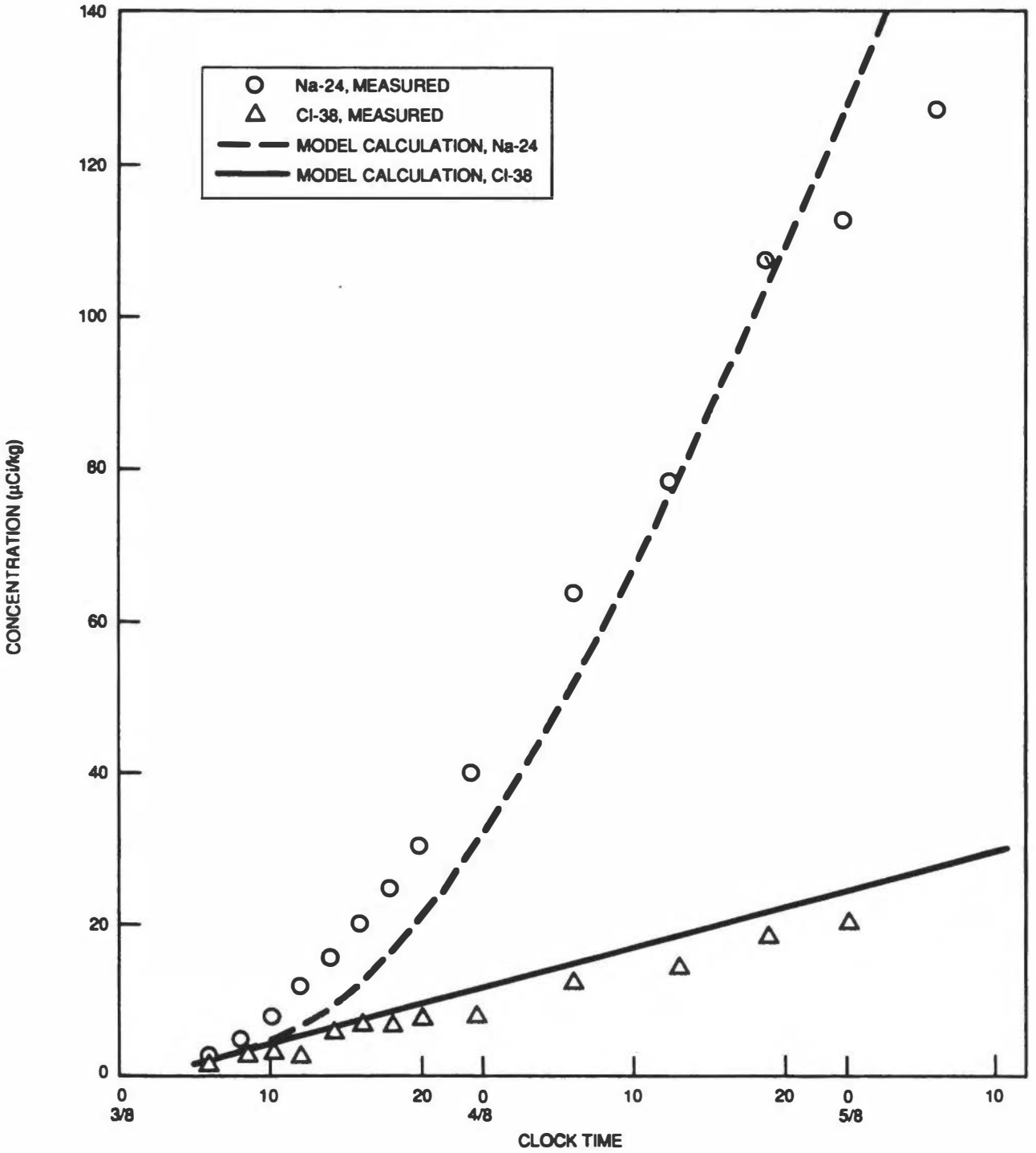

Figure 8-4. Variation of Na-24 and Cl-38 Concentrations in Reactor Water during a No-Cleanup Test

8.2.2 Measurement of Iodine Steam Transport

The magnitude of iodine carryover can be measured directly from the ratio of iodine concentration in the condensate to that in the reactor water. However, in a reactor with forward-pumped heater drains, the iodine carryover cannot be measured directly from the condensate because ~75% of the iodine originally carried over by steam is condensed with steam in the high pressure turbine and forward-pumped back to the reactor (see Section 3.4, Figure 3-5).

Another technique for measuring the iodine carryover is to determine the steady-state concentration of iodine in reactor water during normal steady power operation with and without the RWCU system in service. When the RWCU system is removed from the service $\beta_c=0$ in Equation 3-23, the iodine concentration will increase and reach a higher steady state concentration, C_{nc} (Figure 8-5),

$$C_{nc} = \frac{A_i}{(W\lambda_i + \beta_i)} \tag{8-6}$$

From the ratio of

$$\frac{C_{nc}}{C_i} = \frac{\lambda_i + \beta_c + \beta_s}{\lambda_i + \beta_s} \tag{8-7}$$

β_s and the iodine carryover ε can be calculated,

$$\varepsilon = \beta_s \frac{W}{F} ,$$

where all symbols have been defined in Section 3.2.3.

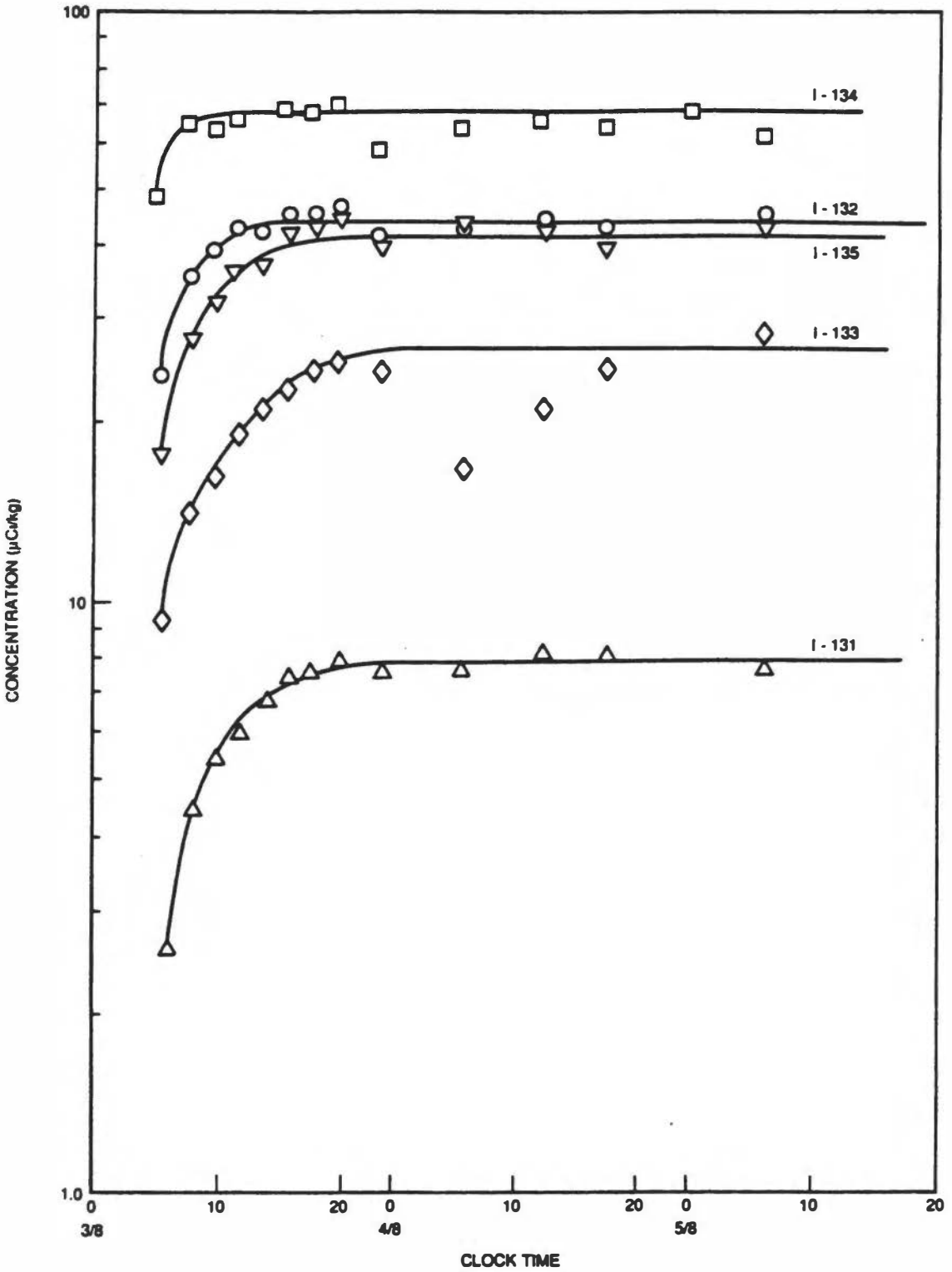

Figure 8-5. Variation of Iodine Activity Concentrations in Reactor Water during a No-Cleanup Test

8.3 RADIOCHEMISTRY OF IODINE

8.3.1 Chemical Forms of Radioiodine in PWR Coolant

The PWR coolant chemistry is more complex than BWR chemistry, particularly during reactor shutdown. During normal operation, the coolant is maintained at pH~9 (25°C) and under reducing conditions with hydrogen. Boration of the coolant during shutdown brings the water pH to ~6, and in some reactors, H_2O_2 is added to oxidize the corrosion film in order to remove the cobalt activities from the primary system surfaces (Section 4.3.2.)

The behavior of iodine activities in the PWR coolant has been studied recently by Voilleque[1]. Most of the iodine activities are found in the reduced form (iodide), as expected, during normal operation, but immediately after shutdown, due to boration and H_2O_2 addition, volatile forms of iodine (mainly I_2) have been found to vary from a few percent to approximately 40%. A few percent of organic iodide are generally found after shutdown. A few percent of iodate (IO_3^-) are also observed after shutdown, but in some cases, up to 70% of iodine activities have been reported when H_2O_2 is added to the coolant.

8.3.2 Chemical Forms of Radioiodine in BWR Coolant*

The chemical forms of radioactive iodine in reactor water have been measured in a number of reactors during normal operation and during shutdown.[2] As shown in Table 8-1, during reactor operation, 60-90% of the iodine in reactor water was found as iodide (I^-) and perhaps HIO, and the remainder was essentially iodate (IO_3^-). Only traces of I_2 and organic iodine were detected and these traces were most likely cross contamination from the other fractions in analytical procedures (see Figure 8-6).

---

* More recently, the chemical behavior of radioiodine in BWR coolant under hydrogen water chemistry conditions has been studied by Lin and the results have been published elsewhere.[16]

Table 8-1

CHEMICAL FORMS OF RADIOIODINE IN BWR PRIMARY COOLANT (%)

Reactor (Date)		I^-	IO_3^-	I_2	Organic
During Normal Operation					
Millstone-1	(7/1972)	80	20	<1	<1
Humbolt	(12/1972)	78	10	8	4
Nine Mile Point-1	(12/1972)	65	34	1	<1
Nine Mile Point-1	(4/1973)	52	48	<1	<1
Nine Mile Point-1	(7/1974)	79	18	3	<1
Monticello	(7/1974)	77	23	<1	<1
Monticello	(9/1975)	84	12	4	<1
Brunswick-2	(5/1977)	67	33	<1	<1
FitzPatrick	(8/1985)	90	10	<1	<1
FitzPatrick (HWC)	(8/1985)	99	1	<1	<1
Hatch-1	(7/1986)	83	17	<1	<1
Hatch-1 (HWC)	(7/1986)	90	10	<1	<1
Nine Mile Point-1	(5/1987)	40	60	<1	<1
Nine Mile Point-1 (HWC)	(5/1987)	95	5	<1	<1
During Reactor Shutdown					
Nine Mile Point-1	(4/1973)	2	98	<1	<1
Nine Mile Point-1	(3/1974)	4	96	<1	<1
Monticello	(9/1975)	63	30	3	<1
Monticello	(2/1976)	18	82	<1	<1

Note: The distribution of I^- and IO_3^- was found to vary from plant to plant, most likely depending on the metallic ion concentration, particularly Cu ions, in reactor water. Similar results of I^-/IO_3^- measurements have been reported in the literature[5,6,7]

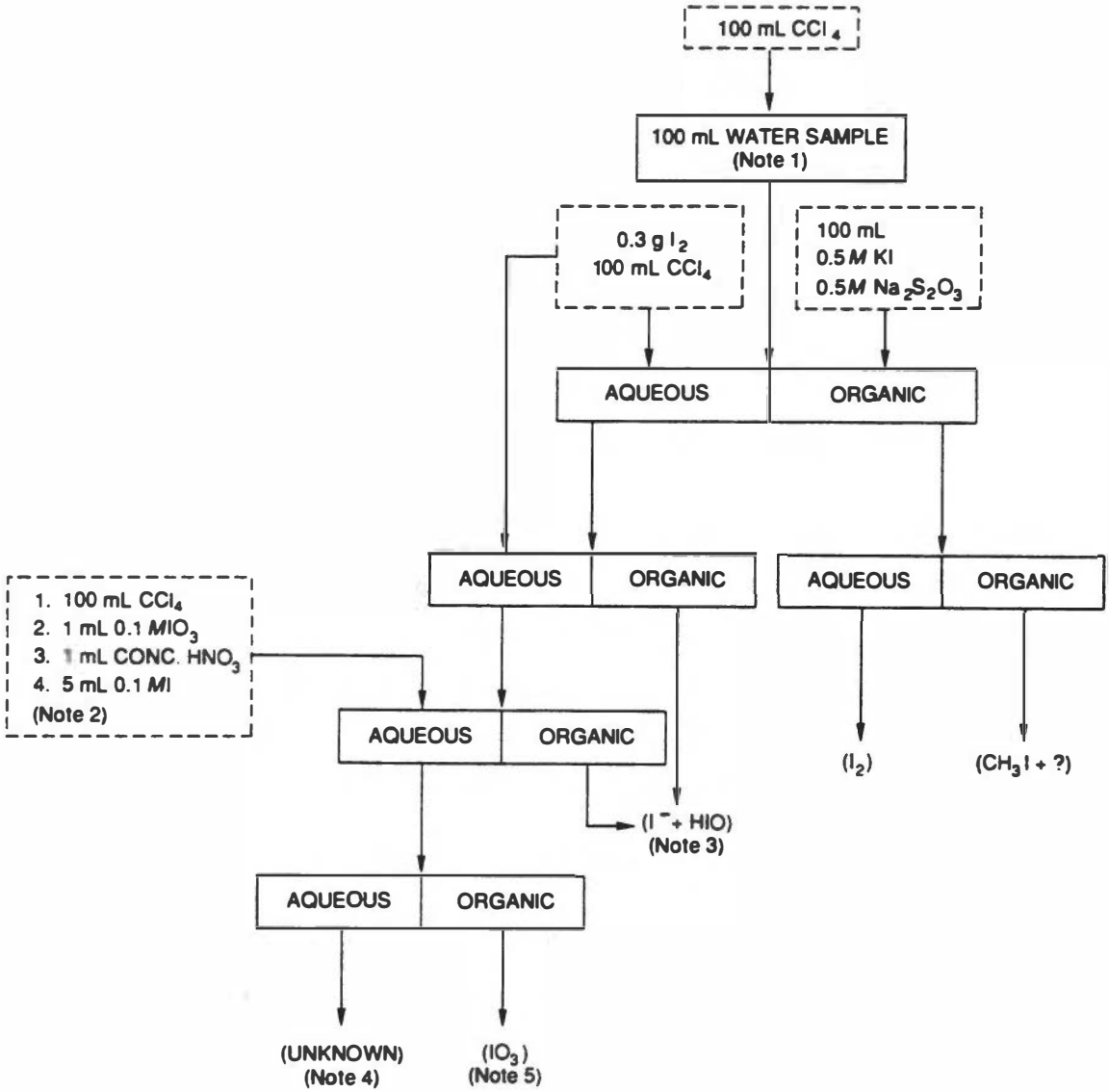

Figure 8-6. Separation of Iodine Chemical Forms by Exchange/Extraction Processes (Ref. 2)

Note 1. The sample size can be reduced for a high activity sample, and the volumes of all reagents are reduced accordingly. The sample is shaken in a separatory funnel for at least two minutes in each separation step.

Note 2. IO_3^- is reduced to I_2 by I^- according to the Dushman reaction. Care is taken that a slight excess of I^- is added to complete the reaction. But to avoid the radioiodine back exchange between produced I_2 and the excess I^-, the process can be carried out in two stages. With approx. 80 mL CCl_4, approx. 4.5 mL I^- solution in the first stage, after the I_2-CCl_4 is removed, 20 ml CCl_4 and additional I^- is added drop by drop until no yellow-brown color appears in the aqueous phase.

Note 3. HIO and I^- are expected to behave similarly. It is recommended to reduce the I_2 in organic phase to I^- for activity counting with 100 mL water containing sufficient Na_2SO_3.

Note 4. Some residual iodine activities may be associated with insoluble impurities.

Note 5. As recommended in Note 3, the I_2 in organic phase is reduced to I^- in aqueous phase for activity counting.

Although it is not certain what form of iodine is released from the fuel, if elemental iodine (I_2) is released at a "carrier free" concentration, I_2 is totally hydrolyzed in neutral water to form I^- and HIO:

$$I_2\ (aq) + H_2O \rightarrow H^+ + I^- + HIO\ (aq)$$

$$K = 5.4 \times 10^{13} \text{ at } 25°C$$

and the reaction should go to completion in less than a second.

Because of its low concentration and a second or third order reaction mechanism, the formation of IO_3^- from the disportionation of HIO,

$$3\ HIO \rightarrow 3H^+ + 2I^- + IO_3^-$$

is almost impossible. Instead, IO_3^- is believed to be produced from I^- by radiation induced oxidation with HIO as a reaction intermediate, which is one of the major forms of iodine in steam transport (see later). The radiation induced oxidation of I^- to IO_3^- has been successfully confirmed in laboratory studies (see Section 6.7). During reactor shutdown, the steam transport stops and the iodine concentration spike occurs in the reactor water. The majority of iodine was found to be oxidized to the IO_3^- form. Recently, during the hydrogen water chemistry (HWC) tests in three reactors, the IO_3^- fraction was found substantially decreased as expected when the reactor water chemistry was switched to more reducing HWC conditions by hydrogen gas addition to suppress the water radiolysis in the coolant. [16]

Organic iodine, commonly represented by CH_3I may be formed (more likely in the gas phase) by the reaction between iodine and organic impurities under radiation fields, CH_3I is also decomposed (hydrolyzed) rapidly in high temperature water:

$$CH_3I + H_2O \rightarrow CH_3OH + I^- + H^+$$

The half-time of the first-order hydrolysis reaction has been reported to be ~20 minutes at 100°C and estimated at <1 s at 250°C.[3,4]

8.3.3 Chemical Forms of Radioiodine Activities in BWR Condensate and Offgas

The iodine species found in the condensate was dominated by I^-, ~90% (Table 8-2), and some traces of I_2 and organic were found. Unlike the reactor water, the trace organic found in the condensate may be real because a large fraction of organic iodine activities has been found in the offgas samples.

The chemical forms of airborne iodine activities are analyzed by using a Science Application Inc. (SAI) type iodine species sampler.[8] The sampler consists of a series of cartridges containing different adsorbents for various iodine species. The particulates are first filtered, I_2 is adsorbed in the first cartridge containing CdI_2 (10% W/W) on inert supporting material chromosorb-P, "hypoiodus acid" (HIO) is adsorbed in the second cartridge containing p-iodophenol (10% W/W) on Al_20_3, the organic iodide is adsorbed in the third cartridge containing Ag-zeolite (100% exchanged), and a backup cartridge containing activated charcoal or Ag-zeolite is used for total adsorption. The results of several measurements are given in Table 8-3. Organic species appear to dominate the airborne iodine activities. It must be pointed out that the species which is separated and collected as "HIO" by the SAI type sample cartridge has never been chemically identified by any other methods. The fraction collected as I_2 could be HI or other volatile inorganic compounds.

It is also of interest to note that the offgas activities are generally much "older" than that measured in the reactor water and the condensate, by comparing the isotopic ratios (Table 8-4). It can be postulated that some of the gaseous iodine activities are not in gaseous forms directly released from the reactor coolant. The apparent aging of the gaseous iodine species in the offgas is probably due to the delay incurred between the iodine deposition on the material surfaces in the steam/turbine system and the subsequent formation and release of organic species. The true mechanism of organic iodine formation in the steam/turbine system is probably related to the production of

Table 8-2

CHEMICAL FORMS OF RADIOIODINE IN CONDENSATE (%)

Reactor	Date	I^-	IO_3^-	I_2	Organic
Millstone-1	7/1972	82	10	6	2
Humbolt	11/1972	85	9	2	4
Nine Mile Pt-1	12/1972	88	3	8	1
Monticello	7/1974	93	4	3	1

Table 8-3

CHEMICAL FORMS OF IODINE ACTIVITIES IN BWR OFFGAS (%)

Reactor	Date	Iodine	HIO	Organic	Particulate
Oyster Creek	1973*	1.5	16.9	81.6	—
Millstone-1	1973*	30.2	34.6	35.0	—
Monticello	1973*	52.3	18.3	29.4	—
Dresden-2	1973*	4.5	20.2	75.3	—
Dresden-3	1973*	6.7	22.6	70.7	—
Millstone-1	7/1972	30	–	(70)**	—
Humbolt	11/1972	2	–	(98)**	—
Nine Mile Pt	12/1972	12	–	(87)**	—
Nine Mile Pt	4/1973	12	6	82	—
Brunswick	5/1977	10	48	42	—

* See Reference 11

** In earlier measurements only I_2 and organic were separated. The organic fraction might include the HIO fraction.

Table 8-4

COMPARISON OF IODINE ISOTOPIC RATIOS IN REACTOR WATER CONDENSATE AND OFFGAS

	Reactor Water		Condensate		Offgas	
Isotope	µCi/kg	Relative to I-131	µCi/kg	Relative to I-131	µCi/cm^3	Relative to I-131
I-131 (8.04 d)	3.35	1.0	0.0358	1.0	0.68E-5	1.0
I-133 (20.8 h)	9.55	2.8	0.105	2.7	1.39E-5	2.0
I-135 (6.6 h)	20.4	6.1	0.216	5.6	2.51E-5	3.7
I-132 (2.29 h)	25.2	7.5	0.27	7.0	2.33E-5	3.4
I-134 (52.6 m)	53.8	16.0	0.5	13.0	4.99E-5	7.3

CH_4 as a result of steel corrosion and carbide-hydrogen interaction[9] in the high temperature steam environment. In a study on the surface effects in the transport of airborne radioiodine, Pelletier[10] has reported up to 12% of the iodine originally released as I_2 in 80% humidity air in contact with galvanized steel at ambient temperatures was converted to organic form in a few days.

8.4 TRANSURANIC NUCLIDES IN BWR COOLANTS

Except for Np-239, which is a beta- and gamma-emitting nuclide with a 2.35 day half-life and beta emitting, 14.4-year Pu-241, the transuranic nuclides observed in the reactor coolant are mostly α-emitting species with relatively long half-lives. Because of the low levels of activity and the difficulties in alpha activity analysis, little attention has been given to measuring these nuclides in the various BWR systems. Even fewer measurements have been made of the β-emitting nuclide Pu-241.

The transuranic elements are produced by successive neutron capture in uranium and in its capture products (Figure 2-9). The fuel inventory of these transuranic elements depends on the power of the reactor, the fuel burnup (or total exposure), and spectral shape. As in the lanthanides, the common and dominant oxidation state for the transuranic (actinide) elements in solution is as a +3 species, and the behavior of actinides is very similar to that of the lanthanides when in this same oxidation state. In neutral solution the +3 state, actinide hydroxides are insoluble, or colloidal, while the +4 oxidation state of Pu polymerizes to become a colloidal aggregate. This chemistry is consistent with the observation that all of the detectable α-emitting isotopes in the reactor water are found in the insoluble fraction, while Np-239 is found in the cationic form, probably as NpO_2^+.

Some results obtained from the analysis of a BWR's reactor water samples are shown in Table 8-5. Because of the unusually high uranium deposit on the reactor core surfaces in this reactor, the total alpha activity in this reactor was approximately two orders of magnitude higher than that normally found in other reactors.[12,13] Curium-242, because of its shorter half-life (163 days), has been the dominant (~90-95%) alpha activity in the samples measured at shorter cooling times. In spite of a difference in concentration, the relative concentration of each transuranic activity remained essentially unchanged in the samples.

In an effort to establish a radiochemical model of BWR coolant,[13] it is assumed that all of the "insoluble" transuranic elements appear in the coolant in the same proportion as they appear in the fuel and in amounts consistent with the insoluble fission products (Zr-95, Ru-106, Ce-141, and Ce-144) present in the coolant. Thus, a determination of any

one of these nuclides is sufficient to establish a fuel level (or an effective fuel level) and the others are evaluated on the basis of their predictable content in fuel depending on burnup. The same data from Table 8-5 are shown in Table 8-6. Irrespective of variation in total alpha concentration, the ratio of α:x is multiplied by a factor of $Y_x(1-e^{-\lambda t})$, a constant number can be obtained. A value of approximately 10^{-3} is calculated for this set of data.

The measured activity ratio of alpha to Zr-95 in the coolant from several reactors at various fuel burnups (average core burnup) is shown in Figure 8-7. This ratio, essentially that of Cm-242 to Zr-95, varies as roughly the cube of the burnup of the fuel present in the sample for nominally enriched UO_2. Experimental data seem to be consistently lower in burnup compared to the calculated ratio. This phenomenon can be explained by assuming that the average core burnup is always lower than the burnup of a particular fuel bundle from which the activity is released into the coolant.

An important application of the relationship between the alpha activity and the insoluble fission products activities in the crud sample is that it is thus possible to estimate the alpha activity in the water sample or radwaste samples (Section 7) from the measurement of insoluble fission products.

Table 8-5

TRANSURANIC ISOTOPES IN REACTOR WATER

Sample I.D.	Tot. α (pCi/kg)	Pu-241 (pCi/kg)	Np-239 (μCi/kg)	% of α Activity			
				Cm-242	Cm-244	Pu-238+ Am-241	Pu-239+ Pu-240
A	144	-	-	92.76	0.867	3.81	2.56
B	140	-	-	93.32	0.788	3.09	2.80
C	160	-	-	93.98	0.674	2.66	2.69
D	968	1946	157.5	93.92	1.055	2.60	2.43
E	579	842	186.0	94.77	1.112	2.13	1.79
Average	398	-	-	93.75	0.899	2.86	2.45
	±369	-	-	±0.76	±0.183	±0.63	±0.40

*Not determined.

Table 8-6

RATIOS OF TOTAL ALPHA ACTIVITY TO INSOLUBLE FISSION PRODUCTS IN REACTOR WATER

Sample ID	$\frac{\alpha}{x}^*$			$(10^3)(\alpha / x)\, Y_x (1 - e^{-\lambda t})^*$		
	Zr-95	Ru-103	Ru-106	Zr-95	Ru-103	Ru-106
A	0.0179	0.0262	-	1.03	1.18	-
B	0.0195	0.0243	-	1.12	1.09	-
C	0.0161	0.023	-	0.926	1.04	-
D	0.0195	0.0275	0.071	1.12	1.24	0.832
E	0.0168	0.0357	0.086	0.967	1.61	1.01
Average	0.018	0.0273	0.0785	1.03	1.23	0.92

* x = Activity concentration of insoluble fission product: Zr-95, Ru-103, Ru-106;
Y_x = Avg. fission yield of insoluble fission products;
t = avg. time of fuel in core.

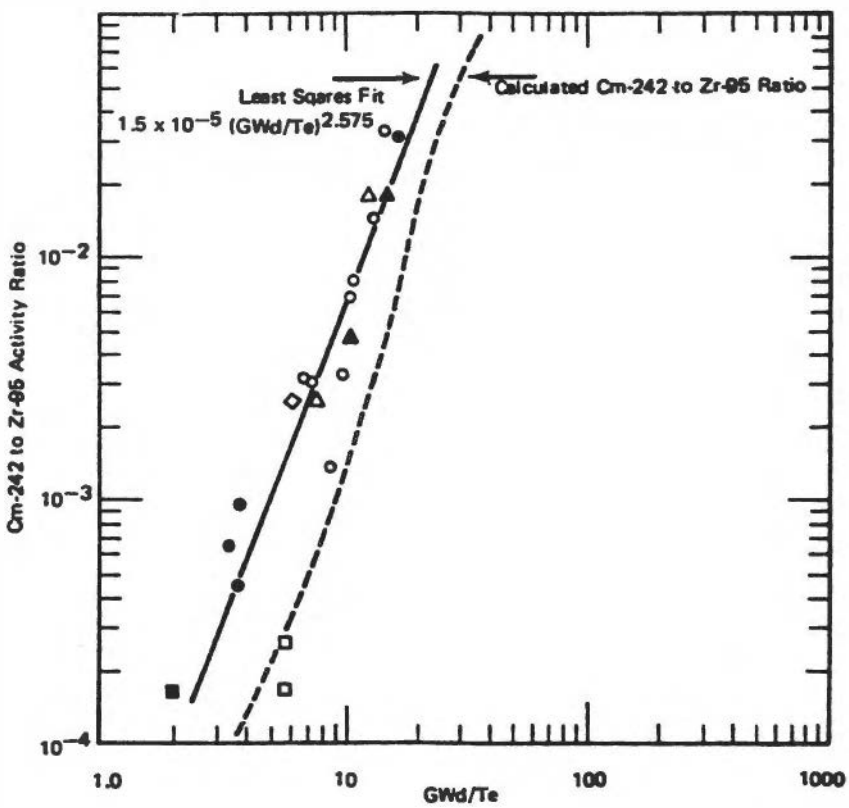

Figure 8-7. Variation of Cm-242 to Zr-95 Activity Ratio in Coolant as a Function of Average Core Burnup

8.5 APPLICATION OF Na-24 TRACER IN FLOW MEASUREMENTS

The measurement of water flow by a radioisotope dilution technique is made by injecting a radioactive tracer solution into the flowing process stream and, after subsequent mixing, sampling the process stream to determine the concentration of tracer in the stream. By knowing the tracer injection rate and the concentrations in the reference solution and the process stream, the flow rate of the process stream can be easily determined by the following equation:

$$F = f \times \frac{c}{C} \qquad (8\text{-}8)$$

where F = water flow rate being determined
f = injection rate of reference solution
c = tracer concentration in reference solution
C = tracer concentration in process stream

Application of this technique has been widely accepted in the nuclear industry, particularly using the Na-24 tracer in feedwater flow measurements. It has been reported by Holloway and Gilbert[14] that the accuracy of ±0.2% relative to a calibrated reference flow nozzle (by ASME) can be obtained. The most obvious advantage of using the Na-24 tracer is the accuracy and high sensitivity of the gamma-ray spectrometric measurement of the Na-24 activity.

In order to achieve a high precision and accuracy of flow measurement, there are a number of parameters that should be carefully determined during a measurement. These parameters are:

(1) Activity concentrations in the reference solution and water samples.
(2) Activity counting time, decay correction and counting geometry correction.
(3) Sample time and sample volume (mass).
(4) Injection time and injection rate.

The combined uncertainty of these parameters should be less than 0.2% in a single measurement.

The only drawback of using the Na-24 tracer is that a heavy shielding is often required to protect the technicians from radiation exposure, particularly during the preparation of highly concentrated tracer solution. A typical procedure of the flow measurement involves the following steps:

(1) Preparation of the Na-24 Reference Solution

The reference solution is prepared by dissolving an irradiated Na_2CO_3 or $NaNO_3$ containing ~ 200 mCi Na-24 in an appropriate container with dilute acid and demineralized water (total volume is about 2 liters). After thoroughly mixing, the solution is transferred to two clean 1-L polyethylene bottles.

(2) Determination of the Na-24 Concentration in Reference Solution

The Na-24 concentration is accurately measured. In order to minimize the counting geometric correction error, the activity sample for counting is prepared identically to the sample collected from the feedwater. Multiple samples should be prepared to obtain the best result. The typical Na-24 concentration in the reference solution is about 2×10^6 cpm/g.

(3) Injection of the Na-24 Reference Solution

The Na-24 reference solution, contained in an 1-L polyethylene bottle, is placed on the platform of a top-loading analytical balance. The solution is injected at a constant rate (approximately 10 g/min) with a minipump into the feedwater upstream of the feedwater pump. The injection rate is determined by determining the weight loss of the solution bottle at predetermined time intervals, generally every 5 minutes. A typical sampling period is ~30 minutes, and total duration of the injection is normally 2 hours for one test.

(4) Sample Collection

The sample is collected at the downstream of the feedwater pump, normally at the regular feedwater sampling station. The water containing the diluted Na-24 activity is passed through two sets of three cation exchange membranes to quantitatively collect the Na-24 in water. Approximately 10 kg of water is collected in a 30 minute period. The exact mass of sample processed through the filter poles is determined by collecting the filter effluent in tared containers and reweighing. The filter holder is a Millipore high pressure filter holder similar to that used in the regular corrosion product sample solution.

(5) Radioactivity Measurement

The Na-24 activity collected on cation membranes is measured with a Ge(Li) detector interfaced to a multichannel gamma-ray spectrometer and a single-channel analyzer. The single-channel analyzer is used to simultaneously measure the gross gamma counting rate detected above the energy of 1.7 MeV. The multichannel analyzer is used to measure the activity of the Na-24 at different photopeaks and other potential background activities in the feedwater.

All samples collected from the feedwater are not counted until about 5 hours after sampling to allow the Cs-138 activity which may be present in the sample to decay away. Generally, the background is found to be less than 0.1% of the sample activity. The gross counting rate is generally used in the flow rate calculation because of its smaller uncertainty in counting statistic.

(6) Calculation

The feedwater flow rate is calculated by Equation 8-8. It is important to include all the possible uncertainties in each parameter, as described earlier, in the overall estimate of uncertainty.

8.6 IDENTIFICATION OF DEFECTIVE FUEL*

In light-water reactors, there are tens of thousands of fuel rods in a reactor. The individual fuel rods and the fuel assemblies are fabricated with exceptional care, to preclude the escape of fission products through even minor cladding defects. However, with such a large number of fuel rods it is possible for cladding failure to develop during an operating cycle. Failure of fuel cladding is indicated when fission-product activity in reactor cooling water rises above normal background levels. (Background radiation is due to uranium impurities previously deposited on reactor internals, or to uranium present in core components).

In operating BWRs, reactor-coolant iodine and fission-gas concentrations in the off-gas system are measured during operation. An on-line, continuously reading off-gas monitor is also used to estimate fission-gas release from the fuel. For PWRs, iodine in the coolant is the basis for evaluating fuel integrity (Section 3.3). The fission product concentrations are determined by analyzing grab samples of coolant or gaseous effluent with gamma-spectrometric techniques (see Appendix C).

Identification of defective fuel is usually accomplished during scheduled refueling outages by a procedure known as "fuel sipping". Three methods are used: wet sipping, dry sipping, and vacuum sipping. All three feature the use of radiation detectors and associated electronics to measure radionuclide releases from defective fuel rods in an isolated sipping container. A comparison of various parameters for three sipping methods is shown in Table 8-7.

It is desirable to identify and remove all defective fuel from the reactor core to prevent the release of fission products into the coolant, and consequently release to the environment. At the same time, however, it is important not to discard expensive sound fuel prematurely. Obviously, precise detection of fuel integrity is particularly desirable.

---

* Information obtained from Reference 17.

Table 8-7

COMPARISON OF FUEL-SIPPING METHODS
(Reproduced with Permission, Power Magazine, Ref. 17)

Method	Fission-Product Driving Force	Typical Nuclides	Analysis Method	Holding Point	Overall Sipping Rate*	Water Requirements
Wet	Temperature	I-131 I-132 Cs-134	Gamma spectrometry of sample	30-60 min	3-5 bundles/hr out-of-core, 4-6 in-core	Demin, 100-200 gal/bundle out-of-core, none in-core
Dry	Temperature	Xe-133 Kr-85	Gamma spectrometry of sample	10-60 min	3-5 bundles/hr	None
Vacuum	Pressure	Xe-133 Kr-85	On-line beta scintillation (no samples)	10 min	3-5 bundles/hr out-of-core, 6-8 near-core	Demineralized or condensate, 65 gal/bundle

* Limited by grapple operator, assuming fuel must be moved from core location.

The method most commonly used for locating malfunctioning fuel elements is wet sipping. Key to monitoring here is the leaching of fission products - primarily iodine-131 and cesium isotopes - from fuel rods into an isolated volume coolant. In a BWR, the primary advantage of wet sipping is that it can sometimes be done without removing fuel from the core.

Most light-water reactors use out-of-core wet sipping. (For PWRs, in fact, in-core wet sipping is not possible.) This requires lifting the fuel assemblies up and out of the core and placing them in sealed containers filled with water. To reduce radionuclide background levels, the pool water is replaced with demineralized water. After a 30-60 minute holding period, the water is sampled and analyzed for the presence of specific radioactive fission products. Injection of hot water into the sipping container to accelerate the activity release has been reported [18].

Dry sipping, as described, depends on forcing the expulsion of fission gas through fuel-cladding defects. This is accomplished by allowing the decay heat from fission to increase fuel bundle temperature. The bundle is removed from the core, placed in a sealed sipping container, and the coolant is displaced with air to expose the fuel rods. When the required temperature is reached, the stagnant air is sampled and analyzed for gaseous fission product activity.

Since fission-gas atoms migrate much more readily than iodine and cesium nuclides, better sensitivity is achieved than in the wet method. The main drawback to dry sipping is potential overheating of the cladding surrounding the fuel rods. This results from the absence of water that would otherwise remove heat generated in the decay of fission products. Due to this safety concern, little development effort has been expended on optimization of this technique.

Vacuum sipping was developed for use with BWRs. It takes the advantage of high sensitivity of measuring the gaseous fission product activity released from cladding defects under partial vacuum in the sipping container. The vacuum-sipper containers are designed so that they can be installed in the control-rod-blade storage rack in the fuel pool, or on the guide rod inside the BWR reactor cavity. This minimizes the time required to transport fuel to and from the sipping containers.

A schematic diagram of a vacuum-sipper system is shown in Figure 8-8. A typical vacuum-sipping cycle starts when a fuel assembly is inserted into the container through the top, which is then closed and sealed by a pneumatically actuated system. Pool water is flushed out of the container with an air-water purge. A gas space is established in the lid above the bundle by aspirating the water out of the lid bottom; at the same time, air is supplied to the top port at a pressure slightly less than the pool pressure outside the lid. The trapped air is then isolated and the space evacuated through a scintillation detector. The remaining low-pressure gas volume is then recirculated through the monitor and back to the can for a predetermined time (3-5 min). After sampling, the container is purged, flooded, and opened for bundle removal. More detailed description of this system has been reported by Green[17].

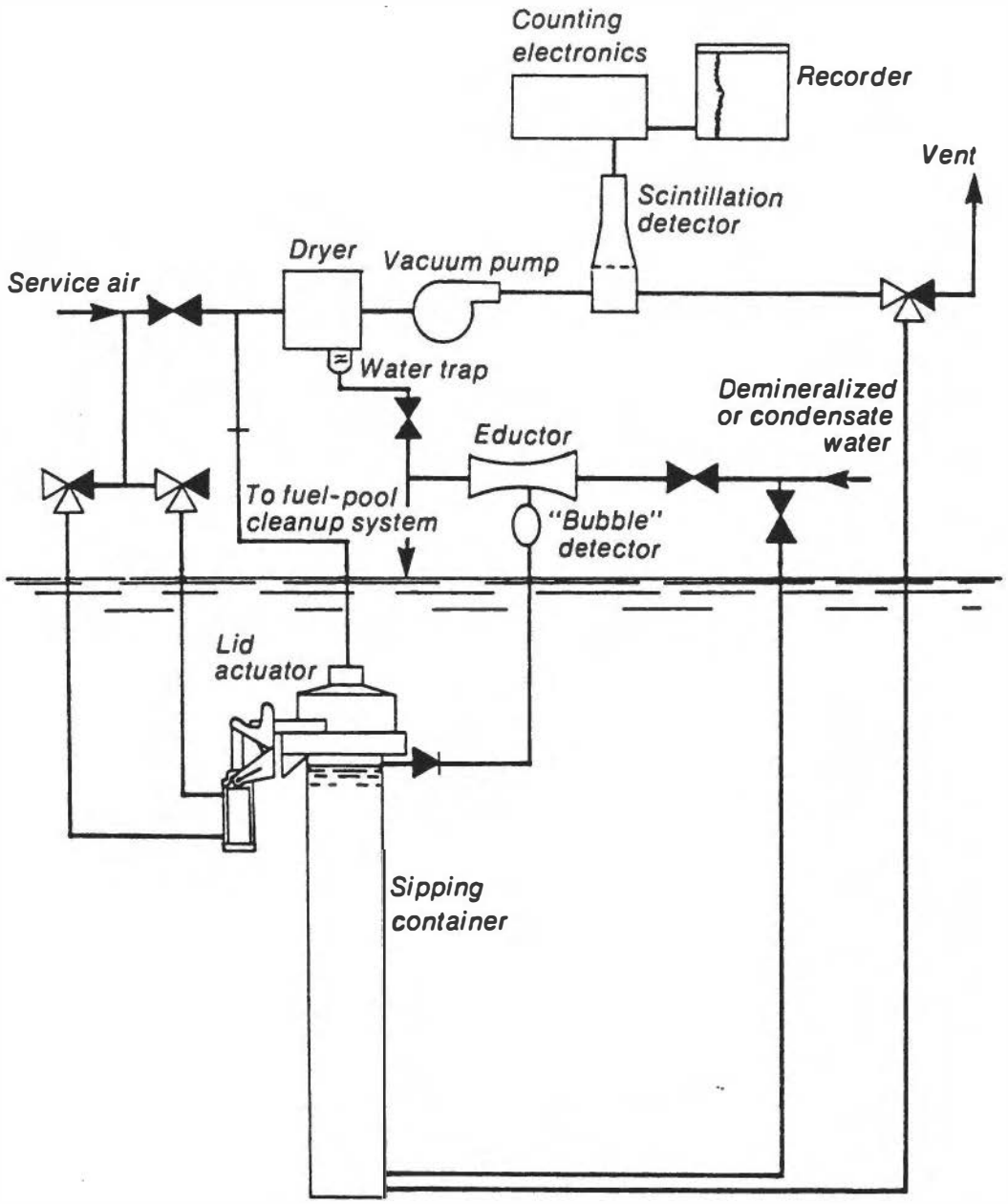

Figure 8-8. Schematic Diagram of a Vacuum-Sipper System (Reproduced with Permission, Power Magazine, Ref. 17)

8.7 REFERENCES

(1) P. G. Voilleque, Nucl. Tech., 90, 23 (1990).

(2) C. C. Lin, J. Inorg. Nucl. Chem., 42, 1043 (1980).

(3) R. L. Hepplette and R. E. Robertson, Proc. Ray. Soc., A252, 273 (1959).

(4) E. A. Moelwyn-Hughes, Proc. Ray. Soc., A220, 386 (1953).

(5) Yu. V. Kuznetsov, et al., Russian Radiochemistry, 23, 744 (1981).

(6) S. W. Duce and J. W. Mondler, Trans. Am. Nucl. Soc., 40, 617 (1985)

(7) E. Linden and D. J. Turner, "Carryover of Volatile Iodine Species in Some Swedish and American BWRs", Water Chemistry of Nuclear Reactor System 3, Vol. I, III (1983) BNES, London.

(8) J. H. Keller, "An Evaluation of Materials and Techniques Used for Monitoring Airborne Radioiodine." 12th AEC Air Cleaning Conference, Vol. I, p. 322 (1972).

(9) E. C. Potter and G. M. W. Mann, J. Br. Corr., 1, 2E (1965).

(10) E. A. Pelletier and R. T. Hempbill, "Nuclear Power Plant Related Iodine Partition Coefficients", EPRI NP-1271 (December 1979).

(11) C. P. Pelletier, Compiler, "Results of Independent Measurements of Radioactivity in Process Systems and Effluent at Boiling Water Reactors", U.S. AEC, Docket RM-50-2, ALAP Exhibit No. 22, May 1973.

(12) J. M. Skarpelos and R. S. Gilbert, "Technical Derivation of BWR 1971 Design Basis Radioactive Material Source Terms", NEDO-10871 (July 1973) (Addendum A).

(13) C. C. Lin, "Transuranic Isotopes in BWR Coolants", May, 1975 (unpublished).

(14) J. H. Holloway and R. S. Gilbert, "Qualification of the Na-24 Tracer Method for Feedwater Flow Nozzle Calibration", NEDM-12454 (September 1973).

(15) W. B. Wilson, et al. Nucl. Safety, 29, 177 (1988).

(16) C. C. Lin "Chemical Behavior of Radioiodine in BWR Systems. (II) Effects of Hydrogen Water Chemistry", Nucl. Tech. 97, 71 (1992).

(17) T. A. Green, "Monitoring Fuel for Defects", Power, P. 56, (August 1978).

(18) S. Uchida, et al. Nucl. Tech., 40, 79 (1978).

Appendix A
NUCLEAR DATA

Table A-1. SUMMARY OF MAJOR NUCLIDES AND RADIATION PROPERTIES

Nuclide	Half-life		Major Gamma-Rays and Intensities keV	%	keV	%	R/hr/Ci at 1 m	Beta E MeV	Gamma E MeV
Ag-110m	249.80	d	657.8	94.6	884.7	72.7	1.654	0.068	2.734
Ar-41	1.82	h	1293.6	99.2	--	--	0.696	0.464	1.284
As-76	26.30	h	559.1	45.0	657.0	6.1	0.274	1.065	0.430
Ba-139	83.76	m	165.9	22.0	--	--	0.029	1.654	0.306
Ba-140	12.79	d	537.2	24.4	162.6	6.7	0.165	0.304	0.191
Ba-141	18.27	m	190.2	49.0	304.2	26.6	0.577	0.858	0.891
Ba-142	10.70	m	255.1	18.0	1204.1	14.0	0.570	0.470	0.905
Br-84	31.80	m	881.5	42.0	1897.3	14.9	0.884	1.249	1.787
Cl-38	37.20	m	2167.5	44.0	1642.4	32.5	0.718	1.529	1.488
Ce-141	32.50	d	145.4	48.2	--	--	0.073	0.170	0.077
Ce-144	284.60	d	133.5	11.1	80.1	1.6	0.023	0.093	0.019
Co-57	271.80	d	122.1	85.9	136.5	10.7	0.151	0.018	0.125
C0-58	70.88	d	810.8	99.4	511.0	30.0	0.614	0.034	0.976
C0-60	5.27	y	1173.2	100.0	1332.5	100.0	1.369	0.096	2.506
Cr-51	27.70	d	320.1	10.1	--	--	0.023	0.004	0.033
Cs-134	2.06	y	604.7	97.6	795.9	85.4	0.070	0.162	1.555
Cs-136	13.16	d	818.5	99.7	1048.1	79.8	1.343	0.133	2.168
Cs-Ba137	30.17	y	661.7	85.2	--	--	0.381	0.171	0.598
Cs-138	32.20	m	1435.9	76.3	462.8	30.7	1.265	1.223	2.361
Cs-139	9.30	m	1283.2	7.0	627.2	1.6	0.158	1.654	0.306
Cu-64	12.70	h	511.0	35.7	1345.9	0.49	0.132	0.123	0.191
F-18	1.83	h	511.0	193.5	--	--	0.696	0.242	0.989
Fe-55	2.73	y	--	--	--	--	--	0.004	--
Fe-59	44.51	d	1099.2	56.5	1291.6	43.2	0.662	0.118	1.189
Hf-181	42.40	d	482.0	82.8	133.0	41.7	0.392	0.194	0.544
I-131	8.04	d	364.5	81.2	637.0	7.3	0.283	0.190	0.381
I-132	2.28	h	667.7	98.7	772.6	76.2	1.421	0.490	2.291
I-133	20.80	h	529.9	86.3	875.3	4.5	0.411	0.410	0.607
I-134	52.60	m	847.0	95.4	884.1	65.3	1.573	0.608	2.625
I-135	6.57	h	1260.4	28.9	1131.5	22.5	0.862	0.369	1.575
I-136	1.39	m	1313.0	69.4	1321.1	25.8	1.265	2.022	2.533
Kr-85	10.73	y	514.0	0.44	--	--	0.002	0.251	0.002
Kr-85m	4.48	h	151.2	75.1	304.9	13.7	0.160	0.255	0.158
Kr-87	1.37	h	402.6	49.6	2554.8	13.2	0.433	1.324	0.793
Kr-88	2.84	h	196.3	26.0	834.8	13.0	1.025	0.365	1.955
Kr-89	3.15	m	220.9	20.0	585.8	16.6	0.973	1.362	1.834
Kr-90	32.30	s	1118.7	37.0	121.8	32.0	0.766	1.315	1.272
La-140	40.27	h	1596.5	95.4	487.0	45.5	1.273	2.022	0.232
La-141	3.90	h	1354.5	2.6	--	--	0.022	0.948	0.043
La-142	1.54	h	641.2	52.5	2397.7	16.3	1.354	0.847	2.719
Mn-54	312.20	d	934.8	100.0	--	--	0.511	0.004	0.836
Mn-56	2.58	h	846.8	98.9	1810.7	27.2	0.925	0.829	1.692
Mo-99	2.79	d	739.6	12.1	181.1	6.2	0.113	0.396	0.155
N-13	9.97	m	511.0	199.6	--	--	0.718	0.491	1.020
Na-24	14.96	h	1368.5	100.0	2754.1	99.9	1.939	0.554	4.121
Nb-95	34.97	d	765.8	99.8	--	--	0.481	0.044	0.764
Nb-97	1.23	h	657.9	98.1	--	--	0.437	0.467	0.665

Table A-1. (continued)

Nuclide	Half-life		Major Gamma-Rays and Intensities keV	%	keV	%	R/hr/Ci at 1 m	Beta E MeV	Gamma E MeV
Nd-147	10.98	d	91.1	27.9	531.0	13.1	0.139	0.268	0.141
Ni-63	100.00	y	--	--	--	--	--	0.017	--
Ni-65	2.52	h	1481.8	23.5	1115.5	14.8	0.297	0.632	0.549
Np-239	2.36	d	277.6	14.1	228.2	10.7	0.514	0.243	0.172
Rb-88	17.70	m	1836.0	21.4	898.0	14.0	0.322	2.071	0.636
Rb-89	15.40	m	1031.9	58.0	1248.1	43.0	1.095	1.020	2.068
Rb-90	2.60	m	831.7	33.3	1060.7	7.8	0.944	1.960	2.164
Rb-90m	4.30	m	831.7	93.4	1375.4	17.4	1.639	1.388	3.273
Rh-105	35.40	h	318.9	19.2	306.1	15.1	0.059	0.153	0.078
Ru-103	39.27	d	497.1	90.9	610.3	5.6	0.332	0.070	0.484
Ru-105	4.44	h	724.5	47.3	469.0	17.5	0.733	0.404	0.784
Ru-Rh106	1.02	y	511.9	20.4	621.8	10.7	0.138	1.412	0.207
Sb-122	2.70	d	563.9	69.3	692.8	3.7	0.304	0.563	0.444
Sb-124	60.20	d	602.7	97.8	1691.0	49.0	1.066	0.380	1.869
Sb-125	2.76	y	427.9	29.4	600.6	17.8	0.381	0.098	0.433
Sn-In113	115.10	d	391.7	64.9	255.1	1.9	0.243	0.131	0.260
Sr-89	50.52	d	--	--	--	--	--	0.585	--
Sr-90	29.10	y	--	--	--	--	--	0.196	--
Sr-91	9.50	h	1024.3	33.4	749.8	23.0	0.414	0.653	0.687
Sr-92	2.71	h	1383.9	90.0	953.3	3.6	0.722	0.200	1.339
Sr-93	7.40	m	590.3	67.2	875.7	24.2	1.358	0.920	2.237
Ta-182	114.43	d	1121.3	34.9	1221.4	27.1	0.773	0.200	1.297
Tc-99m	6.01	h	140.5	89.1	--	--	0.123	0.016	0.127
Tc-101	14.20	m	306.8	88.0	545.1	6.0	0.256	0.474	0.343
Tc-104	18.00	m	358.0	84.4	530.0	14.7	1.051	1.193	1.466
Te-129m	33.60	d	695.7	3.1	729.6	0.7	0.068	0.269	0.039
Te-131m	1.35	d	773.7	38.2	852.2	20.7	0.940	0.190	1.426
Te-132	3.26	d	228.2	88.2	49.7	13.1	0.279	0.098	0.231
W-187	23.90	h	685.8	26.4	479.5	21.1	0.329	0.290	0.476
Xe-133	5.24	d	81.0	38.3	--	--	0.103	0.136	0.045
Xe-133m	2.19	d	233.2	10.3	--	--	0.112	0.190	0.042
Xe-135	9.10	h	249.8	90.2	608.2	2.9	0.189	0.318	0.248
Xe-135m	15.30	m	526.7	80.5	--	--	0.320	0.096	0.431
Xe-137	3.82	m	455.5	31.0	--	--	0.124	1.769	0.188
Xe-138	14.10	m	258.3	31.5	434.5	20.3	0.622	0.632	1.126
Xe-139	39.70	s	219.0	45.0	297.0	18.0	0.286	1.787	0.928
Y-90	2.67	d	--	--	--	--	--	0.931	--
Y-91	58.50	d	1204.9	0.3	--	--	0.002	0.602	0.004
Y-92	3.54	h	934.5	13.9	1405.4	4.8	0.147	1.445	0.252
Y-93	10.20	h	266.9	6.8	947.1	2.0	0.052	1.173	0.089
Zn-65	243.80	d	1115.5	50.7	511.0	2.8	0.330	0.007	0.584
Zn-69m	13.76	h	438.6	94.8	--	--	0.295	0.022	0.416
Zr-95	64.02	d	756.7	54.5	724.2	44.1	0.047	0.116	0.735
Zr-97	16.80	h	743.4	94.8	507.6	5.3	0.108	0.697	0.181

Table A-2. MAJOR GAMMA-RAY ENERGIES AND INTENSITIES

Energy		Half-		γ/d	Associated Major Gamma-ray and Intensity					
(keV)	Nuclide	life		%	keV	%	keV	%	keV	%
49.72	Te132	3.26	h	13.1	228.2	88.2	49.7	13.1	--	--
57.36	Ce143	1.38	d	11.8	293.3	42.0	664.6	5.2	722.0	5.1
66.91	Cs136	13.16	d	12.5	818.5	99.7	1048.1	79.6	340.6	48.5
72.06	W-187	23.90	h	11.9	685.8	26.4	479.5	21.1	134.2	9.5
77.60	Ba142	10.70	m	9.6	255.2	18.0	1204.1	14.0	894.9	11.0
80.10	Ce144	284.60	d	1.6	133.5	11.1	80.1	1.6	--	--
80.18	I-131	8.04	d	2.6	364.5	81.2	637.0	7.3	284.3	6.1
81.00	Xe133	5.24	d	38.3	81.0	38.3	--	--	--	--
86.29	Cs136	13.16	d	6.3	818.5	99.7	1048.1	79.6	340.6	48.5
91.11	Nd147	10.98	d	27.9	91.1	27.9	531.0	13.1	319.4	2.0
93.00	Rb-91	58.50	s	38.0	93.0	38.0	2564.0	20.0	346.0	12.0
99.55	Np239	2.36	d	14.7	103.8	23.7	277.6	14.1	106.1	22.7
102.1	Te131m	1.35	d	7.9	773.7	38.2	852.2	20.7	793.7	13.9
103.8	Np239	2.36	d	23.7	103.8	23.7	277.6	14.1	106.1	22.7
106.1	Np239	2.36	d	22.7	103.8	23.7	277.6	14.1	106.1	22.7
112.0	O-19	26.90	s	2.7	197.0	97.0	1356.0	59.0	112.0	2.7
117.0	Np239	2.36	d	22.7	103.8	23.7	277.6	14.1	106.1	22.7
120.9	Kr-90	32.30	s	2.7	1118.7	37.0	121.8	32.0	539.5	29.0
121.8	Kr-90	32.30	s	32.0	1118.7	37.0	121.8	32.0	539.5	29.0
122.1	Co-57	271.80	d	85.9	122.1	85.9	136.5	10.6	--	--
127.2	Tc101	14.20	m	2.8	306.8	88.0	545.1	6.0	127.4	2.8
133.0	Hf181	42.40	d	41.7	482.0	82.8	133.0	41.7	345.9	17.2
133.5	Ce144	284.60	d	11.1	133.5	11.1	80.1	1.6	--	--
134.2	W-187	23.90	h	9.5	685.8	26.4	479.5	21.1	134.2	9.5
135.4	I-134	52.60	m	3.8	847.0	95.4	884.1	65.3	1072.6	15.3
136.3	Hf181	42.40	d	5.2	482.0	92.8	133.0	41.7	345.9	17.2
136.5	Co-57	271.80	d	10.6	122.1	85.9	136.5	10.6	--	--
138.1	Cs138	32.20	m	1.5	1435.9	76.3	462.8	30.7	1009.8	29.8
140.5	No-99	2.79	d	3.8	739.6	12.8	181.1	6.2	778.0	4.5
140.5	Tc-99m	6.01	h	89.1	140.5	99.1	--	--	--	--
142.7	Fe-59	44.63	d	1.0	1099.2	56.5	1291.6	43.2	192.3	3.1
145.4	Ce141	32.50	d	48.2	145.4	48.2	--	--	--	--
151.2	Kr-85m	4.48	h	75.1	151.2	75.1	304.9	13.7	--	--
153.2	Cs136	13.16	d	7.5	818.5	99.7	1048.1	79.8	340.6	48.5
153.8	Xe138	14.10	m	6.0	258.3	31.5	434.5	20.3	1768.3	16.7
162.6	Ba140	12.75	d	6.7	537.3	24.4	162.6	6.7	304.8	4.5
164.0	Cs136	13.16	d	4.6	818.5	99.7	1048.1	79.8	340.6	48.5
165.9	Ba139	83.76	m	22.0	165.9	22.0	--	--	--	--
166.0	Kr-88	2.84	h	3.1	196.3	26.0	834.8	13.0	1529.8	10.9
168.7	Sr-93	7.40	m	18.2	590.3	67.2	875.7	24.2	888.1	21.9
175.0	Xe139	39.70	s	16.0	219.0	45.0	297.0	18.0	175.0	16.0
176.3	Sb125	2.76	y	6.9	427.9	29.4	600.6	17.8	635.9	11.3
176.6	CS136	13.16	d	13.6	818.5	99.7	1048.1	79.8	340.6	48.5
181.1	Mo-99	2.79	d	6.2	739.6	12.1	181.1	6.2	778.0	4.5
194.1	Tc101	14.20	m	1.6	306.9	88.0	545.1	6.0	127.4	2.8
190.2	Ba141	18.30	m	49.0	190.2	49.0	304.2	26.6	277.0	24.6
192.3	Fe-59	44.51	d	3.1	1099.2	56.5	1291.6	43.2	192.3	3.1

Table A-2 (continued)

Energy		Half-	γ/d	Associated Major Gamma-ray and Intensity					
(keV)	Nuclide	life	%	keV	%	keV	%	keV	%
196.3	Kr-88	2.84 h	26.0	196.3	26.0	934.8	13.0	1529.8	10.9
197.0	O-19	26.90 s	97.0	197.0	97.0	1356.0	59.0	112.0	2.7
200.6	Te131m	1.35 d	7.6	773.7	38.2	852.2	20.7	793.7	13.9
219.0	Xe139	39.70 s	45.0	219.0	45.0	297.0	18.0	175.0	16.0
220.5	I-135	6.57 h	1.8	1260.4	28.9	1131.5	22.5	1678.0	9.5
220.9	Kr-89	3.15 m	20.0	220.9	20.0	585.8	16.6	904.3	7.2
227.8	Cs138	32.20 m	1.5	1435.9	76.3	462.8	30.7	1009.8	29.8
228.2	Te132	3.26 d	88.0	228.2	88.2	49.7	13.1	--	--
228.2	Np239	2.36 d	10.7	103.8	23.7	277.6	14.1	106.1	22.7
231.5	Ba142	10.70 m	10.1	255.1	18.0	1204.1	14.0	894.9	11.0
233.2	Xe133m	2.19 d	10.3	233.2	10.3	--	--	--	--
234.4	Kr-90	32.30 s	2.5	1118.7	37.0	121.8	32.0	539.5	29.0
240.9	Te131m	1.35 d	7.6	773.7	38.2	852.2	20.7	793.7	13.9
241.5	Sr-92	2.71 h	3.3	1383.9	90.0	953.3	3.6	430.6	3.3
242.2	Kr-90	32.30 s	9.6	1118.7	37.0	121.8	32.0	539.5	29.0
242.6	Xe138	14.10 m	3.5	258.3	31.5	434.5	20.3	1768.3	16.7
249.8	Xe135	9.10 h	90.2	249.8	90.2	608.2	2.9	--	--
254.2	Zr-97	16.90 h	1.3	743.4	92.8	507.6	5.3	602.5	1.4
255.1	Ba142	10.70 m	18.0	255.1	18.0	1204.1	14.0	894.9	11.0
255.1	Sn113	115.10 d	1.9	391.7	64.9	255.1	1.9	--	--
258.3	Xe138	14.10 m	31.5	258.3	31.5	434.5	20.3	1768.3	16.7
260.1	Sr-93	7.30 m	7.3	590.3	67.2	875.7	24.2	888.1	21.8
262.9	Ru105	4.44 h	7.2	724.5	47.3	469.0	17.5	676.4	16.7
266.9	Y-93	10.20 h	6.8	266.9	6.8	947.1	2.0	1917.0	1.4
272.5	Rb-89	15.40 m	1.4	1031.9	58.0	1248.1	42.0	2196.0	13.3
273.7	Cs136	13.16 d	12.7	818.5	99.7	1048.1	79.8	340.6	48.5
274.7	Sr-91	9.50 h	1.0	1024.3	33.4	749.8	23.0	652.9	7.8
277.0	Ba141	18.30 m	24.6	190.2	49.0	304.2	26.6	277.0	24.6
277.6	Np239	2.36 d	14.1	103.8	23.7	277.6	14.1	106.1	22.7
284.3	I-131	8.04 d	6.1	364.5	81.2	637.0	7.3	284.3	6.1
288.5	I-135	6.57 h	3.1	1260.4	28.9	1131.5	22.5	1678.0	9.5
293.3	Ce143	1.38 d	42.0	293.3	42.0	664.6	5.2	722.0	5.1
297.0	Xe139	39.70 s	18.0	219.0	45.0	297.0	18.0	175.0	16.0
304.2	Ba141	18.30 m	26.6	190.2	49.0	304.2	26.6	277.0	24.6
304.8	Ba140	12.75 d	4.5	537.2	24.4	162.6	6.7	304.8	4.5
304.9	Kr-85m	4.48 h	13.7	151.2	75.1	304.9	13.7	--	--
306.1	Rh105	35.40 h	5.1	318.9	19.2	306.1	5.1	--	--
306.8	Tc101	14.20 m	88.0	306.8	88.0	545.1	6.0	127.4	2.8
315.9	Np239	2.35 d	1.6	103.8	23.7	106.1	22.7	277.6	14.1
316.5	Ru105	4.44 h	11.7	724.5	47.3	469.0	17.5	676.4	16.7
318.9	Rh105	35.40 h	19.2	318.9	19.2	306.1	5.1	--	--
319.4	Nd147	10.98 d	2.0	91.1	27.9	531.0	13.1	319.4	2.0
320.1	Cr-51	27.70 d	10.1	320.1	10.1	--	--	--	--
328.8	La140	40.27 h	20.5	1596.5	95.4	487.0	45.5	815.9	23.5
334.3	Np239	2.35 d	2.0	103.8	23.7	277.6	14.1	106.1	22.7
334.3	Te131m	1.35 h	9.6	773.7	38.2	852.2	20.7	793.7	13.9
340.6	Cs136	13.16 d	48.5	818.5	99.7	1048.1	79.8	340.6	48.5
343.7	Ba141	18.27 m	15.0	190.2	49.0	304.2	26.6	277.0	24.6

Table A-2 (continued)

Energy		Half-		γ/d	Associated Major Gamma-ray and Intensity					
(keV)	Nuclide	life		%	keV	%	keV	%	keV	%
344.7	I-136	83.00	s	2.5	1313.0	69.4	1321.1	25.8	2289.6	10.8
345.9	Hf181	42.40	d	17.2	482.0	82.8	133.0	41.7	345.9	17.2
346.0	Rb-91	58.50	s	12.0	93.0	38.0	2564.0	20.0	346.0	12.0
346.5	Sr-93	7.30	m	3.2	590.3	67.2	875.7	24.2	888.1	21.8
350.6	Ce143	33.00	h	3.4	293.3	42.0	664.6	5.2	722.0	5.1
355.4	Zr-97	16.80	h	2.3	743.4	94.8	507.6	5.3	355.4	2.3
355.5	Nb-98	51.10	m	10.0	787.2	95.0	722.3	77.0	1169.0	18.0
356.1	Kr-89	3.15	m	4.1	220.9	20.0	585.8	16.6	904.3	7.2
358.0	Tc104	18.00	m	84.4	358.0	84.4	530.0	14.7	883.0	12.2
362.2	Kr-88	2.84	h	2.2	196.3	26.0	834.8	13.0	1529.8	10.9
363.8	Ba142	10.70	m	3.9	255.1	18.0	1204.1	14.0	894.9	11.0
364.5	I-131	8.04	d	81.2	364.5	81.2	637.0	7.3	284.3	6.1
366.3	Ni-65	2.52	h	4.6	1481.8	23.5	1115.5	14.8	366.3	4.6
366.4	Mo-99	2.79	d	1.37	739.6	12.8	181.1	6.2	778.0	4.5
380.4	Sb125	2.76	y	1.5	427.9	29.4	600.6	17.8	635.9	11.3
391.7	Sn113	115.10	d	64.9	391.7	64.9	255.1	1.9	--	--
393.4	Ru105	4.44	h	4.2	724.5	49.0	469.0	17.5	676.4	16.7
394.0	Xe139	39.70	s	5.4	219.0	45.0	297.0	18.0	175.0	16.0
396.4	Xe138	14.10	m	6.3	258.3	31.5	434.5	20.3	1768.3	16.7
401.4	Xe138	14.10	m	2.2	258.3	31.5	434.5	20.3	1768.3	16.7
402.6	Kr-87	1.37	m	49.6	402.6	49.6	2554.8	13.2	845.4	7.3
405.5	I-134	52.60	m	7.3	847.0	95.4	884.1	65.3	1072.6	15.3
409.0	Cs138	32.20	m	4.7	1435.9	76.3	462.8	30.7	1009.8	29.8
417.6	I-135	6.57	h	3.5	1260.4	28.9	1131.5	22.5	1678.0	9.5
423.7	Ba140	12.75	d	3.2	537.3	24.4	162.6	6.7	304.8	4.5
425.0	Ba142	10.70	m	5.0	255.1	18.0	1204.1	14.0	894.9	11.0
427.7	Sb125	2.76	y	29.4	427.9	29.4	600.6	17.8	635.9	11.3
430.6	Sr-92	2.71	h	3.3	1383.9	90.0	953.3	3.6	430.6	3.3
432.5	La140	40.27	h	2.9	1596.5	95.4	487.0	45.5	815.9	23.5
433.4	I-134	52.60	m	4.2	847.0	95.4	884.1	65.3	1072.6	15.3
434.5	Xe138	14.10	m	20.3	258.3	31.5	434.5	20.3	1768.3	16.7
437.6	Ba140	12.75	d	2.0	537.3	24.4	162.6	6.7	304.8	4.5
438.6	Zn-69m	13.76	h	94.8	438.6	94.8	--	--	--	--
439.9	Nd147	10.98	d	1.2	91.1	28.0	531.0	13.1	319.4	2.0
446.8	Ag110m	249.80	d	3.6	657.8	94.4	884.7	72.6	937.5	34.2
448.5	Y-92	3.54	h	2.3	934.5	13.9	1405.4	4.8	561.1	2.4
455.5	Xe137	3.82	m	31.0	455.5	31.0	--	--	--	--
457.4	Cs134	2.06	y	1.5	604.7	97.6	795.9	85.4	569.3	15.4
457.6	Ba141	18.27	m	5.1	190.2	49.0	304.2	26.6	277.0	24.6
462.8	Cs138	32.20	m	30.7	1435.9	76.3	462.8	30.7	1009.8	29.8
463.4	Sb125	2.76	y	10.4	427.9	29.4	600.6	17.8	635.9	11.3
467.3	Ba141	18.27	m	5.1	190.2	49.0	304.2	26.6	277.0	24.6
469.0	Ru105	4.44	h	17.5	724.5	47.3	469.0	17.5	676.4	16.7
479.5	W-187	23.90	h	23.4	685.8	26.4	479.5	21.1	134.2	9.5
482.0	Hf181	42.40	d	82.8	48.2	82.8	133.0	41.7	345.9	17.2
487.0	La140	40.27	h	45.5	1596.5	95.4	487.0	45.5	815.9	23.5
490.4	Ce143	33.00	h	2.0	293.3	42.0	664.6	5.2	722.0	5.1
497.1	Ru103	39.27	d	90.9	497.1	90.9	610.3	5.6	--	--

Table A-2 (continued)

Energy (keV)	Nuclide	Half-life		γ/d %	Associated Major Gamma-ray and Intensity					
					keV	%	keV	%	keV	%
497.5	Kr-89	3.15	m	6.6	220.9	20.0	585.8	16.6	904.3	7.2
505.9	I-132	2.28	h	5.0	667.7	98.7	772.6	76.2	954.6	18.1
507.6	Zr-97	16.80	h	5.3	743.4	94.8	507.6	5.3	355.4	2.3
511.0	N-13	9.97	m	199.6	511.0	199.6	--	--	--	--
511.0	F-18	1.83	m	193.5	511.0	193.5	--	--	--	--
511.0	Na-24	14.96	h	--	1368.5	100.0	2754.1	99.8	--	--
511.0	Co-58	70.88	d	30.0	810.8	99.4	511.0	30.0	--	--
511.0	Cu-64	12.70	h	35.7	511.0	35.7	1345.9	0.49	--	--
511.0	Zn-65	243.80	d	2.8	1115.5	50.7	511.0	2.8	--	--
511.9	Ru106	1.02	y	20.6	511.9	20.4	621.8	10.7	1050.5	1.7
514.0	Kr-85	10.73	y	0.44	514.0	0.44	--	--	--	--
522.7	I-132	2.28	h	16.1	667.7	98.7	772.6	76.2	954.6	18.1
526.7	Xe135m	15.30	m	80.5	526.7	80.5	--	--	--	--
529.9	I-133	20.80	h	86.3	529.9	86.3	875.3	4.5	1298.2	2.3
530.0	Tc104	18.00	m	14.7	358.0	84.4	530.0	14.7	983.0	12.2
531.0	Nd147	10.98	d	13.1	91.1	27.9	531.0	13.1	319.4	2.0
531.5	Tc101	14.20	m	1.0	306.8	88.0	545.1	6.0	127.4	2.8
537.3	Ba140	12.75	d	24.4	537.3	24.4	162.6	6.7	304.8	4.5
539.5	Kr-90	32.30	s	29.0	1118.7	37.0	121.8	32.0	539.5	29.0
540.8	I-134	52.60	m	7.8	847.0	95.4	884.1	65.3	1072.6	15.3
545.1	Tc101	14.20	m	6.0	306.8	98.0	545.1	6.0	127.4	2.8
546.6	I-135	6.57	h	7.1	1260.4	28.9	1131.5	22.5	1678.0	9.5
546.9	Cs138	32.20	m	10.8	1435.9	76.3	462.8	30.7	1009.8	29.8
551.0	Y-94	19.00	m	6.3	919.0	73.6	1139.0	7.8	551.0	6.3
551.6	W-187	23.90	h	5.4	685.8	26.4	479.5	21.1	134.2	9.5
554.4	Kr-90	32.30	s	4.8	1118.7	37.0	121.8	32.0	539.5	29.0
556.7	Te129m	33.60	d	0.1	695.9	3.3	729.6	0.8	556.7	0.1
557.6	Y-91m	49.71	m	95.1	557.6	95.1	--	--	--	--
559.1	As-76	26.20	h	45.0	559.1	45.0	657.0	6.1	1216.0	3.8
561.1	Y-92	3.54	h	2.4	934.5	13.9	1405.4	4.8	561.1	2.4
563.2	Cs134	2.06	y	8.4	604.7	97.6	795.9	95.4	569.3	15.4
563.9	Sb122	2.70	d	69.3	563.9	69.3	692.8	3.7	--	--
569.3	Cs134	2.06	y	15.4	604.7	97.6	795.9	85.4	569.3	15.4
577.0	Kr-89	3.15	m	5.6	220.9	20.0	585.8	16.6	904.3	7.2
585.8	Kr-89	3.15	m	16.6	220.9	20.0	585.8	16.6	904.3	7.2
590.3	Sr-93	7.40	m	67.2	$90.3	67.2	875.7	24.2	888.1	21.8
595.4	I-134	52.60	m	11.4	847.0	95.4	894.1	65.3	1072.6	15.3
600.6	Sb125	2.76	y	17.8	427.9	29.4	600.6	17.8	635.9	11.3
602.5	Zr-97	16.80	h	1.4	743.4	94.8	507.6	5.3	355.4	2.3
602.7	Sb124	60.20	d	97.8	602.7	97.8	1691.0	49.0	722.8	11.1
604.7	Cs134	2.06	y	97.6	604.7	97.6	795.9	85.4	569.3	15.4
604.8	Br-84	31.80	m	1.8	881.5	42.0	1897.3	14.9	1015.9	6.2
606.6	Sb125	2.76	y	5.0	427.9	29.4	600.6	17.8	635.9	11.3
608.2	Xe135	9.10	h	2.9	249.8	99.9	608.2	2.9	--	--
610.3	Ru103	39.27	d	5.6	497.1	90.9	610.3	5.6	--	--
618.4	W-187	23.90	h	6.7	685.8	26.4	479.5	21.1	134.2	9.5
620.1	Sr-91	9.50	h	1.7	1024.3	33.4	749.8	23.0	652.9	7.8
621.8	I-134	52.60	m	10.6	847.0	95.4	884.1	65.3	1072.6	15.3

Table A-2 (continued)

Energy		Half-		γ/d	Associated Major Gamma-ray and Intensity					
(keV)	Nuclide	life		%	keV	%	keV	%	keV	%
621.8	Ru106	1.02	y	10.7	511.9	20.4	621.8	10.7	1050.5	1.7
627.2	Cs139	9.30	m	1.6	1283.2	7.0	627.2	1.6	1680.7	0.6
630.2	I-132	2.28	h	13.7	667.7	98.7	722.6	76.2	954.6	18.1
635.9	Sb125	2.76	y	11.3	427.9	29.4	600.6	17.8	635.9	11.3
637.0	I-131	8.04	d	7.3	364.5	81.2	637.0	7.3	284.3	6.1
641.2	La142	1.54	h	52.5	641.2	52.5	2397.7	16.3	2542.6	11.2
644.6	Nb-98	51.10	m	4.5	787.2	95.0	722.3	77.0	1169.0	18.0
645.9	Sb124	60.20	d	7.3	602.7	97.8	1691.0	49.0	722.8	11.4
647.9	Ba141	18.27	m	5.9	190.2	49.0	304.2	26.6	277.0	24.6
652.9	Sr-91	9.50	h	7.8	1024.3	33.4	749.8	23.0	652.9	7.8
657.0	As-76	26.30	h	6.1	559.1	45.0	657.0	6.1	1216.0	3.8
657.7	Rb-89	15.40	m	10.0	1031.9	58.0	1248.1	42.0	2196.0	14.1
657.8	Ag110m	249.80	d	94.6	657.8	94.6	884.7	72.7	937.5	34.2
657.9	Nb-97	1.23	h	98.1	657.9	98.1	--	--	--	--
661.7	Cs137	30.17	y	85.2	661.7	85.2	--	--	--	--
664.6	Ce143	1.38	d	5.2	293.3	42.0	664.6	5.2	722.0	5.1
667.7	I-132	2.28	h	98.7	667.7	98.7	772.6	76.2	954.6	18.1
669.8	I-132	2.28	h	4.9	667.7	98.7	772.6	76.2	954.6	18.1
671.6	I-132	2.28	h	5.2	667.7	98.7	772.6	76.2	954.6	18.1
673.9	Kr-87	1.39	h	1.9	402.6	49.6	2554.8	13.2	845.4	7.3
676.4	Ru105	4.44	h	16.7	724.5	47.3	469.0	17.5	676.4	16.7
677.3	I-134	2.30	h	8.5	947.0	95.4	884.1	65.3	1072.6	15.3
677.6	Ag110m	249.80	d	10.7	657.8	94.4	884.7	72.6	937.5	34.2
685.8	W-187	23.90	d	26.4	685.8	26.4	479.5	21.1	134.2	9.5
687.0	Ag110m	249.80	d	6.5	657.8	94.4	884.7	72.6	937.5	34.2
692.8	Sb122	2.70	d	3.7	563.9	69.3	692.8	3.7	--	--
694.7	Tc101	14.20	m	1.1	306.8	98.0	545.1	6.0	127.4	2.8
695.9	Te129m	33.60	d	3.3	695.7	3.1	729.6	0.7	556.7	0.1
706.6	I-133	20.80	h	1.5	529.9	86.3	875.3	4.5	1298	2.3
706.7	Ag110m	249.50	d	16.7	657.8	94.4	884.7	72.6	937.5	34.2
709.3	Sb124	60.20	d	1.4	602.7	97.9	1691.0	49.0	722.8	11.1
710.4	Sr-93	7.40	m	21.5	590.3	67.2	875.7	24.2	888.1	21.8
713.6	Nb-98	51.10	m	8.7	787.2	95.0	722.3	77.0	1169.0	18.0
713.8	Sb124	60.20	d	2.4	602.7	97.9	1691.0	49.0	722.8	11.1
722.0	Ce143	1.38	d	5.1	293.3	42.0	664.6	5.2	722.0	5.1
722.3	Nb-98	51.10	m	77.0	787.2	95.0	722.3	77.0	1169.0	18.0
722.8	Sb124	60.20	d	11.1	602.7	97.8	1691.0	49.0	722.8	11.1
722.9	I-131	8.04	d	1.8	364.5	81.2	637.0	7.3	284.3	6.1
724.2	Zr-95	64.02	d	44.1	756.7	54.5	724.2	44.1	--	--
724.5	Ru105	4.44	h	47.3	724.5	47.3	469.0	17.5	676.4	16.7
727.1	I-132	2.28	h	5.4	667.7	98.7	772.6	76.2	954.6	18.1
729.6	Te129m	33.60	d	0.7	695.9	3.1	729.6	0.7	556.7	0.1
736.5	Br-84	31.80	m	1.3	881.5	42.0	1897.3	14.9	1015.9	6.2
738.4	Kr-89	3.15	m	4.2	220.9	20.0	585.8	16.6	904.3	7.2
739.1	Ba141	18.27	m	4.5	190.2	49.0	304.2	26.6	277.0	24.6
739.6	Mo-99	2.79	d	12.8	739.6	12.1	181.1	6.2	778.0	4.5
743.4	Zr-97	16.80	h	94.8	743.4	94.8	507.6	5.3	355.4	2.3
744.3	Ag110m	249.80	d	22.3	657.8	94.6	884.7	72.7	937.5	34.2

Table A-2 (continued)

Energy		Half-	γ/d	Associated Major Gamma-ray and Intensity					
(keV)	Nuclide	life	%	keV	%	keV	%	keV	%
749.8	Sr-91	9.50 h	23.0	1024.3	33.4	749.8	23.0	652.9	7.8
751.8	La140	40.27 h	4.4	1596.5	95.4	487.0	45.5	815.9	23.5
756.7	Zr-95	64.02 d	54.5	756.7	54.5	724.2	44.1	--	--
765.8	Nb-95	34.97 d	99.8	765.8	99.8	--	--	--	--
772.6	I-132	2.28 h	76.2	667.7	98.7	772.6	76.2	954.6	18.1
772.9	W-187	23.90 h	4.4	685.8	29.2	479.5	23.4	134.2	9.5
773.7	Te131m	1.35 d	38.2	773.7	38.2	852.2	20.7	793.7	13.9
778.0	Mo-99	2.79 d	4.5	739.6	12.1	181.1	6.2	778.0	4.5
787.2	Nb-98	51.10 m	95.0	787.2	95.0	722.3	77.0	1169.0	18.0
793.7	Te131m	1.35 d	13.9	773.7	38.2	852.2	20.7	793.7	13.9
795.9	Cs134	2.06 y	95.4	604.7	97.6	795.9	95.4	569.3	15.4
801.9	Cs134	2.06 y	8.7	604.7	97.6	795.9	85.4	569.3	15.4
802.2	Br-84	31.80 m	6.1	881.5	42.0	1897.3	14.9	1015.9	6.2
802.4	Br-85	2.87 m	2.6	802.4	2.6	924.6	1.6	--	--
809.8	I-132	2.28 h	2.9	667.7	98.7	772.6	76.2	954.6	18.1
810.8	Co-58	70.88 d	99.4	810.8	99.4	511.0	30.0	--	
812.2	I-132	2.28 h	5.6	667.7	98.7	772.6	76.2	954.6	18.1
815.9	La140	40.27 h	23.5	1596.5	95.4	487.0	45.5	815.9	23.5
818.0	Ag110m	249.80 d	7.3	657.8	94.6	884.7	72.7	937.5	34.2
818.5	Cs136	13.16 d	99.7	818.5	99.7	1048.1	79.8	340.6	48.5
822.8	Te131m	1.35 d	6.1	773.7	38.2	852.2	20.7	793.7	13.9
831.7	Rb-90	2.60 m	33.3	831.7	33.3	1060.7	7.8	--	--
831.7	Rb-90m	4.30 m	93.4	831.7	93.4	1375.4	17.4	1060.7	9.5
833.3	Nb-98	51.10 m	10.0	787.2	95.0	722.3	77.0	1169.0	18.0
834.8	Kr-88	2.84 h	13.0	196.3	26.0	834.8	13.0	1529.8	10.9
834.8	Mn-54	312.20 d	100.0	834.8	100.0	--	--	--	--
836.8	I-135	6.57 h	6.7	1260.4	28.9	1131.5	22.5	1678.0	9.5
844.3	Y-92	3.54 h	1.3	934.5	13.9	1405.5	4.8	561.1	2.4
845.4	Kr-87	1.37 h	7.3	402.6	49.6	2554.8	13.2	845.4	7.3
846.8	Mn-56	2.58 h	98.9	846.8	98.9	1810.7	27.2	2113.1	14.3
847.0	I-134	52.60 m	95.4	947.0	95.4	894.1	65.3	1072.6	15.3
852.2	Te131m	1.35 d	20.7	773.7	38.2	852.2	20.7	793.7	13.9
857.3	I-134	52.60 m	7.0	947.0	95.4	884.1	65.3	1072.6	15.3
861.6	La142	1.54 h	2.0	641.2	52.5	2397.7	16.3	2542.6	11.2
967.1	Kr-89	3.15 m	5.9	220.9	20.0	585.8	16.6	904.3	7.2
867.8	La140	40.27 h	6.2	1596.5	95.4	497.0	45.5	815.9	23.5
871.8	Cs138	32.20 m	5.1	1435.9	76.3	462.8	30.7	1009.8	29.8
875.3	I-133	20.80 h	4.5	529.9	86.3	875.3	4.5	1298.2	2.3
875.7	Sr-93	7.40 m	24.2	590.3	67.2	875.7	24.2	888.1	21.8
875.8	Ru105	4.44 h	3.4	724.5	49.0	469.0	17.5	676.4	16.7
876.3	Ba141	18.27 m	3.6	190.2	49.0	304.2	26.6	277.0	24.6
881.5	Br-84	31.80 m	42.0	881.5	42.0	1897.3	14.9	1015.9	6.2
883.0	Tc104	18.00 m	12.2	358.0	84.4	530.0	14.7	883.0	12.2
884.1	I-134	52.60 m	65.3	847.0	95.4	994.1	65.3	1072.6	15.3
884.7	Ag110m	249.80 d	72.6	657.8	94.6	884.7	72.7	937.5	34.2
888.1	Sr-93	7.40 m	21.8	590.3	67.2	975.7	24.2	888.1	21.8
894.9	La142	1.54 h	9.4	641.2	52.5	2397.7	16.3	2542.6	11.2
894.9	Ba142	10.70 m	11.0	255.1	18.0	1204.1	14.0	894.9	11.0

Table A-2 (continued)

Energy		Half-		γ/d	Associated Major Gamma-ray and Intensity					
(keV)	Nuclide	life		%	keV	%	keV	%	keV	%
898.0	Rb-88	17.70	m	14.0	1936.0	21.4	898.0	14.0	2677.8	1.9
904.3	Kr-89	3.15	m	7.2	220.9	20.0	585.8	16.6	904.3	7.2
919.0	Y-94	19.00	m	73.6	919.0	73.6	1139.0	7.8	551.0	6.3
919.6	La140	40.22	h	2.9	1596.5	95.5	497.0	45.5	815.9	23.5
924.6	Br-95	2.87	m	1.6	802.4	2.6	924.6	1.6	--	--
925.2	La140	40.27	h	7.1	1596.5	95.4	487.0	45.5	815.9	23.5
925.8	Sr-91	9.50	h	3.7	1024.3	33.4	749.8	23.0	652.9	7.8
934.5	Y-92	3.54	h	13.9	934.5	13.9	1405.4	4.8	561.1	2.4
937.5	Ag110m	349.80	d	34.2	657.8	94.6	884.7	72.7	937.5	34.2
946.8	Ba142	10.70	m	8.9	255.1	18.0	1204.1	14.0	894.9	11.0
947.1	T-93	10.20	h	2.0	266.9	6.8	947.1	2.0	1917.0	1.4
947.7	Rb-89	15.40	m	9.2	1031.9	58.0	1248.1	42.0	2196.0	13.3
953.3	Sr-92	2.71	h	3.6	1383.9	90.0	953.3	3.6	430.6	3.3
954.6	I-132	2.28	h	18.1	667.7	98.7	772.6	76.2	954.6	18.1
969.4	Ru105	4.44	h	2.3	724.5	49.0	469.0	17.5	676.4	16.7
972.6	I-135	6.57	h	1.2	1260.4	28.9	1131.5	22.5	1679.0	9.5
976.5	I-136	1.39	m	2.8	1313.0	69.4	1321.1	25.8	2289.6	10.8
985.8	Kr-88	2.84	h	1.3	196.3	26.0	$34.8	13.0	1529.8	10.8
1009.8	Cs138	32.20	m	29.8	1435.9	76.3	462.9	30.7	1009.8	29.8
1011.4	La142	1.54	h	4.4	641.2	52.5	2397.7	16.3	2542.6	11.2
1015.9	Br-84	31.80	m	6.2	881.5	42.0	1897.3	14.9	1015.9	6.2
1024.3	Sr-91	9.50	h	33.4	1024.3	33.4	749.8	23.0	652.9	7.8
1031.9	Rb-89	15.40	m	58.0	1031.9	58.0	1248.1	42.0	2196.0	13.3
1038.8	I-135	6.57	h	7.9	1260.5	28.9	1131.5	22.5	1678.0	9.5
1040.6	Sr-93	7.40	m	3.2	590.3	67.2	875.7	24.2	988.1	21.8
1043.7	La142	1.54	h	3.0	641.2	52.5	2397.7	16.3	2542.6	11.2
1048.1	Cs136	13.16	d	79.6	818.5	99.7	1048.1	79.8	340.6	48.5
1050.5	Ru106	1.02	y	1.7	$11.9	20.4	621.8	10.7	1050.5	1.7
1060.7	Rb-90	2.60	m	7.8	831.7	33.3	1060.7	7.8	--	--
1060.7	Rb-90m	4.30	m	9.5	831.7	93.4	1375.4	17.4	1060.7	9.5
1072.6	I-134	52.60	m	15.3	947.0	95.4	884.1	65.3	1072.6	15.3
1078.5	Ba142	10.70	m	9.3	255.1	18.0	1204.1	14.0	894.9	11.0
1099.2	Fe-59	44.51	d	56.5	1099.2	56.5	1291.6	43.2	192.3	3.1
1115.5	Ni-65	2.52	h	14.8	1481.9	23.5	1115.5	14.8	366.3	4.6
1115.5	Zn-65	243.80	d	50.7	1115.5	50.7	511.0	2.8	--	--
1118.7	Kr-90	32.30	s	37.0	1118.7	37.0	121.8	32.0	539.5	29.0
1122.5	Sr-93	7.40	m	4.0	590.3	67.2	875.7	24.2	888.1	21.8
1124.0	I-135	6.57	h	3.6	1260.4	28.9	1131.5	22.5	1678.0	9.5
1125.5	Te131m	1.35	d	11.4	773.7	38.2	852.2	20.7	793.7	13.9
1131.5	I-135	6.57	h	22.5	1260.4	28.9	1131.5	22.5	1678.0	9.5
1136.0	I-132	2.28	h	2.9	667.7	98.7	772.6	76.2	954.6	18.1
1136.2	I-134	52.60	m	9.7	847.0	95.4	884.1	65.3	1072.6	15.3
1139.0	Y-94	19.00	m	7.8	919.0	73.6	1139.0	7.8	551.0	6.3
1141.3	Kr-88	2.84	h	1.3	196.3	26.0	834.8	13.0	1529.8	10.9
1142.3	Sr-92	2.71	h	2.9	1383.9	90.0	953.3	3.6	430.6	3.3
1169.0	Nb-98	51.10	m	18.0	787.2	95.0	722.3	77.0	1169.0	18.0
1173.2	Co-60	5.27	y	100.0	1173.2	100.0	1332.5	100.0	--	--
1175.4	Kr-87	1.39	h	1.1	402.6	49.6	2554.8	13.2	845.4	7.3

Table A-2 (continued)

Energy (keV)	Nuclide	Half-life	γ/d %	Associated Major Gamma-ray and Intensity					
				keV	%	keV	%	keV	%
1197.5	Ba141	18.27 m	4.9	190.2	49.0	304.2	26.6	277.0	24.6
1202.2	Ba142	10.70 m	5.3	255.1	18.0	1204.1	14.0	894.9	11.0
1204.1	Ba142	10.70 m	14.0	255.1	18.0	1204.1	14.0	894.9	11.0
1204.9	Y-91	58.50 d	0.3	1204.9	0.3	--	--	--	--
1206.6	Te131m	1.35 d	9.8	773.7	38.2	852.2	20.7	793.7	13.9
1213.3	Br-84	31.80 m	2.6	881.5	42.0	2897.3	14.9	1015.9	6.2
1216.0	As-76	26.30 h	3.8	559.1	45.0	657.0	6.1	1216.0	3.8
1235.3	Cs136	13.16 d	19.7	818.5	99.7	1048.1	79.8	340.6	48.5
1242.8	Rb-90m	4.30 m	3.12	831.7	93.4	1375.4	17.4	1060.7	9.5
1248.1	Rb-89	15.40 m	42.0	1031.9	58.0	1248.1	42.0	2196.0	13.3
1260.4	I-135	6.57 h	28.6	1260.4	28.9	1131.5	22.5	1678.0	9.5
1269.5	Sr-93	7.40 m	7.1	590.3	67.2	875.7	24.2	888.1	21.8
1283.2	Cs139	9.30 m	7.0	1283.2	7.0	627.2	1.6	1680.7	0.6
1291.6	Fe-59	44.51 d	43.2	1099.2	56.5	1291.6	43.2	192.3	3.1
1293.6	Ar-41	1.82 h	99.2	1293.6	99.2	--	--	--	--
1298.2	I-133	20.80 h	2.3	529.9	86.3	875.3	4.5	1298.2	2.3
1313.0	I-136	1.39 m	69.4	1313.0	69.4	1321.1	25.8	2298.6	10.8
1321.1	I-136	1.39 m	25.8	1313.0	69.4	1321.1	25.8	2289.6	10.8
1332.5	Co-60	5.27 y	100.0	1332.5	100.0	1173.2	100.0	--	--
1345.9	Cu-64	12.70 h	0.49	511.0	35.7	154.9	0.49	--	--
1354.5	La141	3.90 h	2.6	1354.5	2.6	--	--	--	--
1356.0	O-19	26.90 s	59.0	197.0	97.0	1356.0	59.0	112.0	2.7
1365.2	Cs134	2.06 y	3.0	604.7	97.6	795.9	85.4	569.3	15.4
1368.2	Sb124	60.20 d	2.5	602.7	97.9	1691.0	49.0	722.8	11.1
1368.5	Na-24	14.96 h	100.0	1368.5	100.0	2754.1	99.8	--	--
1372.1	I-132	2.28 h	2.5	667.7	98.7	772.6	76.2	954.6	18.1
1375.4	Rb-90m	4.30 m	17.4	831.7	93.4	1375.4	17.4	1060.7	9.5
1379.9	Ba142	10.70 m	3.4	251.1	18.0	1204.1	14.0	894.9	11.0
1383.9	Sr-92	2.71 h	90.0	1383.9	90.0	953.3	3.6	430.6	3.3
1384.3	Ag110m	249.80 d	24.3	657.8	94.6	894.7	72.7	937.5	34.2
1398.6	I-132	2.28 h	7.1	667.7	98.7	772.6	76.2	954.6	18.1
1405.4	Y-92	3.54 h	4.8	934.5	13.9	1405.4	4.8	561.1	2.4
1420.0	Sr-94	1.29 m	100.0	1420.0	100.0	--	--	--	--
1423.8	Kr-90	32.30 s	2.8	1118.7	37.0	121.8	32.0	539.5	29.0
1435.0	Nb-98	51.10 m	7.2	787.2	95.0	722.3	77.0	1169.0	18.0
1435.9	Cs138	32.20 m	76.3	1435.9	76.3	462.8	30.7	1009.8	29.8
1440.0	O-19	26.90 s	2.7	197.0	97.0	1356.0	59.0	112.0	2.7
1457.6	I-135	6.57 h	8.6	1260.4	28.9	1131.5	22.5	1678.0	9.5
1463.8	Br-84	31.80 m	2.0	881.5	42.0	1897.3	14.9	1015.9	6.2
1472.7	Kr-89	3.15 m	6.9	220.9	20.0	585.8	16.6	904.3	7.2
1481.8	Ni-65	2.52 h	23.5	1481.9	23.5	1115.5	14.8	366.3	4.6
1505.0	Ag110m	249.80 d	13.1	637.8	94.6	894.7	72.7	937.5	34.2
1511.0	Nb-98	51.10 m	6.1	787.2	95.0	722.3	77.0	1169.0	18.0
1529.8	Kr-88	2.84 h	10.9	196.3	26.0	834.8	13.0	1529.8	10.9
1533.7	Kr-89	3.15 m	5.1	220.9	20.0	585.8	16.6	904.3	7.2
1537.9	Kr-90	32.30 s	9.3	1118.7	37.0	121.8	32.0	539.5	29.0
1545.0	Nb-98	51.10 m	6.3	787.2	95.0	722.3	77.0	1169.0	18.0
1545.8	La142	95.40 m	3.3	641.2	52.5	2347.7	16.3	2542.6	11.2

Table A-2 (continued)

Energy		Half-		γ/d	Associated Major Gamma-ray and Intensity					
(MeV)	Nuclide	life		%	keV	%	keV	%	keV	%
1596.5	La140	40.27	h	95.4	1596.5	95.4	487.0	45.5	815.9	23.5
1642.4	Cl-38	37.20	m	32.5	2167.5	44.0	1642.4	32.5	--	--
1665.6	Rb-90m	4.30	m	4.6	831.7	93.4	1375.4	17.4	1060.7	9.5
1678.0	I-135	6.57	h	9.5	1260.4	28.9	1131.5	22.5	1678.0	9.5
1680.7	Cs139	9.30	m	0.6	1283.2	7.0	627.2	1.6	1680.7	0.6
1691.0	Sb124	60.20	d	49.0	602.7	97.8	1691.0	49.0	722.8	11.1
1693.7	Kr-89	3.15	m	4.4	220.9	20.0	585.8	16.6	904.3	7.2
1706.5	I-135	6.57	h	4.1	1260.4	28.9	1131.5	22.5	1678.0	9.5
1732.0	Na-24	14.96	h	--	1368.5	100.0	2754.1	99.8	--	--
1740.5	Kr-87	1.39	h	2.1	402.6	49.6	2554.8	13.2	845.4	7.3
1756.4	La142	95.40	m	3.3	641.2	52.5	2397.7	16.3	2542.6	11.2
1768.3	Xe138	14.10	m	16.7	258.3	31.5	434.5	20.3	1768.3	16.7
1780.0	Kr-90	32.30	s	6.4	1118.7	37.0	121.8	32.0	539.5	29.0
1791.2	I-135	6.57	h	7.7	1260.4	28.9	1131.5	22.5	1678.0	9.5
1810.7	Mn-56	2.58	h	27.2	846.8	98.9	1810.7	27.2	2113.1	14.3
1836.0	Rb-88	17.70	m	21.4	1836.0	21.4	898.0	14.0	2677.8	1.9
1897.3	Br-84	31.80	m	14.9	881.5	42.0	1897.3	14.9	1015.9	6.2
1901.3	La142	1.54	h	8.7	641.2	52.5	2397.7	16.3	2542.6	11.2
1917.0	Y-93	10.20	h	1.4	266.9	6.8	97.1	2.0	1917.0	1.4
2004.0	Xe138	14.10	m	5.4	253.8	31.5	434.5	20.3	1768.3	16.7
2007.5	Rb-89	15.40	m	2.4	1031.9	58.0	1248.1	42.0	2196.0	13.3
2015.8	Xe138	14.10	m	12.3	253.8	31.5	434.5	20.3	1768.3	16.7
2029.8	Kr-88	2.84	h	4.3	196.3	26.0	834.8	13.0	1529.8	10.9
2091.0	Sb124	60.20	d	5.7	602.7	97.8	1691.0	49.0	722.8	11.1
2113.1	Mn-56	2.58	h	14.3	946.8	98.9	1810.7	27.2	2113.1	14.3
2128.3	Rb-90m	4.30	m	5.4	831.7	93.4	1375.4	17.4	1060.7	9.5
2167.5	Cl-38	37.20	m	44.0	2167.5	44.0	1642.4	32.5	--	--
2195.8	Kr-88	2.84	h	13.2	196.3	26.0	834.8	13.0	1529.8	10.9
2196.0	Rb-89	15.40	m	13.3	1031.9	58.0	1248.1	42.0	2196.0	13.3
2218.0	Cs138	32.20	m	15.2	1435.9	76.3	462.8	30.7	1009.8	29.8
2289.6	I-136	1.39	m	10.8	1313.0	69.4	1321.1	25.8	2289.6	10.8
2392.4	Kr-88	2.84	h	34.6	196.3	26.0	934.9	13.0	1529.8	10.9
2397.7	La142	1.54	h	16.3	641.2	52.5	2397.7	16.3	2542.6	11.2
2494.1	Br-84	31.80	m	6.8	881.5	42.0	1897.3	14.9	1015.9	6.2
2521.7	La140	40.27	h	3.5	1596.5	95.4	487.0	45.5	815.9	23.5
2542.6	La142	1.54	h	11.2	641.2	52.5	2397.7	16.3	2542.6	11.2
2554.8	Kr-87	1.37	h	9.3	402.6	49.6	2554.8	13.2	945.4	7.3
2558.1	Kr-87	1.37	h	3.9	402.6	49.6	2554.8	13.2	845.4	7.3
2564.0	Rb-91	58.50	s	20.0	93.0	38.0	2564.0	20.0	346.0	12.0
2639.6	Cs138	32.20	m	7.6	1435.9	76.3	462.8	30.7	1009.8	29.8
2677.8	Rb-88	17.70	m	1.9	1836.0	21.4	898.0	14.0	2677.8	1.9
2752.7	Rb-90m	4.30	m	11.8	831.7	93.4	1375.4	17.4	1060.7	9.5
2754.1	Na-24	14.96	h	99.8	1368.5	100.0	2754.1	99.8	--	--
2868.9	I-136	1.39	m	4.1	1313.0	69.4	1321.1	25.8	2289.6	10.8

Table A-3. CUMULATIVE YIELDS OF MAJOR FISSION PRODUCTS IN THERMAL NEUTRON FISSION OF U-235 AND Pu-239

Nuclide	Half-life	Decay constant λ, 1/s	Fission yields(Y),% U-235	Pu-239	(U+Pu) 2	Y*λ U-235	(U+Pu)/2
Br-84	31.80 m	3.63E-04	0.967	0.444	0.706	3.51E-06	2.56E-06
Kr-85m	4.48 h	4.30E-05	1.300	0.565	0.933	5.59E-07	4.01E-07
Kr-85	10.72 y	2.05E-09	0.285	0.128	0.207	5.86E-12	4.24E-12
Kr-87	1.37 h	1.41E-04	2.520	0.990	1.755	3.54E-06	2.47E-06
Kr-88	2.84 h	6.78E-05	3.550	1.320	2.435	2.41E-06	1.65E-06
Kr-89	3.15 m	3.67E-03	4.600	1.440	3.020	1.69E-04	1.11E-04
Kr-90	32.30 s	2.15E-02	4.860	1.400	3.130	1.04E-03	6.72E-04
Rb-88	17.70 m	6.53E-04	3.570	1.360	2.465	2.33E-05	1.61E-05
Rb-89	15.40 m	7.50E-04	4.770	1.680	3.225	3.58E-05	2.42E-05
Rb-90	2.60 m	4.44E-03	4.500	1.390	2.945	2.00E-04	1.31E-04
Rb-90m	4.30 m	2.69E-03	1.240	0.680	0.960	3.33E-05	2.58E-05
Rb-91	58.00 s	1.19E-02	5.670	2.160	3.915	6.77E-04	4.67E-04
Sr-89	50.50 d	1.59E-07	4.780	1.690	3.235	7.59E-09	5.14E-09
Sr-90	29.10 y	7.55E-10	5.910	2.110	4.010	4.46E-11	3.03E-11
Sr-91	9.51 h	1.93E-04	5.930	2.490	4.210	1.14E-05	8.11E-06
Sr-92	2.71 h	7.10E-05	5.910	3.040	4.475	4.20E-06	3.18E-06
Sr-93	7.40 m	1.56E-03	6.370	3.920	5.145	9.94E-05	8.03E-05
Y-90	2.67 d	3.00E-06	5.920	2.110	4.015	1.78E-07	1.21E-07
Y-91	58.50 d	1.37E-07	5.930	2.490	4.210	8.13E-09	5.77E-09
Y-92	3.54 h	5.44E-05	5.980	3.060	4.520	3.25E-06	2.46E-06
Y-93	10.20 h	1.89E-05	6.370	3.920	5.145	1.20E-06	9.71E-07
Zr-95	64.00 d	1.25E-07	6.490	4.890	5.690	8.14E-09	7.13E-09
Zr-97	16.80 h	1.15E-05	5.930	5.320	5.625	6.80E-07	6.45E-07
Nb-95	34.97 d	2.29E-07	6.490	4.890	5.690	1.49E-08	1.31E-08
Nb-97	1.23 h	1.57E-04	5.950	5.370	5.660	9.31E-06	8.86E-06
Mo-99	2.79 d	2.88E-06	6.120	6.160	6.140	1.76E-07	1.77E-07
Mo-101	14.60 m	7.91E-04	5.180	5.940	5.560	4.10E-05	4.40E-05
Tc-98m	6.02 h	3.20E-05	5.380	5.420	5.400	1.72E-06	1.73E-06
Tc-101	14.20 m	8.14E-04	5.180	5.950	5.565	4.21E-05	4.53E-05
Tc-104	18.00 m	6.42E-04	1.920	5.960	3.940	1.23E-05	2.53E-05
Ru-103	39.27 d	2.04E-07	3.040	6.950	4.995	6.21E-09	1.02E-08
Ru-105	4.44 h	4.34E-05	0.972	5.360	3.166	4.22E-07	1.37E-06
Ru-106	1.02 y	2.15E-08	0.403	4.280	2.342	8.68E-11	5.05E-10
Rh-105	35.40 h	5.44E-06	0.972	5.360	3.166	5.29E-08	1.72E-07
Sb-125	2.76 y	7.96E-09	0.029	0.115	0.072	2.31E-12	5.73E-12
Te-129m	33.60 d	2.39E-07	0.127	0.270	0.199	3.03E-10	4.74E-10
Te-132	3.26 d	2.46E-06	4.280	5.230	4.755	1.05E-07	1.17E-07
I-131	8.04 d	9.98E-07	2.880	3.850	3.365	2.87E-08	3.36E-08
I-132	2.28 h	8.44E-05	4.320	5.390	4.855	3.65E-06	4.10E-06
I-133	20.80 h	9.26E-06	6.690	6.930	6.810	6.19E-07	6.30E-07
I-134	52.60 m	2.20E-04	7.710	7.270	7.490	1.69E-05	1.65E-05
I-135	6.57 h	2.93E-05	6.300	6.450	6.375	1.85E-06	1.87E-06
I-136	1.39 m	8.31E-03	2.970	1.740	2.355	2.47E-04	1.96E-04

Table A-4

MAJOR WATER AND IMPURITY ACTIVATION PRODUCTS IN REACTOR COOLANT

Nuclide	Half-Life	Reaction	Natural Isotopic Abundance (%)	Average Activation Cross Section[a]
^{3}H	12.3 y	$^{2}H(n,\alpha)^{3}H$	0.015	0.53 mb(T)
		$^{6}Li(n,\alpha)^{3}H$	7.5	942 b (F)
		$^{10}B(n,2\alpha)^{3}H$	-	5.6 mb (F)
		$^{10}B(n,\alpha)^{7}Li$	-	3838 b (F)
		$^{235}U(n,f)^{3}H$	-	0.01% fy
^{14}C	5730 y	$^{13}C(n,\gamma)^{14}C$	1.11	0.9 mb (T)[b]
		$^{14}N(n,p)^{14}C$	99.63	1.8 b (F)[b]
		$^{17}O(n,\alpha)^{14}C$	0.038	240 mb (F)[b]
^{15}C	2.45 s	$^{18}O(n,\alpha)^{15}C$	0.204	1.5 mb (F)
^{13}N	9.97 m	$^{16}O(p,\alpha)^{13}N$	99.76	50 mb (P)[c]
^{16}N	7.13 s	$^{16}O(n,p)^{16}N$	99.76	19 mb (F)
^{19}O	26.9 s	$^{18}O(n,\gamma)^{19}O$	0.204	160 mb (T)
^{18}F	1.83 h	$^{18}O(p,n)^{18}F$	0.204	300 mb (P)
^{24}Na	14.96 h	$^{23}Na(n,\gamma)^{24}N$	100	528 mb (T)
^{32}P	14.28 d	$^{31}P(n,\gamma)^{32}P$	100	190 mb (T)
		$^{32}S(n,p)^{32}P$	95	69 mb (F)
^{38}Cl	37.2 m	$^{37}Cl(n,\gamma)^{38}Cl$	24.23	430 mb (T)

(a) Data for 20°C; T, F, and P in the parentheses indicate thermal and fast neutron and proton reactions, respectively; the activation cross-section data are adopted from References 1 and 2.

(b) P. J. Magno, et al, Proc. 13th AEC Air Cleaning Conf., P1047 (1972).

(c) M. S. Singh and L. Ruby, Nucl. Tech., 17, 104 (1973).

Table A-5

MAJOR ACTIVATED CORROSION PRODUCTS IN LIGHT WATER REACTORS

Nuclide	Half-Life	Formation Reaction	Nature Isotopic Abundance (%)	Activation Cross Section (Barns)[a]		
				Thermal	Epithermal	Fast
^{51}Cr	27.7 d	$^{50}Cr(n,\gamma)^{51}Cr$	4.35	16.0	0.68	
^{54}Mn	312.2 d	$^{54}Fe(n,p)^{54}Mn$	5.8			0.11
^{56}Mn	2.58 h	$^{55}Mn(n,\gamma)^{56}Mn$	100	13.3	1.13	
^{55}Fe	2.73 y	$^{54}Fe(n,\gamma)^{55}Fe$	5.8	2.5	0.1	
^{59}Fe	44.51 d	$^{58}Fe(n,\gamma)^{59}Fe$	0.3	1.14	0.1	
^{58}Co	70.88 d	$^{58}Ni(n,p)^{58}Co$[b]	68.3			0.146
^{60}Co	5.27 y	$^{59}Co(n,\gamma)^{60}Co$	100	37.5	6.05	
^{63}Ni	100 y	$^{62}Ni(n,\gamma)^{63}Ni$	3.6	14.6	0.77	
^{65}Ni	2.52 h	$^{64}Ni(n,\gamma)^{65}Ni$	0.9	1.50	0.07	
^{64}Cu	12.7 h	$^{63}Cu(n,\gamma)^{64}Cu$	69.2	4.4	0.40	
^{65}Zn	243.8 d	$^{64}Zn(n,\gamma)^{65}Zn$	48.6	0.82	0.13	
^{76}As	26.3 h	$^{75}As(n,\gamma)^{76}As$	100	4.4	5.08	
^{95}Zr	64.02 d	$^{94}Zr(n,\gamma)^{95}Zr$	17.4	0.075	0.031	
^{110m}Ag	249.8 d	$^{109}Ag(n,\gamma)^{110m}Ag$	48.17	4.7		
^{113}Sn	115.1 d	$^{112}Sn(n,\gamma)^{113}Sn$	1.01	0.71	2.2	
^{124}Sb	60.2 d	$^{123}Sb(n,\gamma)^{124}Sb$	42.7	4.0	9.7	
^{181}Hf	42.4 d	$^{180}Hf(n,\gamma)^{181}Hf$	35.2	12.6	2.26	
^{182}Ta	114.43 d	$^{181}Ta(n,\gamma)^{182}Ta$	100	22.0	56.4	
^{187}W	23.9 h	$^{186}W(n,\gamma)^{187}W$	28.6	37.2	33.9	

[a]Data for 20°C.
[b]Burnup cross section, σ_b, for Co-58 is 1.9×10^{-21} cm^2.

Table A-6

RECOMMENDED GAMMA-RAY STANDARDS

Nuclide	Half-life	Photon Energy (KeV)	Emission Probability (γ/d)
Na-22	2.605y	1274.54	1.0
Mn-54	312.2 d	834.84	1.0
Co-57	271.8 d	122.06	0.859
Co-60	5.27 y	1173.24	0.999
		1332.50	1.0
Zn-65	243.8 d	1115.55	0.507
Kr-85	10.73 y	514.01	0.00434
Sr-85	64.84 d	514.01	0.983
Y-88	106.6 d	898.04	0.937
		1836.06	0.9924
Cd-109	462.0 d	88.03	0.0375
Sn-113	115.1 d	391.7	0.6489
Sb-125	2.758y	27.4	0.619
		176.4	0.06979
		380.5	0.0151
		427.9	0.294
		463.4	0.1037
		600.6	0.1735
		635.9	0.112
Cs-137	30.17 y	661.66	0.852
Ba-133	10.53 y	81.0	0.343
		302.85	0.183
		356.02	0.621
Ce-139	137.6 d	165.9	0.80
Eu-152	13.48 y	121.78	0.2837
		244.7	0.0751
		344.38	0.2658
		443.98	0.0312
		778.9	0.1296
		964.13	0.1462
		1085.91	0.1016
		1112.12	0.1356
		1408.01	0.2085

Table A-6

RECOMMENDED GAMMA-RAY STANDARDS (Continued)

Nuclide	Half-life	Photon Energy (KeV)	Emission Probability (γ/d)
Eu-154	8.59 y	42.8	0.131
		123.1	0.408
		248.0	0.0691
		591.7	0.0494
		723.3	0.201
		873.2	0.122
		996.4	0.1043
		1004.8	0.1808
		1274.4	0.344
		1596.5	0.0185
Eu-155	4.71 y	42.8	0.117
		86.6	0.311
		105.3	0.215
Hg-203	45.61 d	279.20	0.815
Bi-207	32.2 y	569.7	0.977
		1063.66	0.74
Am-241	432.7 y	26.34	0.024
		59.54	0.359

CHART OF THE NUCLIDES

KNOLLS ATOMIC POWER LABORATORY

Operated by the General Electric Company under direction of

NAVAL REACTORS, U.S. DEPARTMENT OF ENERGY

FOURTEENTH EDITION—REVISED TO APRIL 1988

A-21

PREPARED BY:
F. WILLIAM WALKER
JOSEF R. PARRINGTON
FRANK FEINER

ACKNOWLEDGMENTS: The author is indebted to General Electric Company for reproducing selected portions of the Chart.

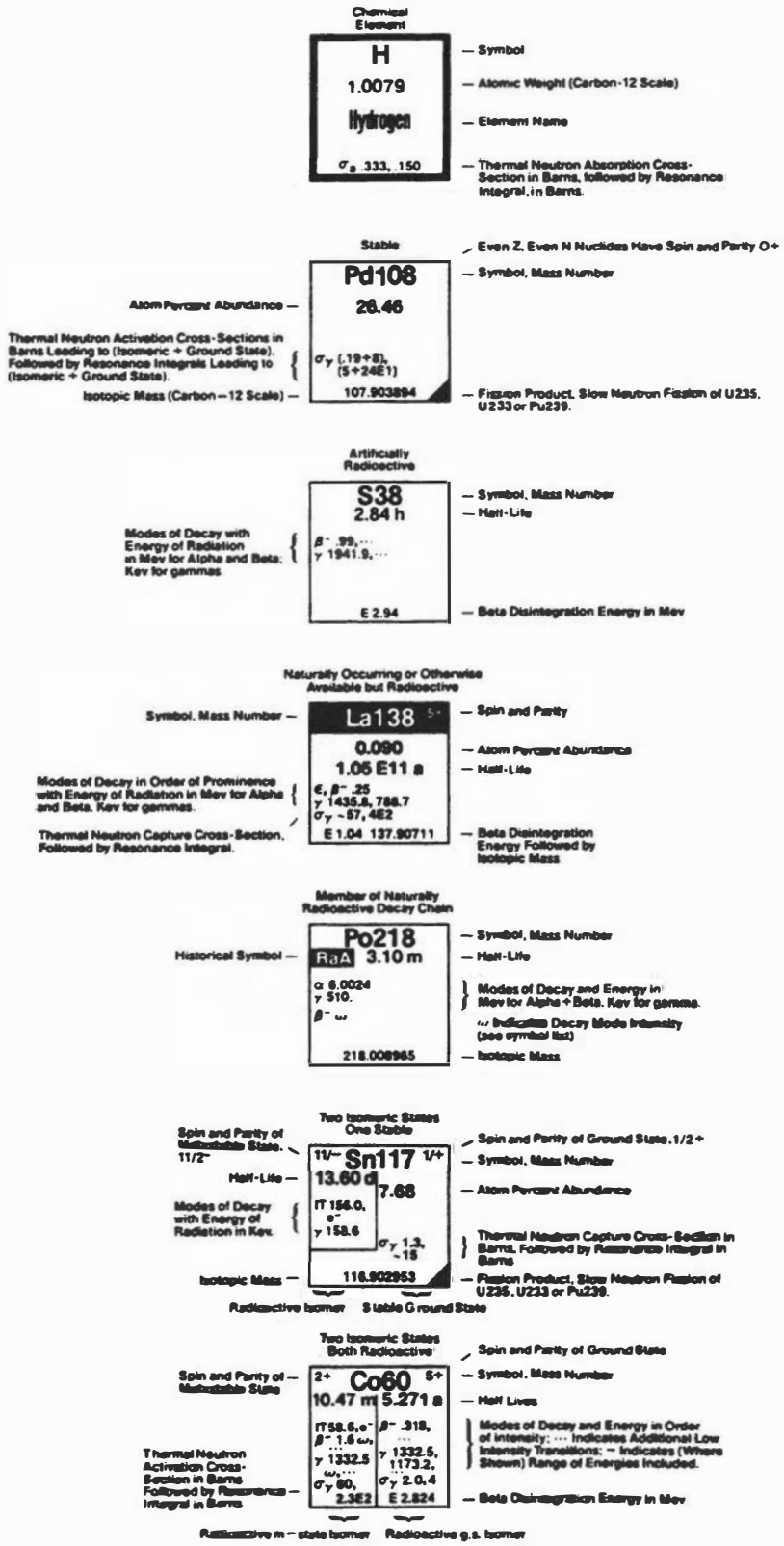

SYMBOLS

α	alpha particle
β^-	negative electron
β^+	positron
γ	gamma ray
n	neutron
p	proton
d	deuteron
t	triton
€	electron capture
IT	isomeric transition
D	delayed radiation
SF	spontaneous fission
E	disintegration energy
e^-	conversion electron
$\beta^-\beta^-$	double beta-decay
C14	particle emission
Ne	particle emission

TIME

μs	microseconds (1.0E-6 sec.)
ms	milliseconds (1.0E-3 sec.)
s	seconds
m	minutes
h	hours
d	days
a	years

Displacements Caused by Nuclear Bombardment Reactions

	α, 3n	α, 2n ³He, n	α, n
	p, n	p, γ d, n ³He, np	α, np t, n ³He, p
	p, pn γ, n n, 2n	Original Nucleus n, n	d, p n, γ t, np	t, p
p, α	n, t γ, np n, nd	n, d γ, p n, np	n, p t, ³He
	n, α n, n ³He	n, ³He n, pd	

Relative Locations of the Products of Various Nuclear Processes

			³He in	α in
	β^- out	p in	d in	t in
	n out	Original Nucleus	n in	
t out	d out	p out	β^+ out e^-	
α out	³He out			

Group 1.
Light Element Nuclides

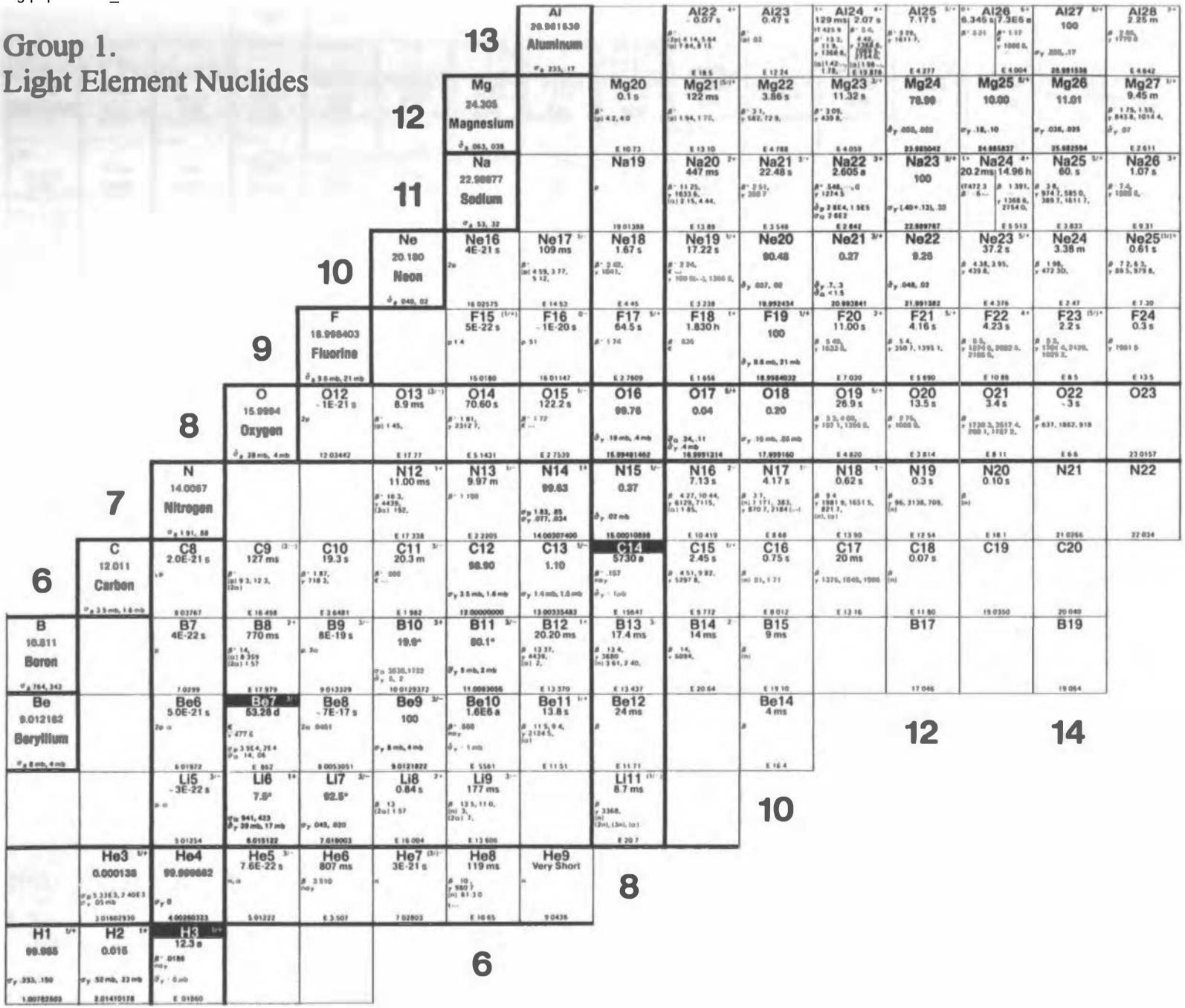

Group 2.
Transtion Metal Nuclides

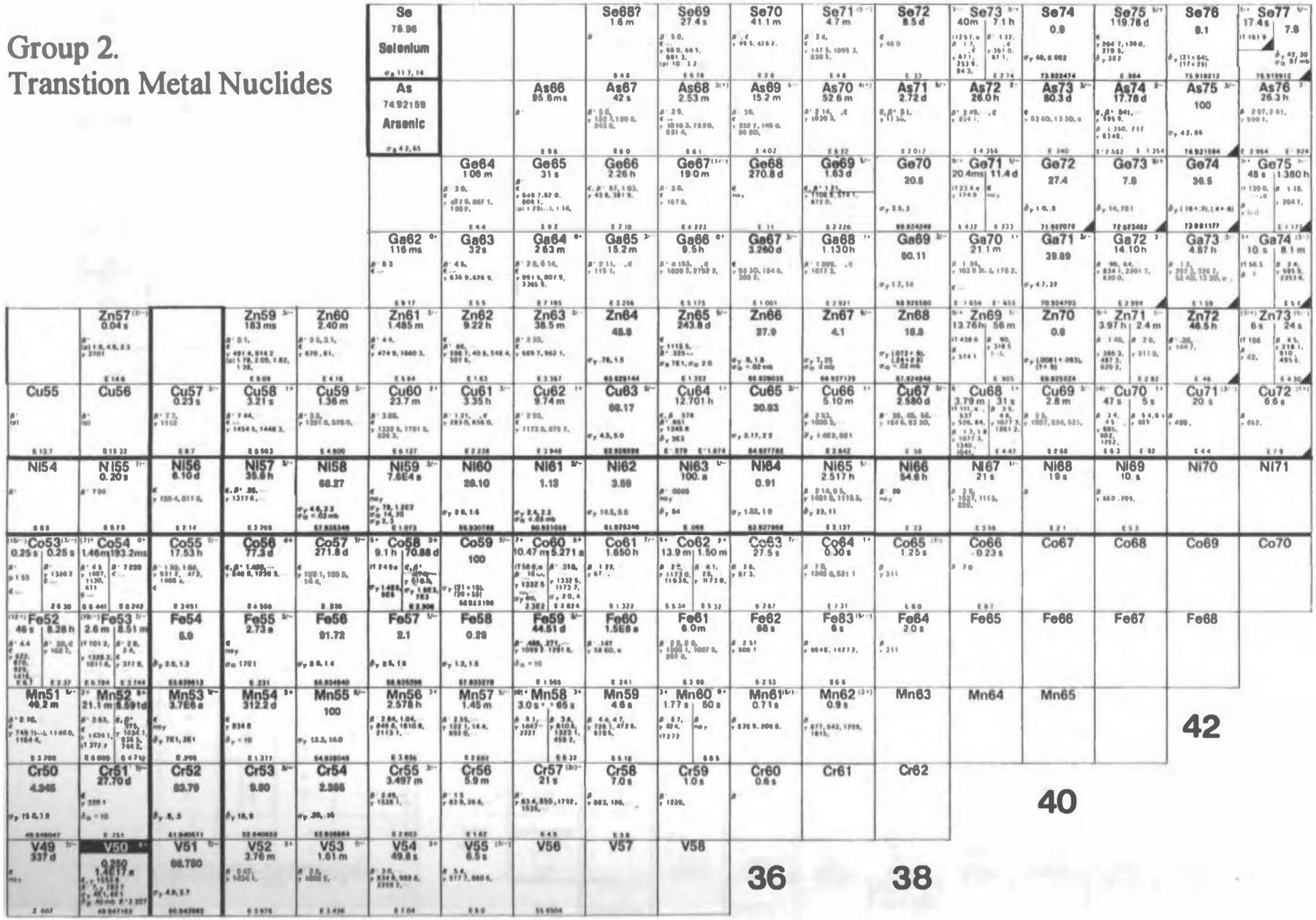

Group 3.
Light Fission Products

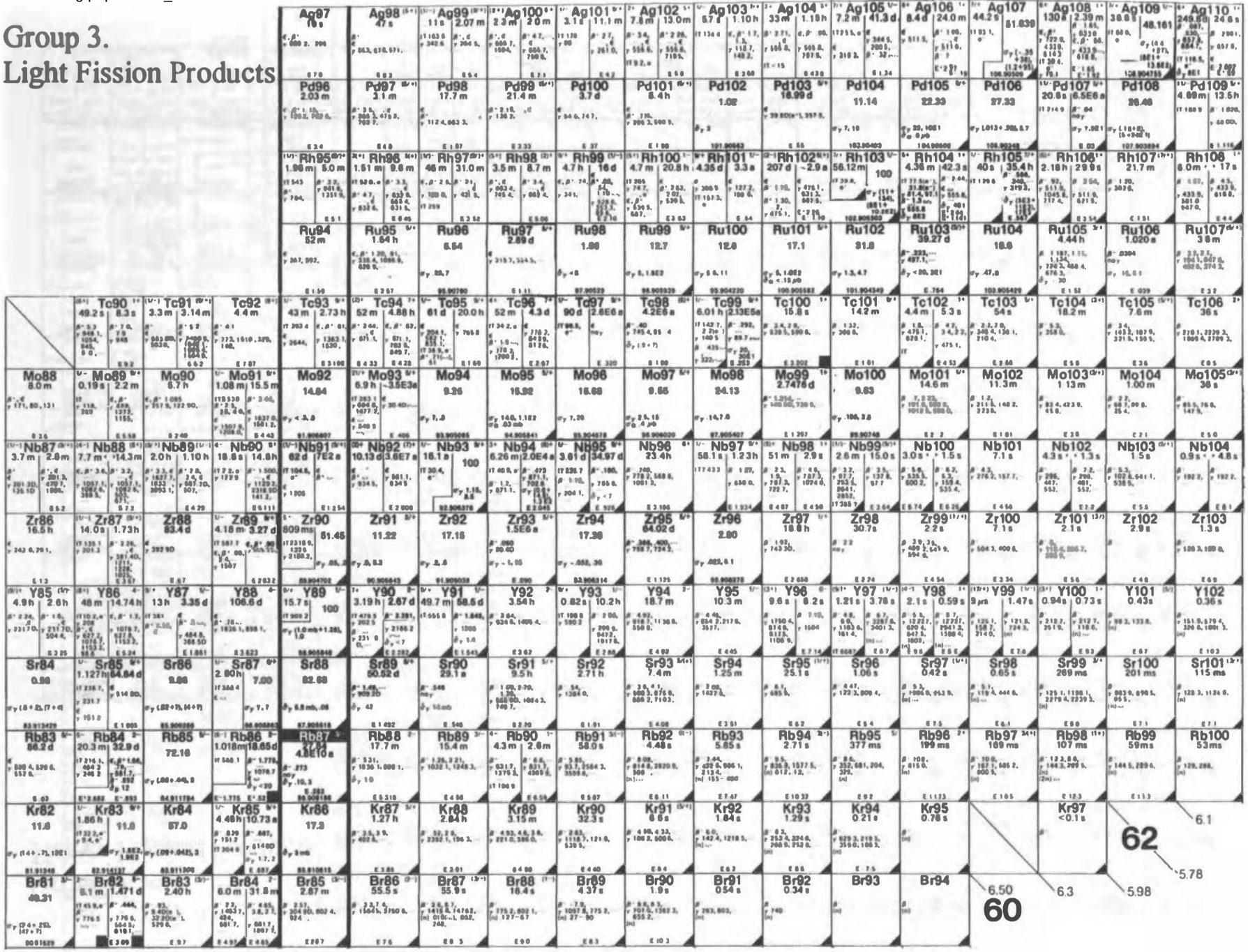

Group 4.
Heavy Fission Products

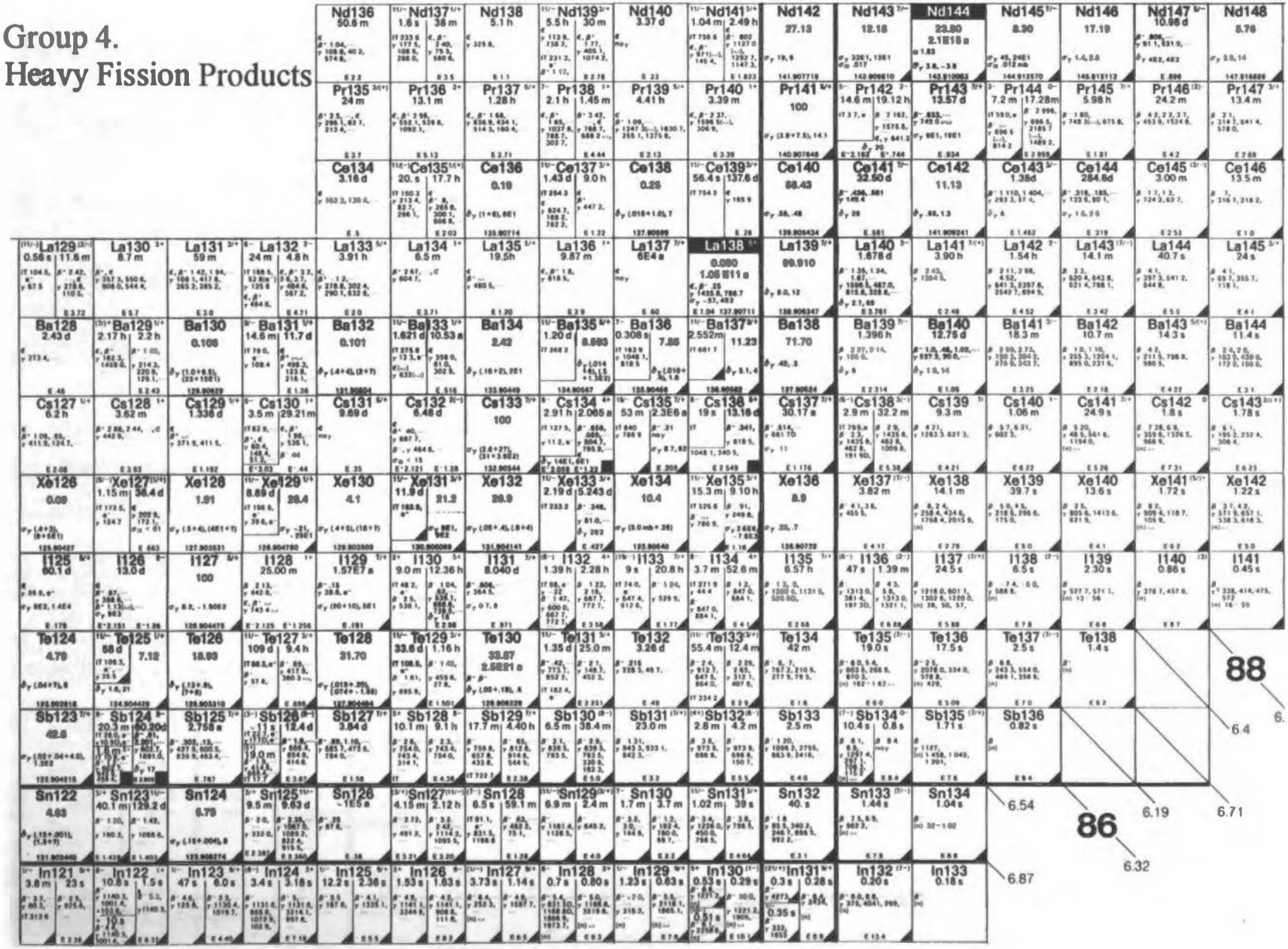

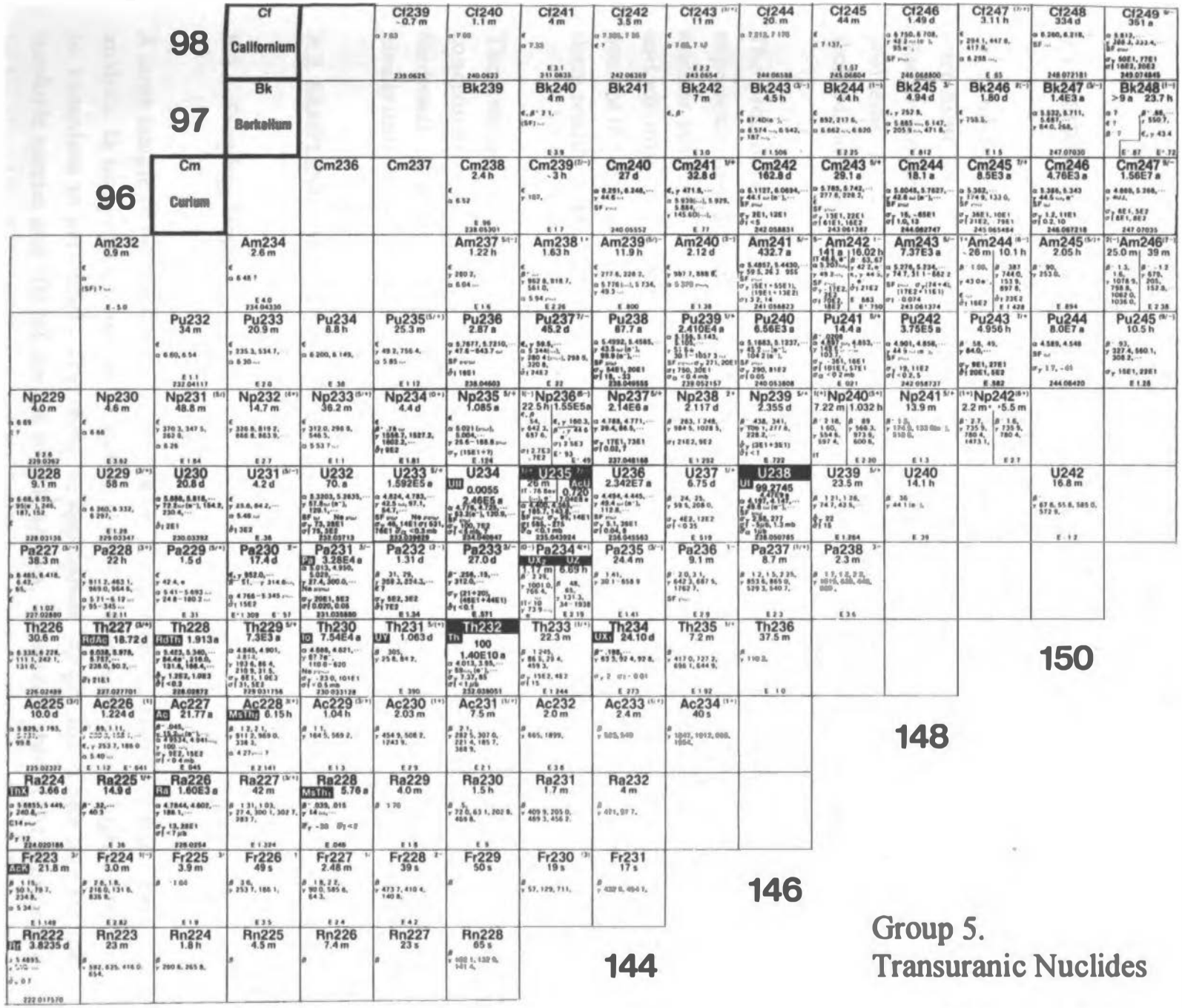

A-27 / A-28

Group 5.
Transuranic Nuclides

Appendix B

SAMPLING PRACTICES AND SAMPLE PREPARATION FOR RADIOCHEMICAL ANALYSES

B.1 INTRODUCTION

In a nuclear power plant, one of the most frequent mistakes and largest errors introduced in radiochemical analysis is sampling and sample preparation. Sampling the reactor coolant, offgas, liquid waste, and airborne samples, etc., may present different problems in each case for an inexperienced radiochemist. Some problems can be avoided, but some can only be minimized.

The procedures described in this and following appendices reflect nearly twenty years of experience in sampling and measuring the radioactivities in various types of samples in nuclear power plants. Some techniques are standard, some modified to suit the needs, and still others developed at GE Vallecitos Nuclear Center. The author has attempted to present the technologies in a simple and concise manner but in sufficient detail to make them readily usable.

The commercially available ion-exchange membranes have been successfully used to concentrate the trace metallic impurities and radioactive species in reactor coolant and feedwater. The speed and simplicity of filtration make the sampling techniques almost ideally suited for concentrating solutions containing trace amounts of materials.

B.2 SAMPLING BWR PRIMARY COOLANT - LABORATORY FILTRATION

B.2.1 Sampling Method

A large sample of reactor water is preferred for accurate chemical and/or radiochemical analysis. In many cases, however, the radiation level from reactor water is high enough to be hazardous to personnel. Therefore, an appropriate sample size is one liter for the insoluble species and 100 mL for the soluble species. In no case should the sample size be less than 10 mL because such small samples may not be representative. Solubles and

(3) Shake the bottle vigorously. Then measure a 100 mL water sample using a clean graduated cylinder.

(4) Filter the 100 mL sample through the filters. Adjust the vacuum so that the filtering flow rate is approximately 50 mL per minute to complete the filtration in approximately 2 minutes.

(**Note**: If radiation levels permit, use the entire liter sample for both particulates and solubles.)

(5) Turn off the vacuum, remove the cation and anion exchange membranes from the holder and place each in a separate petri dish for activity measurement.

(6) Return the Millipore (or equivalent) filter to the filtration apparatus. Filter the remaining 900 mL of water sample to collect the insolubles on the filter.

(7) When the sample is completely filtered, rinse the sample bottle and filtration funnel with approximately 200 mL of deionized water. Then filter the rinse water through the same filter.

(8) When the rinse water is completely filtered, remove the filter from the holder and place it in a petri dish for activity measurement.

B.2.3 Major Nuclides Commonly Observed in Reactor Coolant

The major nuclides separately collected in each fraction are as follows:

Insoluble		Cation		Anion
Ag-110 m	Rh-105	Ba-129	Rb-89	As-76
As-76	Ru-103	Ba-140	Rb-90	Br-84
Ce-141	Ru-105	Ba-141	Rb-90m	Cl-38
Ce-144	Ru(Rh)-106	Ba-142	Sr-87	Cr-51
Co-57	Sb-122	Co-57	Sr-90	F-18

Insoluble		Cation		Anion
Co-58	Sb-124	Co-58	SR-91	I-131
Co-60	Sb-125	Co-60	SR-92	I-132
Cr-51	Sn(IN)-113	Cs-134	Zn-63	I-133
Fe-55	Te-129m	Cs-136	Zn-65	I-134
Fe-59	Te-129m	Cs(Ba)-137	Zn-69m	I-135
Hf-181	Te-132	Cs-138		Mo-99
La-140	W-187	Cs-139		N-13
La-141	Y-91	Cu-64		Tc-99m
La-142	Y-92	Mn-54		Tc-101
Mn-54	Y-93	Mn-56		Tc-104
Nb-95	Zn-65	N-13		
Nb-97	Zr-95	Na-24		
Nd-147	Zr-97	Ni-63		
Ni-63		Ni-65		
Ni-65		Np-239		
Transuranic Isotopes				

In some cases, one nuclide can be found in both the soluble and insoluble fractions (e.g., N-13, Co-58, Co-60). In other cases, the insoluble species (e.g., Ce-141, Ce-144, Y-91, Y-92, Y-93) are frequently found in the soluble cation fraction after the soluble parent nuclides have decayed in the cation membranes.

B.2.4 Further Chemical Separation

Among the radioactive nuclides collected by filtration, only a few α, β, and low-energy gamma emitting nuclides require further chemical separation before their activities can be measured. After the gamma spectrometric analysis is completed, the following procedures are commonly used in further separation:

(1) **Millipore Filter** - When the crud level is low the filter can be counted directly for the gross α activity and α-spectrometric analysis for the transuranic isotopes, Pu-238, Pu-239, Pu-240, Pu-241, Cm-242, Cm-244, Am-241, etc.

The particulate collected on the filter can be easily dissolved in ~10 mL of warm 6N HCl. A few drops of concentrated HNO_3 may be helpful to

accelerate dissolution. The Millipore filter is removed from the solution and rinsed with ~5 mL of fresh 6N HCl. Combine the rinse with the solution for further chemical separation. The solution may contain β-emitting Fe-55 and Ni-63, in addition to the transuranic isotopes and other gamma-emitting nuclides.

(2) **Cation Membranes** - Cationic species can be readily removed from the ion exchange membranes by digesting the membranes in a beaker containing ~10 mL of warm 3N HNO_3. After ~2 minutes, the membranes are removed from the solution and repeat the process with a fresh acid solution. Combine the solutions for further chemical separation. The solution contains the β-emitting nuclides, Ni-63, Sr-89 and Sr-90, and all other cationic gamma-emitting nuclides.

(3) **Anion Membranes** - For a routine radiochemical analysis, there is no anionic species which cannot be measured by gamma spectrometric analysis directly from the anion membranes.

B.3 SAMPLING HIGH PURITY WATER CONTAINING LOW-LEVEL RADIOACTIVITIES - IN-LINE FILTRATION

(1) The water sample is collected by using a standard design of corrosion product sampler connected directly to the sample line. A schematic of a typical sampler is shown in Figure B-1.

(2) Flash the sample line through a bypass line in the sampler at a water flow rate ≥1 kg/min for at least 10 min, or 3 sample line lengths of water flow.

(3) Place one 0.45 μm Millipore filter (on top), 3 cation exchange membranes (in middle) and 3 anion exchange membranes (at bottom) in a high pressure Millipore filter holder to collect and concentrate the insoluble, cationic and anionic activities separately.

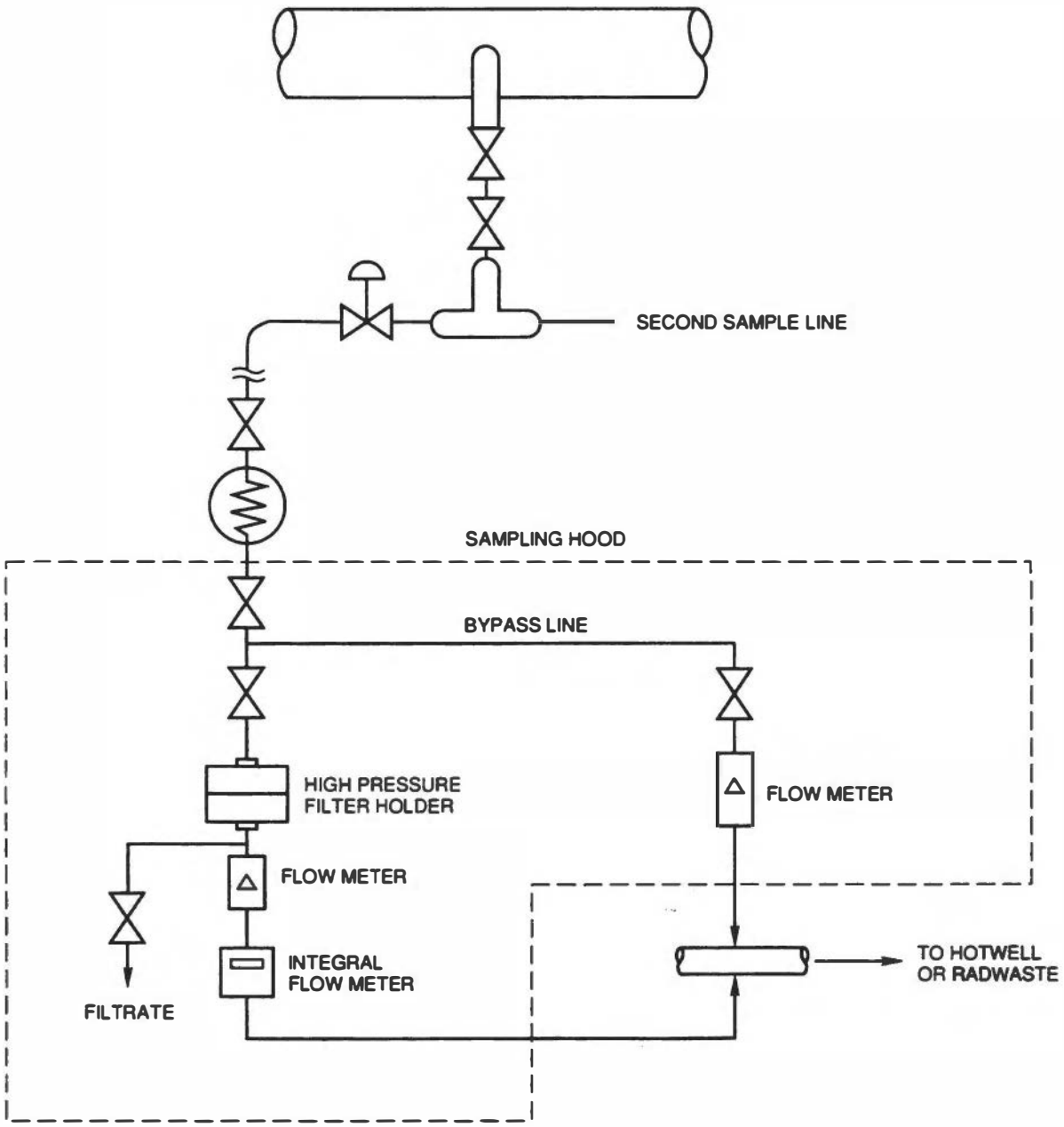

Figure B-1. A Typical In-line Filtration Sampling Arrangement

(4) While maintaining the same bypass flow rate, carefully/slowly open the inlet valve to allow water to pass through the filter holder at a flow rate of 0.1-0.2 kg/min.

(5) Record the time, flow rate and the reading on the water flow accumulator. Collect the desirable amount (at least 1 kg) of water sample at a constant flow rate.

(6) Stop the water flow and record the time and meter reading again.

(7) Remove the filters from the holder and the Millipore, cation and anion membranes are placed separately in petri dishes for activity measurements.

B.4 PWR PRIMARY COOLANT

B.4.1 General Comments and Precautions

Problems in withdrawing representative samples from a PWR primary coolant through long sample lines are well known [1,2]. Unlike the high purity water in the BWR coolant, the PWR coolant chemistry is rather complex, and it presents a special environment for some radiochemical species which may easily change their solubilities and undergo certain interactions with the oxide film on the sample line when the coolant is cooled down and water pH is changed. Experience at Ringhals[3] suggests that, in general, the measured concentrations of some activated corrosion products do not bear any useful relationship to the concentrations of corrosion products in the coolant at operating temperatures. The measured concentrations of some corrosion products (e.g., soluble Co-60 and Mn-54) are strongly dependent on sampling flow rate and the boron concentration. The Cs-137 concentration was also found to correlate directly with boron concentration.

In order to minimize the sample error and to maintain a consistency of sampling for radioactivities, the sample line purge at a constant flow rate is necessary and should not be compromised for reducing the liquid radwaste generation.

B.4.2 Sampling Procedure

(1) If the volatile species is not desired, the grab sample can be withdrawn from the sample line using the sampling procedures described earlier for the BWR coolant. Separation of radioactivities in a grab sample by filtration through a particulate filter and cation/anion change membrane has been reported by Polley and Andersson[3].

(2) If the volatile species is also to be measured, a pressurized sample cylinder ("bomb") is used to collect the sample for subsequent analyses of liquid and gaseous constituents after appropriate manipulation in the laboratory. The following steps are followed at many plants[4]:

(a) The reactor coolant sample is collected at primary system pressure employing a sample cylinder at the primary coolant sampling sink.

(b) The pressurized cylinder is transferred to the laboratory and installed in the sample manipulation panel. (See below for panel operation procedures.)

(c) The cylinder is vented, and the liquid and gas equilibrated at approximately atmospheric pressure by recirculating the gas.

(d) The volume of the total gas evolved is measured and employed to calculate total gas concentration in the sample.

(e) Aliquots of the gas and liquid are withdrawn for analysis.

(3) No standard sample manipulation panel design presently exists, and a wide variety of designs are encountered in the industry. A schematic of a representative design is given in Figure B-2. The operating procedure for this sample panel is described below.

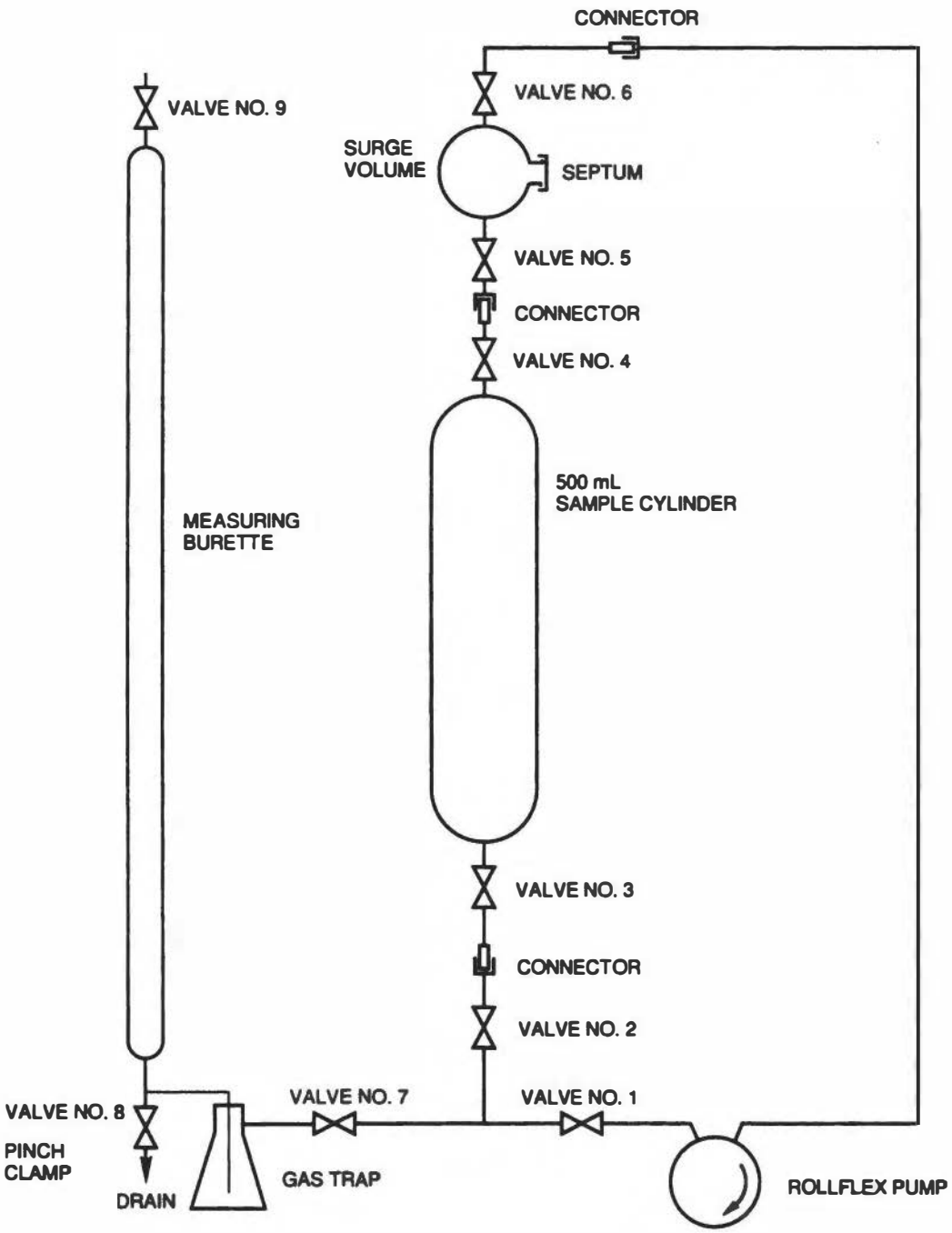

Figure B-2. Primary Coolant Sample Manipulation Apparatus (Ref. 4)

(a) Before connecting the sample cylinder, close valve #1 and introduce water through the sample cylinder connection upstream of valve #2. Fill the portions of the system downstream of valve #7.

(b) Establish a starting level in the buret by draining as necessary through the pinch clamp (valve #8). Record the initial buret level.

(c) Attach the sample cylinder to the apparatus with valve #3 and valve #4 closed.

(d) With valves #2, #7 and #9 open and valve #1 closed, allow the sample to expand slowly through valve #3 into the measuring buret. Record the new buret level.

(e) Close valve #7 and open valves #1, #2, #3, #4, #5, and #6.

(f) Start the Rollflex pump.

(g) Periodically, stop the pump, close valve #1, and open valve #7 to allow expansion of the system gases. Record all changes in level in the measuring buret.

(h) When no changes in buret level are noted, the stripping of gases from the sample is complete.

(i) Aliquots of gas sample can now be taken through the surge volume septum cap and transferred to a calibrated sample vial for radio activity measurement.

(j) Break a connection downstream of the surge volume to allow air into the system. Aliquots of water sample are taken from the cylinder for chemical separation and analysis.

B.5 SAMPLING PROCEDURE FOR THE BWR OFFGAS

(1) Prepare three standard 14.1 mL glass sample vials with rubber caps (septum). Clearly mark sample I.D.

(2) Record the sample date, reactor power level, offgas monitor readings, stack monitor readings, the offgas flow rate, and the offgas monitor flow rate.

(3) Follow the operation instruction at the sample station to obtain the samples:

   (a) Purge the sample system for 2 min.

   (b) Carefully insert the sample vial to sampling position with the vial holder, making sure that the hypodermic needle is inserted in the center of the rubber cap to evacuate the sample vial.

   (c) Check the vacuum gauge reading to be sure it is approaching 29.5 in. and remains constant for at least 1 min.

   (d) Allow the system to purge again for 30 seconds.

   (e) Fill the sample vial with sample gas and keep the vial at position for 10 s. Record the sample time and remove the sample vial.

   (f) Repeat sampling with a new vial starting with Step (a).

(4) Properly timed samples should have been collected exactly every 3 min. Transfer the samples to the counting room as soon as the last sample is taken.

(5) Immediately after the samples are brought back to the counting room, place the first sample in an upright position on a NaI(Tl) detector and count for 1 min.

(6) Repeat counting for samples 2 and 3 as in Step (5), making sure that each sample is counted exactly 3 min apart, or exactly the time between each sample is taken.

(7) On the basis of gross gamma counts, if all three sample counts are within ±5%, the last sample is selected for further detailed gamma-ray spectrometric analysis (see Section 9).

(8) If all the sample count rates are within ±10%, the highest activity sample is chosen for detailed analysis. If all the sample count rates are not within ±10%, a new set of samples should be taken for analysis.

(9) If the sample vial is not properly evacuated, or the sample vial after filling is still under partial vacuum, the activity concentration in the final analysis should be corrected for the actual sample gas volume (at 760 mm).

B.6 REFERENCES

(1) C. A. Bergmann and J. Roesmer, "Coolant Chemistry Effects on Radioactivity at Two Pressurized Water Reactor Plants," EPRI NP-3463 (March 1984).

(2) N. R. Large, et al., "Studies of Problems of Corrosion Product Sampling from PWR Primary Coolant," Water Chemistry of Nuclear Reactor System 5, Vol. 1, p. 63, BNES, London (1984).

(3) M. V. Polley and P. O. Andersson, "Study of the Integrity of Radioisotope Sampling From the Primary Coolant of Ringhals 3 PWR," ibid, p. 71, (1989).

(4) PWR Primary Water Chemistry Guidelines Committee, "PWR Primary Water Chemistry Guidelines: Revision 2," EPRI NP-7077, Final Report (November 1990).

Appendix C

GAMMA-RAY SPECTROMETRIC ANALYSIS

C.1 INTRODUCTION

The measurement of radioactivities by gamma-ray spectrometry using a high resolution solid state detector is the most frequently used technique in a nuclear power plant to monitor the radioactivity concentration in the reactor coolant as well as in the process effluents. The powerful computer has made the gamma-ray spectrometric analysis easier and faster, but some fundamentals which cannot be done by a machine should be carefully exercised. In this section some applications of gamma-ray spectrometric analysis in a nuclear power plant will be presented. More fundamental aspects of gamma-ray spectrometry can be found in the literature [1,2].

C.2 DETECTOR CALIBRATION

C.2.1 Standard Sources

(1) **Certified Radioactivity Source** – A NIST (National Institute of Standard and Technology), formerly National Bureau of Standards (NBS) standard source, or a calibrated radioactive source, with stated accuracy, whose calibration is certified by the source supplier as traceable to NIST, should be used in energy and efficiency calibrations.

The standard sources to be used in energy and efficiency calibrations should contain gamma-ray energies ranging from ~60 to ~2000 keV. A standard source may be a single nuclide with a single gamma-ray (e.g., Cs-137, Co-57) or multiple gamma rays (e.g., Co-60, Ba-133, Eu-152), or a mixture of many nuclides covering a good range of gamma-ray energies (e.g., NIST Standard SRM 4215-B). It is also important to note that the half-lives of the standards selected for routine calibration should be ~5 years or longer to minimize the error in decay correction. A list of commonly used standards is given in Appendix A, Nuclear Data.

(2) **Radioactivity Check Source** – a radioactive source, not necessarily calibrated but preferred to contain long-lived isotopes with both low and high-energy gamma rays (e.g., Eu-152), which should be used to confirm the continuing satisfactory operation of the counting instrument.

(3) **Radioactivity Source Strength** – a radioactive source selected as either a check source, or a calibration standard, should contain radioactivity high enough to produce a statistically reliable count rate in the full-energy gamma-ray peak of interest. However, it should be cautioned that when a source is counted at any distance from the detector, or in any geometry, the count rates should be low enough to reduce the effect of random summing of gamma rays to a level where it may be neglected. A better criterion may be the indication of counting system dead time when the source is placed at the counting position. Any source with ≥5% dead time should not be used in calibration at that position.

(4) **Physical Form of Standard Source** – the radioactive source can be in any physical form or size. However, the result of the calibration is applied to the same physical form and size of the standard used only (more discussion on source geometry in Section C.4.3).

C.2.2 Calibration Procedure

(1) **Energy Calibration** – Determine the energy calibration (channel number versus gamma-ray energy) of the detector system at a fixed gain by determining the full energy peak channel numbers from gamma rays emitted from one or more known energy standard sources. A linear correlation is normally obtained.

(2) **Efficiency Calibration** –

(a) Accumulate an energy spectrum using calibrated radioactivity standards at a desired and reproducible source-to-detector distance. At least 20,000 net counts should be accumulated in each full-energy gamma-ray peak of interest using Certified Radioactivity Standard Sources.

(b) Obtain the net count rate (total count rate of region of interest minus the Compton continuum count rate and, if applicable, the ambient background count rate within the same region) in the full energy gamma-ray peak, or peaks.

(c) Correct the peak net count rate for random summing, decay during counting and coincidence summing (see Section C.4) if applicable.

(d) Correct the standard source emission rate for decay to the count time.

(e) Calculate the full-energy peak efficiency E_γ as follows:

$$E_\gamma = \frac{C_\gamma}{N_\gamma}$$

where E_γ = full energy peak efficiency (counts per gamma ray emitted)

C_γ = net gamma ray count in the full energy peak (c/s)

N_γ = gamma ray emission rate (gamma rays per second)

If the standard source is calibrated as to activity, the gamma ray emission rate is given by

$$N_\gamma = AP_\gamma$$

where A = number of nuclear decays per second

P_γ = probability or intensity per decay for the gamma ray

(f) After obtaining the full energy peak efficiency for at least 10 gamma rays, spreading from ~60 to ~2000 keV, plot the values for full energy

peak efficiency versus gamma ray energy, or fit to an appropriate mathematical function.

(g) The expression or curve showing the variation of efficiency with energy must be determined for a particular detector with a particular source geometry, and must be checked for changes with time. The form of the calibration curve or function will be better defined by using more gamma ray standards, particularly in the ~60-300 keV region.

C.3 MEASUREMENT OF GAMMA RAY EMISSION RATE OF THE SAMPLE

(1) Place the sample to be measured at the source-to-detector distance for efficiency calibration.

(2) Accumulate the gamma-ray spectrum, recording the count duration.

(3) Determine the energy of the gamma rays present by use of the energy calibration curve.

(4) Obtain the net count rate in each full-energy gamma ray peak of interest as described in Efficiency Calibration.

(5) Determine the full-energy peak efficiency for each energy of interest from the curve or function obtained in Efficiency Calibration.

(6) Apply any sample geometric correction factors, if the sample is not in the same geometry as the calibrating standard.

(7) Calculate the number of gamma rays emitted per unit time for each full energy peak as follows:

$$N_\gamma = \frac{C_\gamma}{E_\gamma}$$

When calculating a nuclear disintegration rate from a gamma ray emission rate determined for a specific radionuclide, a knowledge of the gamma ray intensity per decay is required. That is,

$$A = \frac{N_\gamma}{P_\gamma}$$

C.4 CORRECTIONS OF COUNTING DATA

C.4.1 Decay Corrections

(1) Simple Decay Correction

The measured activities are corrected for the decay between the times of sampling and counting by using

$$A_o = Ae^{\lambda t}$$

where A = measured activity

A_o = activity at t=0

t = time between counting and t=0

λ = decay constant

Generally, the midpoint of the sampling and counting is used for decay correction if the sampling or counting duration is less than 1/3 of the decay half-life. When the sampling or counting duration is longer than 1/3 of the decay half-life, correction for the decay during counting or sampling should be applied (see below), and the end of sampling and the beginning of counting are used in decay correction.

(2) Correction for Decay During Counting and Sampling

If the value of a net count rate is determined by a measurement that spans a significant fraction of a half-life, and the value is assigned to the beginning of the counting period, a multiplicative correction factor, F, must be applied.

$$F = \frac{\lambda t}{1 - e^{-\lambda t}}$$

$$A_c = AF = A \frac{\lambda t}{1 - e^{-\lambda t}}$$

where F = correction factor

A = activity or 'average' counting rate during the counting period

A_C = activity at beginning of count (T=0)

T = duration of counting

λ = decay constant

The same correction factor is also used in correction for decay during sampling. In this case

$$A_T = A_m = \frac{\lambda T}{1 - e^{-\lambda T}}$$

where A_T = total activity collected in the sample

A_m = activity measured at end of sampling

T = duration of sampling

λ = decay constant

C.4.2 Coincident Photon Summing Correction

When another gamma ray or x-ray is emitted in cascade with the gamma ray being measured, in many cases a multiplicative coincidence summing correction C must be applied to the net full-energy-peak count rate if the sample-to-detector distance is 10 cm or less. Coincident summing correction factors for the primary gamma rays of Co-60 and Y-88 are approximately 1.09, 1.04, and 1.01 for a 65 cm^3 detector at 1 cm, 4 cm, and 10 cm sample-to-detector distances, respectively. The data for cascade-summing corrections for some major nuclides can be found in the literature[3].

Similarly, when a weak gamma ray occurs in a decay scheme as an alternate decay mode to two strong cascade gamma rays with energies that total to that of the weak gamma ray, a negative correction would be applied to the weak gamma ray. However, the correction factors may be negligible for most of the radionuclides observed in nuclear power plants.

C.4.3 Sample Geometry Calibration

The gamma-ray full energy peak efficiency is sensitive to the following counting geometry factors: (1) source-to-detector distance; (2) physical form of the source (gas, liquid, solid); and (3) size and shape of the source or source container (point source, filter papers of various sizes, charcoal cartridge, liquid bottles of various sizes, gas vials of various sizes, Marinelli beakers of various sizes). For most accurate results, the source to be measured must duplicate, as closely as possible, the calibration standards in all aspects. If this is not practical, appropriate corrections must be determined and applied. The methods of determining geometric correction factors and the preparation of standard source for various geometric calibration are described in Appendix D.

C.5 RESOLUTION OF A COMPOSITE DECAY CURVE

For a mixture of several independent activities, the result of plotting log A versus t is always a curve concave upward (convex toward the original). This curvature results because the shorter-lived components become relatively less significant as time passes. In fact, after sufficient time, the longest-lived activity will entirely predominate, and its half-life may be read from this late portion of the decay curve. Now, if this last portion, which

is a straight line, is extrapolated back to t=0 and the extrapolated line subtracted from the original curve, the residual curve represents the decay of all components except the longest-lived. This curve may be treated again in the same way, and in principle any complex decay curve may be analyzed into its components. In actual practice, experimental uncertainties in the observed data may be expected to make it difficult to handle systems of more than three components, and even two-component curves may not be satisfactorily resolved if the two half-lives differ by less than about a factor of two.

An example of reactor water sample containing N-13, F-18 and Cu-64 is given in Section C.9.

C.6 ACTIVITY DECAY-GROWTH CALCULATIONS

The parent-daughter decay-growth relationship, described in the following equations, is used in correction for activities which may grow into the sample from the decay of its parent nuclide:

$$A = \frac{\lambda_2}{\lambda_2 \lambda_1} A_1^{\circ} (e^{-\lambda 1 t} - e^{-\lambda 2 t}) + A_2^{\circ} e^{-\lambda 2 t}$$

or

$$A_2 = \frac{\lambda_2}{\lambda_2 - \lambda_1} A_1 [1 - e^{-(\lambda_2 - \lambda_1)t} + A_2^{\circ} e^{-\lambda 2 t}]$$

where A_1° = parent activity at time, 0,

A_1 = parent activity at time, t,

A_2° = daughter activity at time, 0,

A_2 = daughter activity at time, t.

If the sample is purified for the parent activity free from the daughter activity, then $A_1^\circ = 0$ at separation time. If the sample contains both daughter activities at sampling time, the activity A_2° is calculated by the following equation:

$$A_2^\circ = A_2\, e^{\lambda 2 t} - \frac{\lambda_2}{\lambda_2 - \lambda_1} A_1^\circ \left[e^{(\lambda_2 - \lambda_1)t} - 1\right]$$

The frequently observed activities requiring decay-growth calculations include Mo-99(Tc-99), Zr-95(Nb-95), and Cs-139(Ba-139).

C.7 IODINE ACTIVITY MEASUREMENTS*

(1) Place the sample on a shelf position at which the system dead time should be less than 5%. In order to obtain the best result, a sample should be counted several times similar to the following schedule:

Time After Sampling (hrs)	Count Time** (min)
0.5	10
1.0	10
2.0	20
5 - 10.0	20
10 - 24.0	20-60

It is important to count the sample as soon as the sample is prepared to measure the shorter-lived isotopes, I-134 and I-132, and to count the sample after most of the shorter-lived isotopes have decayed so that the lower intensity longer-lived isotope, I-131 can be measured accurately.

*The procedure for sample preparation is given in Appendix B.
**The count time may vary depending on the level of activity in the sample.

(2) The following gamma ray energies and intensities for five major iodine nuclides should be used in gamma ray spectrometric analysis:

Isotope	$T_{1/2}$	Gamma Ray 1 keV (%)	Gamma Ray 2 keV (%)
I-131	8.04 d	364.5 (81.2)	
I-132	2.28 h	667.7 (98.7)	772.6 (76.2)
I-133	20.8 h	529.9 (86.3)	
I-134	52.6 m	847.0 (95.4)	884.1 (65.3)
I-135	6.57 h	1260.4 (28.9)	1131.5 (22.5)

More complete decay characteristics of iodine isotopes and other nuclides are given in Appendix A.

C.8 OFFGAS SAMPLE ANALYSIS*

(1) Place the sample vial on a shelf position where the counting geometric factor, or the vial sample calibration, is available. The system dead time should not be higher than 5%.

(2) In order to obtain the best result, a sample should be counted several times similar to the following schedule.

Time After Sampling	Count Time** (min)
<10 min	5
20 min	5
1-2 hrs	10-20
2-5 hrs	10-20
10-24 hrs	20-60

* The sampling procedure is described in Appendix B.
** The count time may vary depending on the level of activity in the sample.

It is important to count the sample as soon as the sample is taken to measure the shorter-lived isotopes (Xe-138 and others), and to count the sample after most of the shorter-lived isotopes have decayed so that the lower intensity longer-lived isotope, Xe-133, can be measured accurately.

(3) The following gamma-ray energies and intensities for major nuclides in the offgas sample should be used in gamma ray spectrometric analysis:

Isotope	$T_{1/2}$	Gamma Ray 1 keV (%)	Gamma Ray 2 keV (%)	Gamma Ray 3 keV (%)
*Kr-85m	4.48 h	151.2(75.1)	304.9(13.7)	
*Kr-87	1.37 h	402.6(49.6)		
*Kr-88	2.84 h	196.3(26.0)	834.8(13.0)	1530(10.9)
Kr-89	3.15 h	220.9(20.0)	585.8(16.6)	
*Xe-133	5.24 d	81.0(38.3)		
Xe-133m	2.19 d	233.2(10.3)		
*Xe-135	9.10 h	249.8(90.2)		
Xe-135m	15.30 m	526.7(80.5)		
Xe-137	3.82 m	455.5(31.0)		
*Xe-138	14.10 m	258.3(31.5)	434.5(20.3)	1768.3(16.7)
N-13	9.97 m	511.0(199.6)		

More complete decay characteristics of noble gases and other nuclides are given in Appendix A.

*Nuclides used in fuel performance evaluations.

C.9 SPECTROMETRIC ANALYSIS OF THE NUCLIDES EMITTING 511 keV PHOTONS

The following nuclides have been identified to decay by emitting 511 keV photons (annihilation radiation) in a reactor coolant sample:

Nuclide	Half-Life	Photon Intensity	Associated Major Gamma-rays (keV) and Intensity
N-13	9.97 m	200%	–
F-18	109.8 m	193.5%	–
Na-24	15.0 m	~2%	1368.5 (100%)
Co-58	70.8 d	30.0%	810.8 (99.4%)
Cu-64	12.7 h	35.7%	1345.9 (0.5%)
Zn-65	243.8 d	2.8%	1115.5 (50.7%)

Among these nuclides, Zn-65, Co-58 and Na-24 are normally determined by their major gamma-rays at 1115 keV, 810 keV and 1368 keV, respectively. Their contribution to the 511 keV peak is generally small and can be easily estimated.

The easiest way to accurately measure the other three nuclides is to perform a simple cation-anion separation by using ion-exchange membranes (see Appendix B, Sampling Practices and Sample Preparation). F-18 is in the anion fraction, Cu-64 is on the cation fraction, and N-13 can be in either the cation or anion fraction (see Section 5.4). Both cation and anion fractions are counted separately for several times to follow the decay of activities. The sample should be counted as soon as possible so that the 10 min N-13 can be measured. The decay curves obtained from the 511 keV photopeak in each fraction can be easily constructed and graphically resolved into two components: 10 min N-13 and 110 min F-18 in the anion fraction, and 10 min N-13 and 12.7 hr Cu-64 in the cation fraction. Any tailing from the contribution from Zn-65, Co-58 and/or Na-24 in the cation fraction should be subtracted before analysis.

It should be pointed out that although there is a low intensity Cu-64 gamma ray at 1346 keV, it cannot be accurately measured in a gamma spectrum containing a mixture of numerous nuclides.

C.10 GOOD PRACTICES IN GAMMA RAY SPECTROMETRIC ANALYSIS

By using a high resolution solid-state detector with associated electronics and computer system, a complex spectrum may be analyzed. However, in many cases some nuclides could be misidentified if the sample contains two or more nuclides which emit photons of identical or similar energies. In other cases, the activity levels of some nuclides may be too low to be detected in a spectrum which is dominated by other high level activities. For the best results of analysis, the counting schedules for the offgas and iodine (anion fraction) have been recommended in Sections C.7 and C.8. Similar counting schedules may be developed for the insoluble and cation fractions.

A well-trained radiochemist should be able to exercise the following practices to obtain the best analysis of the sample (more nuclides are measured accurately):

(1) Make sure the updated nuclear data (Appendix A) are used in gamma-ray spectrometric analysis.

(2) Always count the sample at an appropriate distance from the detector so that good counting statistics are obtained at the lowest counting dead time. Always apply the geometric correction factors, if needed.

(3) Always examine the spectrum to see for any energy shift and/or poor gamma peak resolution, which may lead to misidentification of nuclides.

(4) Search for the expected gamma rays which may be missing due to energy shift or interference from high intensity gamma rays, particularly in high-energy regions.

(5) For a nuclide with more than one major gamma ray, compare the activities calculated from two or three different gamma rays.

(6) Determine what can be done in order to obtain the best analysis of the sample (more nuclides are measured accurately).

(7) The decay of activities in the sample should be followed by counting the sample several times over a period of a few hours or approximately a week, depending on the half-lives of the activities, so that (a) activities of the nuclides with identical gamma energy, but different half-lives, can be calculated by resolving a composite decay curve (Section C.5), and (b) the longer-lived and low intensity activities can be measured after most of the shorter-lived nuclides have decayed away.

(8) Chemical separation in sample preparation (Appendix B) should always be considered, if necessary, as an ultimate method for measuring the low-level activities.

C.11 DATA PROCESSING FOR FISSION PRODUCT RELEASE CHARACTERISTICS

(1) Calculate the measured individual nuclide concentrations at the sampling time. Use the concentration units recommended in Section 2.2.

(2) Correct the concentration values for counting geometry and (see Appendix D) and sample line delay, if necessary.

(3) Calculate the activity release rate by:

(a) multiplying the off-gas flow rate for the off-gas sample, or

(b) Using Equation 3-21 for the iodine activities in the BWR coolant, or Equation 3-34 for the iodine activities in the PWR coolant.

(4) Convert the activity release rate values in μCi/s to fission/s and characterize the fission product release patterns according to the procedures described in Section 3.

(5) For a step by step instruction, the reader is referred to a procedure described by H.R. Helmholz[4].

C.12 REFERENCES

(1) American National Standard, "Calibration and Usage of Germanium Detectors for Measurement of Gamma-Ray Emission of Radionuclides," ANSI N41.14-1978.

(2) "A Handbook of Radioactivity Measurements Procedures," second edition NCRP Report No. 58, NCRP (1985).

(3) F. J. Schima and D.D. Hoppes, Int. J. Appl. Rad. Isot., 34, 1109 (1983).

(4) H.R. Helmholz, "Chemistry Measurement Methods and Data Interpretation", Appendix A to "Failed Fuel Action Plant Guidelines", EPRI NP-5521-SR (November 1987).

Appendix D

COUNTING GEOMETRIC CORRECTIONS IN GAMMA-RADIATION MEASUREMENTS

D.1 INTRODUCTION

The gamma-ray full energy peak efficiency is sensitive to the following counting geometry factors: (1) source-to-detector distance; (2) physical form of the source (gas, liquid, solid); and (3) size and shape of the source or source container (point source, filter papers of various sizes, charcoal cartridge, liquid bottles of various sizes, gas vials of various sizes, Marinelli beakers of various sizes). For most accurate results, the source to be measured must duplicate, as closely as possible, the calibration standards in all aspects. If this is not practical, appropriate corrections must be determined and applied. The preparation of standard sources for various geometric calibration, and the methods of determining geometric correction factors are described in this procedure.

D.2 STANDARD SOURCES

(1) NIST or certified point source containing appropriate standard radioactivities.

(2) NIST or certified liquid source containing appropriate standard radioactivities.

(3) Some standard sources in various forms may be commercially available from the NIST, Analytics, Inc., and other vendors.

D.3 CALIBRATION FOR LIQUID SAMPLES

(1) Use a calibrated micropipette for transferring the standard solution.

(2) Carefully weigh a dry and clean micropipette in an analytical balance to the nearest 0.1 mg.

(3) Evenly distribute the solution on the encircled area of the paper. Care must be exercised to deliver the solution in very small droplets.

(4) After the paper is air dried, cover the entire filter paper with plastic wrap.

(5) The disc source should be checked for its activity content and the uniformity of activity distribution on the surface area by the following two methods:

(a) The activity content in the disc source is calibrated by counting the source at a position 30 cm away from detector where the effect of size variation is negligible. The measured activity is compared with a certified standard point source counted at the same position.

(b) The uniformity of activity distribution is checked by counting the disc source at 1 cm from the detector. The disc source is first counted at the position slightly away from the center of the detector. Repeat counting the disc source at the same center position with the disc turned around 30° and 180°. The measured activity should be consistent within ±5%.

(6) By using the disc standard source, a series of calibration curves can be obtained at various distances from the detector.

D.4.2 Calibration by a Point Source

Alternatively, a standard point source is counted at the same positions, and the correction factors for a disc source (relative to a point source) can be calculated. The method (similar to that reported in Ref. 1) to determine the correction factor is described below:

(1) Using a single gamma-ray point source (e.g., Cs-137) counts from the source placed on a calibrated shelf are obtained at 0.2 cm intervals, starting from the center of the detector and proceeding to the front and back.

(2) The data points (count rate at a distance, R, from the center) are fitted to a polynominal function:

$$f(R) = 1.0 + aR + bR^2 + cR^3 + dR^4 + eR^5 + \ldots .$$

(3) The count rate of a disc source relative to the count rate of a point source with the same amount of activity can be estimated by

$$F(R) = \frac{\int_0^{2\pi}\int_0^{R} f(R)R\,dR\,d\theta}{\int_0^{2\pi}\int_0^{R} R\,dR\,d\theta} = 1 + \frac{2}{3}aR + \frac{2}{4} + bR^2 + \frac{2}{5}cR^3 + \frac{2}{6}dR^4 \ldots .$$

D.5 CALIBRATION FOR GAS SAMPLES

A 14.1 mL glass vial is a standard sample container for the offgas samples. A larger size glass vial (e.g., 100 mL, or a Marinelli container) may also be used to obtain the offgas and stack gas samples, if needed.

The calibration method is based on a publication given in Reference 2, in which Vermiculite is used as a "weightless" supporting material for radioactivities.

(1) An aliquot of known standard solution is diluted to an appropriate volume (~3 mL for a 14 mL vial and the volume may be proportionally increased for a larger volume container) with water in a beaker.

(2) Pour the diluted standard solution over a pre-measured amount (to fill the sample container exactly) of Vermiculite in another beaker. The empty beaker is rinsed twice with ~1 mL water and each time the rinse water is added to Vermiculite.

(3) The wet Vermiculite is dried in air, mixed gently, and transferred to the sample container. Effort should be made to have the Vermiculite containing activity homogeneously mixed and tightly packed in the container.

(4) Wash the beaker and measure the activity that is not transferred with Vermiculite.

(5) Measure the activity at various positions from the detector, and a series of calibration curves can be obtained directly.

(6) Alternatively, a standard point source can be counted at the same positions, and a series of correction factors (relative to a point source) can be calculated.

D.6 CALIBRATION FOR CHARCOAL (OR Ag-ZEOLITE) CARTRIDGES

The calibration procedure is similar to that described in Section D.5, except Vermiculite is replaced with charcoal or Ag-Zeolite granular material. The calibration data obtained are applicable only for the activities homogeneously distributed in the cartridge. For an actual sample, the activity is generally not homogeneously distributed in the cartridge, and it is impractical to open the cartridge and manually mix the granular materials each time the sample is counted.

Alternatively, the cartridge sample is counted twice, with one side facing up and down, and an average count rate is obtained for activity calculation.

If a sample is counted at a close distance, ≤3 cm, an average count rate may differ significantly from a sample with homogeneous activity distribution. An appropriate correction may be empirically obtained by the following method:

(1) Obtain a number of actual samples with various sample flow rates and sampling duration. It is expected that the penetration of airborne activity in a cartridge may be different at different flow rates and sampling duration.

(2) Count the sample cartridge twice, with face up and down, and obtain an average count rate.

(3) Open the cartridge, thoroughly mix the solid adsorbent, and re-pack the materials into the cartridge.

(4) Count the sample again at the same position, and compare the count rate with the previously obtained average count rate. A necessary correction factor can be calculated.

D.7 REFERENCES

1. R. G. Helmer, Int. J. Appl. Rad. Isot., 34, 1105 (1983).

2. C. C. Lin, Int. J. Appl. Rad. Iso., 32, 657 (1981).

Appendix E

SELECTED RADIOCHEMICAL PROCEDURES

E.1 DETERMINATION OF RADIOACTIVE IODINE IN WATER

E.1.1 Principle

Iodine is separated from the other radioactive species by extraction into carbon tetrachloride. Before this extraction is made, a complete interchange must be affected between the added iodine carrier and the tracer iodine present in the sample. The carrier iodide (I^-) is oxidized to periodate (IO_4^-) in alkaline solution by NaOCl. The IO_4^- is reduced to I_2 by hydroxylamine hydrochloride ($NH_2OH \bullet HCl$) and extracted into CCl_4. The I_2 is back-extracted by reduction to I^- with $NaHSO_3$. Iodide is then precipitated as silver iodide for chemical yield measurement and radioactivity counting.

E.1.2 Reagents

CCl_4 (Note 1)
Ethyl alcohol, 95%
HNO_3, concentrated
Iodine carrier, 10.0 mg I^-/mL (Note 2)
NaOH, 5M
NaOCl, 5%
HN_2OH HCl, 1 M
$NaHSO_3$, 0.5 M
$AgNO_3$, 0.1 M

E.1.3 Procedure

a. In a 250 mL separatory funnel containing 100 mL water sample (Note 3), add 2 mL of I^- carrier solution, 2 mL of NaOH, and 4 mL of NaOCl. Shake funnel for 2 minutes.

b. Add 50 mL of CCl_4, 4 mL of 1M NH_2OH HCl and 3 mL of conc. HNO_3.

c. Shake the funnel for 2 minutes, and allow phases to separate.

d. Transfer CCl_4 to a 125 mL separatory funnel. Add 20 mL water containing a 1 mL conc. HNO_3 and shake for 2 minutes. Allow phases to separate.

e. Transfer CCl_4 to a clean 125 mL separatory funnel containing 20 mL H_2O. Add, dropwise, 0.5 M $NaHSO_3$. Shake until the purple color in CCl_4 disappears. Allow phases to separate (Note 4).

f. Transfer the aqueous phase to a 40 mL centrifuge cone. Add 0.5 mL conc. HNO_3 and 2 mL of 0.1 M $AgNO_3$.

g. Stir and heat the solution in a hot water bath for ~5 minutes.

h. Filter the AgI precipitate onto a tared No. 542 Whatman paper. Wash with water and alcohol.

i. Dry the sample in an oven at 115°C for 15 minutes.

j. Cool, weigh and mount for activity measurement.

k. Follow the procedure described in Appendix C.1 for gamma spectrometric analysis of iodine activities.

Notes:

(1) 1,1,1-trichloroethane or cyclohexane can be used in place of CCl_4.

(2) Iodide carrier should be prepared monthly in slightly basic solution to prevent air oxidation.

(3) The sample size may vary, depending on the activity concentration in the sample. If 20 mL or less sample is used, the sample is diluted with appropriate volume of water.

(4) If further purification is desired, discard the organic phase. Add 20 mL of CCl_4, 1 mL of conc. HNO_3, and 2 mL of 1M $NaNO_2$. Repeat the procedure starting at Step C.

E.1.4 References

(1) "Standard Test Methods for Radioactive Iodine in Water", D2334, ASTM Standards, Part 31.

(2) L.E. Glendenin and R.P. Metcalf, "Radiochemical Studies of the Fission Products", Book 3, p. 1625, National Nuclear Energy Series.

E.2 DETERMINATION OF STRONTIUM-89/90

E.2.1 Principle of Analysis

Chemical separation of strontium from other fission and corrosion products involves precipitations of $SrCO_3$ and $Sr(NO_3)_2$. The gross activities of purified Sr-89 and Sr-90 are first measured. Yttrium-90 is then allowed to grow into the strontium sample, and at a later time, the Y-90 activity is separated and measured. The Sr-90 activity is calculated from the Y-90 activity, and the Sr-89 activity is calculated from the difference between the total Sr-89 and Sr-90 activities measured and the calculated Sr-90 activity. A general scheme of analysis is shown below:

(1) Chemical separation for Sr-89 and Sr-90. Record time of separation, t_1.
(2) Mount $SrCO_3$ and count immediately.
(3) Hold $SrCO_3$ for at least 10 days for Y-90 growth.
(4) Milk Y-90 from $SrCO_3$ and record time of separation, t_2.
(5) Mount Y_2O_3 and count Y-90 activity at t_3.
(6) Recount Y_2O_3 for a 64.1 hr half-life decay to check purity of separation.
(7) Calculate Sr-90 activity from Y-90 activity.
(8) Calculate Sr-89 activity from total and Sr-90 activities.

The following three procedures are described:

(1) Strontium separation
(2) Yttrium separation
(3) Preparation of counting efficiency curves for Sr-89, Sr-90 and Y-90.

E.2.2 Strotium Separation

(1) Reagents

Sr carrier (10.0 mg/mL)
Cs scavenger carrier (10 mg/mL)
Co scavenger carrier (10 mg/mL)
Mn scavenger carrier (10 mg/mL)
Fe scavenger carrier (10 mg/mL)
Ba scavenger carrier (10 mg/mL)
La scavenger carrier (10 mg/mL)
Conc. HNO_3
Conc. NH_4OH
3N or 6N HCl
Sat. Na_2CO_3
Fuming HNO_3
$K_2Cr_2O_7$, 10% solution
Ice bath

(2) Procedure

a. Obtain the water sample directly or the leaching solution from cation membranes.

b. Add 2.0 mL Sr carrier, and 4 drops each of Co, Cs, Mn, and Ba scavenger carrier to 100 mL sample in a 250 mL beaker. (Note: If the sample volume is less than 25 mL, use a 40 mL cone and omit the next step.)

c. Add 5 mL of conc. HNO_3 and boil down to ~10 mL. Transfer solution to a 40 mL cone with H_2O.

d. Add 2 mL 10% $K_2Cr_2O_7$ and conc. NH_4OH until solution is basic. Check with pH paper.

e. Centrifuge and discard ppt.

f. Add sat. Na_2CO_3 to solution to ppt. $SrCO_3$.

g. Centrifuge and discard supernate.

h. Wash $SrCO_3$ with 20 mL H_2O and centrifuge and discard supernate.

i. Add 20 mL of fuming HNO_3 and place in ice bath for 10 minutes.

j. Centrifuge and discard fuming HNO_3.

k. Add 20 mL H_2O to dissolve $Sr(NO_3)_2$ and add 6 drops of Fe scavenger carrier.

l. Add conc. NH_4OH to ppt. $Fe(OH)_3$.

m. Centrifuge and discard ppt.

n. Add sat. Na_2CO_3 to the supernate to ppt. $SrCO_3$.

o. Repeat steps (g.) through (m.) and go to step (p.).

p. Filter supernate through Whatman 41. Record time of separation.

q. Add sat. Na_2CO_3 to filtrate to form $SrCO_3$.

r. Filter through Whatman 542 (tare) and wash with 10 mL of H_2O and final rinse with 5 mL of acetone.

s. Dry in oven 110°C for 15 minutes. Cool in desiccator for 10 minutes and weigh. Cover sample with 1/4 mil Mylar.

t. Count the β activity in the sample immediately.

E.2.3 Separation of Yttrium-90

(1) Reagents

Y carrier (10.0 mg/mL)
HNO_3 - concentrated
HCl - concentrated and 6N
HF - concentrated
NH_4OH - concentrated
$AgNO_3$ - 0.1M
$(NH_4)_2C_2O_4$ - saturated
Methyl Alcohol
H_3BO_3 - saturated

(2) Procedure

a. Allow the purified strontium sample to decay for ≥ 10 days.

b. Pipet 2 mL Y carrier, 3 mL conc. HNO_3, and 10 mL H_2O into a 40 mL cone.

c. With a scalpel, cut through the Mylar and around the Whatman 542 filter paper containing the purified strotium sample. Place Mylar, sample, and filter paper into the cone that contains the carrier and mix well.

d. Add 10 drops of 0.1M $AgNO_3$ and 1 mL conc. HCl and heat to boiling.

e. Centrifuge and discard filter paper, Mylar, and ppt.

f. Add 3 mL conc. HF to the solution and mix. Centrifuge and discard supernate.

g. Wash YF_3 ppt. with 10 mL H_2O. Centrifuge and discard washing. (Note: Record separation time.)

h. Add 2 mL sat. H_3BO_3 and mix well. Add 2 mL conc. HNO_3 and 10 mL H_2O. Place in hot bath for 10 minutes. [Note: If solution appears turbid, centrifuge and discard sediment (AgCl).]

i. Add 5 mL conc. NH_4OH and mix well. Centrifuge and discard supernate.

j. Wash $Y(OH)_3$ with 10 mL H_2O. Centrifuge and discard washing.

k. Dissolve $Y(OH)_3$ with 5mL 6N HCl and 15 mL H_2O and place in hot bath for 5 minutes.

l. Add 20 mL $(NH_4)_2C_2O_4$ mix and place in hot bath for 5 minutes. [Note: If a white ppt. does not form after addition of $(NH_4)_2C_2O_4$, add a few drops of conc. NH_4OH and mix.]

m. Chill in ice bath for 5 minutes. Filter onto a Whatman 542 and place in a porcelain crucible and ignite at 1000°C for 60 minutes.

n. Cool to room temperature and grind the ppt. (Y_2O_3) to a fine powder with a stirring rod.

o. With the aid of methyl alcohol, transfer the Y_2O_3 powder to a tared filter paper #542 Whatman.

p. Oven dry at 110°C for 20 minutes. Cool in a desiccator for 10 minutes and weigh.

q. Cover sample with 1/4 mil Mylar and count.

r. Recount the sample in 1 to 2 weeks and check for a 64.1 hr half-life decay, checking purity of separation.

E.2.4 Preparation of Counting Efficiency (Self-Absorption) Curves

(1) Self-absorption Curve for Sr-89

a. Pipet 25.0 mL of Sr carrier and appropriate amount of Sr-89 standard into a 125 mL erlenmeyer flask that contains a magnetic stirring rod.

b. Place erlenmeyer flask on a magnetic stirring plate and stir solution gently.

c. Add conc. NH_4OH until solution is just basic.

d. Add sat. Na_2CO_3 to ppt. $SrCO_3$.

e. Pipet desired volumes of slurry into the tower of a Millipore glass filter holder that contains 10 mL H_2O. (A minimum of 10 samples with varying amounts of slurry should be prepared.)

f. Wash ppt. with 5 mL of H_2O and rinse with 5 mL acetone. Oven dry at 110°C for 15 minutes. Cool in a desiccator for 10 minutes and weigh.

g. Cover samples with 1/4 mil Mylar and count.

h. Calculate the counting efficiency for each sample.

i. Plot counting efficiency vs. sample weight. (see Figure E-1)

(2) Self-absorption Curve for Sr-90

a. Pipet 25.0 mL Sr carrier and appropriate amount of Sr-90 standard into a 40 mL centrifuge cone. Mix.

b. Add 1 mL Y carrier and mix.

c. Add conc. NH_4OH dropwise to ppt. $Y(OH)_3$.

d. Centrifuge and then add 1 drop of conc. NH_4OH to supernate to ascertain completion of $Y(OH)_3$.

e. Decant the supernate to a clean cone and adjust the pH to less than 7 with conc. HNO_3.

f. Repeat steps (b.) through (e.), then go to step (g.).

g. Filter the supernate through Whatman 41 into a clean cone.

h. Add sat. Na_2CO_3 to ppt. $SrCO_3$. Centrifuge and discard the supernate.

i. Wash ppt. with 20 mL H_2O and centrifuge, discarding the washing. (Note: Record time for separation time for Sr-90.)

j. Dissolve the $SrCO_3$ in a minimum amount of 4N HNO_3 and transfer the solution into a 125 mL erlenmeyer flask.

k. Add H_2O to make a total volume of 100 mL and place a magnetic stirring rod into the flask.

l. Place the flask on a magnetic stirring plate and stir solution gently.

m. Add conc. NH_4OH until solution is just basic.

n. Add sat. Na_2CO_3 to ppt. $SrCO_3$.

o. Using a transfer pipette and a syringe, pipet desired volume of slurry into the tower of a Millipore that contains about 10 mL of H_2O. (A minimum of 10 samples with varying amounts of slurry should be prepared.)

p. Wash ppt. with 5 mL of H_2O and rinse with 5 mL acetone. Oven dry at 110°C for 15 minutes. Cool in a desiccator for 10 minutes and weigh.

q. Cover samples with 1/4 mil Mylar and count.

r. Calculate the counting efficiency for each sample.

s. Plot counting efficiency vs. sample weight. (see Figure E-1)

(3) Self-absorption Curve for Y-90

a. Pipet 25.0 mL of Y carrier and appropriate amount of Sr-90 standard into a 40 mL centrifuge cone. (Note: Complete steps b. through h. within 30 minutes.)

b. Add ~8 mL conc. NH_4OH to ppt. $Y(OH)_3$. Centrifuge and discard supernate.

c. Wash $Y(OH)_3$ with 25 mL H_2O and thoroughly mix with stirring rod. Centrifuge and discard supernate.

d. Add 4 mL conc. HNO_3 to dissolve $Y(OH)_3$, then add 2 mL of Sr carrier and mix well.

e. Add 20 mL of fuming HNO_3 and place in ice bath for 5 minutes to form $Sr(NO_3)_2$. Centrifuge and discard $Sr(NO_3)_2$.

f. Add 1 mL of Sr carrier to supernate and mix. Place in ice bath for 5 minutes to form $Sr(NO_3)_2$.

g. Centrifuge and discard $Sr(NO_3)_2$. Record time for Y-90 decay.

h. Add 2 mL of conc. HF to supernate to form YF_3. Centrifuge and discard supernate.

i. Wash YF_3 with 20 mL H_2O. Mix thoroughly with stirring rod. Centrifuge and discard washing.

j. Add 10 mL sat. H_3BO_3 and mix well. Add 5 mL conc. HNO_3 to dissolve YF_3.

k. Add ~10 mL conc. NH_4OH to ppt. $Y(OH)_3$. Centrifuge and discard supernate.

l. Wash $Y(OH)_3$ with 10 mL of H_2O. Centrifuge and discard washing.

m. Add 2 mL sat. H_3BO_3 and 3 mL conc. HNO_3 to dissolve $Y(OH)_3$. Mix well.

n. Add 10 mL H_2O and heat in hot bath for 10 minutes.

o. Add 10 mL of sat. ammonium oxalate and reheat in hot bath for 5 minutes.

p. Chill sample in ice bath for 10 minutes.

q. Filter the solution through a Whatman 41 filter paper and wash ppt. with 15 mL H_2O, with final rinse with 10 mL of acetone.

r. Place filter paper in a porcelain crucible and heat under a heat lamp for 5 minutes. Then place in furnace at 1000°C for 60 minutes to form Y_2O_3.

s. Cool to room temperature and, with a glass stirring rod, grind the ppt. to a fine powder.

t. Transfer the powder to a 125 mL erlenmeyer flask (that contains a magnetic stirring bar) with methyl alcohol. Make up total volume to ~100 mL with methyl alcohol.

u. Gently stir the solution. Pipet desired volumes of slurry to a tare filter paper #542 and wash with 5 mL methyl alcohol. (A minimum of 10 samples with varying amounts of slurry should be prepared.)

v. Oven dry at 110°C for 20 minutes, cool in a desiccator for 10 minutes and weigh. Cover sample with 1/4 mil Mylar and count. Follow decay on one sample for two weeks to check purity of separation.

w. Calculate the counting efficiency for each sample.

x. Plot counting efficiency vs. sample weight. (see Figure E-1)

E.2.5 Calculations

$$^{90}\text{Y dpm at } t_2 = (^{90}\text{Y cpm})\ (e^{\lambda_2(t_3-t_2)})\ (\text{c.y.f.})/(\text{eff. for } ^{90}\text{Y})$$

$$^{90}\text{Sr dpm/mL at } t_1 = \frac{^{90}\text{Y dpm}}{[1-e^{-\lambda_2(t_2-t_1)}]}\ (\text{c.y.f. of Sr})/\text{mL of sample}$$

$$^{89}\text{Sr dpm/mL} = \frac{\left[\frac{(\text{cpm}\ ^{89}\text{Sr}+^{90}\text{Sr})\ (\text{c.y.f. of Sr})}{\text{mL of sample}}\right] - [^{90}\text{Sr (dpm/mL)}\ (^{90}\text{Sr eff.})]}{^{89}\text{Sr eff.}}$$

where

t_1 = strontium separation time (sample contains ^{89}Sr, ^{90}Sr, but no ^{90}Y)

t_2 = ^{90}Y separation time

t_2-t_1 = time allotted for ^{90}Y ingrowth

t_3 = ^{90}Y count time

c.y.f. = chemical yield factor, $\frac{100}{\%\ \text{yield}}$

eff = counting efficiency (see Figure E-1)

E.2.6 Reference

(1) H.L. Krieger and S. Gold, "Procedures for Radiochemical Analysis of Nuclear Reactor Aqueous Solutions", EPA-RA-73-014, US BPA, May 1973.

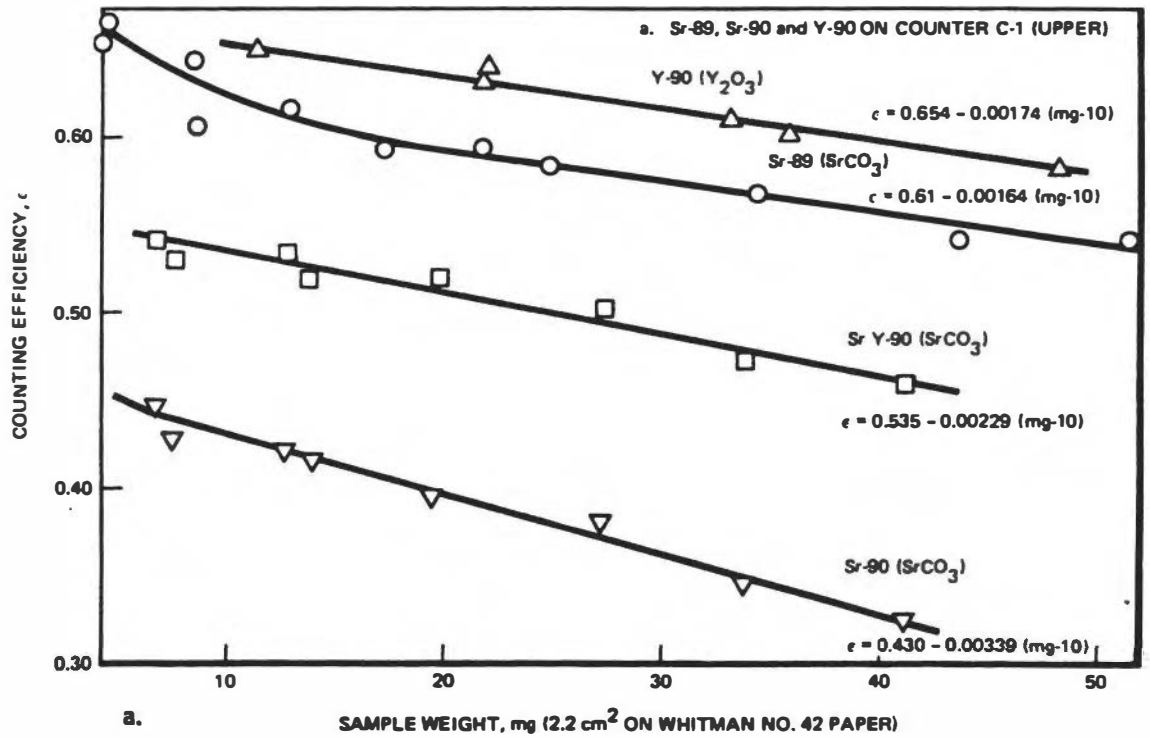

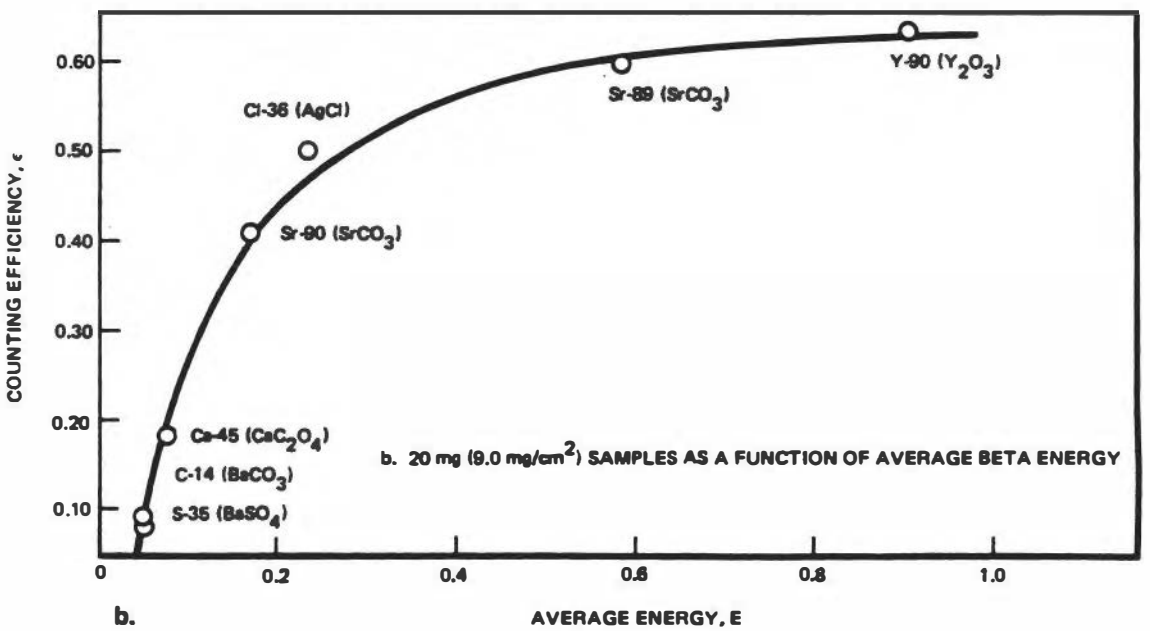

Figure E-1 Counting Efficiency Curves of Beta Activities Using WIDEBETA II

E.3 DETERMINATION OF IRON-55

E.3.1 Principle of Analyses

This procedure is to determine the Fe-55 content in the presence of Fe-59 in water or solid samples. Iron isotopes Fe-55 and Fe-59 are separated from fission and corrosion products by ion exchange and organic extraction. The organic phase is then transferred into a counting vial containing toluene base scintillator cocktail. The sample is counted with a liquid scintillation detector.

E.3.2 Separation and Purification Procedures

(1) Reagents

Fe carrier (10.0 mg/mL)
Co, Cs, Mn, Cr hold-back carrier (~10 mg/mL)
HCl - concentrated, 1N, 6N, 9N
NaOH - 1N and 3N
NH_4OH - concentrated
Anion resin - AG 1x10 50-100 mesh in chloride form
Bis(2-ethylhexyl) Hydrogen Phosphate
Toluene
Buffer solution - pH 2.2

1. Dissolve 14.9 gm KCl in 1000 mL H_2O, label as 0.2M KCl
2. Dilute 16.5 mL of conc. HCl to 1000 mL of H_2O and label as 0.2N HCl
3. Mix 500 mL of 0.2M KCl with 78 mL of 0.2N HCl for buffer solution

Analytical Ash-free filter pulp
Isopropyl ether
Liquid scintillation cocktail (POPOP solution)

(2) Separation Procedure

a. Pipet 250λ of Fe carrier, add 4 drops each of Co, Cs, Mn, Cr, hold back carrier in a 1-L beaker containing 500 mL water sample. (Note: If the sample is a solution from solid, or filter paper dissolution, use 20 mL sample solution and add all carrier as specified above. Continue on step g.)

b. Add 10 mL of conc. HCl to sample and mix well and heat to near boiling.

c. Add conc. NH_4OH until solution is basic to precipitate $Fe(OH)_3$.

d. Warm the solution and allow the precipitate to settle.

e. Cool solution to room temperature, then carefully decant the clear solution as much as possible, or until about 30 mL slurry remaining.

f. Carefully transfer the slurry to a 40 mL centrifuge tube. Rinse the beaker with 5 mL H_2O and add the rinse to the centrifuge tube. Continue on step h.

g. If a smaller size sample is used, add conc. NH_4OH to precipitate $Fe(OH)_3$.

h. Centrifuge and discard the supernate.

i. Wash the precipitate with 20 mL water containing a few drops of NH_4OH. Centrifuge and discard the supernate.

j. Add 6N HCl to dissolve the precipitate.

k. Quantitatively transfer the dissolved Fe into a 50 mL flask. Use 6N HCl to complete the transfer to 50 mL volumetric flask. DO NOT USE ANY WATER.

l. Pipet 1 mL for Fe analysis by A.A. for 100% yield.

m. After pipetting 1 mL for Fe analysis, add 1 drop of Co, Cs, Mn, Cr carrier directly into flask and mix well.

n. Transfer the entire solution to a preconditioned anion column which has been rinsed with 6N HCl.

o. After loading the column, rinse column with additional 15 mL 6N HCl.

p. Upon completion of 6N HCl rinse, add 25 mL H_2O.

q. Continue to allow the effluent to drip into a waste beaker. CAREFULLY watch for the yellow effluent and collect only THIS effluent into a 40 mL centrifuge tube.

(3) Fe-Purification

a. Dilute the solution to ~10 mL. Add conc. NH_4OH to precipitate $Fe(OH)_3$.

b. Centrifuge and discard the supernate.

c. Dissolve the precipitate in 10 mL of 9N HCl and extract the iron with 10 mL of isopropyl ether in a 50 mL separatory funnel.

d. Separate the phase and discard the aqueous phase.

e. Back extract with ~8 mL H_2O and transfer the aqueous phase into a 10 mL volumetric flask.

f. Add H_2O to make up total volume and mix well.

g. Pipet 1 mL for Fe analysis to determine chemical yield by A.A.

h. Pipet 5 mL to a centrifuge tube and add 5 mL Buffer solution.

i. Add 1N or 3N NaOH dropwise to adjust to pH 2. Check with pH paper. (Note: Adjusting to pH 2 is a critical step. This will insure 100% extraction into organic.)

j. Add 5 mL of 50% bis(2-ethylhexyl)hydrogen-phosphate and SHAKE for 30 seconds.

k. Transfer organic layer to a 12 mL conical centrifuge cone with the aid of a transfer pipet.

l. Centrifuge for 2 minutes at medium rpm.

m. Transfer the organic layer with a pipet to a counting vial that contains 10 mL liquid scintillation cocktail solution.

n. Shake for 5 seconds and allow to stand for 12 hours before counting in a liquid scintillation counter.

o. Using the calibrated counting efficiency to calculate the Fe-55 activity content (see below).

p. Using the same sample, determine the Fe-59 activity content with a gamma-ray spectrometer.

E.3.3 Standard Calibration and Radioactivity Measurement

(1) Prepare a standard calibration curve as follows:

a. Pipet various known amounts (50λ to 5000λ) of Fe carrier to several culture tubes.

b. Pipet 100λ of Fe-55 standard into each tube.

c. Pipet 5 mL of pH 2.2 buffer into each tube.

d. Add 3N or 1N NaOH dropwise to adjust to pH 2. Check with pH paper.

e. Add 5 mL of 50% bis(2-ethylhexyl)hydrogen phosphate and SHAKE for 30 seconds.

f. Allow culture tube to stand for 5 minutes in rack for organic layer to separate.

g. Transfer the organic layer (upper) to a 12 mL conical cone (use a transfer pipet) and centrifuge for 2 minutes at medium rpm.

h. Transfer the organic layer to a counting vial containing 10 mL liquid scintillation cocktail.

i. Shake well and store in a dark area for 12 hours before counting in a liquid scintillation detector with appropriate energy discrimination settings.

(**Note**: The energy discrimination settings are determined by using pure Fe-55 and Fe-59 isotopes separately in the counting samples. The lower energy channel should include most of the Fe-55 counting but minimizing the interference from Fe-59 which is counted in the higher energy channel.)

j. Calculate the Fe-55 counting efficiency from each standard sample and prepare a calibration curve of % eff. Fe-55 vs. external standard ratio (ESR).

(2) For the analytical samples count the sample in the predetermined energy channel. Obtain the count rate and the ESR from the calibration curve. The counting efficiency for the sample is estimated and the activity content in the sample is calculated.

E.3.4 Reference

(1) S.E. Graber, et al, J. Lab. Clin. Med. G9, 170 (1967).

E.4 DETERMINATION OF NICKEL-63

E.4.1 Principle of Analyses

Nickel-63 is separated from fission and corrosion products by anion ion-exchange resins and organic extractions. Nickel-63 is purified in chloroform as nickel dimethylglyoxime and back extracted with dilute HCl and then complexed with ammonium thiocyanate and precipitated with pyridine. Nickel precipitate is then dissolved in cocktail for counting with a liquid scintillation counter.

E.4.2 Separation and Purification

(1) Reagants

Ni carrier (10.0 mg/mL)
Fe, Co, Cs, Mn hold-back carrier (~10 mg/mL)
HCl - 6N concentrated
NaOH - 1N
NH_4OH - concentrated
Anion resin - AG 1x10 50-100 mesh chloride form
Dimethylglyoxime - 1% solution in Ethanol
Liquid scintillation (POPOP solution) cocktail
Toluene
Chloroform
Analytical filter paper pulp - Ash free
Pyridine
NH_4SCN 1% solution + Pyridine 1% solution = rinse solution
NH_4SCN - 20% solution
HAC - 1N
Alconex - 0.25%

(2) Separation Procedure

a. To 500 mL of water sampled in a 1-L beaker, add 500λ of Ni carrier, 4 drops each of Cs, Fe, Co and Mn hold-back carrier, and 3 mL conc. HCl. (Note: If the sample is a solution from filter dissolation, use only 20 mL sample in a 40 mL centrifuge tube. Add all the carriers as specified above and continue on step g.)

b. Heat the solution to near boiling.

c. Slowly add 100 mL of 1N NaOH. Stir and warm the solution for about 10 min.

d. Chill sample in ice bath to room temperature.

e. Allow the precipitate to settle and carefully decant the clear solution as much as possible, or until ~30 mL slurry remains in beaker.

f. Carefully transfer the slurry to a 40 mL centrifuge tube. Use 5 mL 1N NaOH to rinse the beaker and add the rinse to the centrifuge tube. Continue on step h.

g. If smaller size sample is used, add enough 6N NaOH to precipitate the Ni carrier. Stir and warm the solution for about 10 minutes.

h. Centrifuge to separate the precipitate. Discard the supernate.

i. Rinse the precipitate with 10 mL 1N NaOH. Centrifuge again and discard the supernate.

j. Dissolve the precipitate with conc. HCl and quantitatively transfer the solution to a 50 mL volumetric flask using conc. HCl to complete the transfer. DO NOT USE ANY WATER.

k. Add 2 drops of Co and Mn carrier, make up to final 50 mL by adding conc. HCl.

l. Prepare an anion exchange column and rinse with 25 mL of 6N HCl.

m. Pipet 1 mL into a 50 mL flask for Atomic Absorption analysis. Determine 100% chemical yield for Ni.

n. Load the remaining sample onto the resin column using conc. HCl for rinsing.

o. Collect the effluent (~50 mL) from the column into a 250 mL beaker.

p. Heat the solution to near boiling and reduce the volume to ~25 mL.

(3) Ni Purification

a. To the solution obtained in step p. in separation procedure, slowly add conc. NH_4OH until solution is just basic, using pH paper as indicator.

b. Add 10 mL of 10% sodium citrate and allow solution to cool to room temperature and then transfer to a separatory funnel.

c. Add 20 mL of 1% dimethylglyoxime and mix well.

d. Add 10 mL of chloroform and shake well and allow the layers to separate and transfer the chloroform (lower layer) to another separatory funnel.

e. Back extract Ni-63 by adding 10 mL 0.1N HCl and shake well.

f. Transfer aqueous layer to a 100 mL beaker. Repeat steps a. through e., and continue on step g.

g. Transfer aqueous layer to a 25 mL volumetric flask. Fill up to the mark with 0.1 N HCl. Mix well.

h. Pipet 1 mL into a 50 mL volumetric flask for determining Ni chemical yield by atomic absorption analysis.

i. Pipet 20 mL to a 40 mL centrifuge tube, add 1N NaOH or 1N HAc to adjust to pH 6-7 using pH paper as indicator.

j. Add 10 mL of 20% solution NH_4SCN and mix, then add 3 drops of alconex.

k. Add 5 drops of pyridine and mix well. Allow to stand for 10 minutes, then centrifuge and discard supernate.

l. Wash ppt. with 1% NH_4SCN + 1% Pyridine wash solution, centrifuge and discard supernate.

m. Dissolve ppt. with 15 mL of liquid scintillation cocktail and transfer to a counting vial and store in darkness for 12 hours before counting in a liquid scintillation counter with predetermined energy discrimination setting.

E.4.3 Standard Calibration and Radioactivity Measurement

a. Prepare a series of samples containing a known amount of Ni-63 activity and variable amount (0.5, 1.0, 2.0 5.0, 10.0 mg) of Ni carrier in 0.1N HCl solution in a 25 mL volumetric flask.

b. Process each standard sample starting from step i. through step m. in Ni Purification.

c. Obtain the counting rate, as well as external standard ratio (ESR) for each standard with an energy discriminator setting to include ≥80% of the counting. (Use the C-14 channel if the liquid scintillation counter has no variable energy discriminator.)

d. Prepare a counting efficiency curve, i.e., efficiency vs. weight of Ni or efficiency vs. E.S.R.

e. Determine the counting efficiency for a sample from either the determined Ni content in the sample or the measured E.S.R. from the counter.

E.4.4 References

(1) C. Yonizawa, et al, J. Radioanal. Chem., 78, 7 (1983).